Thrombus Analogue Material: Mechanical Characterisation and Use in the *in-vitro* Modelling of Acute Ischemic Stroke Treatment

Sarah Johnson B.E.

A thesis submitted to the National University of Ireland as fulfilment of the requirements for the Degree of Doctor of Philosophy

January 2020

Discipline of Biomedical Engineering,

College of Engineering and Informatics,

National University of Ireland, Galway

Primary Supervisor: Prof. Peter E. Mc Hugh

Co-supervisor: Dr. Patrick McGarry

Table of Contents

Abstract

Acute ischemic stroke (AIS), which accounts for approximately 85% of all strokes globally, is among the leading causes of death and long-term disability. It occurs when a blood clot causes an occlusion in a blood vessel, resulting in reduced blood flow to an area of the brain. Mechanical thrombectomy (MT), where the clot is removed from the occluded vessel, has become the new standard of care in stroke treatment. *In-vitro* thrombus analogs are very useful in the pre-clinical testing of devices intended for use in thrombectomy, where amongst other things they can be used to evaluate the number of attempts required to remove the thrombus and the associated risk of embolisation. Some key determinants for success of the thrombectomy procedure are the mechanical properties and composition of the occluding thrombus.

In this thesis, a range of clot analogues with varying compositions and mechanical behaviour are developed. A repeatable test method, that can be used to test a broad range of clot types, is presented and for the first time, an investigation of the mechanical behaviour of clot analogues, as a function of composition, is reported. The effect of platelet-driven contraction on the mechanical properties and microstructure of the clot analogues is also investigated. An appropriate hyper-viscoelastic constitutive model is identified and fitted to the experimental results.

The clot analogues were then used in the development of an appropriate *in-vitro* model of AIS. This model was used to compare the effectiveness of various MT techniques on clots with varying mechanical properties. Finally, the *in-vitro* model was used to investigate the effect of clot mechanical properties and composition on the occlusion dynamics and deformation of an occluding clot under physiological conditions of pressure and flow, using the previously characterised clot analogues.

The compression test set-up was found to be robust enough to test a broad range of clots, and the clot analogues were found to have similar mechanical behaviour to the human thromboemboli. Clot analogue composition was found to strongly affect the observed mechanical behaviour. Similarly, platelet-contraction was found to significantly affect clot volume and microstructure, and in turn, clot stiffness. The proposed hyper-viscoelastic constitutive model was found to successfully capture the material test data.

The feasibility of the *in-vitro* AIS mode was demonstrated and a limited evaluation of different MT approaches was performed. Although a more comprehensive analysis is required to draw definitive conclusions when comparing techniques, the clot mechanical behaviour was found to impact the effectiveness of various MT techniques. Similarly, the clot mechanical behaviour and composition was also found to affect the clot behaviour and angiographic appearance when lodged in the *in-vitro* model under physiological conditions. This behaviour may be useful in the identification of particular clot types prior to treatment, and could assist the physician in selecting the most appropriate treatment method to administer or on what MT technique to use, to ensure a greater success rate in each case.

In conclusion, the work performed in this thesis has led to an enhanced understanding of the mechanical behaviour of thrombus material. The mechanical characterisation and modelling presented are of key importance and offer a framework that could be used as an aid in the future development of treatment devices and procedures for AIS.

Acknowledgements

Firstly, I wish to express my sincere thanks to my academic supervisors Prof. Peter McHugh and Dr Patrick McGarry for their invaluable guidance, encouragement and support throughout this project.

I would also like to convey my sincere appreciation to Michael Gilvarry (Cerenovus), my employment mentor, for his continued support, input and feedback on this project, but more importantly for providing me the opportunity to work in this exciting field.

Equally, I would like to thank Dr Ray McCarthy (Cerenovus), for his advice, feedback and supervision throughout the latter part of my research. His input and guidance has been invaluable and has greatly enhanced this research endeavour.

I wish to thank my colleagues from the NTI team at Cerenovus, particularly Brian, Sharon and Anu for their encouragement and assistance in the lab and also for their words of support when I needed it most! To Eimear and Aoife, thank you for all the blood collections….

Sincere thanks to the Irish Research Council and the College of Engineering and Informatics in NUIG for funding this research. I also wish to extend my sincere appreciation to the technical staff in the Engineering Department, in particular to Dave Connolly, Maja Drapiewska, Boni Kennedy, Pat Kelly and William Kelly for their assistance and support throughout the experimental testing and lab work.

To “the gals”- Ciara, Eimear, Emily, Hollie, Laura, Lizanne, Marissa and Orla - thanks for all of the social activities, from the nights in - filled with book clubs and movie nights - to the ‘occasional’ night out; not forgetting all of the tea breaks, steps challenges and lunchtime runs, with even the odd holiday thrown in! You have provided many welcome distractions and laughs throughout the last 4 years and I greatly appreciate your friendship. To the rest of the postgrads and postdocs (past and present), the nights out, tag fun, quizzes, conference trips and lunchtime chats are treasured memories and will not be forgotten!

To Paul, thank you for your endless support, patience and encouragement, but most especially for always listening and caring, and for always being just a phone call away!

Finally, and most importantly, I would like to thank my family, whose support and love have helped me all along this journey. Big thanks to Daniel and Emma, for the laughs and distractions at home. To Mom and Dad, I owe so much to you both. Thank you for your unending love, encouragement and advice throughout my life, without which I could never have gotten this far.

List of Publications

The work presented in this thesis has appeared in the following publications:

Chapter 2: Johnson S, Duffy S, Gunning G, Gilvarry M, McGarry JP, and McHugh PE. Review of Mechanical Testing and Modelling of Thrombus Material for Vascular Implant and Device Design, *Annals of Biomedical Engineering*, 45(11):2494-2508, 2017.

Chapter 3: Johnson S, Chueh JY, Gounis MJ, McCarthy R, McGarry JP, McHugh PE, Gilvarry M. Mechanical Behaviour of In-Vitro Blood Clots and the Implications for Acute Ischemic Stroke Treatment, *Journal of Neurointerventional Surgery*, In Press, 2019.

Chapter 4: Johnson S, McCarthy R, Gilvarry M, McHugh PE, McGarry JP. Investigating the Mechanical Behaviour of Clot Analogues with varying Hematocrit, through Experimental and Computational Analysis, *in preparation.*

Chapter 5: Johnson S, McCarthy R, Fahy B, Mereuta OM, Fitzgerald S, Gaudric J, Remadi JP, Shotar E, Sourour N, Doyle K, Gilvarry M, McGarry JP, McHugh PE, Clarençon F. Treatment of Calcified Cerebral Emboli in Acute Ischemic Stroke, a Comparison of Mechanical Thrombectomy Approaches Using an In-Vitro Model, *Journal of Neurointerventional Surgery*, In Press, 2020.

Chapter 6: Johnson S, McCarthy R, Gilvarry M, McGarry JP, McHugh PE, Consoli, A. Investigating the Effect of Mechanical Properties and Composition on Clot Behaviour during Vessel Occlusion, *in preparation.*

Conference Proceedings

International Conference Proceedings

- Johnson, S., Duffy, S., Gilvarry, M., McGarry, J.P., and McHugh, P.E., "Mechanical Characterisation and Modelling of Thrombus Material", Summer Biomechanics, Bioengineering, and Biotransport Conference 2017 (SB3C 2017), Tucson, AZ, USA, June 21–24, 2017 (poster presentation).

- Johnson, S., Gilvarry, M., McGarry, J.P. and McHugh, P.E., "Biomechanical Characterisation of Thrombus Material through Experimental and Computational Analysis", 10th European Solid Mechanics Conference (ESMC 2018), Bologna, Italy, July 2-6, 2018 (oral presentation).

- Johnson, S., Gilvarry, M., McGarry, J.P. and McHugh, P.E., "Experimental and Computational Analysis of the Mechanical Behaviour of Thrombus Material", 8th World Congress of Biomechanics (WCB 2018), Dublin, Ireland, July 8-12, 2018 (oral presentation).

- Johnson, S., Chueh, J.Y., Gounis, M., Gilvarry, M., McCarthy, R., McGarry, J.P. and McHugh, P.E., "Clot Contraction: Investigating the Impact on Clot Mechanical Behaviour and Microstructure", Summer Biomechanics, Bioengineering and Biotransport Conference (SB3C 2019), Seven Springs, Pennsylvania, USA, June 25-28, 2019 (poster presentation).

- Johnson, S., McCarthy, R., "Mechanical Behaviour of Thrombus", SLICE – Stroke Live Conference 2019, Nice, France, September 30 – October 2, 2019 (Oral Presentation & Live Demonstration).

- Johnson, S., Chueh, J.Y., Gounis, M., Gilvarry, M., McCarthy, R., McGarry, J.P. and McHugh, "Investigating the Effect of Platelet Contraction on the Mechanical Properties and Microstructure of Clot Analogues with Varying Hematocrit", 15th Congress of the World Federation of Interventional and Therapeutic Neuroradiology (WFITN 2019), Naples, Italy, October 21-24, 2019 (oral presentation).

National Conference Proceedings

- Annual Bioengineering in Ireland Conference, the Annual Conference of the Section of Bioengineering of the Royal Academy of Medicine in Ireland, January 2017-2019 (oral presentations).

- Johnson, S., Duffy, S., Gilvarry, M., McGarry, J.P. and McHugh, P.E., "Mechanical Characterisation and Modelling of Thrombus Material", 20th Sir Bernard Crossland Symposium and Postgraduate Research Workshop, Dublin Institute of Technology, Grangegorman Campus, Dublin, 26-27 April, 2017 (oral & poster presentation).

Chapter 1

Introduction

1.1 Background

Stroke is the second leading cause of death worldwide, with an estimated 5.5 million deaths in 2016 (Gorelick 2019). In Ireland alone, over 10,000 people have a stroke each year, with approximately 2,000 of these resulting in death (Irish Heart Foundation 2017). According to the heart disease and stroke statistics from 2019, an additional 4% of the adult population will have experienced a stroke by 2030 (Benjamin *et al*. 2019). In the USA, it is forecast that the number of strokes will double by 2050 (Gorelick 2019).

Acute Ischemic Stroke (AIS) accounts for 85% of all strokes (Van Der Worp & Van Gijn 2007), and is characterised by the sudden loss of blood to an area of the brain, resulting in the loss of neurological function, making AIS an emergency that requires hyperacute treatment. The looming increase of AIS patients around the world, due the aging population, highlights the necessity for the further development and implementation of improved therapies to improve outcomes (Catanese *et al.*, 2017).

The key factor that determines the effectiveness of stroke treatment is the time to recanalisation (Gomis & Dávalos 2014; Muchada *et al*. 2014). Current treatment for AIS involves thrombus lysis using the thrombolytic drug, Recombinant Tissue Plasminogen (rt-PA) and/or thrombus removal via endovascular therapy (EVT). EVT for AIS has undergone a major evolution since its origin in the 1980s, when it was

purely utilised to administer thrombolytic agents directly to the clot (Catanese *et al.*, 2017). The era of mechanical thrombectomy commenced in 2004 with the approval of the MERCI device (Mechanical Embolus Removal in Cerebral Ischemia) by the U.S. Food and Drug Administration (FDA) (Smith *et al*. 2008; Smith *et al*. 2005).

Since then, recent randomised control trials have demonstrated a convincing benefit from stent retriever-mediated mechanical thrombectomy for selected AIS patients with large vessel occlusion in the anterior circulation (Berkhemer *et al.*, 2014; Campbell *et al.*, 2015; Goyal *et al.*, 2015; Saver *et al.*, 2015).

There has been a rapid evolution in thrombectomy devices and approaches over the past decade, with the FDA clearing the extended use of the Trevo clot retrieval device (Stryker Neurovascular) from 6 to 24 hours after stroke onset, based on the results of the DAWN trail in 2018 (Nogueira, Jadhav, *et al*. 2018). However, to date, there are no universally accepted standards for device or treatment selection due to the paucity of scientific evidence on what combinations of techniques or devices will yield the best outcome (Spiotta *et al*. 2015).

Despite significant developments in the treatment of AIS, EVT is unsuccessful in some patients (Flint *et al*. 2010; Kulcsár *et al*. 2010; Menon *et al*. 2015). The reasons for this are multifaceted and include variations in vessel anatomy and tortuosity (Kaymaz *et al*. 2017), poor vessel access (Ribo *et al*. 2013; Leischner *et al*. 2018), occlusion location and size, patient co-morbidities and the composition of the occluding thrombus (Dobrocky *et al*. 2018; O'Cearbhaill *et al*. 2016). The advent of mechanical thrombectomy has however permitted the analysis of retrieved thrombi in AIS (Fitzgerald *et al*. 2019; Duffy *et al*. 2019; De Meyer *et al*. 2017).

Analysis of thrombus material from human sources can often be expensive and highly regulated, making specimens difficult to obtain. Therefore analogue clot materials, formed *in-vitro* from human or animal blood, present an alternative option for the preclinical testing and development of treatment devices (Robinson *et al*. 2013). Additionally, they are also a useful tool for the investigation and characterisation of clot material properties and their mechanical behaviour as a function of their constituents.

A variety of protocols have been proposed for the fabrication of clot analogues, involving numerous variables, such as donor species, concentration of thrombin and the addition of barium sulphate as a radiopaque additive (Duffy *et al*. 2016; Krasokha *et al*. 2010; Chueh *et al*. 2011; Liebig *et al*. 2008), and the effect of these variables on the mechanical behaviour of the clot analogues have also been explored. However, clot composition can differ substantially with varying red blood cell (RBC) and fibrin content (Marder *et al*. 2012; Liebeskind *et al*. 2011), and to date, the effect of clot composition and hematocrit (%H), i.e. the volume percentage of RBCs in the mixture, on mechanical behaviour of the material has not been adequately investigated. This work builds on the previously reported clot protocols reported by Cerenovus (Duffy *et al*. 2016; Gunning *et al*. 2016; Weafer *et al*. 2019), and presents the next generation of clot analogues which include contracted clots and calcified clots.

The dependencies of the efficacy and safety of EVT on clot composition and mechanics were highlighted in prior studies (Chueh *et al*. 2013; Gunning *et al*. 2016). Current *in-vitro* clot modelling techniques produce clinically representative clot analogues with different mechanical features for device efficacy testing and with various histological patterns (Duffy *et al*. 2016; Chueh *et al*. 2011), with the aim of providing clinicians with treatment strategies based on laboratory findings. Therefore,

it is critical to have *in-vitro* clot models that are clinically representative in terms of their mechanical behaviour as well as compositional features.

In the context of analytical and computational modelling that can support the mechanical analysis of clot material and *in-vitro* model development, the literature is relatively limited. A few studies have reported constitutive models (van Dam *et al.*, 2008; Schmitt *et al.*, 2011; Slaboch *et al.*, 2012; van Kempen *et al.*, 2015; Malone *et al.*, 2018) to capture the mechanical behaviour of clot material, yet the loading-unloading hysteresis due to the rate-dependent viscoelasticity of thrombus material has largely been neglected. This material behaviour is particularly important for several reasons. Firstly, although the stent expansion rate is constant, there are varying strain distributions and, as a result, varying the strain rates within the clot material. Hence, gaining an understanding of the material strain rate dependence, over a range of strain rates, is important. Secondly, as complete as possible an understanding of the rate dependence and the viscoelasticity of the clot material is necessary in order to define an appropriate constitutive law for the material, and data on strain rate dependence, loading-unloading hysteresis, and stress relaxation response are all important elements for selecting and calibrating a suitable constitute law. Such a constitutive law could then be used to simulate and evaluate the effect of important clinical parameters such as stent embedding time during MT, and to simulate the behavior of the clot during aspiration, in terms of variation in aspiration time and the effects of applying a constant or cyclic pressure.

Finite element analysis (FEA) is commonly accepted as a powerful tool used in the medical device industry to analyse performance of devices during development. While predictive computational models simulating clot behaviour *in-vivo* would be very valuable for vascular research and device design, relatively little has been reported on

the computational modelling of clot tissue mechanics in the literature to date. Very few finite element models have been developed to simulate even simple experiments (Fogelson and Guy, 2008; Slaboch *et al.*, 2012; Xie *et al.*, 2005).

Under the current FDA guidance for non-clinical testing of neurothrombectomy devices, devices must be shown to have the capability of capturing clots of variable size, coagulation and composition in order to determine device effectiveness (Center for Devices and Radiological Health 2007). Currently the majority of this testing is performed *in-vitro*. The use of finite element modelling to simulate these procedures could significantly reduce the number of *in-vitro* experiments required and provide a more time and cost effective approach to device testing and development. However, in order to simulate these procedures, an accurate constitutive model capable of capturing the material behaviour of thrombus is required.

1.2 Thesis Objectives

In the field of AIS treatment, there is an immediate need to develop improved and more clinically representative *in-vitro* models for device testing. A critically important aspect of this is the use of clots that are similar in composition to those retrieved from AIS patients. In this context, the first overall objective of this thesis is to develop clot analogues with varying compositions and to use these to gain a better understanding of the mechanical behaviour of clot material than has been possible to date. The second overall objective is to use these analogues in *in-vitro* AIS models to allow for the analysis of the mechanics of an occluding clot and for the performance assessment of various AIS treatment techniques. The clot analogues were lodged in patient-specific silicone models provided by Cerenovus to create more realistic models of AIS for mechanical thrombectomy simulation.

In this thesis, an investigation of the mechanical behaviour of clot analogues under compressive loading and unloading, as a function of composition, is presented for the first time. The experimental results are then used to identify an appropriate constitutive model to capture the material behaviour. Finally, the clot analogues are used in the development of *in-vitro* models to simulate AIS and to evaluate various mechanical thrombectomy techniques. The models and results presented in this thesis are of key importance to the evaluation and future development of mechanical thrombectomy devices and procedures.

The specific objectives of this thesis are as follows:

- To develop a range of repeatable clot analogues, with varying compositions and mechanical behaviour that span the range of human thromboemboli.
- To investigate the mechanical behaviour of clot analogues as a function of clot composition and to develop a reliable test method that can be used to test the broad range of clot types.
- To evaluate how platelet-driven contraction can affect clot mechanical properties and microstructure, and in turn, how this can have implications for the treatment of AIS.
- To identify an appropriate visco-hyperelastic constitutive law to capture the rate-dependent mechanical behaviour of the clot analogue material.
- To use the developed clot protocols to generate a calcified clot analogue and to assess the effect of calcification on clot mechanical properties and retrieval therapies.
- To develop an *in-vitro* model of AIS using the clot analogues, that can be used to compare the effectiveness of various mechanical thrombectomy techniques on clots with varying mechanical properties.
- To use the *in-vitro* AIS model to analyse the occlusion dynamics and deformation of an occluding clot under physiological conditions, supported by computational modelling.

1.3 Thesis Overview

Chapter 2 reviews stroke pathology and the current state of the art in terms of therapies and endovascular treatment options for AIS, and provides a general literature review of the previous research on the characterisation of *in-vivo* thrombi retrieved from AIS patients and *in-vitro* clot replicates that have been reported to date. An overview of the constitutive and computational modelling of thrombus material in the published literature is also provided.

This background is intended to support the chapters that follow and included in each of the subsequent technical studies (Chapters 3-6) is a critical literature review directly pertinent to each study, while Chapter 2 gives a more general background to the literature.

Chapter 3 outlines the preparation and characterisation of both platelet-contracted and non-contracted clot analogues with varying hematocrit and demonstrates the effect of platelet-driven clot contraction and clot composition on the microstructure and mechanical behaviour of the material. Mechanical testing is performed to compare the behaviour of the analogues with previously tested human thromboemboli. Scanning electron microscopy and histology investigates the clot microstructure and composition. The association between clot properties and their behaviour during mechanical thrombectomy is also investigated.

Chapter 4 further investigates the mechanical behaviour of the clot analogues using two loading protocols; cyclic compression and stress-relaxation, and provides an improved understanding of the relationship between clot composition and the rate-dependent non-linear mechanical behaviour of the material. The experimental results are then used to identify an appropriate constitutive model to capture the visco-

hyperelastic behaviour of the material. The effect of clot aging and storage methods on the microstructure and mechanical behaviour of the clot analogues are also investigated.

Chapter 5 describes the development of an *in-vitro* calcified clot model to evaluate different procedural approaches, using contemporary endovascular treatment devices, for the retrieval of a calcified clot analogue. The development and preparation of an appropriate calcified clot analogue, based on the clot preparation protocols described in Chapters 3 and 4, and the characterisation of human calcified tissues that represent likely sources of calcified emboli, are also described. The feasibility of this *in-vitro* calcified clot model, to test different endovascular strategies to recanalise a large vessel occlusion, is demonstrated.

Chapter 6 investigates the occlusion dynamics of clots with various mechanical properties over the relevant timeline for stroke. The previously characterised clot analogues, described in Chapters 3 and 4, were used to investigate the effect of clot mechanical properties and composition on the deformation and angiographic appearance of clot when lodged in an *in-vitro* model under physiological conditions of pressure and flow. A finite element model of the experiment is also presented to allow a comparison with the experimental results.

Finally, **Chapter 7** provides an overview of the work performed. The key findings of this thesis are summarised and the outcomes of each result chapters are discussed, followed by overall conclusions in this thesis. Suggestions for experimental and computational future works are also proposed.

1.4 References

Benjamin, E. J. *et al.* (2019) 'Heart Disease and Stroke Statistics—2019 Update: A Report From the American Heart Association', Circulation, 139(10). doi: 10.1161/CIR.0000000000000659.

Berkhemer, O. A. *et al.* (2014) 'A Randomized Trial of Intraarterial Treatment for Acute Ischemic Stroke', New England Journal of Medicine. Massachusetts Medical Society, (372), pp. 11–20.

Campbell, B. C. V. *et al.* (2015) 'Endovascular Therapy for Ischemic Stroke with Perfusion-Imaging Selection', New England Journal of Medicine. Massachusetts Medical Society, 372(11), pp. 1009–1018. doi: 10.1056/NEJMoa1414792.

Catanese, L., Tarsia, J. and Fisher, M. (2017) 'Acute Ischemic Stroke Therapy Overview', Circulation Research, 120(3), pp. 541–558. doi: 10.1161/CIRCRESAHA.116.309278.

Center for Devices and Radiological Health (2007) Guidance for Industry and FDA Staff Pre-Clinical and Clinical Studies for Neurothrombectomy Devices.

Chueh, J. Y. *et al.* (2013) 'Reduction in Distal Emboli With Proximal Flow Control During Mechanical Thrombectomy', Stroke, 44(5), pp. 1396–1401. doi: 10.1161/STROKEAHA.111.670463.

Chueh, J. Y. *et al.* (2011) 'Mechanical characterization of thromboemboli in acute ischemic stroke and laboratory embolus analogs.', AJNR. American journal of neuroradiology, 32(7), pp. 1237–44. doi: 10.3174/ajnr.A2485.

van Dam, E. A. *et al.* (2008) 'Non-linear viscoelastic behavior of abdominal aortic aneurysm thrombus', Biomechan Model Mechanobiol, 7, pp. 127–137.

Dobrocky, T. *et al.* (2018) 'Thrombectomy of calcified emboli in stroke. Does histology of thrombi influence the effectiveness of thrombectomy?', Journal of neurointerventional surgery. British Medical Journal Publishing Group, 10(4), pp. 345–350. doi: 10.1136/neurintsurg-2017-013226.

Duffy, S. *et al.* (2016) 'Novel methodology to replicate clot analogs with diverse composition in acute ischemic stroke', Journal of Neurointerventional Surgery, 0, pp. 1–7.

Duffy, S. *et al.* (2019) 'Per-Pass Analysis of Thrombus Composition in Patients With Acute Ischemic Stroke Undergoing Mechanical Thrombectomy', Stroke, 50(5), pp. 1156–1163. doi: 10.1161/STROKEAHA.118.023419.

Fitzgerald, S. T. *et al.* (2019) 'Platelet-rich clots as identified by Martius Scarlet Blue staining are isodense on NCCT.', Journal of neurointerventional surgery. British Medical Journal Publishing Group, 11(11), pp. 1145–1149. doi: 10.1136/neurintsurg-2018-014637.

Flint, A. C. *et al.* (2010) 'Predicting Long-Term Outcome after Endovascular Stroke Treatment: The Totaled Health Risks in Vascular Events Score', American Journal of Neuroradiology, 31(7), pp. 1192–1196. doi: 10.3174/ajnr.A2050.

Fogelson, A. L. and Guy, R. D. (2008) 'Immersed-boundary-type models of intravascular platelet aggregation', Computer Methods in Applied Mechanics and Engineering, 197(25–28), pp. 2087–2104. doi: 10.1016/j.cma.2007.06.030.

Gomis, M. and Dávalos, A. (2014) 'Recanalisation and Reperfusion Therapies of Acute Ischemic Stroke: What have We Learned, What are the Major Research Questions, and Where are We Headed?', Frontiers in neurology. Frontiers Media SA, 5, p. 226. doi: 10.3389/fneur.2014.00226.

Gorelick, P. B. (2019) 'The global burden of stroke: persistent and disabling.', The Lancet. Neurology. Elsevier, 18(5), pp. 417–418. doi: 10.1016/S1474-4422(19)30030-4.

Goyal, M. *et al.* (2015) 'Randomized assessment of rapid endovascular treatment of ischemic stroke.', The New England journal of medicine. Massachusetts Medical Society, 372(11), pp. 1019–30. doi: 10.1056/NEJMoa1414905.

Gunning, G. M. *et al.* (2016) 'Clot friction variation with fibrin content; implications for resistance to thrombectomy', Journal of Neurointerventioal Surgery, 372(1), pp. 1019–1030. doi: 10.1136/.

Irish Heart Foundation (2017) Irish Heart Stroke - Irish Heart Foundation.

Kaymaz, Z. *et al.* (2017) 'Influence of carotid tortuosity on internal carotid artery access time in the treatment of acute ischemic stroke', Interventional Neuroradiology. SAGE PublicationsSage UK: London, England, 23(6), pp. 583–588. doi: 10.1177/1591019917729364.

van Kempen, T. H. S., Peters, G. W. M. and van de Vosse, F. N. (2015) 'A constitutive model for the time-dependent, nonlinear stress response of fibrin networks.', Biomechanics and modeling in mechanobiology, 14(5), pp. 995–1006.

Krasokha, N. *et al.* (2010) 'Mechanical properties of blood clots - a new test method. Mechanische Eigenschaften von Thromben - Neue Untersuchungsmethoden', Materialwissenschaft und Werkstofftechnik, 41(12), pp. 1019–1024. doi: 10.1002/mawe.201000703.

Kulcsár, Z. *et al.* (2010) 'Penumbra System: A Novel Mechanical Thrombectomy Device for Large-Vessel Occlusions in Acute Stroke', American Journal of Neuroradiology, 31(4), pp. 628–633. doi: 10.3174/ajnr.A1924.

Leischner, H. *et al.* (2018) 'Reasons for failed endovascular recanalisation attempts in stroke patients', Journal of NeuroInterventional Surgery , 0, pp. 1–5.

Liebeskind, D. S. *et al.* (2011) 'CT and MRI Early Vessel Signs Reflect Clot Composition in Acute Stroke', Stroke, 42(5), pp. 1237–1243. doi: 10.1161/STROKEAHA.110.605576.

Liebig, T. *et al.* (2008) 'Comparative in vitro study of five mechanical embolectomy systems: effectiveness of clot removal and risk of distal embolisation.', Neuroradiology, 50(1), pp. 43–52. doi: 10.1007/s00234-007-0297-y.

Malone, F. *et al.* (2018) 'The Mechanical Characterisation of Bovine Embolus Analogues Under Various Loading Conditions', Cardiovascular Engineering and Technology. Springer US, 9(3), pp. 489–502. doi: 10.1007/s13239-018-0352-3.

Marder, V. J. *et al.* (2012) Hemostasis and Thrombosis: Basic Principles and Clinical Practice. Lippincott Williams & Wilkins.

Menon, B. K. *et al.* (2015) 'Trends in Endovascular Therapy and Clinical Outcomes Within the Nationwide Get With The Guidelines-Stroke Registry', Stroke, 46(4), pp. 989–995. doi: 10.1161/STROKEAHA.114.007542.

De Meyer, S. F. *et al.* (2017) 'Analyses of thrombi in acute ischemic stroke: A consensus statement on current knowledge and future directions', International Journal of Stroke, 12(6), pp. 606–614. doi: 10.1177/1747493017709671.

Muchada, M. *et al.* (2014) 'Impact of time to treatment on tissue-type plasminogen activator-induced recanalisation in acute ischemic stroke.', Stroke, 45(9), pp. 2734–8. doi: 10.1161/STROKEAHA.114.006222.

Nogueira, R. G. *et al.* (2018) 'Thrombectomy 6 to 24 Hours after Stroke with a Mismatch between Deficit and Infarct', New England Journal of Medicine. Massachusetts Medical Society, 378(1), pp. 11–21. doi: 10.1056/NEJMoa1706442.

O'Cearbhaill, R. M. *et al.* (2016) 'Calcified cerebral emboli: A case series and review of literature', Journal of Systems and Integrative Neuroscience, 2(3), pp. 180–13.

Ribo, M. *et al.* (2013) 'Difficult catheter access to the occluded vessel during endovascular treatment of acute ischemic stroke is associated with worse clinical outcome.', Journal of neurointerventional surgery. British Medical Journal Publishing Group, 5 Suppl 1(suppl 1), pp. i70-3. doi: 10.1136/neurintsurg-2012-010438.

Robinson, R. A. *et al.* (2013) 'Limitations of using synthetic blood clots for measuring in vitro clot capture efficiency of inferior vena cava filters.', Medical devices (Auckland, N.Z.), 6, pp. 49–57. doi: 10.2147/MDER.S42555.

Saver, J. L. *et al.* (2015) 'Stent-Retriever Thrombectomy after Intravenous t-PA vs. t-PA Alone in Stroke', New England Journal of Medicine, 372(24), pp. 2285–2295. doi: 10.1056/NEJMoa1415061.

Schmitt, C., Hadj Henni, A. and Cloutier, G. (2011) 'Characterization of blood clot viscoelasticity by dynamic ultrasound elastography and modeling of the rheological behavior', Journal of Biomechanics, 44(4), pp. 622–629. doi: 10.1016/j.jbiomech.2010.11.015.

Slaboch, C. L. *et al.* (2012) 'Mechano-rheological properties of the murine thrombus determined via nanoindentation and finite element modeling.', Journal of the

mechanical behavior of biomedical materials, 10, pp. 75–86. doi: 10.1016/j.jmbbm.2012.02.012.

Smith, W. S. *et al.* (2005) 'Safety and Efficacy of Mechanical Embolectomy in Acute Ischemic Stroke', Stroke, 36(7), pp. 1432–1438. doi: 10.1161/01.STR.0000171066.25248.1d.

Smith, W. S. *et al.* (2008) 'Mechanical Thrombectomy for Acute Ischemic Stroke', Stroke, 39(4), pp. 1205–1212. doi: 10.1161/STROKEAHA.107.497115.

Spiotta, A. M. *et al.* (2015) 'Evolution of thrombectomy approaches and devices for acute stroke: a technical review.', Journal of neurointerventional surgery, 7(1), pp. 2–7. doi: 10.1136/neurintsurg-2013-011022.

Weafer, F.M. *et al.*, 2019. Characterization of strut indentation during mechanical thrombectomy in acute ischemic stroke clot analogs. Journal of NeuroInterventional Surgery, p.neurintsurg-2018-014601.

Van Der Worp, H. B. and Van Gijn, J. (2007) 'Acute Ischemic Stroke', The New England journal of medicine, 357(6), pp. 572–579.

Xie, H. *et al.* (2005) 'Correspondence of ultrasound elasticity imaging to direct mechanical measurement in aging DVT in rats', Ultrasound in Medicine & Biology, 31(10), pp. 1351–1359. doi: 10.1016/j.ultrasmedbio.2005.06.005.

Chapter 2

Background

2.1 Chapter Overview

This chapter provides an overview of the literature and background relevant to the subject area of this thesis. While this chapter provides a general overview of the literature relevant to this body of work, it should be noted that each technical chapter of this thesis provides a focused discussion of the critical literature in the context of the key results and findings.

The content of this chapter has appeared in a review paper published in the *Annals of Biomedical Engineering* (Johnson *et al.*, 2017).

2.2 Acute Ischemic Stroke (AIS)

Stroke a leading cause of death and disability worldwide (Mozaffarian *et al*. 2015). In Ireland alone, of the 10,000 strokes annually approximately 2,000 result in death. This is a higher mortality rate than breast cancer, prostate cancer and bowel cancer combined (Irish Heart Foundation 2017).

There are two types of stroke; ischemic, accounting for 85% of all strokes, and hemorrhagic. Acute ischemic stroke occurs when a blood clot causes an occlusion in a blood vessel, resulting in reduced blow flow to an area of the brain (Figure 2.1 A). Within areas of the brain that are severely deprived of blood, necrotic cell death occurs almost immediately, and the affected tissue undergoes irreversible damage. This is

referred to as the ischemic core. The ischemic penumbra, which is the area surrounding the ischemic core, receives some blood supply from the collateral circulation (Figure 2.1 B), and may be salvaged if there is prompt and adequate reperfusion of the area (González 2006).

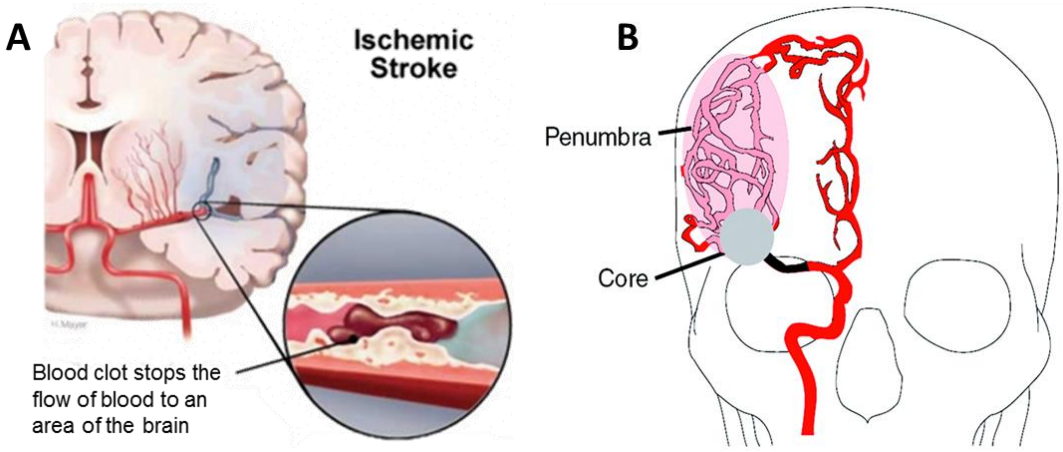

Figure 2.1 (A) Ischemic stroke caused by a blood clot obstructing blood flow to an area of the brain. (B) Irreversible damage caused to brain tissue in AIS, referred to as the 'core' and the brain tissue at risk of ischemia referred to as the 'penumbra'.

Clots are classified as either thrombotic or embolic, depending on the area in the body where they are formed. A thrombotic clot forms within a vessel in the brain, whereas embolic clots are formed elsewhere in the body, with part of the clot becoming dislodged (embolus) and travelling to and occluding a narrower vessel in the brain. Identifying the underlying cause of AIS could be important for guiding treatment decisions and for secondary stroke prevention measures. Attempts have been made to identify clot etiology using histology to predict where clots with certain compositions originated as this could impact the treatment technique used. However it has been proven to be extremely difficult to develop an accurate correlation between the two (Marder *et al*. 2006).

Similarly, understanding clot adhesion could also improve AIS treatment. If an occluding clot is thrombotic, it is likely to have some level of adhesion to the vessel wall through biological processes. However, in the case of an embolic clot, adhesion to the vessel wall is not fully understood. To-date the interaction between the clot and the vessel wall is not fully understood as it is difficult to replicate these *in-vivo* processes in an *in-vitro* environment. However, clot adhesion to the vessel wall could impact treatment success by making the clot more difficult to remove.

2.2.1 Thrombus Formation

Thrombus material is a critically important diseased tissue component associated with AIS and a range of vascular disease conditions, such as myocardial infarction, atherosclerosis and deep vein thrombosis (DVT) (Stary 1999). Thrombus formation can be initiated in many ways, for example due to vascular injury, as a result of low flow/stasis, or in very high shear flow conditions.

Coagulation Cascade

Hemostasis is the main process that maintains the integrity of a vessel after vascular damage (Furie & Furie 2008). The hemostatic system *in-vivo* acts to prevent blood loss at the site of injury by forming a hemostatic plug. The coagulation pathway describes the cascade of events which leads to hemostasis (Figure 2.2) (MacFarlane 1964; Davie & Ratnoff 1964). Two major pathways, the extrinsic and intrinsic pathways, originate separately but converge at a specific point, leading to the formation of fibrin monomers (Chaudhry & Babiker 2019).

The intrinsic pathway is localised within the blood and occurs due to trauma to blood cells and exposure of blood cells to collagen. The activation of FXII occurs when blood comes into contact with prekallikrein (a serine protease) and high molecular

weight kininogen (a non-enzymatic cofactor). Subsequently, activated FXII activates FXI which in turn activates FIX. FX is activated by FIXa in the presence of FVIII (activated by traces of thrombin and calcium ions). Factor IXa goes on to serve as a catalyst for turning factor X into factor Xa, also known as the prothrombin activator, which converts prothrombin to thrombin.

The extrinsic pathway occurs due to vessel damage. In this pathway plasma factor (F) VII is activated in the presence of calcium (Ca^{2+}) and its cofactor, tissue factor (TF). This FVIIa/TF complex is responsible for activation of factor X into factor Xa. It is as this point that both extrinsic and intrinsic pathways become one (Chaudhry & Babiker 2019).

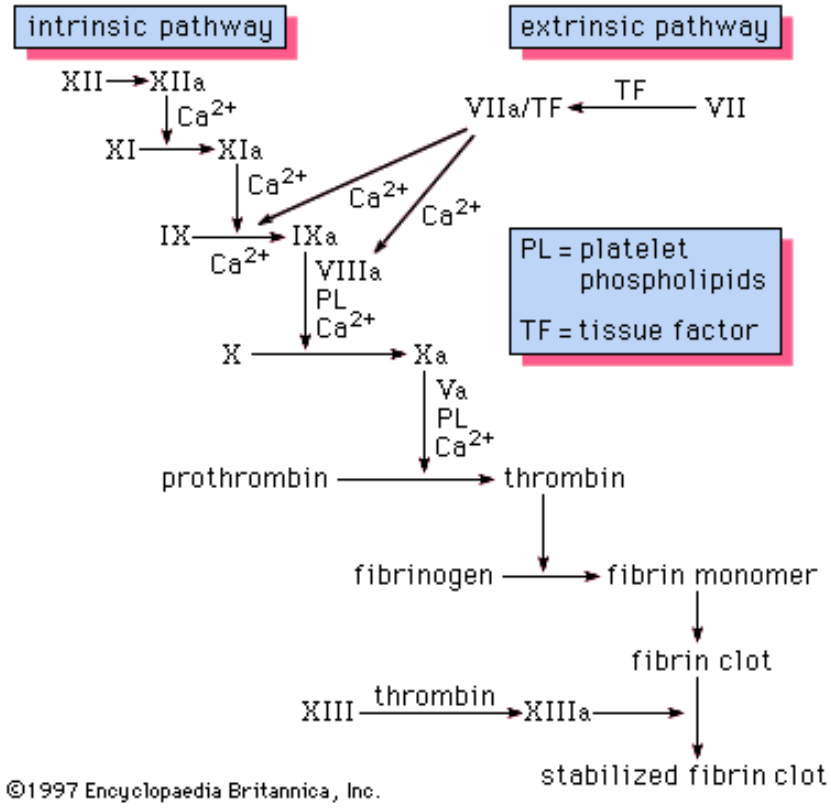

Figure 2.2 The blood coagulation cascade. Each protein circulates in the blood in an active form (Furie 1999).

Cell-based Model of Coagulation

Although the classic coagulation model contributed significantly to the understanding of coagulation, more recent research has shown that the cascade hypothesis does not adequately reflect *in-vivo* hemostasis. The cell-based model of coagulation has replaced this original cascade model, and has significantly modified current understanding of how hemostasis occurs *in-vivo* (Hoffman 2003; Ferreira *et al*. 2010).

The cell-based model proposes that coagulation occurs on different cell surfaces. Tissue factor (TF) bearing cells are an important component of the cell-based system. TF is expressed on a number of cell types which include endothelial cells, mononuclear cells, macrophages and fibroblasts (Hoffman 2003). Under normal flow conditions with an intact endothelium, cells expressing TF are separated from the blood by the vascular endothelium. When the endothelium is disrupted, collagen and TF become exposed to the flowing blood, thus initiating formation of a thrombus (Furie & Furie 2008) (Figure 2.3 A). FVIIa binds to the exposed TF, which activates small amounts of FIX and FX. Xa associated with its cofactor, FVa, forms a complex called prothrombinase on the surface of cells that express TF. This complex transforms small amounts of prothrombin (Factor II) to thrombin; amounts too small to complete the fibrin clot formation process, but this is critical in the coagulation amplification phase (Ferreira *et al.*, 2010).

The coagulation process proceeds to the amplification phase only when there is vascular damage. The exposed collagen triggers the accumulation and activation of circulating platelets at the site of vessel injury, where they become a major component of the developing thrombus. The formation of a blood clot accompanies the

aggregation of platelets at the site of injury and forms a plug that prevents blood loss from the vessel (Weisel, 2008).

TF is the sole initiator of the generation of thrombin, and in turn the formation of fibrin (Furie & Furie 2008). The soluble precursor protein of fibrin in blood is fibrinogen, which is converted by cleavage of small peptides to fibrin (Weisel, 2008). As TF becomes exposed, it initiates the production of thrombin, which begins the conversion of fibrinogen to fibrin, as well as the continued activation of platelets. Von Willebrand Factor, a glycoprotein secreted by platelets, allows the platelets to adhere to collagen in the subendothelial matrix forming a polymeric mesh at the base of the wound with the accumulated fibrin (van Galen *et al*. 2012).

Fibrin polymerises and the growing strands stabilise the clot, with a great diversity of structural, biological, physical and chemical properties, depending on the conditions of formation (Weisel 2007). Thrombin in the presence of Ca2+ produces Factor XIIIa that crosslinks the meshes to form a stable fibrin scaffold (Litvinov *et al*. 2012). The scaffold then fills with red blood cells and platelets to form a stable blood clot that plugs the wound and allows healing of the tissues (Figure 2.3 B).

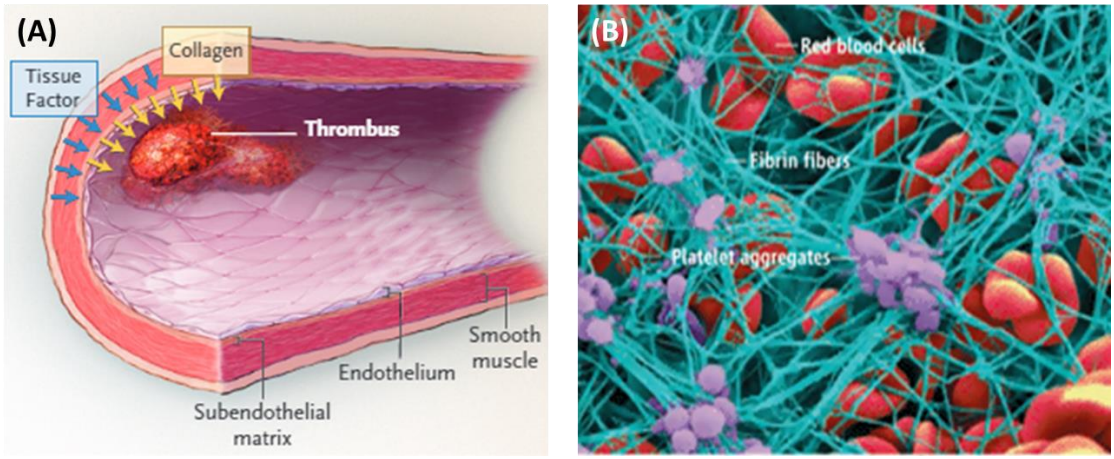

Figure 2.3 (A) Collagen (yellow arrows), located in the subendothelial matrix beneath the endothelium, is not exposed to flowing blood under normal conditions. Tissue factor (blue arrows), located in the medial (smooth muscle) and adventitial layers of the vessel wall, comes in contact with flowing blood when the vessel is disrupted or punctured. Both collagen and thrombin initiate thrombus formation (Furie & Furie 2008). (B) Schematic of thrombus microstructure showing the branched network of fibrin fibres (blue), platelets (purple) and red blood cells (Weisel, 2008).

2.2.2 Thrombus Contraction

Thrombus contraction/retraction is the tightening and shrinking of the thrombus network (Figure 2.4). It occurs as activated platelets rearrange within the clot structure, pulling on the fibrin threads, thus causing the fibrin network to contract and reduce in volume (Kim *et al*. 2017). Although previous studies have described the components necessary for clot contraction, the physical mechanism is still unknown. Activated platelets have been found to bend and shorten individual fibrin fibres, via their filopodia, that undergo sequential extension and retraction, similar to pulling hand-over-hand on a rope (Kim *et al*. 2017). Contracting platelets have been found to actively remodel the fibrin network by increasing the density followed by enhanced clot stiffness.

Figure 2.4 Blood mixture before contraction (left) and contracted/retracted clot (right) (Duffy *et al.*, 2016).

Although the physical mechanisms of clot contraction remain unknown, certain correlations between blood clot cellular composition and clot contraction mechanics have been identified. For example, the extent of clot contraction has been found to be hematocrit-dependent (Tutwiler *et al*. 2018), as clots with a greater hematocrit were found to exhibit less contraction than clots with a lower hematocrit. It is likely that the presence of red blood cells (RBCs) prevent the clot contraction as the fibrin network must compress around them until they are tightly packed and cannot compact any further. RBCs have also been found to get compacted into the core, with the redistribution of platelets and fibrin to the outside of the clot. Interestingly, these RBCs at the core of the contracting clot undergo a shape transformation from their native biconcave shape to that of polyhedra, hence named polyhedrocytes (Cines *et al.*, 2014). It is believed that the presence of these polyhedrocytes reduce clot permeability and consequently they are thought to play a role in hemostasis. These remarkable polyhedral shaped RBCs were first described by Gottlob *et al.* (1971) and rediscovered later is a natural morphological form of erythrocytes in addition to echinocytes, acanthocytes, spheroechinocytes, ovalocytes, elliptocytes, stomatocytes, and more (Lim *et al.,* 2002). This polyhedrocyte shape allows for the efficient packing of RBCs within the clot, thus minimizing the interface area and space between cells, which helps to create an impermeable seal at the site of vessel injury to prevent bleeding. This in turn may impact the effectiveness of stroke treatments such as thrombolysis and mechanical thrombectomy respectively.

Although the effect of clot contraction on the clot microstructure has been reported in the literature, the effect of the microstructural reorganisations on the clot mechanical behaviour and stiffness has not been thoroughly investigated.

2.3 Treatment of AIS

In recent years, significant developments have been made in the field of AIS treatment. The majority of AIS cases are treated using mechanical thrombectomy (MT) or dissolved using Recombinant Tissue Plasminogen Activator (rt-PA).

2.3.1 Thrombolytic Drug Treatment

Early reperfusion of the ischemic penumbra is associated with favourable outcomes and reduced mortality (Berkhemer *et al.*, 2014; Chueh *et al.*, 2013; Gralla *et al.*, 2006; Gunning *et al.*, 2016; Ryan *et al.*, 1999).

rt-PA is currently the only thrombolytic drug approved by the Food and Drug Administration (FDA) for the treatment of AIS. However the use of rt-PA has many limitations, and is available for less than 10% (Chueh *et al*. 2011; Schwamm *et al*. 2013; Menon *et al*. 2015) of stroke patients, mainly due to the narrow therapeutic time-window of 4.5 hours after symptom onset (Hacke *et al*. 2008) and several contraindications that limit its use, such as use of anticoagulants, patient history of coagulopathy such as hemophilia, or if the patient has undergone recent surgery. Moreover, with large clot burdens in proximal vessels, rt-PA is less effective in achieving recanalisation (Asakura *et al*. 2007).

rt-PA results in early reperfusion in only 13-50% of patients with occlusions of the intracranial internal carotid artery or the first segment of the middle cerebral artery (Saqqur *et al*. 2007; De Silva *et al*. 2010; Paciaroni *et al*. 2012). These low rates of early perfusion may be due to the occlusion site, clot composition, clot length/size, clot microstructure (permeable/impermeable) and exposure time to rt-PA. Similarly, reduced rt-PA perfusion has also been observed in clots that fully occlude the vessel as there is less surface area exposed to the rt-PA than in clots with residual flow around

them (Mishra *et al.,* 2014). However, there is incontrovertible evidence that MT with stent-retrievers is superior to rt-PA in the management of AIS with large vessel occlusions (Andersson *et al*. 2019). Similarly, the effectiveness of MT in combination with thrombolytic therapy had been shown to be superior to thrombolytic therapy alone in recent trials such as the REVASCAT (Jovin *et al*. 2015), EXTEND-IA (Campbell *et al*. 2015), MR CLEAN (Berkhemer *et al*. 2015), SWIFT PRIME (Saver *et al*., 2015) and ESCAPE (Goyal *et al.*, 2015) trials (Table 2.1).

Recent studies have also shown that combining intravenous thrombolysis (IVT) with rt-PA and MT is superior to direct MT in terms of clinical outcomes at 90 days (Robinson *et al.*, 2013; Kan *et al.*, 2010; Yuki *et al.*, 2012). It has been hypothesized that IVT before MT may increase recanalisation rates by softening the thrombus and, thus, reducing the duration of the procedure with fewer passes of stent retrievers. However, most of these studies compared intravenous thrombolysis (IVT)-eligible and IVT-ineligible patients, although both groups are inherently different. Lower recanalization rates in patients ineligible for IV tPA may be an epiphenomenon of different clot histology and clot characteristics. Patients ineligible for medical treatment are more likely to have thrombi of cardiogenic origin, and these cardiogenic thrombi have been found to have a higher fibrin content, which is associated with lower rates of successful reperfusion. In contrast, when analysis was confined to studies with a low risk of selection bias (i.e. comparable IVT-eligible patients in both treatment groups), the results indicate that direct MT may offer comparable safety and efficacy to IVT+MT (van der Bom *et al*. 2012). It has also been suggested that rt-PA may cause harm as it may induce thrombus fragmentation, as a result of softening the thrombus, which may lead to more challenging interventions (Haider *et al*. 2016).

Table 2.1 Table outlining key characteristics and outcomes from the major clinical trials.

Trial Name:	Key Characteristics:	Outcome:
REVASCAT	- Aimed to assess the safety and efficacy of thrombectomy for the treatment of stroke. - Patients received either medical therapy (including intravenous alteplase when eligible) and endovascular therapy with the Solitaire stent retriever (thrombectomy group) or medical therapy alone (control group).	- Stent retriever thrombectomy reduced the severity of post-stroke disability and increased the rate of functional independence.
EXTEND-1A	- Randomly assigned patients to undergo endovascular thrombectomy with the Solitaire FR (Flow Restoration) stent retriever or to continue receiving alteplase alone.	- The trial was stopped early because of efficacy after 70 patients had undergone randomization. - Early thrombectomy with the Solitaire FR stent retriever, as compared with alteplase alone, improved reperfusion, early neuro-logic recovery, and functional outcome.
SWIFT PRIME	- Randomly assigned eligible patients continue with t-PA alone (control group) or to undergo endovascular thrombectomy with the use of a stent retriever within 6 hours after symptom onset (intervention group).	- The study was stopped early because of efficacy. - Thrombectomy with a stent retriever within 6 hours after onset improved functional outcomes at 90 days.
MR CLEAN	- Randomly assigned eligible patients to either intraarterial treatment (arterial catheterization with a microcatheter to the level of occlusion and delivery of a thrombolytic agent, mechanical thrombectomy, or both) plus usual care or usual care alone.	- Intraarterial treatment in patients with acute ischemic stroke was effective and safe when administered within 6 hours after stroke onset.
ESCAPE	- Randomly assigned participants to receive standard care (control group) or standard care plus endovascular treatment with the use of available thrombectomy devices (intervention group).	- The trial was stopped early because of efficacy. - Rapid endovascular treatment improved functional outcomes and reduced mortality.

2.3.2 Mechanical Thrombectomy

Mechanical thrombectomy (MT) treatments, where the thrombus is excised from the vessel, are seeing increasing use and have recently been added to the standard of care for the treatment of acute ischemic stroke (AIS) (Saver *et al*. 2012; Fransen *et al*. 2014; Goyal *et al*. 2016), where it greatly improves outcomes for eligible patients. Mechanical thrombectomy as a treatment method was initially considered if patients presented beyond the recommended time window for rt-PA, if they failed to recanalise using rt-PA or if they had any contraindications to thrombolysis, such as coagulopathy, or a history of intracranial hemorrhage (Fugate & Rabinstein 2015). Recent randomised clinical trials have shown that mechanical thrombectomy is an effective treatment for patients with large vessel occlusion in the anterior circulation and these devices are emerging as the new standard of care (Berkhemer *et al*. 2014).

Thrombectomy involves the delivery of a device by endovascular access to the site of the occlusion and all devices act by engaging with the thrombus in order to remove it and to restore blood flow. The latest generation of mechanical thrombectomy devices includes ‘‘stent-retriever’’ devices, which are retrievable stents (Figure 2.5). A catheter is advanced across the thrombus, and the stent-retriever is unsheathed. The stent component expands and interacts with the thrombus to temporarily restore blood flow. After several minutes, the stent-retriever has engaged with the thrombus, and it is carefully pulled back into the catheter (Akbik *et al*. 2016).

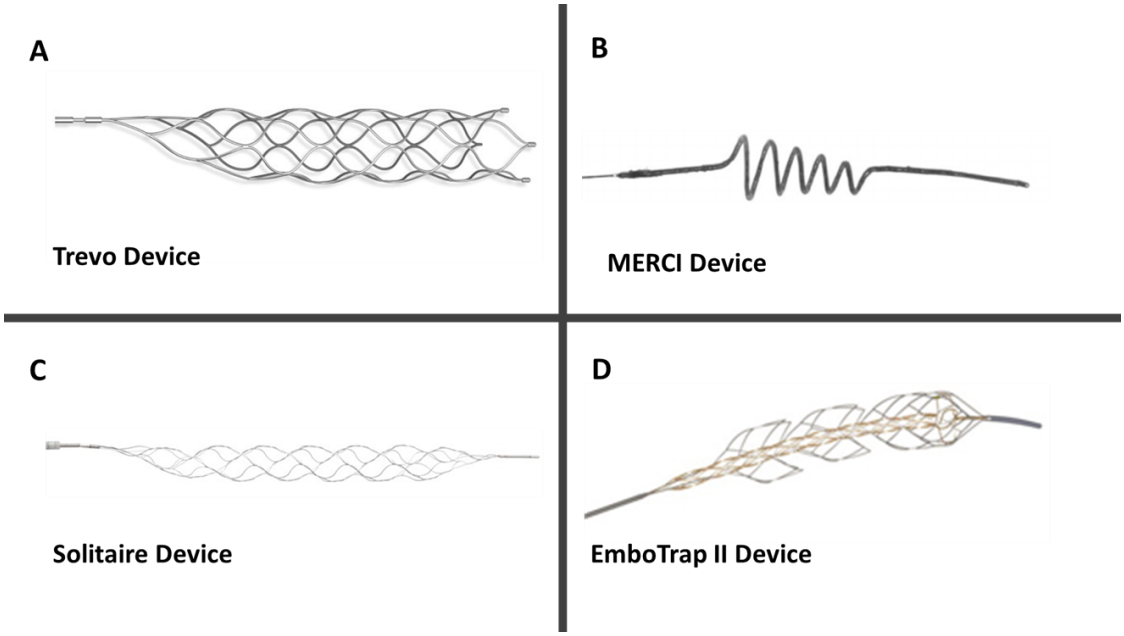

Figure 2.5 Images of various thrombectomy devices. (A) Trevo device. (B) MERCI Device. (C) Solitaire Device. (D) EmboTrap II device.

The majority of patients in the recent randomised trials of endovascular treatment of stroke that established the role of mechanical thrombectomy were treated with stent-retrievers (Campbell *et al.*, 2015; Goyal *et al.*, 2015; Nogueira *et al.*, 2012; Saver *et al.*, 2012). However, an alternative technique of thrombectomy through direct aspiration has been gaining popularity (Fargen *et al*. 2017; Andersson *et al*. 2019), where the clot is removed through suction applied through a large bore distal access catheter at the face of the clot. The direct aspiration technique has been found to produce rapid and reliable recanalisation, but with increased risk of distal embolisation, particularly in the case of red elastic clots (Chueh *et al*. 2016). Therefore although direct aspiration has a faster puncture-to-recanalisation time and thus is more cost-effective than stent-retriever thrombectomy, it may cause an increase in emboli breaking off distally during withdrawal, creating a greater need for bail-out techniques, which in-turn would have an impact on the cost and recanalisation time.

While several clinical trials have shown better recanalisation rates with thrombectomy devices than previous treatment methods, this is not synonymous with better clinical outcomes (Berkhemer *et al.*, 2014; Campbell *et al.*, 2015; Goyal, Demchuk, *et al.*, 2015; Saver *et al.*, 2015). The leading hypothesis to explain this is that patients who benefit from thrombectomy need to be correctly identified. Other possible factors for poor patient outcome may be due to the presence of distal emboli, arterial wall response to the thrombectomy devices, baseline NIH stroke scale, difficulties navigating the device intracranially and beyond the aortic arch, which in turn can affect the time to recanalisation (Flint *et al*. 2010; Kulcsár *et al*. 2010; Menon *et al*. 2011).

Clot debris generated during mechanical thrombectomy or that form *in-situ*, due to local vessel damage during thrombectomy, can result in distal embolisation. Several endovascular techniques such as balloon guide catheter assisted stent-retriever thrombectomy, as well as stent-retriever thrombectomy with aspiration via a distal access catheter, have been used in acute stroke interventions to reduce the risk of distal embolisation (Mayer *et al.*, 2002; Imai *et al.*, 2006; Brekenfeld *et al.*, 2008; Velasco *et al.*, 2016; Lee *et al.*, 2017). According to previous *in-vitro* studies with the use of the thrombin-induced clot models, thousands of micro-emboli were formed during the thrombectomy procedure (Chueh *et al.*, 2013, 2017). It is hypothesised that red emboli have increased risk of embolisation (Chueh *et al*. 2016), however there is little information in the literature on the relationship between clot composition and distal embolisation.

Overall, mechanical thrombectomy helps to overcome some of the limitations associated with rt-PA, in particular the short therapeutic window for treatment and the increased risk of cerebral hemorrhage. There has been rapid evolution in

thrombectomy devices and approaches over the past decade; however, to date, there are no universally accepted standards for device or treatment selection due to very limited scientific information about what combinations of techniques or devices will yield the best outcome (Spiotta *et al*. 2015). With the increasing prevalence of such devices, the need to characterise the mechanical properties of clot material has never been greater as the material undergoes large deformation *in-vivo* during these procedures. Developing a deeper understanding of the device-clot interaction has many potential benefits for the development of future devices.

2.4 Human AIS Thrombi

The recent development of mechanical thrombectomy devices affords the opportunity to examine the composition of fresh thrombi retrieved from AIS patients. Analysis of retrieved thrombi can provide information to enhance our understanding of AIS pathophysiology and can allow correlation between thrombus composition and pre-treatment imaging.

Histopathological examination of AIS thrombi retrieved from AIS has shown the thrombi to be RBC dominant, fibrin dominant or have a mixture of both RBCs and fibrin (Liebeskind *et al*. 2011; Boeckh-Behrens *et al*. 2016). Liebeskind *et al.* (2011) performed a histological analysis of thrombi retrieved from 50 AIS patients. They found that 26% of thrombi were RBC dominant, 44% were fibrin dominant and 30% were mixed. Boeckh-Behrens (2016) also analysed thrombi from 34 AIS patients using histology and displayed a mean RBC, fibrin and WBC content of 32% ± 23%, 60% ± 21% and 8% ± 5% respectively (Boeckh-Behrens *et al.* 2016). Not withstanding that these studies focus on different data classifications, these studies of AIS thrombus

composition have shown a large variation in the RBC and fibrin composition of the retrieved thrombi.

Methods of characterising clot material are described in detail later in this chapter. The results from AIS thrombus studies are extremely informative and have the potential to contribute to larger scale, multi-centre studies and facilitate the standardisation of thrombus characterisation through the development of a central repository for retrieved thrombi. This could potentially further our knowledge on thrombus composition and help identify potential correlations between procedural data pertaining to the case and thrombus properties (De Meyer *et al*. 2017).

2.4.1 Calcified Emboli

With the recent advancements in MT devices, failure in recanalising the occluded vessel is only observed in 10 to 15% of cases (Goyal *et al*. 2016; Berkhemer *et al*. 2014; Campbell *et al*. 2015; Leischner *et al*. 2018) and is often due to difficulties navigating the device intracranially and beyond the aortic arch. Calcified Cerebral Emboli (CCE) represent an uncommon cause of acute ischemic stroke, present in approximately 1-3% of all cases (Walker *et al.*, 2014; Koh *et al*, 2017; Dobrocky *et al.*, 2018), and are usually secondary to cardiac valve surgery or carotid endarterectomy (Walker *et al.*, 2014; Ramírez-Moreno *et al.*, 2017). They consist of one, or several, build up(s) of calcium that embolize in the cerebral vasculature. The presence of dense calcified material enables reliable identification of CCEs using non-contrast CT (Figure 2.6) (Christian *et al.*, 2009; Walker *et al.*, 2014), however they remain among the most difficult clots to recanalise (Walker *et al.*, 2014; O'Cearbhaill *et al.*, 2016), accounting for part of this 10-15% of MT failures. Contemporary treatment of AIS relies on targeting the occlusive clot using medical and endovascular therapy, which exploit the properties of thrombus to lyse and breakdown, or capture

the occlusive material, respectively. Resistant calcified emboli represent a different paradigm, they are neither amenable to fibrinolysis or mechanical engagement in the same way as thrombi (Koh *et al.,* 2017; Dobrocky *et al.*, 2018).

Since CCEs in clinical cases prove difficult to retrieve by endovascular means (Walker *et al.*, 2014; O'Cearbhaill *et al.*, 2016; Koh *et al.*, 2017), analysis of their composition is usually not possible. However, further understanding of the mechanical properties of these clots is required as a different treatment strategy or purpose-designed device appears to be required for this unresolved clinical scenario.

Figure 2.6 Non-contrast CT image of a brain with a calcified embolus present, indicated by the white arrow.

2.5 *In-vitro* Thrombus Analogues

Analysis of thrombus material from human sources can often be expensive and highly regulated, making specimens difficult to obtain. Therefore analogue clot material, that

is formed *in-vitro* from human or animal blood to simulate real blood clots, is an alternative option for the preclinical testing and development of treatment devices (Robinson *et al*. 2013). Such analogue materials present an attractive option because they can be constructed from blood proteins and components present in the clotting cascade, and therefore have a similar chemical structure to native clots. In addition, they are also a useful tool for the investigation and characterisation of clot material properties and their mechanical behaviour as a function of their constituents (Figure 2.7).

The variation in hematologic values from different donors along with the pH and ionic strength of the clotting environment can result in different composition and structure of the analogues (Ryan *et al*. 1999). The mechanical and structural properties of these constructs, such as elastic modulus, permeability, and strength, can also be manipulated by varying the concentrations of fibrinogen, thrombin, factor XIII, fibronectin, platelets, red blood cells and calcium (Ashton *et al*. 2009). This leads to the hypothesis that commonly used clot analogues have varying mechanical properties. However, results from previous experimentation suggest that current analogue materials have been successful at mimicking various clot types. These clot analogues can offer an alternative method to gain a better understanding of clot material behaviour and are gaining popularity among researchers as a more accessible alternative. The growing use of experimental clot models for thrombectomy device testing continues with a goal to provide clinicians with treatment strategies based on laboratory findings; therefore it is critical to have clot models that are clinically representative in terms of their mechanical behaviour as well as compositional features.

Figure 2.7 Gross images of a spontaneously formed clot (left), a red blood cell rich clot (middle), and fibrin rich clot (right) (Duffy *et al.*, 2016) all formed from ovine blood.

2.5.1 Clot Analogues Made with Biological Blood Components

There are many protocols reported in the literature for the manufacture of clot analogues. Common variables include donor species, addition of thrombin or barium sulphate and the variation in red blood cell and fibrin content (Gralla *et al.*, 2006; Marder *et al.*, 2006; Duffy *et al.*, 2016). The variation in hematologic values from different donors, as well as varying concentrations of thrombin, barium, fibrinogen, platelets and calcium, can result in very different clot composition and structure (Ryan *et al*. 1999).

Bovine Blood Models

A common clot analogue model is the Gralla model (Gralla *et al.*, 2006), formed by mixing autologous venous blood with bovine thrombin. To generate the clot analogue, after mixing for 10 seconds, the blood was injected into a silicone tube and left at room temperature for 60 minutes. The clots were then washed in saline solution and left for

a further 20 minutes at room temperature before use. To increase the radiographic absorption of the thrombus analogues, barium sulphate was added to the mixture of blood and bovine thrombin. The barium sulphate was found to provide the analogues with good mechanical stability and good radiopacity. Enhancement of clot visibility by incorporating this radiopaque agent during experimental clot preparation has been helpful in highlighting the challenges of different clot removal techniques.

A similar protocol was adopted by Chueh *et al.* (2011) who formed clot analogues from bovine blood, with and without the presence of thrombin. Bovine thrombin-induced clotting was initiated by simultaneously injecting whole blood/anticoagulant citrate dextrose (ACD) mixture and calcium chloride/thrombin solution into silicone tubing. Without the presence of thrombin, spontaneous coagulation was initiated by mixing the blood/ACD mixture with calcium chloride ($CaCl_2$). This procedure was also followed by Malone *et al.* (2018). Fibrin clots have also been formed by combining bovine fibrinogen and thrombin with calcium chloride (Ashton *et al*. 2009).

Porcine Blood Models

Porcine blood is also commonly used for the preparation of clot analogue material. The protocol by Chueh *et al.* (2011), mentioned previously, has also been used to make porcine clot analogues, by mixing porcine blood with bovine thrombin and barium sulphate. A similar procedure was adopted by Krasokha *et al.* (2010) to prepare samples for mechanical testing.

A more simplified approach was used by Schmitt *et al.* (2011) where fresh porcine whole blood (WB) was coagulated using $CaCl_2$ within 16 hours of collection. Similarly, Huang *et al.* (2013) used fresh porcine blood and clot analogues were formed within 12 hours of collection. EDTA (ethylenediaminetetraacetic acid) was

added immediately to the blood to prevent coagulation. The blood was then passed through the sponge to filter out impurities. The WB was centrifuged and washed twice with a saline buffer solution to separate the erythrocytes from the plasma. WB samples with varying hematocrits were then obtained. $CaCl_2$ was added to artificially induce blood coagulation.

van Kempen *et al.* (2015) formed clots from porcine WB, platelet-rich plasma (PRP) and platelet-poor plasma (PPP). It has been observed that clots made from platelet-rich plasma (PRP) generate a bulk contractile force that begins shortly after the clot is formed and increases over minutes to hours to a maximum of about 1500 to 4500 dyn/cm (Cines *et al.*, 2014). In the van Kempen *et al.* (2015) method, the blood was collected in a beaker with sodium citrate to prevent clotting, and kept at room temperature. The WB was centrifuged at a low spin to obtain the PRP. The PRP was then centrifuged at a high spin to obtain the PPP. Clotting was initiated by adding clotting buffer (composed of $CaCl_2$, human thrombin and HEPES) to the WB, PRP or PPP and the solutions were mixed gently.

Asakura *et al.* (2007) adopted another approach, collecting porcine blood without heparin. The blood was then added to citric acid to remove calcium, and the mixture was centrifuged. The plasma was then extracted and mixed with lactic acid Ringer's solution and stirred. Finally a fibrin clot was formed.

Other Animal Models

Ovine blood has been demonstrated to be a suitable substitute for human blood for coagulation studies (Siller-Matula *et al.*, 2008) and the corresponding blood clots have been shown to be histologically similar (Duffy *et al*. 2016; Gunning *et al*. 2016). Duffy *et al.* (2016) used citrated ovine blood for the preparation of seven different clot

analogues with varying RBC and fibrin content. The WB was centrifuged and separated into the plasma, buffy layer and erythrocyte-rich layer. The plasma and erythrocytes were then harvested separately and recombined in controlled ratios to give clot analogues with varying compositions – 0%, 5%, 40% and 80% RBC content (clot type G, E, D & B respectively). $CaCl_2$ was then added to the solution to reverse the action of the sodium citrate and the samples were incubated at 37°C for 30 minutes to initiate clotting.

One of the clot models (clot type C) was prepared using thrombin and platelets to promote clot retraction. Prostaglandin E1 solution was added to the citrated blood prior to centrifugation to minimize the platelet activation during centrifugation. The extracted buffy coat and plasma were subsequently mixed with RBCs and adenosine diphosphate was added to reverse the effects of the prostaglandin E1. This study also formed a whole blood clot (clot type A). This clot analogue was formed by spontaneous coagulation of the whole blood after it was collected in the syringe. The sample was left to clot for 12 hours at room temperature. Clot type F was a heterogeneous clot formed by adding calcium chloride to WB and by allowing it to form under dynamic conditions in a Chandler Loop.

Murine blood has also been used in the formation of clot analogues. Slaboch *et al.* (2012) centrifuged citrated murine blood at a low spin. The PRP layer was then collected and brought to 37°C in a water bath. The thrombus was formed by adding $CaCl_2$ and thrombin to the PRP. The clot analogue was left at room temperature for 2 hours until fully coagulated before testing.

Human Clot Models

Many *in-vitro* clot models have also been formed using human blood collected from donors. Krasokha *et al.* (2010) and Chueh *et al.* (2011) both adapted their previously discussed protocols to form clots using human blood with the addition of human thrombin and barium sulfate. Similarly, Liebig *et al.* (2008) added bovine thrombin to human blood to form their samples. Krueger *et al.* (2004) allowed human blood samples to clot spontaneously without any thrombogenic substances.

Kim *et al.* (2014) prepared fibrin clots by pooling human citrated PPP with $CaCl_2$ and human thrombin. The samples were allowed to form for 30-100 minutes at room temperature. Fibrin clots were also formed by Shah and Janmey (1997) who obtained human blood from healthy volunteers. The blood samples were centrifuged at a slow spin of 110 g for 15 minutes to remove the PRP. The PRP was then spun at a high spin at 1000 g for 15 minutes to yield the PPP. Gel-filtered platelets were prepared from the PRP and were stored in platelet buffer at 37°C for up to 2 hours. Human fibrinogen was also partially purified from the PPP by adding saturated ammonium sulphate and incubating at 4°C for 1 hour. The precipitate was then centrifuged at 100 g for 30 minutes and the pellet was re-suspended in tris-buffered saline. Human fibrinogen was also used by Saldívar *et al.* (2002) to create fibrin clots. The fibrinogen was completely depleted of plasminogen and von Willebrand factor, and subsequently diluted with HEPES-buffered saline. Fibrin gels were then formed in plastic moulds by quickly mixing the fibrinogen with diluted thrombin and allowing them to set for 2 hours at 37°C.

Clot Models Formed Under Dynamic Conditions

Another experimental approach to *in-vitro* thrombogenesis is Chandler's loop technique, whereby the clot is formed under dynamic flow conditions in a closed loop. This technique has been found to produce a more heterogeneous clot (Krueger *et al*. 2004; Campbell *et al*. 2015).

Duffy *et al.* (2016) used a modified version of this approach to prepare one of their clot analogues (clot type F). Silicone tubing was mounted on a multi rotator device and partially filled with citrated ovine whole blood. $CaCl_2$ was injected into the tubing and the ends of the tubing were then fixed, thus forming a closed loop. The tubing was rotated at a rate of 25 rpm for approximately 1 hour. A similar method was adopted by Shao *et al.* (2014) forming clots from swine blood mixed with barium sulphate and bovine thrombin. The mixture was injected into a polyvinyl chloride (PVC) tube, ensuring there were no air bubbles. The tube was coiled using a connector and set into a Plexiglas ring rotation unit, which was mounted on a rotating shaft of an MR-16 blood clot detector and slowly rotated for 15 minutes at 15 rpm. Poole (1959) also produced clots using a similar modified Chandler method from citrated human, bovine, murine and leporine blood mixed with $CaCl_2$.

2.5.2 Thrombus Analogues Made of Polymeric Materials

Clot analogues have also been produced from polymeric materials. Robinson *et al.* (2013) prepared moderately stiff synthetic clots using polyacrylamide. The clots were used to evaluate the clot capture efficiency of various vena cava filters in a physiological venous flow loop. These devices were also tested using clots formed *in-vitro* from both human and ovine blood. This study found that although the polymeric clots were more convenient and easier to use than the clots formed from blood, there

were differences in shape, density and elasticity, and this in turn affected the device performance.

Synthetic clot material formed by combining polyacrylamide and alginate (PAAM-Alg) with a crosslinking agent was tested by Merritt *et al.* (2018). Rheometry was used to compare the shear and dynamic moduli of the synthetic polymeric clots with clots formed *in-vitro* using human blood. The PAAM-Alg analogues were found to closely mimic the clots formed using human blood and were easily adjustable to mimic various thrombi classifications.

2.5.3 Aging and Storage

There are few reports in the literature on the effects of storage conditions and aging on clot material. It is believed that aged clot material behaves differently to fresh clot material. Previously published experiments have been carried out on clot material with substantial variations in age, from 1 hour to 19 days (Krasokha *et al*. 2010; Krueger *et al*. 2004). Krasokha *et al.* (2010) found that aged human thromboemboli had reduced elasticity when compared to soft, highly elastic fresh red thromboemboli. These fresh thromboemboli are also less likely to fragment when compared to aged specimens.

Krueger *et al.* (2004) investigated the effect of clot aging and storage temperature on clot samples. Spontaneous and thrombin-induced samples were aged for 1 or 5 days at 4°C or 21°C. The results from the study show that thrombus type can affect the results of the thrombectomy procedure and clot stability appeared to decrease with age. It was hypothesised that this was due to cell lysis. Storage temperature as a singular factor was not found to affect the results and only had an effect in combination with other parameters tested. Further examination of the effect of storage conditions

and aging of the clot material is necessary to fully understand the impact on clot mechanical behaviour.

2.5.4 Comparison with Human Thrombi

Analog clot material is becoming increasingly prevalent in preclinical testing of devices as a cheaper and more readily available alternative to human clot tissue (Johnson *et al.*, 2017). However, a limitation of this material is the fundamental difference between the clot analogues formed *in-vitro* and the complex human material that they are intended to represent (Chueh *et al*. 2011).

Human thrombi have been found to be very heterogeneous, with large variation in structure and composition (Chueh *et al*. 2011; Merritt *et al*. 2018; Marder *et al*. 2006; Liebeskind *et al*. 2011; De Meyer *et al*. 2017; Kirchhof *et al*. 2003). Most analogue clot material has a homogeneous composition, though some heterogeneous clots have been formed (Merritt *et al*. 2018; Chandler 1958; Kan *et al*. 2010). A study by Chandler (1958) proposed forming the clot samples in a closed loop in order to simulate the physiological blood flow environment. Clots formed using this method are found to have a fibrin rich pattern and are firmer and more elastic when compared to clots formed under static conditions, which are generally RBC dominant. This has been shown to increase heterogeneity (Duffy *et al.*, 2016).

There are limitations however to the previously described analogue clot models. The addition of barium sulphate can alter the clot mechanical properties by significantly decreasing clot elasticity (Gralla *et al.*, 2006; Krasokha *et al.*, 2010). In addition, the histological characteristics of the analogues have been found to be inconsistent with thrombi from AIS patients. Research on the morphology of AIS thrombi has revealed that no two thrombi are histologically identical, with ranging fibrin and RBC

composition (Marder *et al*. 2006; Liebeskind *et al*. 2011; Kim *et al*. 2015). Although it is not possible to reproduce the morphological characteristics of all thrombi, clot analogues have been proposed with a range of compositions that are clinically relevant and histologically similar to thrombi removed from AIS patients (Chueh *et al.* 2011; Duffy *et al.* 2016; Marder *et al.* 2006). Another limitation of analogue material is the absence of calcified material, although calcifications in AIS thrombi are rarely observed suggesting that it is not a common pathogenic process in AIS (Chueh *et al*. 2011).

Although clot analogues do not fully accurately mimic the complex structural nature of human specimens, they are still an extremely valuable tool for pre-clinical evaluation of thrombectomy devices and have been proven to predict clinical performance of various treatment strategies. These materials are becoming more prevalent as material from human sources are often expensive and highly regulated, making specimens difficult to obtain (Johnson, Duffy, Gunning, Gilvarry, J.P. McGarry, *et al*. 2017).

Clot material has been developed *in-vitro* with varying compositions and mechanical properties to mimic the large range of stiffness and elasticity of AIS thrombi found *in-vivo*, to assess the effect of clot composition on device performance (Chueh *et al.* 2011; Duffy *et al.* 2016; Malone *et al.* 2018). Clot analogues are often used for *in-vitro* occlusion models for training in interventional techniques. The analogue material may also facilitate the future development of diagnostic imaging technologies to visualise clot composition *in-vivo*.

2.6 Characterisation of Thrombus Material

Thrombus mechanical behaviour and its characteristics are strongly dependent on the thrombus structural and molecular origins (Krasokha *et al*. 2010), as well as the composition of the thrombus. Multiple investigations into these basic structural origins have been reported.

As previously mentioned, clot properties can differ greatly depending on a variety of factors; the prevalence of fibrin, platelets and other blood components, tissue factor or thrombin levels and many other environmental conditions (Weisel, 2008). For example, fibrinogen concentration has been found to influence clot mechanical and functional properties; high levels of fibrinogen can result in improved mechanical stability and improved interaction of platelets with the fibrin network (Dempfle *et al*. 2008). Carr and Carr (1995) showed that an increase in fibrinogen content and a decrease in calcium content resulted in an increased elastic modulus of thrombus mimics. Similarly Ryan *et al.* (1999) concluded that these factors also decreased fibre length and diameter, thus demonstrating that clot types can vary significantly depending on their constituents. Blood clots have also been found to be viscoelastic polymers with both viscous and elastic properties (Weisel, 2008; Weisel, 2010).

2.6.1 Mechanical Characterisation

A variety of mechanical testing studies on thrombus material have been reported as illustrated in Table 2.2 Early studies of the mechanical properties of blood clots date back to 1940s and 1950s with the work of J.D. Ferry and co-workers (Ferry & Morrison 1944), and considerable work still continues today. For the types of thrombus material that have been studied, the material has generally been found to be incompressible, nonlinearly elastic, heterogeneous, and is generally assumed to be isotropic (Wang *et al*. 2001; Gasser *et al*. 2008).

Table 2.2 Summary of experimental characterisation experiments used to determine the mechanical behaviour of thrombus material.

Author	Clot Type	Aim of Study	Test Method
Di Martino *et al.* (1998)	*In-vivo* Intraluminal thrombus (ILT) removed from human patients	To determine the biomechanical and geometrical parameters of endoluminal thrombus	Tensile testing
Gasser *et al.* (2006)	*In-vivo* Intraluminal thrombus (ILT) removed from human patients	To determine failure data for intraluminal thrombus	Tensile testing
Vande Geest *et al.* (2006)	*In-vivo* Intraluminal thrombus (ILT) removed from human patients	To determine the biaxial mechanical behaviour of ILT	Biaxial testing
O'Leary *et al.* (2014)	*In-vivo* Intraluminal thrombus (ILT) removed from human patients	To determine the biaxial mechanical behaviour of ILT	Biaxial testing
Teng *et al.* (2015)	*In-vivo* Intraluminal thrombus (ILT) removed from human patients	To determine layer- and direction-specific material properties, extensibility and ultimate material strength of AAA	Tensile testing
Wang *et al.* (2001)	*In-vivo* Intraluminal thrombus (ILT) removed from human patients	To determine the mechanical properties and microstructure of ILTfrom AAA	Tensile testing
Krasokha *et al.* (2010)	*In-vitro* clots formed from human and porcine whole blood	To determine compressive and tensile strength of aged human and animal clots	Tensile testing Compression testing
Saldívar *et al.* (2002)	*In-vitro* clots generated from human fibrinogen and thrombin	To determine the relationship between tensile destruction and partial proteolysis of fibrin clots	Tensile testing
Xie *et al.* (2005)	*In-vivo* clots formed in the IVC of rats	To determine Young's modulus of ex vivo thrombus	Compression testing Ultrasound elastography
Chueh *et al.* (2011)	*In-vitro* clots formed from bovine, porcine and human whole blood *In-vivo* thromboemboli removed from patients with AIS	To determine the mechanical properties and composition of thromboemboli from clinical cases and compare them with clot analogues	Compression testing
Ashton *et al.* (2009)	*In-vivo* Intraluminal thrombus (ILT) removed from human patients	To determine the viscoelastic properties of thrombus material	Compression testing
Kim *et al.* (2014)	*In-vitro* clots formed from human platelet-poor plasma mixed with calcium chloride and thrombin	To establish correlations between structural changes and mechanical responses of fibrin networks exposed to compressive loads.	Rheological compressive loads
van Dam *et al.* (2006)	*In-vivo* Intraluminal thrombus (ILT) removed from human patients	To determine whether the linear viscoelastic properties of an abdominal aortic aneurysm thrombus can be determined by rheometry	Shear rheometry
van Kempen *et al.* (2015)	*In-vitro* clots formed from porcine whole blood, platelet-rich plasma and platelet-poor plasma	To develop a constitutive model describing the nonlinear viscoelastic properties of the fibrin network, using experimental results	Large amplitude oscillatory shear deformation
Schmitt *et al.* (1997)	*In-vitro* clots formed from porcine whole blood	Study mechanical behaviour and determine the viscoelastic properties of porcine clot samples	Dynamic ultrasound elastography
Slaboch *et al.* (2012)	*In-vitro* clot material produced from platelet-rich murine plasma	Determine the elastic modulus of murine thrombus using the elastic contact theory	Nanoindentation
Gunning *et al.* (2016)	*In-vitro* clots produced from ovine whole blood *in-vitro*	To determine if there is a relationship between clot composition and the friction which might contribute to resistance to clot removal	Friction Testing
Huang *et al.* (2013)	*In-vitro* clots formed from porcine whole blood	To estimate the viscoelastic modulus of a thrombus using an ultrasonic shear-wave approach	Shear-wave dispersion Ultrasound vibrometry

2.6.1.1 Tensile Testing

In-vivo Thrombus

Tensile testing of thrombus material has been widely used to determine its tensile strength and elastic modulus. Since thrombus material is quite soft in nature, it can be quite difficult to grip for testing. Therefore, various techniques to combat the slipping of the samples during testing have been developed. Di Martino *et al.* (1998) performed uniaxial tensile tests on aortic thrombus specimens that were removed from six male patients undergoing elective resection of abdominal aortic aneurysm (AAA). A custom designed die was used to cut tensile dog-bone shaped specimens from thrombus material (Figure 2.8 A), which encourages rupture away from the grips. The results from this research showed a linear load–displacement relationship for each of the samples.

Similar results were obtained by Gasser *et al.* (2008) who carried out tensile testing on intraluminal thrombus (ILT) tissue also removed from AAA patients (Figure 2.8 B). Their goal was to determine the ultimate tensile strength and fatigue strength of the material, comparing the luminal, medial and abluminal layers of the tissue. The luminal layer is the layer that is in contact with the blood flow in the vessel, while the abluminal layer is in contact with the vessel wall. The medial layer resides between them. Similar dog-bone shaped specimens were used and the test was performed until failure. The results from this study again depict an almost linear relationship of the load with respect to specimen elongation, indicating that the ILT exhibits a linear stress–strain behaviour. Vande Geest *et al.* (2006) also found that the ILT material displayed an almost linear response under biaxial tensile loading. These results are quite unusual for biological tissues (Polzer *et al.* 2012) and may be due to the strain

rates at which the samples were tested. However, more recent research has found that the material exhibits nonlinear elastic behaviour (O'Leary *et al*. 2014; Teng *et al*. 2015a; Wang *et al*. 2001). O'Leary *et al.* (2014) found that the ILT samples they obtained and tested biaxially exhibited mild non-linearity, while the uniaxial tensile testing completed by Teng *et al.* (2015) on similar samples showed that the material clearly demonstrated non-linear elastic behaviour and that the material was highly extensible.

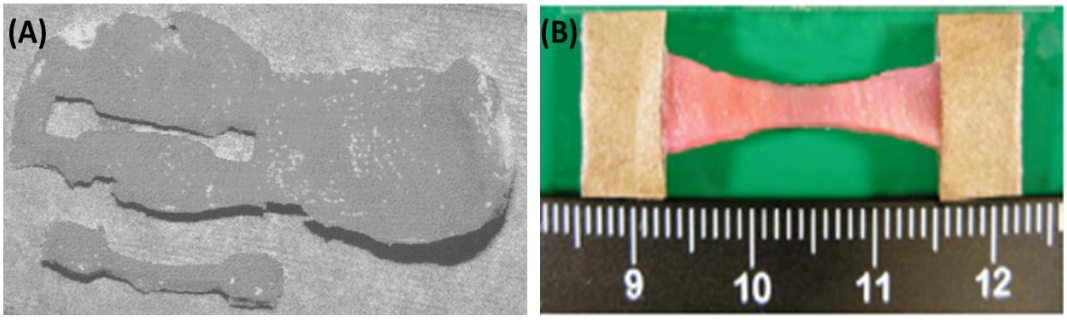

Figure 2.8 Dog-bone specimens for tensile testing cut from intraluminal thrombus by (a) Di Martino *et al*. (1998) and (b) Gasser *et al.* (2008).

In-vitro Thrombus

Krasokha *et al.* (2010) investigated the tensile strength of clot analogues, produced *in-vitro* from porcine blood and combined with thrombin and barium sulphate. The experimental setup for the tensile tests was custom designed and built; the specimen was positioned between the two sample holders and fixed by pinch clamps. The authors found that the analogue material reached high levels of stress and strain, approximately 9 kPa and 240% respectively, before failure. The presence of heparin in the clot analogues was found to increase these values to a stress of 10 kPa and a strain of 300%, although a mechanism for this was not described. The findings of Brown *et al.* (2009) from their extension testing of fibrin clots, formed from purified

human fibrinogen further supported these results. The samples were stretched to three times their relaxed length before failing.

Similar failure strains were observed by Saldívar *et al.* (2002) from tensile testing of their clot analogues formed *in-vitro* from thrombin and human fibrinogen. The unique test set up used a lever mechanism to test the sample in which a calibration weight was placed on the holder, and the vertical displacement of the lever was monitored. It was found that mechanical failure was a consequence of fibrinolytic activity due to an increased concentration of plasmin. Results from these experiments found that the sample showed progressive recovery over time after the removal of the tensile load, indicating a viscoelastic response.

Although many studies have investigate the tensile properties of clot material, it can often prove to be quite challenging due to the fragile nature of the clot material, and can often result in the sample tearing/rupturing at the grips (Krasokha *et al*. 2010; Malone *et al*. 2018), a feature that is common when testing soft biological materials. Therefore, developing a reliable test method that is suitable to test the broad range of clot types is essential when examining the mechanical behaviour of clot material.

2.6.1.2 Compression Testing

In-vivo Thrombus

As mentioned, mechanical testing of soft tissues, such as clot material, can be quite challenging. Therefore, very soft tissues are often tested in compression to determine their mechanical behaviour. Also, thrombus material can experience compressive deformation *in-vivo* due to physiological conditions, such as blood flow/pressure, vasoconstriction, and clot retraction, therefore it is important to characterise the compressive mechanical behaviour specifically.

Xie *et al.* (2005) developed a customised measurement device to determine the mechanical properties of thrombus, formed *in-vivo* in the inferior vena cava (IVC) of rats, under compression. From the results, the stress had a nonlinear relationship with the strain. Chueh *et al.* (2011) presented similar results. They tested human thromboemboli, obtained from patients with AIS using aspiration devices and from carotid atherosclerotic plaques harvested during endarterectomy. They found that the material demonstrated a small increase in stress at low strains and a large increase in stress when strains above approximately 80% were experienced by the material, which is the expected soft-tissue response. It was also found that the aged thromboemboli lacked elasticity compared to the soft, highly elastic fresh red thromboemboli.

Compression testing has also been used to investigate the viscoelastic properties of thrombus material. Ashton *et al.* (2009) performed stress-relaxation tests by applying and holding a 5% compressive strain for 20 min, and measuring the corresponding decrease in compressive load over time. Strains of 10 and 15% were also subsequently applied for 20 minutes each. Both human ILT samples and clot analogue samples were tested. The ILT specimens were procured from the elective open AAA repairs of six patients and were placed in an isotonic phosphate buffered solution (PBS), immediately after extraction from the aorta and stored at 4°C until testing. Gentle physical manipulation was used to separate the ILT specimens into three layers based on relative position and colour: abluminal, medial, and luminal. The clot analogues were formed *in-vitro* from bovine fibrinogen and thrombin and calcium chloride. This study showed that the load on the material samples decreased over time when held at a constant strain, indicating that the clot material is viscoelastic.

In-vitro Thrombus

Similarly, compression testing has been used to determine the mechanical properties of clot analogues. Krasokha *et al.* (2010) performed unconfined compression testing of clots formed *in-vitro* using porcine and human whole blood and investigated the effect of the addition of barium sulphate. It was found that both the porcine and human clot analogues demonstrated increased stiffness due to the addition of barium sulphate. These results were validated by Chueh *at al.* (2011), who also determined that the addition of barium sulphate greatly reduced the elasticity of clot analogues formed from bovine, porcine and human whole blood. This was supported by a notable difference in clot microstructure in the clots with added barium sulphate, as there is evidence that the metallic particles enhance the number and stability of the branch points, which may account for the increased stiffness. Malone *et al.* (2018) showed that analogue stiffness was also increased with increased thrombin concentration.

Chueh *et al.* (2011) also compared the mechanical behaviour of thromboemboli removed from stroke patients and laboratory embolus analogues under compression. The results indicated that thrombin-induced clot analogues made with human blood *in-vitro* were similar to cerebral thromboemboli retrieved from patients with AIS, in terms of elasticity and stiffness. There was no significant difference in stiffness between thrombin-induced bovine or porcine *in-vitro* analogues and clot samples collected by carotid endarterectomy.

Kim *et al.* (2014) also carried out compression testing to determine the mechanics of fibrin clots under compression. Fibrin clot analogues were prepared by mixing human citrated platelet-poor plasma (PPP) with calcium chloride and human thrombin. The results from this experiment showed that an increase in both the initial clot stiffness

and compression rate resulted in a steeper growth of normal stress. This study also investigated the origin of the non-linear rheology of the fibrin-networks under compression. The structural rearrangements of the 3D fibre networks under compressive loading were analysed using confocal microscopy and rheological measurements. Visual observations of the 3D networks displayed buckling of the fibrin-fibres along the direction of the compressive force. Fibre bending was also found to increase with compressive force and the deformation of the individual fibres depended greatly on their orientation in the network. Saldívar *et al.* (2002) also found that fibrin clots formed *in-vitro* also showed plastic deformation under compressive loading as cross-linked clot samples did not recover or spring-back (Figure 2.9). This suggests that fibre integrity is essential for sustaining clot integrity when samples experience large levels of stress both *in-vitro* and *in-vivo.*

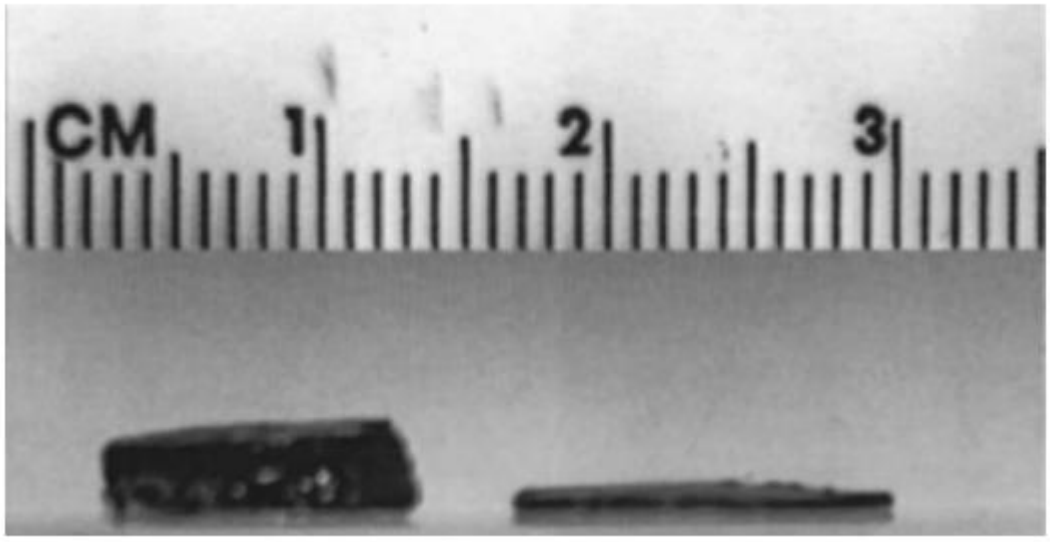

Figure 2.9 Macroscopic view of the effects of normal compressive stress on fibrin clots. The image shows the lateral view of the clots before (left) and after (right) an unconfined compression experiment. Both samples had the same original volume (Saldívar *et al.* 2002).

2.6.1.3 Other Test Methods

A number of other characterisation techniques have been used to study clot material. Rheometry is one such technique that has been adopted by many studies (Burghardt *et al*.; Fukada *et al*. 1984; Kim *et al*. 2014). van Dam *et al.* (2006) performed shear rheometry using a parallel plate rheometer to determine the storage (G') and loss (G'') modulus of thrombus samples removed from patients undergoing AAA repair. A limitation of this study is that the test requires flat specimens that must also have the same diameter as the rheometer parallel plates, to ensure accurate results are achieved. However, this study did indicate that the determination of thrombus material properties is possible using rheometry.

van Kempen *et al.* (2015) also used rheology and large amplitude oscillatory shear (LAOS) deformations to study the effect of red blood cells, platelets and fibrin on the non-linear viscoelastic properties of clots analogues, formed form whole porcine blood (WB), platelet-rich plasma (PRP) and platelet-poor plasma (PPP). The rheology results indicate that clots formed from PRP had the highest stiffness, followed by clots formed with WB and PPP respectively. This behaviour can be explained by platelet contraction, which causes the increased stiffness of the network. The high volume of RBCs in the WB prevents this contraction. This also explains the difference in clot behaviour, between clots formed from PRP and WB, during the LAOS experiments as the fibrin network is stiffer when there are no RBCs present, as they have been found to prevent regular network formation and platelet binding (van Kempen *et al.*, 2015). Similar rheology results were described by Riha *et al.* (1999). Clots were found to have a decreased elastic modulus when a greater amount of red blood cells were present, and clots made from PRP had the highest values of elastic moduli. Alternatively, Schmitt *et al.* (2011) implemented a dynamic ultrasound elastography

technique to evaluate the storage and loss moduli of analogue thrombus material formed *in-vitro* using porcine whole blood. This technique investigated the mechanical behaviour of thrombus by measuring its motion response to propagating shear waves.

Although rheology has been commonly used in the literature for the investigation of clot mechanical properties, compression testing was selected in this thesis as it allowed for the experimental results to be compared to compression data for previously tested human thromboemboli. Similarly, the compression test set-up in this thesis also allowed for the loading-unloading hysteresis and stress-relaxation of the material to be investigated for a range of clot types.

Clot analogues have been manufactured using a variety of different protocols which can have many variables, such as donor species, concentration of thrombin and the addition of barium sulphate as a radiopaque additive (Liebig *et al.*, 2008; Krasokha *et al.*, 2010; Chueh *et al.*, 2011; Duffy *et al.*, 2016) and the effect of these variables on the mechanical behaviour of the clot analogues have been investigated. However, clot composition can also differ substantially with varying red blood cell (RBC) and fibrin content (Marder *et al*. 2012; Liebeskind *et al*. 2011), and to date, only a few studies have investigated the effect of clot composition on mechanical behaviour of the material.

Nanoindentation was performed by Slaboch *et al.* (2012) to determine the mechanical properties of murine clot material produced from PRP *in-vivo*. This test method has many advantages over other test methods as it can obtain small scale measurements: indenter tips are easily customisable and it obtains high resolution load and displacement measurements. The moduli values for the clot material were found to be

within the range for soft materials. Similarly, Weafer *et al.* (2019) investigated the indentation behaviour of clot analogues with varying hematocrit, by subjecting the clot material to indentation forces and embedding times representative of those experienced during thrombectomy. The indenter tip was designed to have the approximate profile of a single strut of a thrombectomy stent-retriever device, and the depth of the strut indentation, in addition to the degree of device-clot integration, following an embedding time of 5 minutes, was correlated to the hematocrit. The study found that greater indentation was identified in clots with higher RBC content, but with an increased level of fibrin rupture, suggesting an increased propensity for fragmentation. Additional embedding time was also found to improve strut integration, especially in fibrin-rich clots, through the mechanism of fibrin stretching.

The resistance to sliding (friction) of clot material as a function of composition was also studied by Gunning *et al.* (2016). During the thrombectomy procedure, the clot experiences sliding contact along the inside of the vessel and/or the inside of the catheter. The aim of this study was to investigate if clot composition may contribute to friction and the resistance to clot removal. Clot samples were formed *in-vitro* with varying RBC content by separating the plasma and erythrocytes from ovine plasma and recombining them in controlled ratios to give clots with varying composition – 0%, 5%, 20%, 40% and 80% RBCs. The study found that fibrin-rich clots had a significantly larger coefficient of friction than clots with high RBC content, which may contribute to fibrin-rich clots requiring more retrieval attempts (Vidmar *et al.* 2015).

Although extensive experimentation of thrombus material has been carried out by the aforementioned previous studies, the viscoelastic behaviour as a function of clot composition is still not fully understood. Experiments have been performed to

determine if clot material exhibits viscoelastic behaviour (Saldívar *et al.*, 2002; Ashton *et al.*, 2009; van Kempen *et al.*, 2015). However, the time-dependence and recovery of the material has not been adequately established.

2.6.2 Histological Characterisation

The efficacy of removing an occluding clot during mechanical thrombectomy has been shown to be influenced by histologic characteristics. Therefore clot composition has been assessed using various histological methods (Yuki *et al.* 2012; Chueh *et al.* 2011; Duffy *et al.* 2016) to determine a potential relationship between thrombus histology and clot stability. Clots with high red blood cell content have been associated with a high rate of successful intra-arterial thrombectomy (Shin *et al*. 2018a); whereas fibrin-rich clots are often resistant to mechanical thrombectomy, resulting in an extended procedure time and unfavourable clinical outcome.

The most commonly used staining methods are Martius Scarlet Blue (MSB) (Figure 2.10 A and C) and haematoxylin–eosin staining (H&E) (Figure 2.10 B and D) (Chueh *et al.*, 2011; Duffy *et al.*, 2017; Duffy *et al.*, 2019). H&E highlights nuclei in blue-black, RBCs in orange red and fibrin in deep pink. MSB stains fresh fibrin red, aged fibrin blue, and RBCs yellow. Immunostaining is required to identify platelets, T-cells and von Willebrand factor (Nouh *et al*. 2017; De Meyer *et al*. 2017). However MSB staining has recently been found to identify platelet-rich regions with the clot, by staining the area blue (Fitzgerald *et al*. 2019).

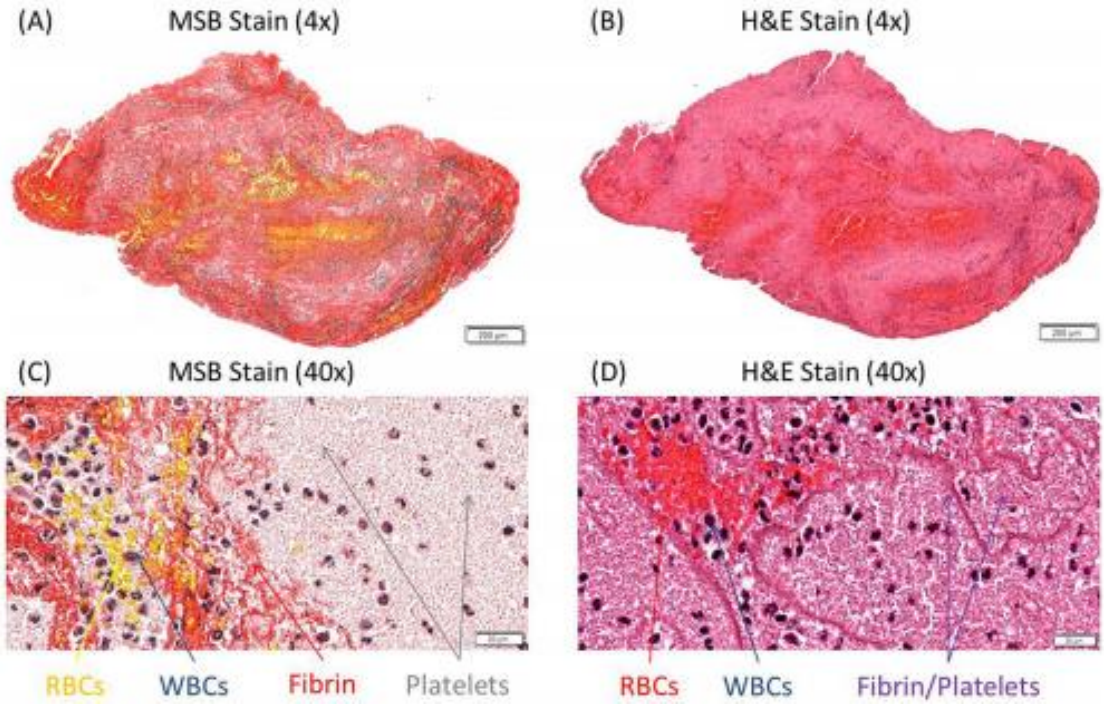

Figure 2.10 Comparison of Martius Scarlet Blue (MSB) and H&E stains in an acute ischemic stroke clot. (A) and (C) are examples of an MSB stained slide from a clot demonstrating the presence of red blood cells (yellow), white blood cells (blue), fibrin strands (red), and platelets (grey, identified by black arrows). (B) and (D) are examples of an H&E-stained slide from the same clot demonstrating the presence of red blood cells (red), white blood cells (blue), and fibrin/platelets (purple) (Fitzgerald *et al*. 2019).

Inflammatory cells such as neutrophils have recently been found to have impacts on clot stability and can be detected with neutrophil elastase staining (Kaesmacher *et al*. 2017). Other methods such as Elastica van Gieson staining stains nuclei black-brown (Boeckh-Behrens *et al*. 2016; De Meyer *et al*. 2017) and van Kossa is used to stain for calcium. Clinical samples are stained with Gomori methenamine silver for fungus (Marder *et al*. 2006). For quantitative measurements of clot components, the stained slide is imaged at low magnification and the clot image is subjected to segmentation to differentiate each clot constituent.

2.6.3 Scanning Electron Microscopy (SEM)

The mechanical properties of clots have been compared to other materials with similar behaviour that are better understood. One such material is lightly cross-linked rubber as it exhibits similar viscoelastic properties to thrombus material (Weisel 2010). Although the mechanical behaviour of these materials is similar, their structure is very different. It is widely known that clots are made up of coarse, three-dimensional networks consisting of fibres that are branched with each other at various points (Weisel, 2008). This differs from the random-coil network of thin, highly flexible strands typically found in rubbers. This fibrin network is a major structural component, that largely determines the mechanical stability, shape, strength and flexibility of the clot (Weisel 2004; Xu *et al*. 2012). Properties such as clot stiffness can also be explained by other microstructural characteristics which include fibre thickness, fibre concentration and branch point density (Krasokha *et al*. 2010). However, calculations of branch point density from clot stiffness can be inaccurate by up to six orders of magnitude, indicating how little we understand about this material (Weisel, 2008; Weisel, 2010).

The fibrin structure can vary significantly due to a number of variables, including pH, ionic strength and concentrations of thrombin, fibrin and calcium present during gelation (Ryan *et al*. 1999; Wolberg & Campbell 2008). Thrombin concentration in particular influences both the fibre thickness and density of the clot. Low thrombin has been found to produce thick loosely-woven fibrin strands, whereas high thrombin content has been found to create a dense network of thin fibrin strands. These varying structures have been shown to affect both the permeability and stability of the clot material (Wolberg & Campbell 2008). In general, higher thrombin concentrations are associated with the formation of stiffer clots (Kaibara & Fukada 1971).

SEM has also been utilised to visualise the polyhedral-shaped RBCs in contracted blood clots. As described earlier, RBCs take on this unique shape to allow for more efficient packing within the fibrin network (Figure 2.11 A-B), thus forming an impermeable barrier. Previous studies have shown that these polyhedrocytes are compacted to the core during clot contraction, with platelets and fibrin redistributing towards the outside of the clot (Figure 12.11 C-D) (Cines *et al*., 2014; Peshkova *et al*., 2017; Tutwiler *et al*., 2016). A fibrous outer shell has also been reported by Di Meglio *et al.* (2019) (Figure 2.11 C). They reported an outer shell made of densely compacted components that included fibrin and aggregated platelets observed when examining AIS thrombi under SEM and suggest that this can impact the effectiveness of rt-PA treatment.

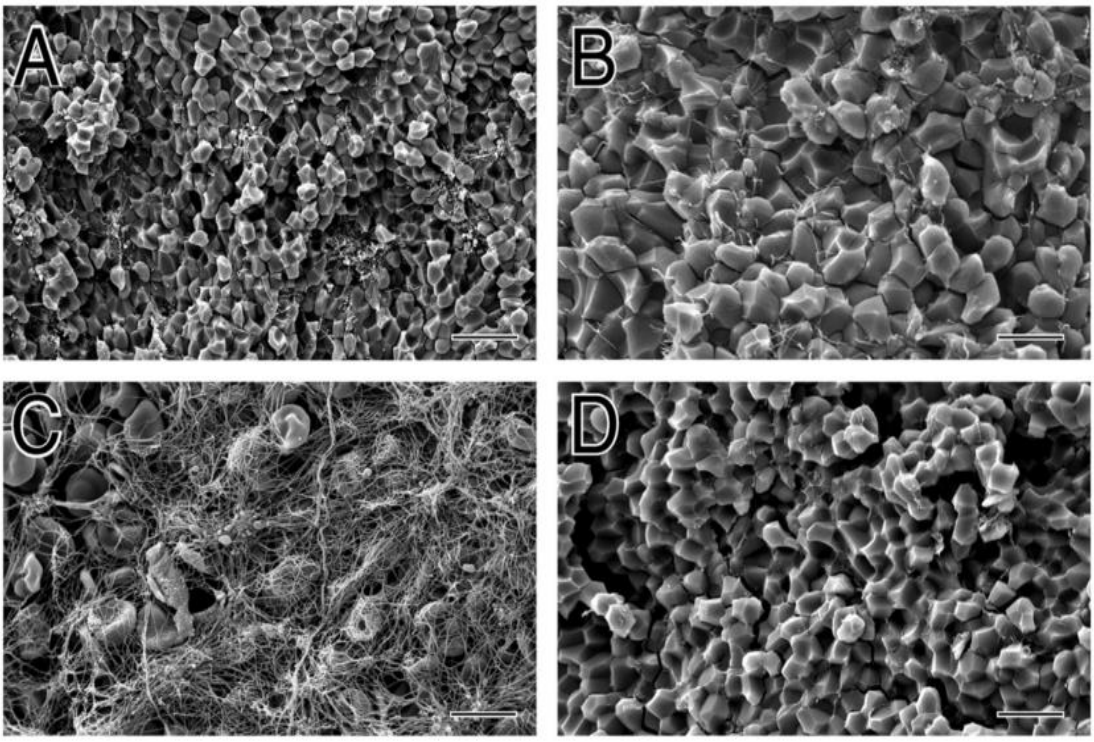

Figure 2.11 The structure of clots made from reconstituted human whole blood activated with kaolin and mouse whole blood. (A-C) Scanning electron micrographs of clots made from reconstituted human whole blood consisting of 2 mg/mL fibrinogen, 167 000 platelets/mL, 37% hematocrit, activated by kaolin following recalcification. (A-B) Inside of these contracted clots, revealing close-packed polyhedra. (C) Outside of contracted clot, showing a thick meshwork of fibrin and platelet aggregates. (D) Scanning electron micrograph of the inside of a mouse whole-blood clot. Magnification bar = 20 μm (A) and 10 μm (B-D) (Cines *et al*., 2014).

2.6.4 Clot Imaging

Imaging techniques are used in patients with AIS to exclude hemorrhage and to assess the extent of infarction. The primary imaging techniques in clinical practice are computed tomography (CT) and magnetic resonance imaging (MRI).

Computed tomography (CT) imaging has been shown to be a feasible option for differentiating thrombi according to their hematocrit. The study by Kirchhof *et al.* (2003) supported this hypothesis by demonstrating that CT is a suitable technique for distinguishing clots as white, mixed and red by estimating the number of erythrocytes present based on the attenuation number. Phantom clot samples were prepared *in-vitro* with varying hematocrit levels. The results from the study show that the CT numbers of white, mixed and red clots vary significantly and suggest that clots with a larger hematocrit level have larger CT numbers than clot samples with a lower hematocrit level. These findings were supported by Riedel *et al.* (2010) who found that erythrocyte-rich clots were shown to have higher attenuation values than platelet-rich clots using non-contrast CT.

Magnetic resonance imaging (MRI) has also been utilised to analyse the histological composition of clots (Fujimoto *et al*. 2013). Erythrocyte-rich and fibrin-rich clots were created *in-vitro* and injected into the common carotid artery in a swine model. Some of the samples were imaged *in-vivo*, while other samples were randomly selected for *in-vitro* imaging. The erythrocyte component of the clots were found to show high fluid-attenuated inversion recovery (FLAIR) signal intensity and iso-intensity in T2-weighted imaging, compared to the fibrin-rich samples which demonstrated low FLAIR and low intensity T2-weighted signals. Similar results were achieved in both the *in-vitro* and *in-vivo* stroke models. Thus, using CT and MRI characteristics have

been found to aid in the differentiation of clot compositions within thrombi (Gasparian *et al*. 2015; Brinjikji *et al*. 2017).

Distinguishing between red and white thrombi and determining clot age could potentially be very useful in evaluating what treatment strategy to pursue (Fang *et al*., 2015). The definition of clot characteristics that are associated with successful recanalisation could help to inform treatment decisions and identify patients at risk. Recent studies by Consoli *et al.* (2018, 2019) have developed a correlation between the angiographic phenotype of M1-middle cerebral artery occlusions, classified as regular and irregular in aspect, and the success of treatment by stent retrievers (SRs) or contact aspiration (CA). The studies found that clots classified as 'irregular' had greater recanalisation rates when treated with SRs as a first-line approach than with CA. Therefore from a clinical aspect, imaging of a clot *in-situ* before treatment could assist in establishing the clot type, and in turn, could assist the physician in selecting the most appropriate treatment method to administer or establish what device to use, that would ensure a greater success rate in each case.

Non-invasive imaging techniques are a promising tool in the characterisation of clot material. Huang *et al.* (2013) used shear-wave dispersion ultrasound vibrometry to measure elasticity and viscosity of clot analogues formed from porcine WB. This approach was found to provide accurate estimations for shear elasticity; however it did not measure viscosity accurately. Alternatively, dynamic ultrasound elastography was implemented by Schmitt *et al.* (2011) to evaluate the storage and loss moduli of similar analogues also formed from porcine WB. Fang *et al.* (2015) also used ultrasound to distinguish between newly formed and aged clots. These clot samples were formed *in-vitro* using porcine WB. This study recognised ultrasound as a useful

tool to distinguish between clot types that in turn, may be used to assist in establishing personalised thrombolytic treatment planning.

While many imaging techniques have been used to examine blood coagulation and clot formation *in-vivo,* few studies have established imaging techniques to determine the mechanical properties of clots *in-vivo*. Xie *et al.* (2005) studied the correspondence of ultrasound measured elasticity with direct mechanical measurement. Thrombi were surgically induced in rats, and good agreement was achieved between the Young's modulus measured *ex-vivo* and the elasticity images reconstructed *in-vivo*. This result supports the ability of elasticity imaging to establish efficient treatment of thrombi. Other studies have used similar imaging techniques to determine the viscoelastic properties of thrombus *in-vivo* (Chen *et al.*, 1996; Chandran *et al.,* 2017). However, the ability to accurately measure these ultrasound parameters *in-vivo* is needed before applying this method for clinical diagnosis (Huang *et al*. 2011)

In the near future, these imaging strategies may enable identification of AIS patients who may or may not benefit from a particular treatment. If certain clot types are shown to be associated with an increased susceptibility to fragmentation and possible distal embolisation, then imaging may be useful to choose the optimum therapy or device, and also offer the physician with an insight into what to expect during the procedure.

2.7 Computational Modelling of Thrombus Material

Despite the fact that thrombus material is of critical importance in relation to the progression of vascular disease, a detailed integrated computational-experimental investigative focus on thrombus material has been lacking in the published literature. A brief overview and key equations of the constitutive models used to represent clot material in the literature are illustrated in Table 2.3.

Table 2.3 Summary of constitutive models and equations used to represent behaviour of thrombus material.

Author	Aim of Study	Model Type	Key Equations
van Dam *et al.* (2006)	Describe the linear viscoelastic properties of ILT	Multi-mode Maxwell Model	$\dot{\tau}_i + \frac{1}{\lambda_i}\tau_i = G_i\dot{\gamma}$ $\tau = \sum_{i=1}^{n} \tau_i$
Kim *et al.* (2011)	Model clot fibre network	Each individual fibre in network represented by a linear spring	$F(\delta L) = K\delta L$ $\lambda = \frac{\left(\sum {}^{F_i}/_{A_i}\right)_{i=1}^{M}}{\varepsilon}$
Brown *et al.* (2009)	To model stress-strain behaviour of fibre networks	Each individual fibre in network represented by a linear spring	$x_f = \lambda_f L_f = L_f(1 + \frac{F}{EA})$
van Dam *et al.* (2008)	Capture the clot material behaviour using non-linear viscoelastic model	Generalized multi-mode Maxwell model	$\sigma^d = \sigma_0^d + \sum_{i=1}^{n} \sigma_i^d$ $\sigma_i^d = G_i B_{e,i}^d$
van Kempen *et al.* (2015)	Capture the non-linear viscoelastic behaviour	Two-arm Maxwell model (two modes)	$\tau = \tau_v + \tau_e + \sum_{i=1}^{2} \tau_{ve,i}$ $\tau_{ve,i} = G_i(B_{e,i} - I)$
Schmitt *et al.* (2011)	Capture the viscoelastic behaviour	Kelvin-Voigt Model Standard Linear Solid Model (SLS) Generalized Maxwell Model	$\sigma(t) = E\varepsilon_0 + \eta\frac{d\varepsilon}{dt}$ $\sigma(t) = \varepsilon_0(E_1 + E_2 e^{-E_2 t/\eta}$ $\sigma(t) = E_0 + \sum_j E_j e^{\frac{-t}{\tau_j}}$
Slaboch *et al.* (2012)	Capture the viscoelastic behaviour	Kelvin Model Standard Linear solid Model (SLS)	$\sigma(t) = E\varepsilon_0 + \eta\frac{d\varepsilon}{dt}$ $\sigma(t) = \varepsilon_0(E_1 + E_2 e^{-E_2 t/\eta}$
Malone *et al.* (2018)	Capture the non-linear stress–strain response and time-dependent properties of clot analogues	Third Order Mooney-Rivlin Model Standard Linear Solid Model (SLS)	$W = a_{10}(I_1 - 3) + a_{01}(I_2 - 3) + a_{11}(I_1 - 3)(I_2 - 3) + a_{20}(I_1 - 3)^2 + a_{30}(I_1 - 3)^3$ $s(t) = \frac{E_1 E_2}{E_1 + E_2}\left(1 + \frac{E_1}{E_2} e^{-t/\tau_2}\right)$ where $\tau_2 = \frac{\mu}{E_1 + E_2}$

2.7.1 Constitutive Models

Constitutive models are essential for the numerical simulation of blood clot behaviour and deformation *in-vivo*. A number of models have been developed to describe the mechanical properties of the components of the blood clot (Xu *et al*. 2008). These models focus mainly on clot formation, coagulation and dissolution in flowing blood or the formation of the fibrin network (van Kempen *et al.*, 2015; Karsaj and Humphrey 2009; Bodnár and Sequeira 2008). The linear viscoelastic properties of the blood clot have also been modelled using results from ultrasound techniques that were fitted to linear viscoelastic models (Schmitt *et al.*, 2011).

Models for ILT in AAA that describe their mechanical properties have been developed in recent years (Polzer *et al*. 2012; van Dam *et al*. 2008). van Dam *et al.* (2006) determined the linear viscoelastic properties of ILT and described this behaviour using a multi-mode Maxwell model as shown in Table 2, and given by

$$\dot{\tau}_i + \frac{1}{\lambda_i}\tau_i = G_i\dot{\gamma} \tag{2.1}$$

where τ_i is the shear stress contribution of mode *i*, with relaxation time λ_i and modulus G_i and where $\dot{\gamma}$ is the applied shear strain rate. The total stress,τ, is the sum of the stress contributions of all *n* modes described as follows

$$\tau = \sum_{i=1}^{n} \tau_i \tag{2.2}$$

This model was calibrated using the shear test results and the material was assumed to be isotropic and incompressible. A similar model was developed by Kim *et al.* (2011) where the clot fibre networks were modelled. Each individual fibre in the network was represented by a linear spring, with the spring force given by

$$F(\delta L) = \kappa \delta L \tag{2.3}$$

where $\kappa = EA/L_0$ is the spring constant, E is the Young's Modulus, A is the cross-sectional area, L_0 is the initial fibre length and δL is the extension of the fibre. The elastic modulus of the network was then calculated by

$$\lambda = \frac{(\sum F_i/A_i)_{i=1}^{M}}{\varepsilon} \tag{2.4}$$

where F_i is the normal component of the force acting on a fibre with thickness A_i, ε is the average strain and M is the total number of fibres.

Brown *et al.* (2009) also investigated approaches to model the stress–strain behaviour of fibrin networks. They developed a model for random networks of folded proteins which uses a system of connected fibres, which leads to an expression for the force-extension (or stress–strain) relation of the network in terms of the force-extension relation of a single fibre. For small forces the fibre behaves as a linear spring and the force-extension can be written as

$$x_f = \lambda_f L_f = L_f(1 + \frac{F}{EA}) \tag{2.5}$$

where x_f is the end-to-end distance of the fibrin fibre after deformation, λ_f is the fibre deformation, L_f is the undeformed length, F is the force, A is the cross-sectional area of the fibre, and E is the Young's Modulus.

However, it was found that the linear models described above were only valid for small strains (up to 5%) as the materials only behaved linearly at small strains. Therefore van Dam *et al.* (2008) later presented a non-linear viscoelastic model to capture the material behaviour at larger strains more accurately. The constitutive model proposed was based on a model used to describe the material properties of brain

tissue (Hrapko *et al*. 2006). Based on the assumption that thrombus material is incompressible (Hinnen *et al*. 2007), the Cauchy stress, σ, was decomposed as follows

$$\boldsymbol{\sigma} = \boldsymbol{\sigma}^{d} + \boldsymbol{\sigma}^{v} \tag{2.6}$$

where σ^{v} is the volumetric part, which depends on the hydrostatic pressure, and σ^{d} is the deviatoric part, where $\boldsymbol{\sigma}^{d}=\boldsymbol{\sigma} - p\boldsymbol{I}$ and pI is the pressure multiplied by the identity tensor. This deviatoric part was then further divided into an elastic part, $\boldsymbol{\sigma}_{0}^{d}$, and into *n* viscoelastic modes, represented by a generalized multi-mode Maxwell model (Table 2). The elastic behaviour of the viscoelastic elements was modelled as Neo-Hookean, where $\boldsymbol{B}_{e,i}^{d}$ is the deviatoric part of the elastic Finger tensor $\boldsymbol{B}_{e}$ of mode *i*. The finger tensor is the left Cauchy Green Tensor given by

$$\boldsymbol{B} = \boldsymbol{F}\boldsymbol{F}^{T} \tag{2.7}$$

where $\boldsymbol{F}$ is the deformation gradient tensor.

A similar model was developed by van Kempen *et al.* (2014) inspired by previously developed models (Hinnen *et al.*, 2007; van Dam *et al.*, 2008). This model was also based on a generalized multi-arm Maxwell model, (van Kempen *et al.*, 2015) which is represented by an elastic spring, a viscous dashpot and a number of Maxwell modes assembled in parallel. A two-arm Maxwell model (2 modes) was used in this study to sufficiently capture the material behaviour (Table 2),

$$\tau = \tau_{v} + \tau_{e} + \sum_{i=1}^{2} \tau_{ve,i} \tag{2.8}$$

where τ_{v}, τ_{e} and $\tau_{ve,i}$ are the Cauchy stress components for the viscous dashpot, elastic spring and Maxwell modes, respectively (van Kempen *et al.*, 2015). The elastic

part of the viscoelastic modes were modelled as Neo–Hookean, similar to the van Dam model (2008), also shown in Table 2,

$$\tau_{ve,i} = G_i\left(\boldsymbol{B}_{e,i} - \boldsymbol{I}\right) \tag{2.9}$$

where G_i represents the modulus of mode *i* and $\boldsymbol{B}_{e,i}$ is the elastic Finger tensor, as described earlier. This was then used to determine the inelastic rate of deformation

$$D_{p,i} = \frac{\tau_{ve,i}}{2\eta_i} \tag{2.10}$$

with η_i representing the viscosity of mode *i*. The contribution to stress from the elastic mode was also modelled as Neo-Hookean by

$$\tau_e = G_0(\boldsymbol{B} - \boldsymbol{I}) \tag{2.11}$$

and the contribution of the viscous mode given by

$$\tau_v = 2\left(\eta_p - \eta_o\right)D \tag{2.12}$$

with η_p representing the plasma viscosity and η_o representing the contribution from the clot. The generalized Maxwell model was then extended to describe the nonlinear viscoelastic behaviour of the thrombus material. As previously described for a fibrin network (van Kempen *et al*. 2014), three nonlinear features were incorporated into the model; softening, strain stiffening and nonlinear viscous dissipation. The shear moduli and viscosities of the generalized Maxwell model were extended to include these three features in the model.

Similar model development was carried out in other studies which investigated the use of simple viscoelastic models, such as the Kelvin-Voigt and Maxwell models, to

capture the viscoelastic behaviour of thrombus. Slaboch *et al.* (2012) found that a standard linear solid (SLS) viscoelastic model more accurately captured the viscoelastic behaviour observed from nano-indentation and rheometry experiments on clot analogues, than the Kelvin model. Similarly, Malone *et al.* (2018) adopted a visco-hyperelastic model to capture the loading curves from tensile testing experiments on clot analogues, using a third order Mooney-Rivlin model, combined with an SLS model to capture viscoelasticity, whereas Schmitt *et al.* (2011) determined that a second or third order generalized Maxwell model could best describe thrombus viscoelasticity observed from dynamic ultrasound elastography of porcine whole blood samples during coagulation.

A limitation of all of the studies described here is that loading data alone was used to fit the constitutive model and the loading-unloading behaviour, and any related hysteresis, was not captured. The consideration of unloading behaviour is of critical importance to the evaluation and future development of mechanical thrombectomy devices and procedures. Therefore, while there have been many advancements in the development of constitutive models for clot material, further progress remains to be achieved in this area.

2.7.2 Computational Models

While predictive computational models simulating the mechanical behaviour of thrombus material *in-vivo* would be very valuable for vascular research and device design, relatively little has been reported in the literature to date.

One of the first finite element models of thrombus material was developed by Di Martino *et al.* (1998) A simplified model of the transverse section of the aneurysmatic wall with the intraluminal thrombus was developed and the effect of the thrombus on

the arterial wall studied. Finite element analysis has also been utilised to replicate simple experimental techniques that were carried out. The aforementioned Xie *et al.* (2005) study, which investigated the mechanical properties of thrombus under compression, used finite element analysis to create a model of the sample under compression. The sample was modelled as elastic, linear, isotropic and quasi-incompressible. The Young's modulus calculated from the experimental data was fed into the model. The results from the simulation indicated that the finite element model could accurately capture the behaviour of the clot as there was a good fit between the experimental and simulated results.

Similarly, an elastic two-dimensional plane stress finite element computational model was used by Gasser *et al.* to validate their experimental tensile testing data (Gasser *et al*. 2008). Due to the symmetry of the dog bone specimens used, a quarter of the specimen was modelled. The incompressible mechanical properties of the ILT tissue were modelled by a one parameter Ogden strain energy function. This constitutive model predicted an approximately linear load–displacement response and hence, was able to capture the experimental findings of ILT tissue.

Slaboch *et al.* developed a two dimensional (2D) axisymmetric, poro-viscoelastic finite element model, which simulated the thrombus sample and the flat punch indenter tip during a nanoindentation experiment (Slaboch *et al*. 2012). Two-node axisymmetric rigid elements were used for the indenter tip (RAX2) and four-node axisymmetric hybrid quadrilateral elements with pore pressure (CAX4P) were used for the thrombus. Frictionless contact was assumed between the indenter and the sample, and a zero pore pressure condition was set on the thrombus surface. The loading conditions applied to the model were the same as used in the experimental nanoindentation testing. The thrombus was modelled as a biphasic material consisting

of a porous solid medium and a fluid. For a biphasic material, the solid phase is described by any solid continuum theory such as elasticity or viscoelasticity. The fluid can flow through the porous solid medium, which is driven by a pore pressure gradient, and can be described by Darcy's Law. Both the solid and the fluid phases bear the total load. In this case, the solid phase of the thrombus is viscoelastic and therefore the model used a standard linear solid model, consisting of a linear spring in parallel with a Maxwell element, similar to the constitutive models outlined in the previous section.

While the development of predictive computational models simulating the clot *in-situ* would be very valuable for basic and applied vascular research, very few computational models of thrombus material have been reported. In particular, an integrated computational-experimental investigative focus on thrombus material is lacking in the published literature and is required in order to inform more complex simulations.

2.8 Summary

It is evident from the literature to date that many studies have focused on the mechanical testing and characterisation of thrombus material, from tensile and compression testing, to investigating the friction coefficient and indentation/integration properties, but considerable work is still required and ongoing. Analogue clot material is becoming more prevalent in preclinical mechanical testing as a cheaper and more readily available alternative to human clot tissue. It is important to characterise clot material with varying compositions and constituents that represent the range of clot types seen *in-vivo*, to determine the associated range of mechanical behavior, and in order to do this a variety of reproducible clot analogues are required.

However, developing a reliable test method that is suitable to test the broad range of clot types remains a challenge due to the fragile nature of the material.

The growing use of clot analogue material for thrombectomy device testing continues, with a goal to provide clinicians with treatment strategies based on laboratory findings. The development of a variety of reproducible clot analogues that span a large range of stiffnesses is essential for preclinical device testing to achieve physiologically accurate results, as the clot properties may affect the level of resistance during removal, and in turn, may affect the success of the procedure. This information may also have many possible implications for the future design of these treatment devices.

From a clinical perspective, imaging of clots *in-situ* before treatment and establishing clot type, could inform the physician on what is the most appropriate treatment method to administer or on what device to use, to ensure more successful outcomes in each case. However, to date few imaging techniques have been successful in determining the clot type, in real-time, prior to treatment. Little is still known about the relationship between the angiographic appearance of an occlusion and the mechanical properties and composition of the thrombus, underlining the importance of understanding the occlusion dynamics and deformation of an occluding clot.

Few studies have reported constitutive models for thrombus material to capture the material behaviour under various loading methods. A limitation of the published studies is that loading data alone has been used to calibrate these models. The loading-unloading behaviour of thrombus material, and related hysteresis due to rate-dependent viscoelasticity, has been largely neglected.

Very few computational models of thrombus material have been presented in the literature, despite the fact that this material is of critical importance in relation to the progression of vascular disease.

In this thesis, a range of repeatable clot analogues with varying compositions are presented. Mechanical characterisation of these clot analogues is performed to gain a better understanding of the mechanical behaviour of clot material, as a function of composition. An appropriate constitutive model is selected to capture the material behaviour based on the experimental results. Finally, the clot analogues are used in the development of *in-vitro* AIS models to allow for the analysis of the mechanics of an occluding clot and for the performance assessment of various AIS treatment techniques.

2.9 References

Akbik, F. *et al.* (2016) 'The Evolution of Mechanical Thrombectomy for Acute Stroke', Current Treatment Options in Cardiovascular Medicine, 18(5), p. 32. doi: 10.1007/s11936-016-0457-7.

Andersson, T. *et al.* (2019) 'The Aspirations of Direct Aspiration for Thrombectomy in Ischemic Stroke: A Critical Analysis.', Journal of stroke. Korean Stroke Society, 21(1), pp. 2–9. doi: 10.5853/jos.2018.02026.

Asakura, F. *et al.* (2007) 'Preclinical testing of a new clot-retrieving wire device using polyvinyl alcohol hydrogel vascular models', Neuroradiology, 49(3), pp. 243–251. doi: 10.1007/s00234-006-0181-1.

Ashton, J. H. *et al.* (2009) 'Compressive mechanical properties of the intraluminal thrombus in abdominal aortic aneurysms and fibrin-based thrombus mimics', Journal of Biomechanics, 42(3), pp. 197–201. doi: 10.1016/j.jbiomech.2008.10.024.

Berkhemer, O. A. *et al.* (2014) 'A Randomized Trial of Intraarterial Treatment for Acute Ischemic Stroke', New England Journal of Medicine. Massachusetts Medical Society, (372), pp. 11–20.

Berkhemer, O. A. *et al.* (2015) 'A Randomized Trial of Intraarterial Treatment for Acute Ischemic Stroke', New England Journal of Medicine, 372(1), pp. 11–20. doi: 10.1056/NEJMoa1411587.

Bodnár, T. and Sequeira, A. (2008) 'Numerical Simulation of the Coagulation Dynamics of Blood', Computational and Mathematical Methods in Medicine. Hindawi Publishing Corporation, 9(2), pp. 83–104.

Boeckh-Behrens, T. *et al.* (2016) 'The Impact of Histological Clot Composition in Embolic Stroke', Clinical Neuroradiology, 26(2), pp. 189–197. doi: 10.1007/s00062-014-0347-x.

van der Bom, I. M. J. *et al.* (2012) 'Quantitative Evaluation of C-Arm CT Cerebral Blood Volume in a Canine Model of Ischemic Stroke', American Journal of Neuroradiology, 33(2), pp. 353–358. doi: 10.3174/ajnr.A2944.

Brekenfeld, C. *et al.* (2008) 'Mechanical Thromboembolectomy for Acute Ischemic Stroke', Stroke, 39(4), pp. 1213–1219. doi: 10.1161/STROKEAHA.107.495614.

Brinjikji, W. *et al.* (2017) 'Correlation of imaging and histopathology of thrombi in acute ischemic stroke with etiology and outcome: a systematic review', Journal of NeuroInterventional Surgery, 9(6), pp. 529–534. doi: 10.1136/neurintsurg-2016-012391.

Brown, A. E. X. *et al.* (2009) 'Multiscale mechanics of fibrin polymer: gel stretching with protein unfolding and loss of water.', Science (New York, N.Y.). American Association for the Advancement of Science, 325(5941), pp. 741–4. doi: 10.1126/science.1172484.

Burghardt, W. R. *et al.* 'Nonlinear viscoelasticity and the thrombelastograph: 1. Studies on bovine plasma clots.', Biorheology, 32(6), pp. 621–30. doi: 10.1016/0006-355X(95)00041-7.

Campbell, B. C. V. *et al.* (2015) 'Endovascular Therapy for Ischemic Stroke with Perfusion-Imaging Selection', New England Journal of Medicine. Massachusetts Medical Society, 372(11), pp. 1009–1018. doi: 10.1056/NEJMoa1414792.

Carr, M. E. and Carr, S. L. (1995) 'Fibrin structure and concentration alter clot elastic modulus but do not alter platelet mediated force development.', Blood coagulation & fibrinolysis : an international journal in haemostasis and thrombosis, 6(1), pp. 79–86.

Chandler, A. B. (1958) 'In vitro thrombotic coagulation of the blood; a method for producing a thrombus.', Laboratory investigation; a journal of technical methods and pathology, 7(2), pp. 110–4.

Chandran, V.D., Kadri, O.E., Voronov, R.S., 2017. Thrombus Yield Stress Calculation From LBM Based on Intravital Laser Injury Images In Mice, in: Northeast Bioengineering Conference (NEBEC).

Chaudhry, R. and Babiker, H. M. (2019) Physiology, Coagulation Pathways, StatPearls Publishing.

Chen, E. J. *et al.* (1996) 'Young's modulus measurements of soft tissues with application to elasticity imaging', IEEE Transactions on Ultrasonics, Ferroelectrics and Frequency Control, 43(1), pp. 191–194. doi: 10.1109/58.484478.

Christian, B. A. *et al.* (2009) 'Showered calcific emboli to the brain, the "salted pretzel" sign, originating from the ipsilateral internal carotid artery causing acute cerebral infarction.', Stroke, 40(5), pp. e319-21. doi: 10.1161/STROKEAHA.108.538009.

Chueh, J. Y. *et al.* (2013) 'Reduction in Distal Emboli With Proximal Flow Control During Mechanical Thrombectomy', Stroke, 44(5), pp. 1396–1401. doi: 10.1161/STROKEAHA.111.670463.

Chueh, J. Y., Puri, A. S. and Gounis, M. J. (2017) 'An in vitro evaluation of distal emboli following Lazarus Cover-assisted stent retriever thrombectomy', Journal of NeuroInterventional Surgery, 9(2), pp. 183–187. doi: 10.1136/neurintsurg-2015-012256.

Chueh, J. Y. *et al.* (2011) 'Mechanical characterization of thromboemboli in acute ischemic stroke and laboratory embolus analogs.', AJNR. American journal of neuroradiology, 32(7), pp. 1237–44. doi: 10.3174/ajnr.A2485.

Chueh, J.Y. *et al.,* (2016). 'Risk of distal embolisation with stent retriever thrombectomy and ADAPT'. Journal of NeuroInterventional Surgery, 8(2), pp.197–202.

Cines, D. B. *et al.* (2014) 'Clot contraction: compression of erythrocytes into tightly packed polyhedra and redistribution of platelets and fibrin.', Blood. American Society of Hematology, 123(10), pp. 1596–603. doi: 10.1182/blood-2013-08-523860.

Consoli, A. *et al.* (2018) 'Thrombectomy for M1-Middle Cerebral Artery Occlusion: Angiographic Aspect of the Arterial Occlusion and Recanalisation: A Preliminary Observation.', Stroke, 49(5), pp. 1286–1289. doi: 10.1161/STROKEAHA.117.018987.

Consoli, A. *et al.* (2019) 'Effect of the phenotype of the M1-middle cerebral artery occlusion on the recanalisation rates in the ASTER trial', Journal of NeuroInterventional Surgery. British Medical Journal Publishing Group. doi: 10.1136/neurintsurg-2019-015002.

van Dam, E. A. *et al.* (2006) 'Determination of linear viscoelastic behavior of abdominal aortic aneurysm thrombus.', Biorheology, 43(6), pp. 695–707.

van Dam, E. A. *et al.* (2008) 'Non-linear viscoelastic behavior of abdominal aortic aneurysm thrombus', Biomechan Model Mechanobiol, 7, pp. 127–137.

Davie, E. W. and Ratnoff, O. D. (1964) 'Waterfall Sequence for Intrinsic Blood Clotting', Science (New York, N.Y.). American Association for the Advancement of Science, 145(3638), pp. 1310–2. doi: 10.1126/science.145.3638.1310.

Dempfle, C.-E. *et al.* (2008) 'Impact of fibrinogen concentration in severely ill patients on mechanical properties of whole blood clots.', Blood coagulation & fibrinolysis : an international journal in haemostasis and thrombosis, 19(8), pp. 765–70. doi: 10.1097/MBC.0b013e32830f1b68.

Dobrocky, T. *et al.* (2018) 'Thrombectomy of calcified emboli in stroke. Does histology of thrombi influence the effectiveness of thrombectomy?', Journal of neurointerventional surgery. British Medical Journal Publishing Group, 10(4), pp. 345–350. doi: 10.1136/neurintsurg-2017-013226.

Duffy, S. *et al.* (2016) 'Novel methodology to replicate clot analogs with diverse composition in acute ischemic stroke', Journal of Neurointerventional Surgery, 0, pp. 1–7.

Duffy, S. *et al.* (2019) 'Per-Pass Analysis of Thrombus Composition in Patients With Acute Ischemic Stroke Undergoing Mechanical Thrombectomy', Stroke, 50(5), pp. 1156–1163. doi: 10.1161/STROKEAHA.118.023419.

Evans, M. R. B. *et al.* (2017) 'Revolution in acute ischaemic stroke care: a practical guide to mechanical thrombectomy.', Practical neurology. BMJ Publishing Group Ltd, 17(4), pp. 252–265. doi: 10.1136/practneurol-2017-001685.

Fang, J. *et al.* (2015) 'Discrimination between Newly Formed and Aged Thrombi Using Empirical Mode Decomposition of Ultrasound B-Scan Image', BioMed Research International. Hindawi, 2015, pp. 1–9. doi: 10.1155/2015/403293.

Fargen, K. M. *et al.* (2017) 'A survey of neurointerventionalists on thrombectomy practices for emergent large vessel occlusions.', Journal of neurointerventional surgery. British Medical Journal Publishing Group, 9(2), pp. 142–146. doi: 10.1136/neurintsurg-2015-012235.

Ferreira, C. N. *et al.* (2010) 'A cell-based model of coagulation and its implications', Revista Brasileira de Hematologia e Hemoterapia. Associação Brasileira de Hematologia e Hemoterapia, 32(5), pp. 416–421. doi: 10.1590/S1516-84842010000500016.

Ferry, J. D. and Morrison, P. R. (1944) 'Chemical, Clinical, And Immunological Studies On The Prodcuts Of Human Plasma Fractionation. XVI. Fibrin Clots, Fibrin Films, And Fibrinogen Plastics.', The Journal of clinical investigation, 23(4), pp. 566–72. doi: 10.1172/JCI101523.

Fitzgerald, S. T. *et al.* (2019) 'Platelet-rich clots as identified by Martius Scarlet Blue staining are isodense on NCCT.', Journal of neurointerventional surgery. British Medical Journal Publishing Group, 11(11), pp. 1145–1149. doi: 10.1136/neurintsurg-2018-014637.

Flint, A. C. *et al.* (2010) 'Predicting Long-Term Outcome after Endovascular Stroke Treatment: The Totaled Health Risks in Vascular Events Score', American Journal of Neuroradiology, 31(7), pp. 1192–1196. doi: 10.3174/ajnr.A2050.

Fransen, P. S. *et al.* (2014) 'MR CLEAN, a multicenter randomized clinical trial of endovascular treatment for acute ischemic stroke in the Netherlands: study protocol for a randomized controlled trial', Trials, 15(1), p. 343. doi: 10.1186/1745-6215-15-343.

Fugate, J. E. and Rabinstein, A. A. (2015) 'Absolute and Relative Contraindications to IV rt-PA for Acute Ischemic Stroke', The Neurohospitalist, 5(3), pp. 110–121. doi: 10.1177/1941874415578532.

Fujimoto, M. *et al.* (2013) 'Characterization of Arterial Thrombus Composition by Magnetic Resonance Imaging in a Swine Stroke Model', Stroke, 44(5), pp. 1463–1465. doi: 10.1161/STROKEAHA.111.000457.

Fukada, E. *et al.* (1984) 'Methods to study rheological properties of blood during clotting.', Biorheology. Supplement : the official journal of the International Society of Biorheology, 1, pp. 9–14.

Furie, B. (1999) 'Bleeding and blood clotting', Encyclopaedia Britannica.

Furie, B. and Furie, B. C. (2008) 'Mechanisms of thrombus formation.', The New England journal of medicine, 359(9), pp. 938–949. doi: 10.1056/NEJMra0801082.

van Galen, K. P. M. *et al.* (2012) 'Von Willebrand factor deficiency and atherosclerosis', Blood Reviews, 26(5), pp. 189–196. doi: 10.1016/j.blre.2012.05.002.

Gasparian, G. G. *et al.* (2015) 'Imaging of Occlusive Thrombi in Acute Ischemic Stroke', International Journal of Stroke, 10(3), pp. 298–305. doi: 10.1111/ijs.12435.

Gasser, T. C. *et al.* (2008) 'Failure properties of intraluminal thrombus in abdominal aortic aneurysm under static and pulsating mechanical loads.', Journal of vascular surgery, 48(1), pp. 179–88. doi: 10.1016/j.jvs.2008.01.036.

Gasser, T. C. *et al.* (2006) 'Hyperelastic modelling of arterial layers with distributed collagen fibre orientations.', Journal of the Royal Society, Interface/the Royal Society, 3(6), pp. 15–35. doi: 10.1098/rsif.2005.0073.

Vande Geest, J. P. *et al.* (2006) 'A planar biaxial constitutive relation for the luminal layer of intra-luminal thrombus in abdominal aortic aneurysms.', Journal of biomechanics. Elsevier, 39(13), pp. 2347–54. doi: 10.1016/j.jbiomech.2006.05.011.

González, R. G. (2006) 'Imaging-guided acute ischemic stroke therapy: From "time is brain" to "physiology is brain".', AJNR. American journal of neuroradiology, 27(4), pp. 728–35.

Gottlob, R. *et al.* (1971) 'Studies on Thrombolysis with Streptokinase', Thrombosis and Haemostasis. Schattauer GmbH, 25(01), pp. 354–378. doi: 10.1055/s-0038-1654310.

Goyal, M. *et al.* (2015) 'Randomized Assessment of Rapid Endovascular Treatment of Ischemic Stroke', New England Journal of Medicine, 372(11), pp. 1019–1030. doi: 10.1056/NEJMoa1414905.

Goyal, M. *et al.* (2016) 'Endovascular thrombectomy after large-vessel ischaemic stroke: a meta-analysis of individual patient data from five randomised trials', The Lancet. Elsevier, 387(10029), pp. 1723–1731. doi: 10.1016/S0140-6736(16)00163-X.

Gralla, J. *et al.* (2006) 'A dedicated animal model for mechanical thrombectomy in acute stroke.', AJNR. American journal of neuroradiology, 27(6), pp. 1357–61.

Gralla, J. *et al.* (2006) 'Mechanical thrombectomy for acute ischemic stroke: thrombus-device interaction, efficiency, and complications in vivo.', Stroke; a journal of cerebral circulation, 37(12), pp. 3019–24. doi: 10.1161/01.STR.0000248457.55493.85.

Gunning, G. M. *et al.* (2016) 'Clot friction variation with fibrin content; implications for resistance to thrombectomy', Journal of Neurointerventioal Surgery, 372(1), pp. 1019–1030. doi: 10.1136/.

Hacke, W. *et al.* (2008) 'Thrombolysis with Alteplase 3 to 4.5 Hours after Acute Ischemic Stroke', New England Journal of Medicine, 359(13), pp. 1317–1329. doi: 10.1056/NEJMoa0804656.

Haider, T. *et al.* (2016) 'New mechanical thrombectomy model in the rabbit: A feasibility study', Journal of Neuroscience Methods, 271, pp. 139–142. doi: 10.1016/j.jneumeth.2016.07.007.

Hinnen, J. W. *et al.* (2007) 'Development of fibrinous thrombus analogue for in-vitro abdominal aortic aneurysm studies.', Journal of biomechanics, 40(2), pp. 289–95. doi: 10.1016/j.jbiomech.2006.01.010.

Hoffman, M. (2003) 'A cell-based model of coagulation and the role of factor VIIa.', Blood reviews, 17 Suppl 1, pp. S1-5.

Hrapko, M. *et al.* (2006) 'The Mechanical Behaviour Of Brain Tissue: Large Strain Response and Constitutive Modelling', Biorheology, 43(5), pp. 623–36.

Huang, C.-C. *et al.* (2011) 'Review: Study of the Blood Coagulation by Ultrasound', Journal of Medical and Biological Engineering, 31(2), pp. 79–86. doi: 10.5405/jmbe.893.

Huang, C.-C., Chen, P.-Y. and Shih, C.-C. (2013) 'Estimating the viscoelastic modulus of a thrombus using an ultrasonic shear-wave approach', Medical Physics. American Association of Physicists in Medicine, 40(4), p. 042901. doi: 10.1118/1.4794493.

Imai, K. *et al.* (2006) 'Clot removal therapy by aspiration and extraction for acute embolic carotid occlusion.', AJNR. American journal of neuroradiology, 27(7), pp. 1521–7.

Irish Heart Foundation (2017) Irish Heart Stroke - Irish Heart Foundation.

Johnson, S. *et al.* (2017) 'Review of Mechanical Testing and Modelling of Thrombus Material for Vascular Implant and Device Design', Annals of Biomedical Engineering, 45(11). doi: 10.1007/s10439-017-1906-5.

Jovin, T. G. *et al.* (2015) 'Thrombectomy within 8 Hours after Symptom Onset in Ischemic Stroke', New England Journal of Medicine, 372(24), pp. 2296–2306. doi: 10.1056/NEJMoa1503780.

Kaesmacher, J. *et al.* (2017) 'Risk of Thrombus Fragmentation during Endovascular Stroke Treatment', American Journal of Neuroradiology, 38(5), pp. 991–998. doi: 10.3174/ajnr.A5105.

Kaibara, M. and Fukada, E. (1971) 'The influence of the concentration of thrombin on the dynamic viscoelasticity of clotting blood and fibrinogen-thrombin systems.', Biorheology, 8(3), pp. 139–47.

Kan, I. *et al.* (2010) 'A Novel Method of Thrombus Preparation for Use in a Swine Model for Evaluation of Thrombectomy Devices', American Journal of Neuroradiology, 31(9), pp. 1741–1743. doi: 10.3174/ajnr.A1991.

Karsaj, I. and Humphrey, J. D. (2009) ‘A mathematical model of evolving mechanical properties of intraluminal thrombus.’, Biorheology, 46(6), pp. 509–27. doi: 10.3233/BIR-2009-0556.

van Kempen, T. H. S. *et al.* (2014) ‘A constitutive model for a maturing fibrin network.’, Biophysical journal, 107(2), pp. 504–13. doi: 10.1016/j.bpj.2014.05.035.

van Kempen, T. H. S. *et al.* (2015) ‘A constitutive model for developing blood clots with various compositions and their nonlinear viscoelastic behavior’, Biomechanics and Modeling in Mechanobiology. doi: 10.1007/s10237-015-0686-9.

van Kempen, T. H. S., Peters, G. W. M. and van de Vosse, F. N. (2015) ‘A constitutive model for the time-dependent, nonlinear stress response of fibrin networks.’, Biomechanics and modeling in mechanobiology, 14(5), pp. 995–1006.

Kim, E. *et al.* (2011) ‘Correlation between fibrin network structure and mechanical properties: an experimental and computational analysis’, Soft Matter. The Royal Society of Chemistry, 7(10), p. 4983. doi: 10.1039/c0sm01528h.

Kim, O. V. *et al.* (2014) ‘Structural basis for the nonlinear mechanics of fibrin networks under compression’, Biomaterials, 35(25), pp. 6739–6749. doi: 10.1016/j.biomaterials.2014.04.056.

Kim, O. V. *et al.* (2017) ‘Quantitative structural mechanobiology of platelet-driven blood clot contraction’, Nature Communications. Nature Publishing Group, 8(1), p. 1274. doi: 10.1038/s41467-017-00885-x.

Kim, S. K. *et al.* (2015) ‘Histologic Analysis of Retrieved Clots in Acute Ischemic Stroke: Correlation with Stroke Etiology and Gradient-Echo MRI’, American Journal of Neuroradiology, 36(9), pp. 1756–1762. doi: 10.3174/ajnr.A4402.

Kirchhof, K. *et al.* (2003) ‘Differentiation of White, Mixed, and Red Thrombi: Value of CT in Estimation of the Prognosis of Thrombolysis—Phantom Study’, Radiology, 228(1), pp. 126–130. doi: 10.1148/radiol.2273020530.

Koh, E. *et al.* (2017) ‘Manual Aspiration Thrombectomy in Patients with Acute Stroke-Related Calcified Cerebral Emboli.’, Journal of stroke and

cerebrovascular diseases : the official journal of National Stroke Association. Elsevier, 26(10), pp. 2050–2054. doi: 10.1016/j.jstrokecerebrovasdis.2016.07.005.

Krasokha, N. *et al.* (2010) 'Mechanical properties of blood clots - a new test method. Mechanische Eigenschaften von Thromben - Neue Untersuchungsmethoden', Materialwissenschaft und Werkstofftechnik, 41(12), pp. 1019–1024. doi: 10.1002/mawe.201000703.

Krueger, K. *et al.* (2004) 'How thrombus model impacts the in vitro study of interventional thrombectomy procedures.', Investigative radiology, 39(10), pp. 641–8. doi: 10.1097/01.RLI.0000139009.65226.17.

Kulcsár, Z. *et al.* (2010) 'Penumbra System: A Novel Mechanical Thrombectomy Device for Large-Vessel Occlusions in Acute Stroke', American Journal of Neuroradiology, 31(4), pp. 628–633. doi: 10.3174/ajnr.A1924.

Lee, D. H. *et al.* (2017) 'Effective use of balloon guide catheters in reducing incidence of mechanical thrombectomy related distal embolisation', Acta Neurochirurgica, 159(9), pp. 1671–1677. doi: 10.1007/s00701-017-3256-3.

Leischner, H. *et al.* (2018) 'Reasons for failed endovascular recanalisation attempts in stroke patients', Journal of NeuroInterventional Surgery , 0, pp. 1–5.

Liebeskind, D. S. *et al.* (2011) 'CT and MRI Early Vessel Signs Reflect Clot Composition in Acute Stroke', Stroke, 42(5), pp. 1237–1243. doi: 10.1161/STROKEAHA.110.605576.

Liebig, T. *et al.* (2008) 'Comparative in vitro study of five mechanical embolectomy systems: effectiveness of clot removal and risk of distal embolisation.', Neuroradiology, 50(1), pp. 43–52. doi: 10.1007/s00234-007-0297-y.

Lim, G., Wortis, M. and Mukhopadhyay, R. (2002) 'Stomatocyte-discocyte-echinocyte sequence of the human red blood cell: evidence for the bilayer-couple hypothesis from membrane mechanics.', Proceedings of the National Academy of Sciences of the United States of America. National Academy of Sciences, 99(26), pp. 16766–9. doi: 10.1073/pnas.202617299.

Litvinov, R. I. *et al.* (2012) 'The α-Helix to β-Sheet Transition in Stretched and Compressed Hydrated Fibrin Clots', Biophysical Journal, 103(5), pp. 1020–1027. doi: 10.1016/j.bpj.2012.07.046.

MacFarlane, R. G. (1964) 'An Enzyme Cascade in the Blood Clotting Mechanism, and its Function as a Biochemical Amplifier', Nature. Nature Publishing Group, 202(4931), pp. 498–499. doi: 10.1038/202498a0.

Malone, F. *et al.* (2018) 'The Mechanical Characterisation of Bovine Embolus Analogues Under Various Loading Conditions', Cardiovascular Engineering and Technology. Springer US, 9(3), pp. 489–502. doi: 10.1007/s13239-018-0352-3.

Marder, V. J. *et al.* (2006) 'Analysis of Thrombi Retrieved From Cerebral Arteries of Patients With Acute Ischemic Stroke', Stroke, 37(8).

Marder, V. J. *et al.* (2012) Hemostasis and Thrombosis: Basic Principles and Clinical Practice. Lippincott Williams & Wilkins.

Di Martino, E. *et al.* (1998) 'Biomechanics of abdominal aortic aneurysm in the presence of endoluminal thrombus: Experimental characterisation and structural static computational analysis', European Journal of Vascular and Endovascular Surgery, 15(4), pp. 290–299. doi: 10.1016/S1078-5884(98)80031-2.

Mayer, T. E. *et al.*. (2002) 'Treatment of basilar artery embolism with a mechanical extraction device: necessity of flow reversal.', Stroke, 33(9), pp. 2232–5.

Di Meglio, L. *et al.* (2019) 'Acute ischemic stroke thrombi have an outer shell that impairs fibrinolysis', Neurology, p. 10.1212/WNL.0000000000008395. doi: 10.1212/WNL.0000000000008395.

Menon, B. K. *et al.* (2011) 'Initial experience with the Penumbra Stroke System for recanalisation of large vessel occlusions in acute ischemic stroke', Neuroradiology, 53(4), pp. 261–266. doi: 10.1007/s00234-010-0725-2.

Menon, B. K. *et al.* (2015) 'Trends in Endovascular Therapy and Clinical Outcomes Within the Nationwide Get With The Guidelines-Stroke Registry', Stroke, 46(4), pp. 989–995. doi: 10.1161/STROKEAHA.114.007542.

Merritt, W. *et al.* (2018) 'Quantifying the mechanical and histological properties of thrombus analog made from human blood for the creation of synthetic thrombus for thrombectomy device testing', Journal of NeuroInterventional Surgery, 10(12), pp. 1168–1173. doi: 10.1136/neurintsurg-2017-013675.

De Meyer, S. F. *et al.* (2017) 'Analyses of thrombi in acute ischemic stroke: A consensus statement on current knowledge and future directions', International Journal of Stroke, 12(6), pp. 606–614. doi: 10.1177/1747493017709671.

Mishra, S.M. *et al.,* (2014). 'Early Reperfusion rates with IV tPA Are determined by CTA clot characteristics'. American Journal of Neuroradiology, 35(12), pp. 2265–2272.

Mozaffarian, D. *et al.* (2015) Heart Disease and Stroke Statistics—2016 Update, Circulation.

Nogueira, R. G. *et al.* (2012) 'Trevo versus Merci retrievers for thrombectomy revascularisation of large vessel occlusions in acute ischaemic stroke (TREVO 2): a randomised trial.', Lancet (London, England). NIH Public Access, 380(9849), pp. 1231–40. doi: 10.1016/S0140-6736(12)61299-9.

Nouh, A. *et al.* (2017) 'Abstract TP210: Histopathological Evaluation of Thrombus in Acute Stroke and Correlation with Stroke Etiology', Stroke.

O'Cearbhaill, R. M. *et al.* (2016) 'Calcified cerebral emboli: A case series and review of literature', Journal of Systems and Integrative Neuroscience, 2(3), pp. 180–13.

O′Leary, S. A. *et al.* (2014) 'The biaxial mechanical behaviour of abdominal aortic aneurysm intraluminal thrombus: Classification of morphology and the determination of layer and region specific properties', Journal of Biomechanics, 47(6), pp. 1430–1437. doi: 10.1016/j.jbiomech.2014.01.041.

Paciaroni, M. *et al.* (2012) 'Systemic Thrombolysis in Patients With Acute Ischemic Stroke and Internal Carotid ARtery Occlusion', Stroke, 43(1), pp. 125–130. doi: 10.1161/STROKEAHA.111.630624.

Peshkova, A. D. *et al.* (2017) 'Activated Monocytes Enhance Platelet-Driven Contraction of Blood Clots via Tissue Factor Expression', Scientific Reports. Nature Publishing Group, 7(1), p. 5149. doi: 10.1038/s41598-017-05601-9.

Polzer, S. *et al.* (2012) 'Impact of poroelasticity of intraluminal thrombus on wall stress of abdominal aortic aneurysms', BioMedical Engineering OnLine, 11(1), p. 62. doi: 10.1186/1475-925X-11-62.

Poole, J. C. (1959) 'A study of artificial thrombi produced by a modification of Chandler's method.', Quarterly journal of experimental physiology and cognate medical sciences, 44, pp. 377–84.

Ramírez-Moreno, J. M. *et al.* (2017) 'Mechanical thrombectomy during ischaemic stroke due to a calcified cerebral embolism', Neurología (English Edition). Elsevier, 32(4), pp. 270–273. doi: 10.1016/j.nrleng.2015.06.008.

Riedel, C. H. *et al.* (2010) 'Assessment of Thrombus in Acute Middle Cerebral Artery Occlusion Using Thin-Slice Nonenhanced Computed Tomography Reconstructions', Stroke, 41(8), pp. 1659–1664. doi: 10.1161/STROKEAHA.110.580662.

Riha, P. *et al.* (1999) 'Elasticity and fracture strain of whole blood clots.', Clinical Hemorheology and Microcirculation, 21, pp. 45–49.

Robinson, R. A. *et al.* (2013) 'Limitations of using synthetic blood clots for measuring in vitro clot capture efficiency of inferior vena cava filters.', Medical devices (Auckland, N.Z.), 6, pp. 49–57. doi: 10.2147/MDER.S42555.

Ryan, E. A. *et al.* (1999) 'Structural Origins of Fibrin Clot Rheology', Biophysical journal, 77(November), pp. 2813-2826.

Saldívar, E., Orje, J. N. and Ruggeri, Z. M. (2002) 'Tensile destruction test as an estimation of partial proteolysis in fibrin clots.', American journal of hematology, 71(2), pp. 119–27. doi: 10.1002/ajh.10199.

Saqqur, M. *et al.* (2007) 'Site of Arterial Occlusion Identified by Transcranial Doppler Predicts the Response to Intravenous Thrombolysis for Stroke', Stroke, 38(3), pp. 948–954. doi: 10.1161/01.STR.0000257304.21967.ba.

Saver, J. L. *et al.* (2012) 'Solitaire flow restoration device versus the Merci Retriever in patients with acute ischaemic stroke (SWIFT): a randomised, parallel-group, non-inferiority trial.', Lancet (London, England). Elsevier, 380(9849), pp. 1241–9. doi: 10.1016/S0140-6736(12)61384-1.

Saver, J. L. *et al.* (2015) 'Stent-Retriever Thrombectomy after Intravenous t-PA vs. t-PA Alone in Stroke', New England Journal of Medicine, 372(24), pp. 2285–2295. doi: 10.1056/NEJMoa1415061.

Schmidt, C. E. *et al.* (1997) 'Stimulation of neurite outgrowth using an electrically conducting polymer.', Proceedings of the National Academy of Sciences of the United States of America, 94(17), pp. 8948–53.

Schmitt, C. *et al.* (2011) 'Characterization of blood clot viscoelasticity by dynamic ultrasound elastography and modeling of the rheological behavior', Journal of Biomechanics, 44(4), pp. 622–629. doi: 10.1016/j.jbiomech.2010.11.015.

Schwamm, L. H. *et al.* (2013) 'Temporal Trends in Patient Characteristics and Treatment With Intravenous Thrombolysis Among Acute Ischemic Stroke Patients at Get With the Guidelines-Stroke Hospitals', Circulation: Cardiovascular Quality and Outcomes, 6(5), pp. 543–549. doi: 10.1161/CIRCOUTCOMES.111.000303.

Shah, J. V. and Janmey, P. A. (1997) 'Strain hardening of fibrin gels and plasma clots', Rheologica Acta. Steinkopff-Verlag, 36(3), pp. 262–268. doi: 10.1007/BF00366667.

Shao, Q. *et al.* (2014) 'New method of thrombus preparation using a fluid model for evaluation of thrombectomy devices in a swine model', Thrombosis Research, 134(5), pp. 1087–1092. doi: 10.1016/j.thromres.2014.07.043.

Shin, J. W. *et al.* (2018) 'High red blood cell composition in clots is associated with successful recanalisation during intra-arterial thrombectomy', PLOS ONE. Edited by H. ten Cate, 13(5), p. e0197492. doi: 10.1371/journal.pone.0197492.

Siller-Matula, J. M. *et al.* (2008) 'Interspecies differences in coagulation profile.', Thrombosis and haemostasis, 100(3), pp. 397–404. Available at: http://www.ncbi.nlm.nih.gov/pubmed/18766254 (Accessed: 9 February 2018).

De Silva, D. A. *et al.* (2010) 'The Benefits of Intravenous Thrombolysis Relate to the Site of Baseline Arterial Occlusion in the Echoplanar Imaging Thrombolytic Evaluation Trial (EPITHET)', Stroke, 41(2), pp. 295–299. doi: 10.1161/STROKEAHA.109.562827.

Slaboch, C. L. *et al.* (2012) 'Mechano-rheological properties of the murine thrombus determined via nanoindentation and finite element modeling.', Journal of the mechanical behavior of biomedical materials, 10, pp. 75–86. doi: 10.1016/j.jmbbm.2012.02.012.

Spiotta, A. M. *et al.* (2015) 'Evolution of thrombectomy approaches and devices for acute stroke: a technical review.', Journal of neurointerventional surgery, 7(1), pp. 2–7. doi: 10.1136/neurintsurg-2013-011022.

Stary, H. (1999) Atlas of Atherosclerosis Progression and Regression. New York/London: Parthenon Publishing.

Teng, Z. *et al.* (2015) 'Layer- and Direction-Specific Material Properties, Extreme Extensibility and Ultimate Material Strength of Human Abdominal Aorta and Aneurysm: A Uniaxial Extension Study.', Annals of biomedical engineering. Springer, 43(11), pp. 2745–59. doi: 10.1007/s10439-015-1323-6.

Tutwiler, V. *et al.* (2016) 'Kinetics and mechanics of clot contraction are governed by the molecular and cellular composition of the blood', Blood. American Society of Hematology, 127(1), pp. 149–159. doi: 10.1182/blood-2015-05-647560.

Tutwiler, V. *et al.* (2018) 'Shape changes of erythrocytes during blood clot contraction and the structure of polyhedrocytes', Scientific Reports. Nature Publishing Group, 8(1), p. 17907. doi: 10.1038/s41598-018-35849-8.

Velasco, A. *et al.* (2016) 'Comparison of a Balloon Guide Catheter and a Non–Balloon Guide Catheter for Mechanical Thrombectomy', Radiology, 280(1), pp. 169–176. doi: 10.1148/radiol.2015150575.

Vidmar, J. *et al.* (2015) 'Unsuccessful percutaneous mechanical thrombectomy in fibrin-rich high-risk pulmonary thromboembolism.', Thrombosis journal. BioMed Central, 13, p. 30. doi: 10.1186/s12959-015-0060-2.

Walker, B. S., Shah, L. M. and Osborn, A. G. (2014) 'Calcified cerebral emboli, a "do not miss" imaging diagnosis: 22 new cases and review of the literature', American Journal of Neuroradiology, 35(8), pp. 1515–1519. doi: 10.3174/ajnr.A3892.

Wang, D. H. *et al.* (2001) 'Mechanical properties and microstructure of intraluminal thrombus from abdominal aortic aneurysm.', Journal of biomechanical engineering, 123(6), pp. 536–9.

Weafer, F. M. *et al.* (2019) 'Characterization of strut indentation during mechanical thrombectomy in acute ischemic stroke clot analogs', Journal of NeuroInterventional Surgery, 11(9), pp. 891-897 neurintsurg-2018-014601. doi: 10.1136/neurintsurg-2018-014601.

Weisel, J. W. (2004) 'The mechanical properties of fibrin for basic scientists and clinicians.', Biophysical chemistry, 112(2–3), pp. 267–76. doi: 10.1016/j.bpc.2004.07.029.

Weisel, J. W. (2007) 'Structure of fibrin: impact on clot stability.', Journal of thrombosis and haemostasis : JTH, 5 Suppl 1, pp. 116–24. doi: 10.1111/j.1538-7836.2007.02504.x.

Weisel, John W (2008) 'Biophysics. Enigmas of blood clot elasticity.', Science (New York, N.Y.), 320(5875), pp. 456–7. doi: 10.1126/science.1154210.

Weisel, J. W. (2010) 'Biomechanics in haemostasis and thrombosis', Journal of Thrombosis and Haemostasis, 8(5), pp. 1027–9. doi: 10.1111/j.1538-7836.2010.03808.x.

Wolberg, A. S. and Campbell, R. A. (2008) 'Thrombin generation, fibrin clot formation and hemostasis.', Transfusion and apheresis science : official journal of the World Apheresis Association : official journal of the European Society for Haemapheresis. NIH Public Access, 38(1), pp. 15–23. doi: 10.1016/j.transci.2007.12.005.

Xie, H. *et al.* (2005) 'Correspondence of ultrasound elasticity imaging to direct mechanical measurement in aging DVT in rats.', Ultrasound in medicine & biology, 31(10), pp. 1351–9. doi: 10.1016/j.ultrasmedbio.2005.06.005.

Xu, Z. *et al.* (2008) 'A multiscale model of thrombus development.', Journal of the Royal Society, Interface / the Royal Society, 5(24), pp. 705–22. doi: 10.1098/rsif.2007.1202.

Xu, Z. *et al.* (2012) 'Multiscale models of thrombogenesis.', Wiley interdisciplinary reviews. Systems biology and medicine, 4(3), pp. 237–46.

Yuki, I. *et al.* (2012) 'The Impact of Thromboemboli Histology on the Performance of a Mechanical Thrombectomy Device', American Journal of Neuroradiology, 33(4), pp. 643–648. doi: 10.3174/ajnr.A2842.

Chapter 3

Mechanical Behaviour of In-Vitro Blood Clots and the Implications for Acute Ischemic Stroke Treatment

3.1 Chapter Overview

This chapter investigates the effect of platelet-driven contraction on blood clot microstructure and mechanical behaviour, and provides insight into some implications for mechanical thrombectomy. Platelet-contracted clot analogues (PCCs) and non-contracted clot analogues (NCCs) were prepared from blood mixtures of various hematocrits (%H), i.e. the volume percentage of red blood cells (RBCs) in the mixture. Mechanical testing was performed to compare the behaviour of the analogues with previously tested human thromboemboli. Scanning electron microscopy and histology investigated the clot microstructure and composition of the clot analogues. The association between clot properties and their behaviour during mechanical thrombectomy was also investigated.

The content of this chapter has been published in the *Journal of NeuroInterventional Surgery* (Johnson *et al*. 2019).

3.2 Introduction

Thrombi, or blood clots, can form through various pathways *in-vivo* due to low flow/stasis, high shear flow conditions or blood being exposed to tissue factor because of vascular injury (Johnson *et al.*, 2017). Thrombi that cause obstruction to the normal flow in blood vessels are associated with a range of life-threatening conditions, such

as acute ischemic stroke (AIS), which accounts for 85% of all strokes (Van Der Worp and Van Gijn, 2007). Many treatment options for these thromboembolism related pathologies involve interventional methods with medical devices. In this chapter, *in-vitro* clot analogues are described, which may be utilised to aid in the understanding of AIS and the devices used to treat this devastating disease.

The formation of blood clots involves the inclusion of several components, mainly fibrin, red blood cells, platelets, white blood cells and extracellular water (Furie & Furie 2008). It has been shown through the examination of explanted human clots that these components vary significantly and are commonly non-uniformly distributed, therefore clots can be regarded as heterogeneous composite materials (Marder *et al*. 2006; Duffy *et al*. 2019). The mechanical properties of clots are determined by the ratio, arrangement and interaction of these components. Examination of clot microstructure shows complex interactions between the components, which can reveal the biochemical processes under which they formed.

A key initiator and regulator of clot formation is the platelet, these cell fragments expel hemostasis regulatory proteins. Transformation from an anti-thrombotic, circulating smooth cell fragment into a pro-thrombotic, ‘sticky’ structure belies the platelets role as a conductor of the coagulation cascade that adapts and changes depending on a host of biochemical and local environmental factors. Fibrin is another main player in coagulation, rapidly polymerising from its soluble form, fibrinogen, into a remarkable network of interconnected branched fibres to locally solidify the blood. The structure of the fibrin polymer network differs based on the hemodynamic conditions at the site of formation and the relative quantity of other blood components included within the network.

After solidification of the blood, platelet-driven clot contraction tightens the fibrin network by gathering fibrin strands to adhered platelets. This process continues and leads to the merging of individual platelets into agglomerates that can exert even greater contractile forces. The effect on the clot is a reduction of volume with expulsion of serum and a close packing of the blood components entrapped in the network. Thus, clot contraction acts twofold to reduce blood loss by creating an impermeable seal at the site of vessel injury and to restore vessel patency by reducing the size of the clot protruding into the vessel. It has been found that the extent of clot contraction is sensitive to hematocrit, i.e. the volume percentage of RBCs in the blood (%H) (Tutwiler *et al*. 2018), fibrinogen concentration and platelet function.

Mechanical thrombectomy (MT) using medical devices has recently been universally added to the standard of care for the treatment of AIS (Goyal *et al*. 2016; Fransen *et al*. 2014; Saver, Goyal, Bonafe, Diener, Levy, Pereira, Albers, Cognard, Cohen, Hacke, Jansen, Jovin, Mattle, Nogueira, Siddiqui, Yavagal, Baxter, Devlin, Lopes, Reddy, du Mesnil de Rochemont, Singer, Jahan, *et al*. 2015), where it greatly improves outcomes for eligible patients. It is implicit that the success of mechanical thrombectomy procedures are significantly affected by the mechanical properties of the thrombus itself.

Analysis of thrombus material from human sources can often be expensive and highly regulated, making specimens difficult to obtain. Therefore clinically relevant thrombus analogues, that are formed *in-vitro,* are an extremely useful and attractive tool in the pre-clinical testing of these devices to evaluate metrics such as the number of attempts required to remove the thrombus and the risk of further embolism (Liebig *et al.*, 2008; Chueh *et al.*, 2011; Duffy *et al.*, 2016). They present an attractive option

because they can be constructed from blood proteins and components present in the clotting cascade, and therefore have a similar chemical structure to native clots.

Several clot analogues have previously been described that can be used in the assessment of medical devices (Chueh *et al.*, 2011; Duffy *et al.*, 2016). Simulated thrombectomy procedures with such clots have effectively aided the evaluation of thrombectomy devices (Fennell *et al*. 2018; Machi *et al*. 2017); additionally these clot analogues have been used for the assessment of specific clot attributes such as coefficient of friction (Gunning *et al*. 2016), indentation/integration (Weafer *et al*. 2019) and appearance in medical imaging modes (Bourcier *et al*. 2018).

The growing use of the experimental clot models for thrombectomy device testing continues with a goal to provide clinicians with treatment strategies based on laboratory findings; therefore it is critical to have clot models that are clinically representative in terms of their bulk mechanical behaviors as well as compositional features.

In this chapter a range of repeatable clot analogues are presented, along with an analysis to advance the understanding of how platelet-driven contraction can affect the clot mechanical properties and microstructure and, in turn, how this can have implications for MT. Platelet-contracted clot analogues (PCCs) and non-contracted clot analogues (NCCs) were prepared from blood mixtures of various hematocrits (%H). Mechanical testing was performed to compare the behaviour of the analogues with previously tested human thromboemboli. Scanning electron microscopy and histology investigates the clot microstructure and composition. Finally, the association between clot properties and their behaviour during MT was investigated.

3.3 Materials and Methods

3.3.1 Sample Preparation

Fresh venous blood was collected from sheep for the preparation of the clot samples for testing (Cummings School of Veterinary Medicine). Ovine blood was chosen as it has been found to be a suitable substitute for human blood for coagulation studies (Siller-Matula *et al.*, 2008) and the clot samples produced using this methodology have been found to be histologically similar to human clots (Duffy *et al*. 2016). Blood was collected in receiving vessels pre-loaded with ACPD (Adenine citrate phosphate dextrose) anticoagulant solution. The blood was then transported to the lab and stored at room temperature until used. All clots were prepared within 5 hours of blood collection.

To begin clot preparation, the blood was centrifuged at 180 g for 10 minutes. The platelet-rich plasma (PRP) was removed and collected into a separate container. The remaining blood mixture was then centrifuged again at 2200 g for 10 minutes to separate the platelet-poor plasma (PPP). The PPP was carefully collected, ensuring that the buffy layer was not disrupted. The buffy layer was then removed as waste and the erythrocyte-rich (RBC) layer remained.

Two families of clot analogues were produced – platelet contracted and non-contracted. Platelet contracted clots were formed from blood mixtures with different hematocrit (%H) by mixing the platelet rich plasma (PRP) with the red blood cells in controlled ratios. Similarly, the non-contracted clots were produced by mixing the platelet poor plasma (PPP) with the red blood cells in the same ratios.

Once the various blood mixtures were produced, coagulation was initiated by the addition of a 2.06% calcium chloride solution to the blood components in a 1:9 ratio.

The samples were formed in cylindrical-shaped moulds (Figure 3.1 A) and were placed standing vertically to mature overnight at 37°C. The extent of contraction was assessed gravimetrically by weighing the solid and liquid phases in the clot moulds. The colour of the serum was monitored to ensure the RBCs had been incorporated.

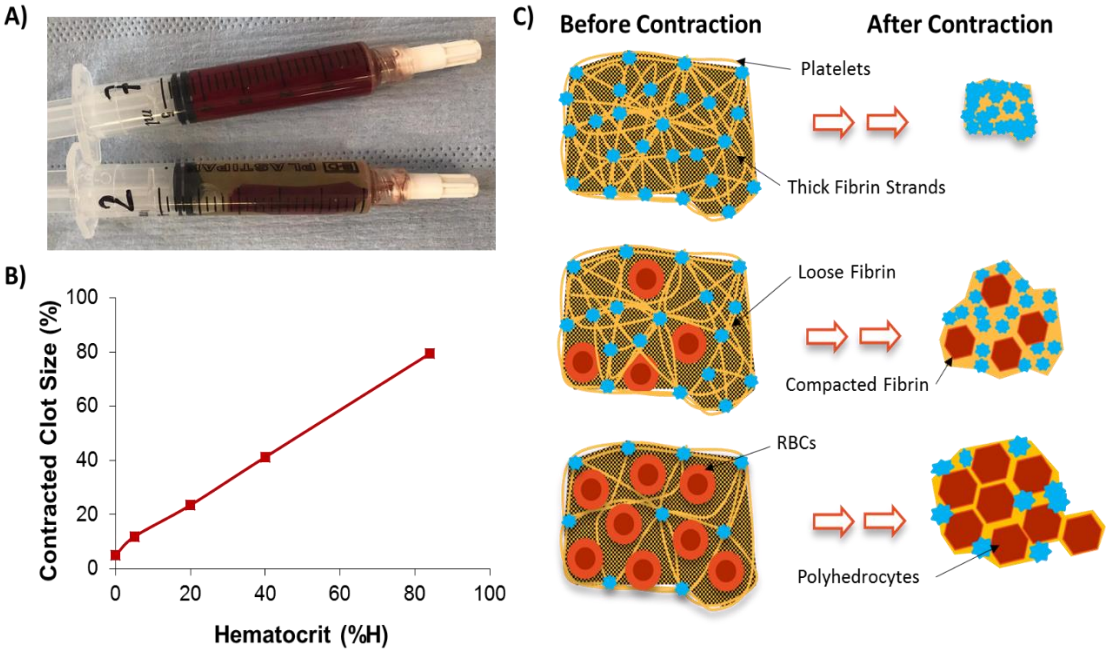

Figure 3.1 (A) Non-contracted clot (NCC) (top) and a platelet-contracted clot (PCC) with expelled serum (bottom). (B) Plot of contracted clot size (expressed as a % of the original weight of blood mixture before clotting) versus hematocrit of the blood mixture. (C) Schematic diagram depicting clot contraction and how it is limited by the red blood cells (RBCs) present. Before contraction, the clots consist of a loose fibrin mesh (yellow) with RBCs (red) scattered throughout and platelets (blue) attached at junctions of thicker fibrin fibres. After contraction, the fibrin compacts around polyhedron-shaped RBCs (polyhedrocytes) and serum is expelled, resulting in reduced clot volume.

3.3.2 Mechanical Characterisation

Compression testing was selected to characterise the analogue material as this method is sufficiently robust to allow reliable testing of a broad range of clot types and it allowed the author to compare the mechanical behaviour of the presented clot analogues with that of previously tested human AIS samples. Tensile testing of the samples was initially attempted, however reliable tensile testing did not prove possible and often resulted in tearing/rupturing at the grips due to the fragile nature of the clots.

A Dynamic Mechanical Analyser (DMA, Q800; TA Instruments, New Castle, Delaware), was used to investigate the mechanical behaviour of the clot analogues. The test was carried out using a submersion compression clamp in the controlled force mode and the samples (minimum of n = 3 for each group) were tested in a 0.9% saline solution (Baxter Healthcare SA, Zurich, Switzerland) at 37°C. Cylindrical clot samples, with a diameter of approximately 5 mm, were cut to have an approximate height of 3 mm, as in the study by Chueh *et al.* (2011). The samples were placed in saline for 30 minutes prior to testing. 220-grit sandpaper was adhered to the compression disk to prevent the samples from slipping out during the test. The test consisted of a force ramp to 15 N at a rate of 0.5 N/min, according to Chueh *et al.* (2011), in compression.

To compare the mechanical behaviour of the materials, tangent stiffnesses were determined from the slopes of straight lines fitted to the initial and final linear portions of the nominal stress-strain curves: a low strain tangent stiffness (over approx. initial 10% strain) and a large strain tangent stiffness (over approx. the final 2% strain). It is worth noting that these quantities are dependent on the specific test conditions and are used here as a convenient measure to compare mechanical performance. True stress-

strain curves could not be generated for these tests as there was no reliable measurements for contact area due to the nature of the test set-up.

An additional indicator of the mechanical behaviour is the onset point (Chueh *et al*. 2011), which was obtained as the intersection point of the aforementioned two lines. Statistical analysis was carried out using the general linear model ANOVA procedure in Minitab (ver. 18.1). A comparison of mean onset point was performed with a Bonferroni model (alpha = 0.05) to compare the onset point of the clot analogues with the human thromboemboli tested by Chueh *et al.* (2011).

3.3.3 Histology

MSB staining was selected as an appropriate method to stain for fibrin and erythrocytes (Chueh *et al*. 2011; Duffy *et al*. 2016). Sections of both the contracted and non-contracted clot analogues were fixed in a 10% buffered formalin solution after removal from the incubator and left for 48 hours. The samples were then embedded in a paraffin wax and cut into 5 μm sections. The sections were dewaxed and hydrated with distilled water in preparation for staining.

Sections were photographed using an Olympus VS120 digital slide scanner. The objective lens, brightness, and height of the condenser, as well as the saturation, brightness, and contrast settings of the image acquisition software were standardised to ensure uniformity of the digitised images. Images were acquired at 40x magnification from 5 randomly chosen areas of the slide. The quantification method followed was previously reported to assess the composition of human thrombi (Liebeskind *et al*. 2011) and clot analogues. Image J software was used for quantitative analysis of the percentage fibrin and RBCs by area by (Duffy *et al.*, 2016) by applying

thresholds to the image and quantifying the various components as a percentage of the total area.

3.3.4 Scanning Electron Microscopy (SEM)

The analogue samples were fixed with 2.5% glutaraldehyde and dehydrated in a series of ethanol concentrations up to 100%. The samples were frozen in liquid nitrogen and fractured so that the interior surface of the clot analogues could be examined. The samples were then critical-point dried, mounted and sputter-coated with iridium.

3.3.5 In-Vitro Simulation of Thrombectomy

An *in-vitro* model based on the human intracranial circulation was used for observational thrombectomy experiments (Figure 3.2). The model consisted of the complete intracranial circulation with both carotids and vertebral arteries, complete circle of Willis, and functional anterior and posterior communicating arteries with distal circulation up to M2 and A2 (Elastrat Sàrl, Geneva, Switzerland) (Matos Casano *et al*. 2019; Navarro-Orozco & Sánchez-Manso 2019).

Saline at 37°C was circulated through the model and the rate of flow was set to be within the range of clinically representative flow rates. To consistently target the same region of the anatomy, both PCCs and NCCs were cut to have dimensions of 3 mm×3 mm×8 mm, introduced into the model and allowed to migrate in the vessel to the target location to facilitate a distal M1 segment occlusion of the middle cerebral artery. Clots that did not reach the M1, or migrated too far distally, were discarded and replaced with a new clot to ensure consistent clot location for each procedure.

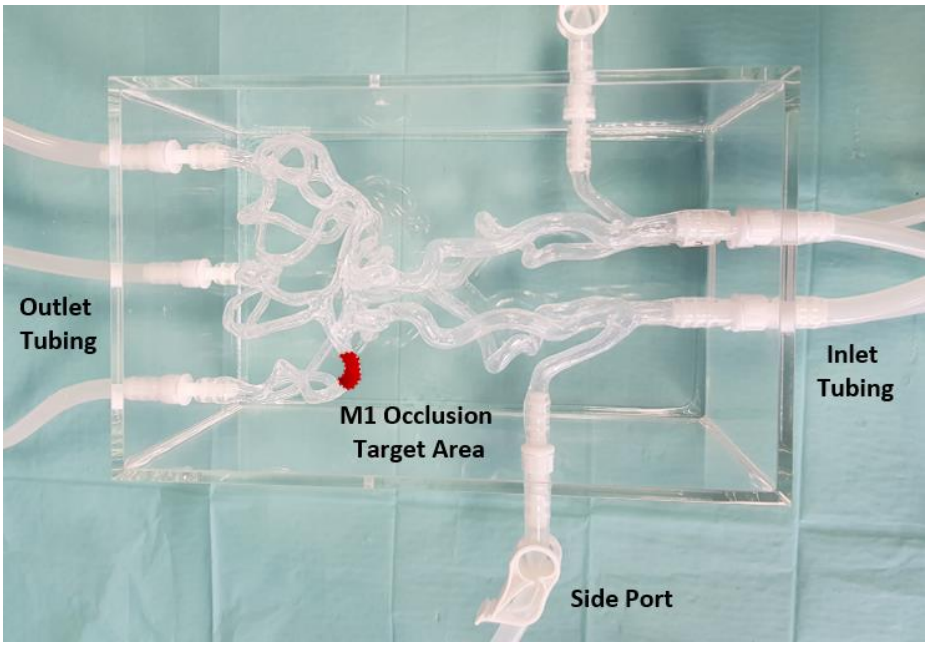

Figure 3.2 Silicone vascular flow model used to complete the *in-vitro* mechanical thrombectomy procedures; highlighting the side port into which clot was introduced and the M1 segment of the middle celebral artery in which occlusions occurred.

Two retrieval techniques were used to remove the clot analogues; contact aspiration with an aspiration catheter and retrieval via stent-retriever combined with local aspiration into an intermediate catheter. An ACE 64 (Penumbra, Alameda, CA, USA) intermediate catheter was used for the former, and a 33x5 mm Embotrap II stent-retriever (Cerenovus, Galway, Ireland) and an ACE 64 intermediate catheter were used for the latter. A Medium Support 0.014” straight tip guidewire (Boston Scientific, Marlborough, USA) and an ev3 Rebar (ev3, Irvine, CA, USA) 0.021” microcatheter were used to cross the clot for the retrievals using the stent-retriever. For contact aspiration alone, the catheter was advanced to the face of the clot over the guidewire and aspiration was applied using a Hersill V7 Plus AC aspiration pump (Hersill Medical Devices, Madrid, Spain), which was set to “high”. The interaction of the clot with the devices was investigated by observing the behaviour of the clot and device during retrieval.

3.4 Results

3.4.1 Gravimetric Analysis of Clot Analogues

For all clots, in the early stage following clotting initiation (within 30 minutes) the entire blood mixture was solidified in to a clot. When subsequent clot contraction occurred, the extent of clot contraction was calculated by weighing the combined serum and clot together and the resultant clots alone using a gravimetric balance. Mass reduction due to contraction was calculated by expressing the weight of the clot as a percentage of the weight of the clot and serum together. No serum was expelled from the NCCs, indicating that there was no mass loss due to contraction. However, PCCs had a reduced weight due to expulsion of serum. The eventual size of the PCCs strongly correlates (R^2 = 0.99) to the %H of the clot mixture (Figure 3.1 B). An additional gravimetric assessment of the NCCs was carried out whereby the NCCs were mechanically compressed by spinning twice in a centrifuge for 10 minutes at 2200 g. The final weight of these mechanically contracted clots also correlated to the %H of the blood mixtures (Figure 3.3), thereby demonstrating that RBCs, entrapped in the clot network, are a limiting factor for the final clot volume.

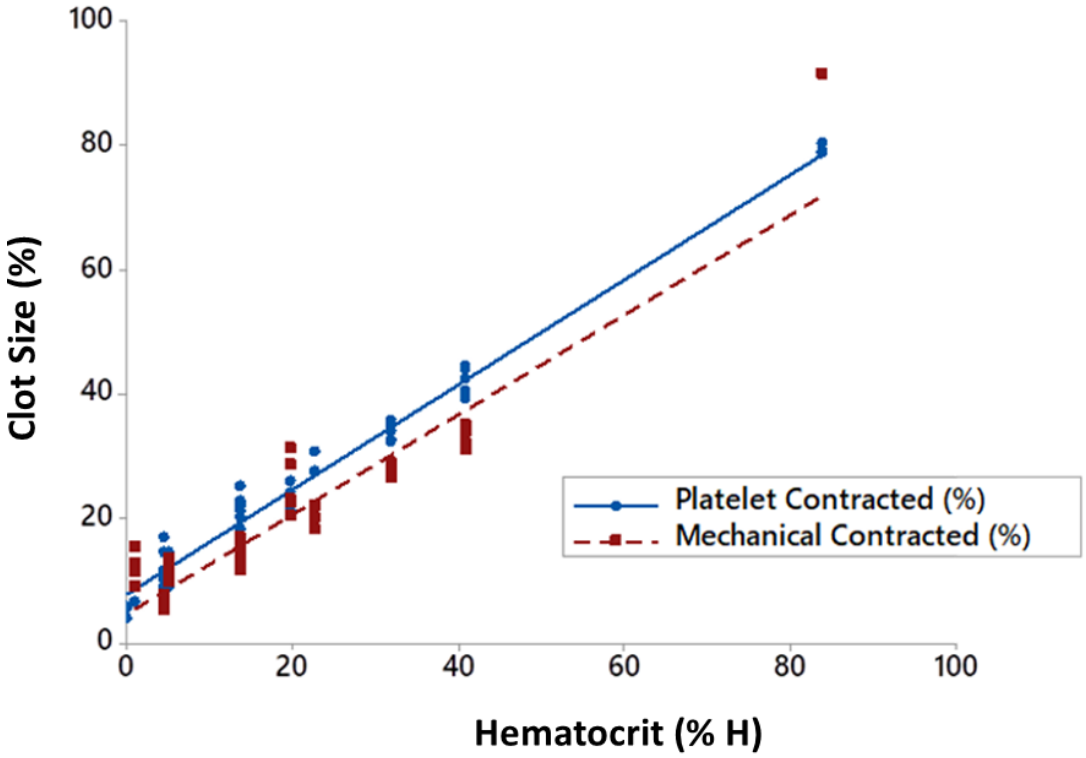

Figure 3.3 Plot of clot size (expressed as a % of the original clot weight of the blood mixture before clotting) versus hematocrit, comparing the clot size after platelet contraction (in blue) and mechanical contraction by centrifuging for 10 minutes at 2200 g (in red). The clot contraction for both methods was found to have a linear correlation with the clot hematocrit i.e. the volume percentage of red blood cells (RBCs) within the clot, highlighting that the RBCs limit the contraction of the clot network due to their incompressibility.

3.4.2 Mechanical Behaviour of Clot Analogues

The mechanical testing shows that all clots exhibit non-linear stress-strain behaviour (Figure 3.4 A). PCCs had earlier onset points than NCCs (Figure 3.4 B), meaning as they deform under an applied force, they begin to stiffen sooner. The 20% H PCC was found to have the earliest onset point, stiffening sooner than the rest of the analogues. A non-linear dependence on hematocrit was observed.

The mechanical behaviour of the clot analogues was compared to thromboemboli tested by Chueh *et al.* (Figure 3.4 A-B). There was a significant difference when comparing the onset of the AIS thrombi with the NCCs and the 0% and 5% H PCCS (Figure 3.4 B). Both groups of analogues were found to have lower stiffnesses than the human thromboemboli at low levels of strain (< 30%) (Figure 3.4 C), by almost an order of magnitude. However, all of the clot analogues were found to reach similar stiffness levels at high strain levels (Figure 3.4 D) and to span the range of large strain stiffnesses measured in the *ex-vivo* emboli.

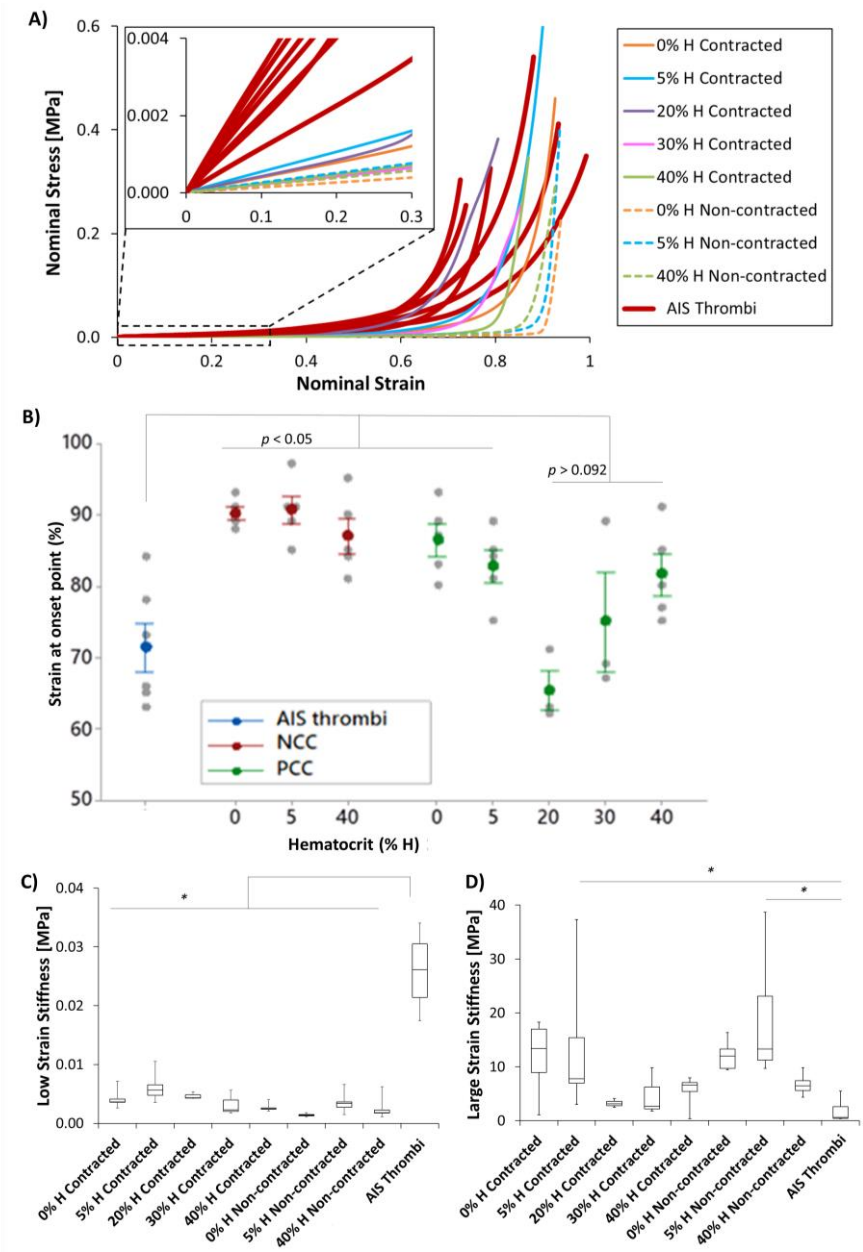

Figure 3.4 (A) Average nominal stress-strain curves for the compression testing (n≥3 for each group), shown as positive values for clarity, comparing the mechanical behaviour of the platelet-contracted clots (PCCs) and non-contracted clots (NCCs), with the raw data for the human AIS red thrombi previously tested by Chueh *et al.* (2011), where each sample tested is represented by an individual red line (n=6). Inset, is a zoomed-in image of the behaviour at low levels of strain. (B) Plot of onset point versus hematocrit, comparing the onset point of both the PCCs and NCCs with the human thromboemboli. (C) Comparison of low strain stiffness and (D) stiffness at large strain for the PCCs and NCCs with the human AIS thrombi. * denotes statistical significance where $p<0.05$.

3.4.3 Composition and Structure of Clot Analogues

Histological examination of the clot analogues shows little difference in the fibrin and RBC content when comparing the PCCs and NCCs at the same hematocrit levels (Figure 3.5).

However, the % content of RBCs measured was found to be slightly higher than the known clot hematocrit. When the clots are formed, controlled ratios of RBCs and plasma are added. However not all of the plasma is converted to fibrin as it contains other clotting factors and components. Therefore, the RBC content is greater than the % H added during clot formation and the percentage of fibrin in the clot is slightly less than estimated. This has also previously been observed in the study by (Duffy *et al.*, 2016).

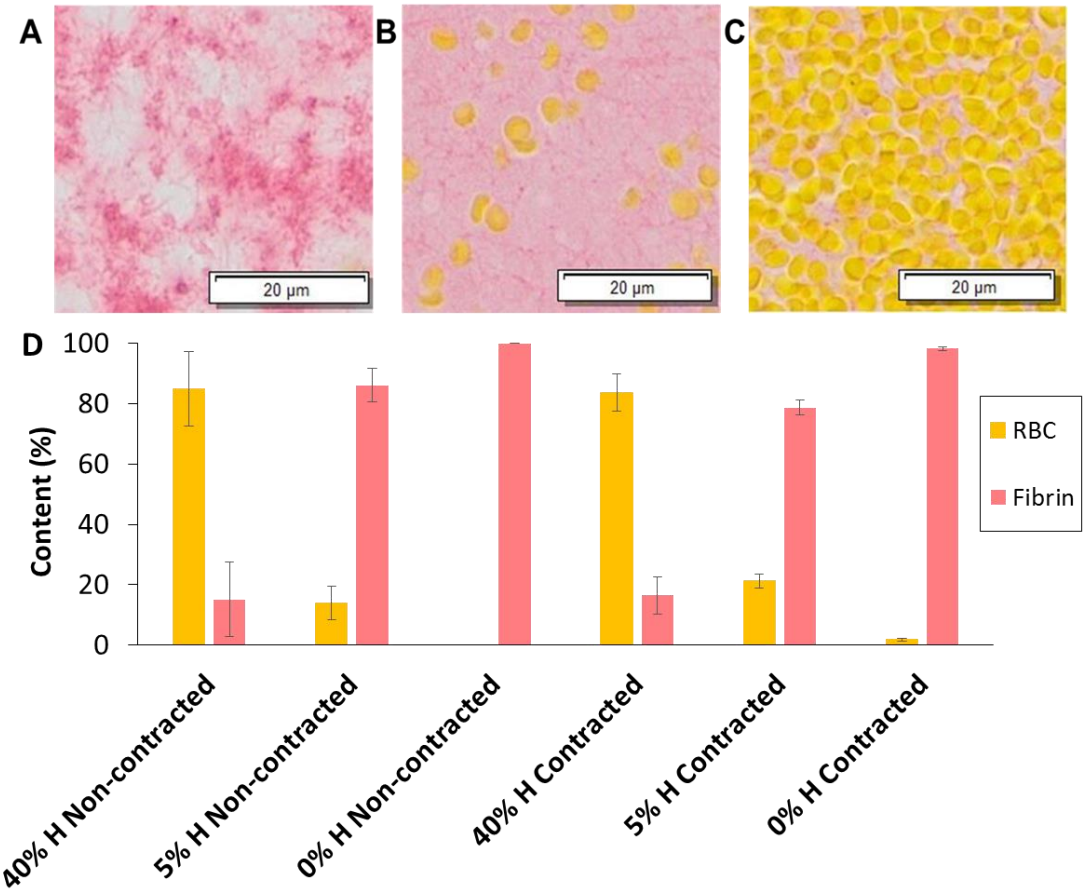

Figure 3.5 MSB staining of A) a 0% H clot, B) a 5% H clot and C) a 40% H clot. MSB stained fibrin in pink and RBCs in yellow. D) Bar graph comparing the % content of fibrin and RBCs in both contracted and non-contracted clot samples across three hematocrits.

However, under SEM the microstructure of both groups are significantly different (Figure 3.6 A-D). Two types of fibrin fibres were observed, thick fibres (179.8 nm ± 80 nm) with relatively few branches and thin hyper branched fibres (45.75 nm ± 11.5) (Li *et al*. 2016). The former is observed in abundance on the exterior of the clots and traversing the interior, while the latter is seen in the interior only. In the NCCs, the thin, highly branched fibrin occupies the spaces between the red blood cells and thicker fibrin fibres (Figure 3.6 A and C). This spongy fibrin network is significantly compressed through the action of clot contraction (Figure 3.6 B & D), appearing as a very thin layer on the faces of closely packed RBCs in Figure 3.6 D.

Noticeable changes in red blood cell shape are also apparent. The typical biconcave-shaped RBCs are clearly observed in the NCCs, whereas the PCCs consist of compressed fibrin structures, compacted around polyhedron-shaped RBCs, called ‘polyhedrocytes’ (Cines *et al.*, 2014). The thicker fibrin fibres are seen to entrap the polyhedrocytes in a latticework of fibres. Imprints seen where the fibrin has come away from the face of the RBCs establishes that contractile forces exerted by platelets, and conveyed through the fibrin, are responsible for the RBC shape change.

All of the clot analogues were found to have a fibrous layer containing thicker fibrin fibres covering the exterior of the clot (Figure 3.6 E and F). In PCCs, a higher concentration of platelets is also visible on the outside of the clot when compared to the interior.

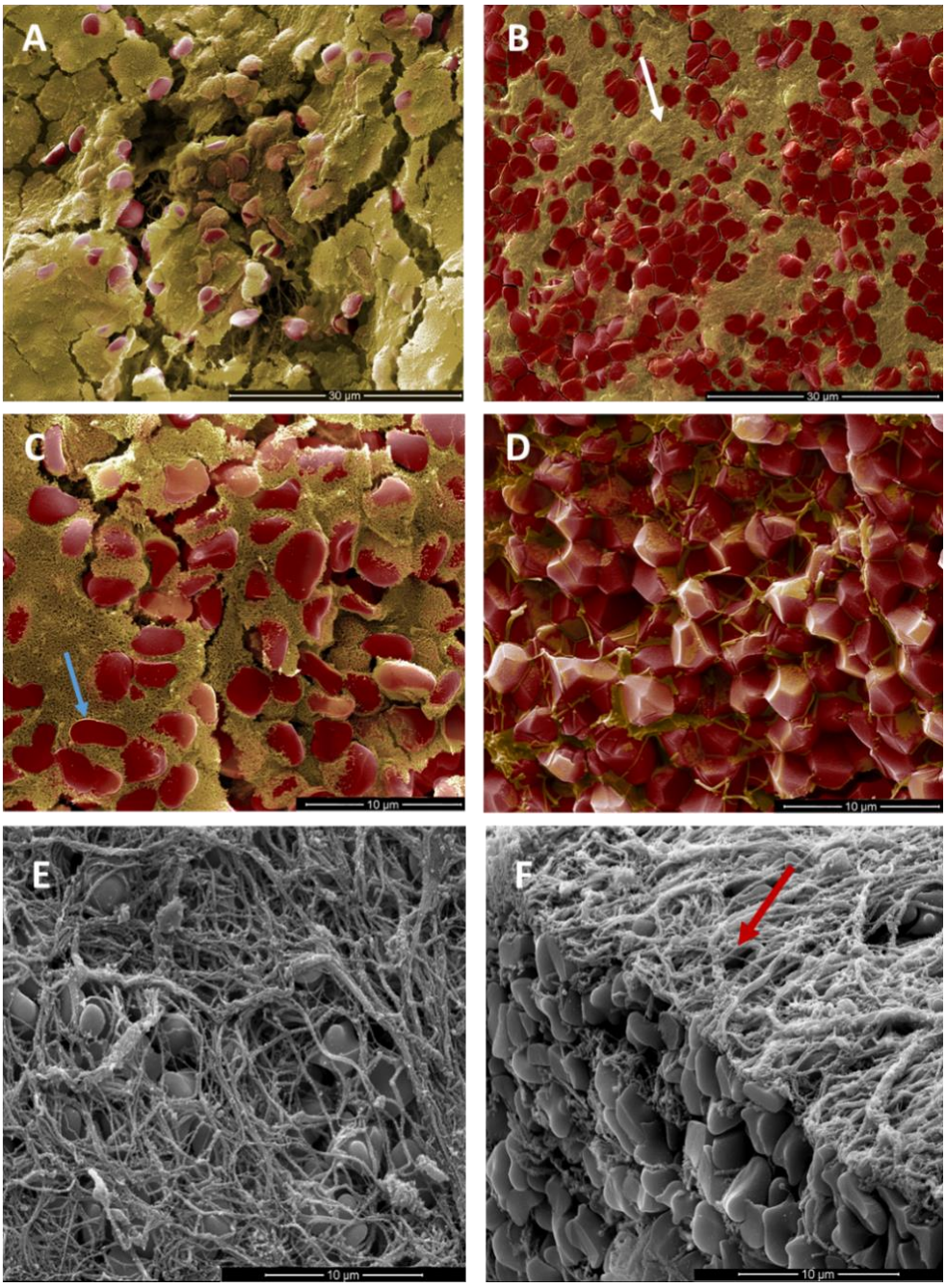

Figure 3.6 Coloured SEM images taken of the clot analogues, with fibrin coloured yellow and RBCs coloured red. Images A & B show the interior of a 5% H non-contracted and contracted clot analogue respectively, with the white arrow indicating an area of compressed fibrin. Image C depicts the interior of a 40% H non-contracted. The blue arrow highlights a typical biconcave-shaped RBC trapped within a loose fibrin mesh. Image D shows the polyhedrocytes present in the interior of a 40% H contracted clot analogue. Images E & F are SEM images illustrating the large fibrin strands covering the exterior surface of the clot analogues (E), comparing the interior and exterior surfaces (F) of the clot, with the red arrow indicating the outer surface.

3.4.4 In-Vitro Retrieval of Clot Analogues

MT was simulated in an *in-vitro* flow model using two approaches – (1) contact aspiration with an aspiration catheter and (2) retrieval via stent-retriever combined with local aspiration into an intermediate catheter (IC). For the aspiration only technique, it was not possible to fully aspirate PCCs formed with 0% H or 5% H into the aspiration catheter, however the clots were subsequently successfully retrieved by removing the catheter and clot en-bloc (Figure 3.7). NCCs were successfully aspirated fully through the aspiration catheter. The results from the combined approach were similar. The lower hematocrit PCCs were not fully retrieved into the IC using the stent-retriever requiring en-bloc removal of the clot with the stent-retriever and IC.

NCCs and PCCs formed from blood mixtures with a higher hematocrit were fully retrieved into the IC, either with aspiration alone or through use of a stent-retriever. However, considerably more fragmentation was observed for the 40% H PCC compared to the 40% H NCC as they entered the IC using both techniques.

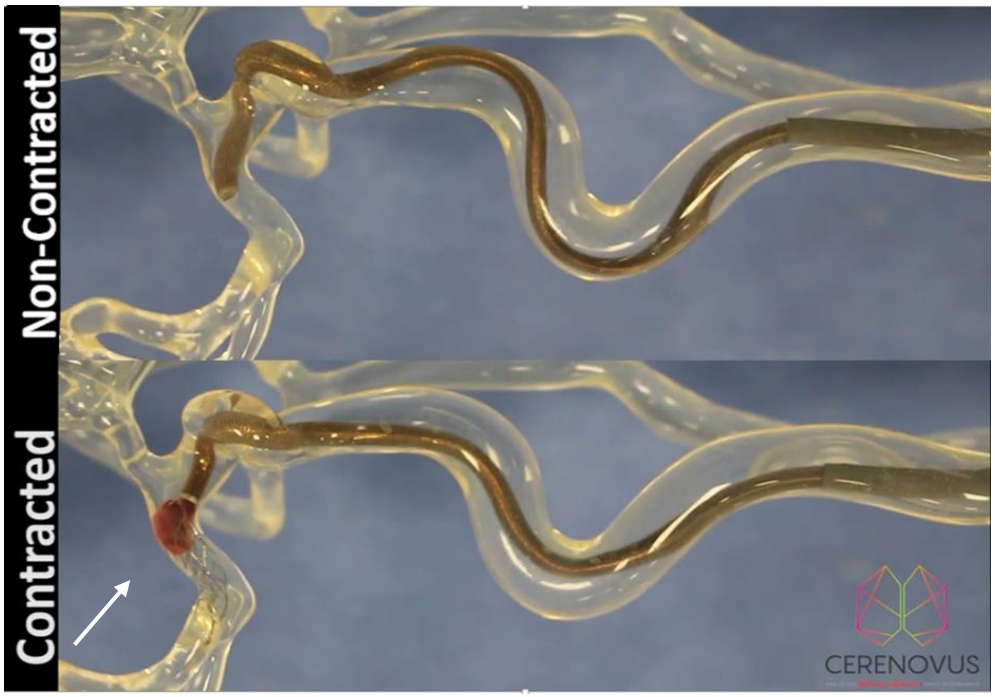

Figure 3.7 Image comparing the full retrieval of the non-contracted clot (above) and partial retrieval of the contracted clot (below) into the intermediate catheter using the stent-retriever. The intermediate catheter was pulled back into the guidecatheter with the contracted clot corked at the end, as highlighted by the white arrow.

3.5 Discussion

Clot mechanical properties, composition and structure are important factors in the treatment of AIS. There are many protocols in the literature for the manufacture of clot analogues for the *in-vitro* testing of these treatment methods, and common variables include the donor species, concentration of thrombin and fibrinogen, and radiopacity. Many studies have demonstrated the effect these variables have on the mechanical properties of clot analogues (Chueh *et al.*, 2011; Duffy *et al.*, 2016; Malone *et al.*, 2018). However, to date few studies have investigated the effect of platelet contraction and hematocrit on the mechanical behaviour and microstructure of clot material.

This chapter has shown that the mechanical properties of clot analogues can be significantly altered by the activation of platelets during clotting and also by varying the hematocrit. The extent of clot contraction was found to be hematocrit-dependent, as clots formed from blood mixtures with a lower hematocrit contracted more than clots with a greater hematocrit. This is due to the incompressible RBCs present.

The clot analogues were found to have a similar, non-linear stress-strain relationship and mechanical behaviour to published data for clot material (Chueh *et al*. 2011; Malone *et al*. 2018; Krasokha *et al*. 2010; Ashton *et al*. 2009). The NCCs were found to be less stiff than the PCCs across all hematocrits. Of the PCCs, the 40% H clot had the lowest low strain stiffness. This is likely due to the lower levels of fibrin present, combined with the increased number of RBCs present, reducing the overall stiffness. However, the clots formed from 20% H blood had a greater compressive stiffness than 0% H and 5% H clots. Similarly, the 20% H and 30% PCCs had the earliest onset points, stiffening sooner than the rest of the analogues but at a similar point to the human AIS thrombi. It is hypothesised that the ratio of fibrin to RBCs in the fibrin matrix is optimal in clots within this range of hematocrit, and the stiffness is increased potentially due to a reinforcement effect of the RBCs within the fibrin matrix. However further testing with a larger sample size is necessary to confirm this result.

The low strain stiffness of the human AIS thrombi appears to be an order of magnitude greater than the clot analogues. This may be due to the heterogeneous nature of the human AIS thrombi causing an increase in stiffness at low strains. However, the large strain stiffnesses of the analogues were found to span the range measured for the human AIS thrombi at large strains. Since MT causes large strain in the clot material, it is considered that clot behaviour at these strains (< 60%) is of most interest when comparing the analogues with the human thrombi.

Contracting platelets actively remodel the fibrin network by tightening the fibres, and therefore the enhanced stiffness of the PCCs can be explained by examining their microstructure. The NCCs were found to consist of a loose fibrin mesh with biconcave–shaped RBCs homogeneously dispersed throughout, whereas the PCCs consisted of compacted fibrin around polyhedrocyte-shaped RBCs. The loose fibrin mesh in PCCs can be easily deformed under compression, thus resulting in lower clot stiffness.

In clots that contained RBCs, the shape of the RBCs and their interaction with the surrounding fibrin can be used to understand how the mechanical properties change through the process of platelet driven contraction. Prior to clot contraction RBCs maintain a biconcave shape and are homogeneously dispersed throughout the fibrin network, following platelet contraction the RBCs are compacted closely with individual cells exhibiting a polyhedrocyte shape (Tutwiler *et al*., 2017). The close packing of red-blood cells creates a watertight seal and allows a maximum reduction in clot volume, both of which are important for reperfusion.

Contracted clots formed from blood mixtures with a high hematocrit are dominated by red blood cells that are homogeneously dispersed throughout, however clots formed from lower hematocrit blood mixtures exhibit grouping of the red blood cells into RBC rich domains, surrounded by compressed fibrin. Thicker fibrin fibres surrounding the RBCs were observed to have left imprints in the faces of the polyhedrocytes, which indicates that it is through these thick fibrin fibres that the platelet-driven contraction of the clots is propagated. The hyperbranched, thin-fibre fibrin was observed to compress significantly after contraction, which indicates that it is the compression of this porous material with the subsequent expulsion of serum, which accounts for the majority of clot volume reduction between initial clot formation and the final

contracted state. The RBCs were found to be homogeneously distributed throughout these statically formed analogues in both groups, with a fibrin rich layer enveloping all clots. For clots that contained platelets, the platelets were also observed in much greater abundance on the outer layer as has previously been described in the literature. Local clustering of RBCs was observed in clots that formed from low hematocrit blood mixtures, which indicates the existence of a mechanism for movement of RBCs out of the fibrin meshwork during clot contraction.

Platelet contraction had the effect of increasing stiffness and together with adjustment of the hematocrit enables close matching of stiffness to representative thromboemboli of AIS origin. The lower stiffness of the NCCs clots is unsurprising considering the large volume of extracellular water (serum) in these clots. However the behaviour of the NCCs is also relevant as patients of AIS often exhibit impaired platelet contraction and therefore there is a mechanism by which NCC clots can arise *in-vivo* (Tutwiler, Alina D. Peshkova, *et al*. 2017).

Polyhedrocytes have been observed in human coronary thrombi (Cines *et al.*, 2014) and it is hypothesised that this shape allows for more efficient packing of RBCs (Tutwiler *et al*. 2018) thus creating an impermeable seal at the site of vessel injury to prevent bleeding (Kim *et al*. 2017). This decreased permeability may impact the effectiveness of medical thrombolytic therapy in AIS. *In-vitro* thrombectomy experiments reported in this chapter show that clot engagement with devices differed for PCCs and NCCs, with PCCs having fewer RBCs incorporated resisting full ingestion or retrieval into catheters. PCCs with a greater hematocrit appeared to be more prone to fragmentation than their NCC counterparts.

Clot composition has been assessed *ex-vivo* (Chueh *et al.*, 2011; Yuki *et al.*, 2012; Duffy *et al.*, 2016) to determine a potential relationship between thrombus histology and difficulty of clot removal. Many medical imaging studies attempting to determine the difficulty of clot removal based on predicting the composition of clots using CT or MRI have also been carried out (Liebeskind *et al*. 2011; Kirchhof *et al*. 2003; Fujimoto *et al*. 2013; Gasparian *et al*. 2015). The quantitative histological measurement of RBC and fibrin composition in this study failed to distinguish clots based on their mechanical properties. Similarly, the histological staining failed to highlight the polyhedrocyte shape of the RBCs in the contracted clots due to the large clusters of RBCs compacted together within the network. However, SEM analysis of the clot microstructure clearly highlighted how clots formed from blood solutions with the same hematocrit can depict varied mechanical behaviour. Taken together, the significant difference in mechanical properties and microstructure but without an appreciable difference in RBC and fibrin composition, implies that histological examination of the fibrin and RBC content of explanted human clots alone should not be used in isolation as a predictor of the mechanical behaviour of the clots in thrombectomy.

3.5.1 Limitations

One limitation of this investigation is the homogeneous nature of the clots, as they are prepared under static conditions in a controlled laboratory environment, whereas clots retrieved from patients tend to have irregular distribution of components. However, for the purposes of understanding the mechanical behaviour of clots it is necessary to use homogeneous samples. Nevertheless, it should be noted that clots *in-vivo* may be heterogeneous.

Another limitation is the use of sandpaper to keep the sample in place and to prevent it from slipping out from between the plates during testing. This increases the friction between the sample and the plates and could prevent the samples from being in a uniform stress-state during the testing.

There are few studies that have investigated the mechanical properties of human AIS thrombi and therefore there is limited data to compare our clot analogues with. In this chapter, we compare the mechanical behaviour to one classification of thromboemboli that were retrieved from patients with AIS via aspiration (Chueh *et al*. 2011). However, these ex-vivo clots may have already experienced severe deformation during aspiration and therefore there is the possibility that their mechanical properties were altered prior to testing.

3.6 Conclusion

This chapter presents a selection of repeatable clot analogues with a range of mechanical properties have been developed for *in-vitro* modelling of AIS. The preparation and characterisation of both platelet-contracted and non-contracted clot analogues with varying hematocrit is outlined and the effect of clot contraction on the microstructure and mechanical behaviour of the material is demonstrated.

Although significant differences in mechanical properties and microstructure was observed between PCCs and NCCs, histological quantification of fibrin and RBCs in these clots did not show an appreciable difference. The implication is that RBC content alone, measured by histology, of explanted human clots may not be predictive of their mechanical behaviour during thrombectomy.

As clot contraction can also affect the clot permeability, it is hypothesised that this may impact the effectiveness of stroke treatments such as thrombolysis and MT. The

clot analogues presented in this chapter have been shown to be useful for the evaluation of different clot behaviour during mechanical thrombectomy.

3.7 References

Ashton, J. H. *et al.* (2009) 'Compressive mechanical properties of the intraluminal thrombus in abdominal aortic aneurysms and fibrin-based thrombus mimics', Journal of Biomechanics, 42(3), pp. 197–201. doi: 10.1016/j.jbiomech.2008.10.024.

Bourcier, R. *et al.* (2018) 'Susceptibility Vessel Sign in the ASTER Trial: Higher Recanalisation Rate and More Favourable Clinical Outcome after First Line Stent Retriever Compared to Contact Aspiration.', Journal of stroke. Korean Stroke Society, 20(2), pp. 268–276. doi: 10.5853/jos.2018.00192.

Chueh, J. Y. *et al.* (2011) 'Mechanical characterization of thromboemboli in acute ischemic stroke and laboratory embolus analogs.', AJNR. American journal of neuroradiology, 32(7), pp. 1237–44. doi: 10.3174/ajnr.A2485.

Cines, D. B. *et al.* (2014) 'Clot contraction: compression of erythrocytes into tightly packed polyhedra and redistribution of platelets and fibrin.', Blood. American Society of Hematology, 123(10), pp. 1596–603. doi: 10.1182/blood-2013-08-523860.

Duffy, S. *et al.* (2016) 'Novel methodology to replicate clot analogs with diverse composition in acute ischemic stroke', Journal of Neurointerventional Surgery, 0, pp. 1–7.

Duffy, S. *et al.* (2019) 'Per-Pass Analysis of Thrombus Composition in Patients With Acute Ischemic Stroke Undergoing Mechanical Thrombectomy', Stroke, 50(5), pp. 1156–1163. doi: 10.1161/STROKEAHA.118.023419.

Fennell, V. S. *et al.* (2018) 'What to do about fibrin rich "tough clots"? Comparing the Solitaire stent retriever with a novel geometric clot extractor in an in vitro stroke model.', Journal of neurointerventional surgery. British Medical Journal Publishing Group, 10(9), pp. 907–910. doi: 10.1136/neurintsurg-2017-013507.

Fransen, P. S. *et al.* (2014) 'MR CLEAN, a multicenter randomized clinical trial of endovascular treatment for acute ischemic stroke in the Netherlands: study protocol for a randomized controlled trial', Trials, 15(1), p. 343. doi: 10.1186/1745-6215-15-343.

Fujimoto, M. *et al.* (2013) 'Characterization of Arterial Thrombus Composition by Magnetic Resonance Imaging in a Swine Stroke Model', Stroke, 44(5), pp. 1463–1465. doi: 10.1161/STROKEAHA.111.000457.

Furie, B. and Furie, B. C. (2008) 'Mechanisms of thrombus formation.', The New England journal of medicine, 359(9), pp. 938–949. doi: 10.1056/NEJMra0801082.

Gasparian, G. G. *et al.* (2015) 'Imaging of Occlusive Thrombi in Acute Ischemic Stroke', International Journal of Stroke, 10(3), pp. 298–305. doi: 10.1111/ijs.12435.

Goyal, M. *et al.* (2016) 'Endovascular thrombectomy after large-vessel ischaemic stroke: a meta-analysis of individual patient data from five randomised trials', The Lancet. Elsevier, 387(10029), pp. 1723–1731. doi: 10.1016/S0140-6736(16)00163-X.

Gunning, G. M. *et al.* (2016) 'Clot friction variation with fibrin content; implications for resistance to thrombectomy', Journal of Neurointerventioal Surgery, 372(1), pp. 1019–1030. doi: 10.1136/.

Johnson, S. *et al.* (2017) 'Review of Mechanical Testing and Modelling of Thrombus Material for Vascular Implant and Device Design', Annals of Biomedical Engineering. Springer US, pp. 1–15. doi: 10.1007/s10439-017-1906-5.

Johnson, S. *et al.* (2019) 'Mechanical behavior of in vitro blood clots and the implications for acute ischemic stroke treatment.', Journal of neurointerventional surgery. British Medical Journal Publishing Group. doi: 10.1136/neurintsurg-2019-015489.

Kim, O. V. *et al.* (2017) 'Quantitative structural mechanobiology of platelet-driven blood clot contraction', Nature Communications. Nature Publishing Group, 8(1), p. 1274. doi: 10.1038/s41467-017-00885-x.

Kirchhof, K. *et al.* (2003) 'Differentiation of White, Mixed, and Red Thrombi: Value of CT in Estimation of the Prognosis of Thrombolysis—Phantom Study', Radiology, 228(1), pp. 126–130. doi: 10.1148/radiol.2273020530.

Krasokha, N. *et al.* (2010) ‘Mechanical properties of blood clots - a new test method. Mechanische Eigenschaften von Thromben - Neue Untersuchungsmethoden’, Materialwissenschaft und Werkstofftechnik, 41(12), pp. 1019–1024. doi: 10.1002/mawe.201000703.

Li, W. *et al.* (2016) ‘Fibrin Fiber Stiffness Is Strongly Affected by Fiber Diameter, but Not by Fibrinogen Glycation.’, Biophysical journal. The Biophysical Society, 110(6), pp. 1400–10. doi: 10.1016/j.bpj.2016.02.021.

Liebeskind, D. S. *et al.* (2011) ‘CT and MRI Early Vessel Signs Reflect Clot Composition in Acute Stroke’, Stroke, 42(5), pp. 1237–1243. doi: 10.1161/STROKEAHA.110.605576.

Liebig, T. *et al.* (2008) ‘Comparative in vitro study of five mechanical embolectomy systems: effectiveness of clot removal and risk of distal embolisation.’, Neuroradiology, 50(1), pp. 43–52. doi: 10.1007/s00234-007-0297-y.

Machi, P. *et al.* (2017) ‘Experimental evaluation of stent retrievers’ mechanical properties and effectiveness.’, Journal of neurointerventional surgery. British Medical Journal Publishing Group, 9(3), pp. 257–263. doi: 10.1136/neurintsurg-2015-012213.

Malone, F. *et al.* (2018) ‘The Mechanical Characterisation of Bovine Embolus Analogues Under Various Loading Conditions’, Cardiovascular Engineering and Technology. Springer US, 9(3), pp. 489–502. doi: 10.1007/s13239-018-0352-3.

Marder, V. J. *et al.* (2006) ‘Analysis of Thrombi Retrieved From Cerebral Arteries of Patients With Acute Ischemic Stroke’, Stroke, 37(8), 2086-93.

Matos Casano, H. A., Tadi, P. and Ciofoaia, G. A. (2019) Anterior Cerebral Artery Stroke, StatPearls. StatPearls Publishing.

Navarro-Orozco, D. and Sánchez-Manso, J. C. (2019) ‘Neuroanatomy, Middle Cerebral Artery’. StatPearls Publishing.

Saver, J. L. *et al.* (2015) ‘Stent-Retriever Thrombectomy after Intravenous t-PA vs. t-PA Alone in Stroke’, New England Journal of Medicine, 372(24), pp. 2285–2295. doi: 10.1056/NEJMoa1415061.

Siller-Matula, J. M. *et al.* (2008) 'Interspecies differences in coagulation profile.', Thrombosis and haemostasis, 100(3), pp. 397–404.

Tutwiler, V. *et al.* (2017) 'Contraction of Blood Clots Is Impaired in Acute Ischemic Stroke', Arteriosclerosis, Thrombosis, and Vascular Biology, 37(2), pp. 271–279. doi: 10.1161/ATVBAHA.116.308622.

Tutwiler, V. *et al.* (2018) 'Shape changes of erythrocytes during blood clot contraction and the structure of polyhedrocytes', Scientific Reports. Nature Publishing Group, 8(1), p. 17907. doi: 10.1038/s41598-018-35849-8.

Weafer, F. M. *et al.* (2019) 'Characterization of strut indentation during mechanical thrombectomy in acute ischemic stroke clot analogs', Journal of NeuroInterventional Surgery, 11(9), pp. 891-897 neurintsurg-2018-014601. doi: 10.1136/neurintsurg-2018-014601.

Van Der Worp, H. B. and Van Gijn, J. (2007) 'Acute Ischemic Stroke', The New England journal of medicine, 357(6), pp. 572–579.

Yuki, I. *et al.* (2012) 'The Impact of Thromboemboli Histology on the Performance of a Mechanical Thrombectomy Device', American Journal of Neuroradiology, 33(4), pp. 643–648. doi: 10.3174/ajnr.A2842.

Chapter 4

Investigating the Mechanical Behaviour of Clot Analogues with varying Hematocrit, through Experimental and Computational Analysis

4.1 Chapter Overview

The aim of this study is to provide a further investigation of the mechanical behaviour of thrombus analogues as a function of composition, through experimental testing and computational analysis.

This chapter presents an investigation of the mechanical behaviour of clot analogues, with varying hematocrit, using two loading protocols; cyclic compression and stress-relaxation. The effect of clot aging and storage conditions on the mechanical behaviour was also investigated. Scanning electron microscopy (SEM) was also used to investigate the clot microstructure at various time-points. A hyper-viscoelastic constitutive law was identified and calibrated based on the experimental mechanical test data.

A journal paper based on the content of this chapter is currently in preparation.

4.2 Introduction

Thrombus material is a critically important tissue component that has the essential role of preventing blood loss in the human organism. However thrombus material is associated with a range of life-threatening conditions, such as acute ischemic stroke

(AIS), which accounts for 85% of all strokes (Van Der Worp & Van Gijn 2007). AIS is often caused by the embolisation of cardiac or vascular originating clots that cause an occlusion in the neuro-vasculature. Mechanical thrombectomy has recently been established as the new standard of care for the treatment of AIS (Goyal, Andrew M Demchuk, *et al*. 2015). However, it is proposed that the success of the thrombectomy procedure can be significantly affected by the mechanical properties of the occluding thrombus (Chueh *et al*. 2011; Johnson *et al*. 2019).

Analysis of thrombus material from human sources can often be expensive and highly regulated, making specimens difficult to obtain. Therefore clinically relevant thrombus analogues that are fabricated *in-vitro* are an extremely useful for pre-clinical testing of thrombectomy devices (Liebig *et al.*, 2008; Chueh *et al.*, 2011; Duffy *et al.*, 2016) and assessment of the effectiveness of a device for a range of clot compositions. Such clot analogues should be constructed from blood proteins and components present in the clotting cascade so that a similar chemical composition to native clots is achieved.

A variety of protocols have been proposed for fabrication of clot analogues involving numerous variables, which include donor species and concentration of thrombin (Duffy *et al*. 2016; Krasokha *et al*. 2010; Chueh *et al*. 2011; Liebig *et al*. 2008; Johnson *et al*. 2019). Other studies have also investigated the effect of barium sulphate on the clot material (Chueh *et al*. 2011; Krasokha *et al*. 2010). The effects of these variables on the mechanical behaviour of the clot analogues under compressive (Saldívar *et al.*, 2002; Krasokha *et al.*, 2010; Chueh *et al.*, 2011; Malone *et al.*, 2018; Johnson *et al.*, 2019) and tensile loading (Saldívar *et al*, 2002; Krasokha *et al.*, 2010; Malone *et al.*, 2018), as well as clot permeability and structure (Kim *et al*. 2017; Johnson *et al*. 2019), have been investigated. Clot composition can also differ

substantially with varying red blood cell (RBC) and fibrin content (Marder *et al*. 2012; Liebeskind *et al*. 2011), and to date, the effect of clot composition and hematocrit (%H), i.e. the volume percentage of RBCs in the mixture, on the rate-dependent mechanical behaviour of the material has not been adequately investigated.

Previous studies have carried out a variety of mechanical testing on thrombus material, including compression testing (Saldívar *et al*, 2002; Ashton *et al.*, 2009; Krasokha *et al.*, 2010; Chueh *et al.*, 2011; Malone *et al.*, 2018), uniaxial and biaxial tensile testing (Di Martino *et al.*, 1998; Riha *et al.*, 1999; Saldívar *et al*, 2002; Vande Geest *et al.*, 2006; Gasser *et al.*, 2008; Teng *et al.*, 2015; Malone *et al.*, 2018), rheometry (Kim & Srinivasan 2005; van Dam *et al*. 2006; Malone *et al*. 2018), nanoindentation (Slaboch *et al*. 2012; Weafer *et al*. 2019) and friction testing (Gunning *et al*. 2016), with the earliest studies dating back to the 1940s and 1950s with the work of Ferry and co-workers (Ferry & Morrison 1944). However, developing a reliable test method that is suitable to test the broad range of clot types and compositions can be challenging due to the fragile nature of the clot material.

Few studies have investigated the viscoelastic behaviour of clot material and have proposed constitutive models to capture this behaviour (van Dam *et al.*, 2008; Schmitt *et al*, 2011; Slaboch *et al.*, 2012; van Kempen *et al*, 2015; Malone *et al.*, 2018), yet the loading-unloading hysteresis and stress-relaxation due to rate-dependent viscoelasticity of thrombus material, as a function of clot composition, has been neglected.

In Chapter 3, we investigated the effect of platelet-driven clot contraction on the clot mechanical properties and microstructure (Johnson *et al*. 2019). This chapter presents a further investigation of the mechanical behaviour of these clot analogues with a focus

on the rate-dependent viscoelasticity of thrombus material, as a function of clot composition. Similar to Chapter 3, compression testing was selected for this study as this method is sufficiently robust to allow reliable testing of a broad range of clot types. The experimental results obtained were then used to identify an appropriate constitutive model to capture the material behaviour and this chapter reports the first model to successfully capture the loading-unloading hysteresis and stress-relaxation of the thrombus material. The results reported in this chapter provide a significant advance in the current understanding of the relationship between clot composition and rate-dependent non-linear mechanical behaviour.

4.3 Materials and Methods

4.3.1 Sample Preparation

The sample preparation methodology, as previously described in chapter 3 (Johnson *et al*. 2019), was followed. Fresh venous blood was collected from the jugular vein of sheep, into receiving vessels that were pre-loaded with ACPD (Adenine citrate phosphate dextrose) anticoagulant solution (Ash Stream vets, Co. Mayo, Ireland), for the preparation of the analogue clot samples for testing (Johnson *et al*. 2019; Duffy *et al*. 2016). The blood was then transported to the lab and stored at room temperature before use. Ovine blood was chosen as it has been found to be a suitable substitute for human blood for coagulation studies (Siller-Matula *et al*. 2008a) and the clot samples produced using this methodology have been found to be histologically similar to human clots (Duffy *et al*. 2016). All clots were prepared within 5 hours of blood collection. The clot samples prepared for this study were produced from 5 separate blood collections.

To begin clot preparation, the blood was centrifuged at 180 g for 10 minutes. The platelet-rich plasma (PRP) was removed and collected into a separate container. The remaining blood mixture was centrifuged at 2200 g for a further 10 minutes to isolate the red blood cells (RBCs). Platelet contracted clots were formed by mixing the PRP with the RBCs in controlled ratios, to represent clots with different levels of hematocrit (%H), i.e. the volume percentage of RBCs in the mixture – 0, 5 and 40 %H.

Once the various clot mixtures were produced, coagulation was initiated by the addition of a 2.06% calcium chloride solution to the blood components in a 1:9 ratio. The samples were formed in cylindrical-shaped moulds (Figure 4.1 A-B) and were allowed to mature overnight at 37°C. A whole blood (WB) clot was also formed by collecting whole blood into a syringe and allowing spontaneous coagulation to occur at room temperature overnight (Duffy *et al*. 2016).

After maturation overnight, the weights of the resultant clots and the expelled serum were measured separately on a gravimetric balance to determine the percentage of clot contraction and to ensure that the clot analogues had contracted fully. The volume reduction due to contraction was calculated by expressing the weight of each clot as a percentage of the weight of the original blood mixture (weight of resultant clot + weight of expelled serum). The platelet contracted clot size was found to have a linear correlation with the hematocrit of the clot mixture ($R^2 = 0.769$) (Figure 4.1 C). There was a slight variation in results as it was found that platelet contraction was reduced in clots formed later than 5 hours after blood collection. Therefore only clots that had sufficient contraction (i.e. %H ± 10%) were used for testing.

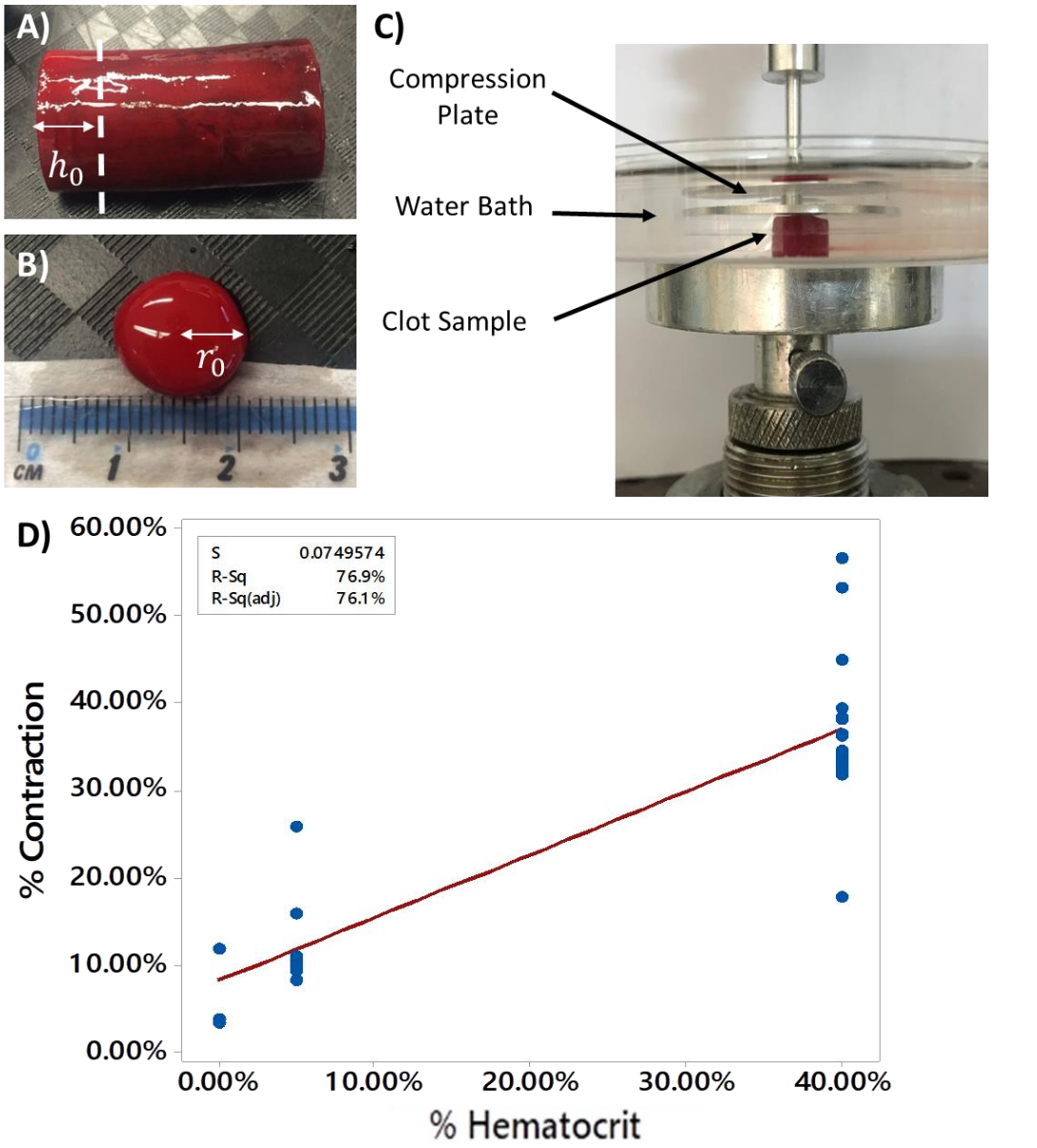

Figure 4.1 Images illustrating (A) the cylindrical shaped clot "slug" after formation, with the white dashed line indicating how the test samples were cut, (B) an example of a test-sample (5% H clot) and (C) the compression test set-up. (D) Plot of percentage contraction of the clot analogues versus the percentage hematocrit of the blood mixture, with a linear correlation fit.

Test samples were then prepared by cutting the clots into cylindrical-shaped samples with an approximate diameter of 10 mm (Figure 4.1 B), and an approximate height of 5 mm. Unconfined compression was used to determine the material behaviour of the analogue clot samples, the day after formation (minimum of n = 15 for each clot type).

The 0%, 5% and 40% H clot analogues were also aged, by storing the samples in serum at 4°C or at 37°C. These samples were then tested at various time-points; 1 day, 4 days, 7 days and 14 days after contraction (n = 9 at each time-point), to investigate the effect of aging and storage temperature on the mechanical behaviour.

A group of 5% and 40% H clots were also aged at 4°C for up to 7 days in saline. These samples were not mechanically tested, although their microstructure was examined under SEM at time points of 1, 4 and 7 days.

4.3.2 Compression Testing

The compression test set-up is shown in Figure 4.1 D, with all samples tested in saline. The testing was performed on a Zwick uniaxial tensile machine (Zwick Z2.5, Ulm, Germany), using a customised aluminium platen.

The samples were placed between two platens and the crosshead position of the machine was adjusted so that the top platen was slightly touching the top of the sample at the beginning of the test. The clot specimens were loaded to a compressive nominal strain of 80% at a constant axial strain-rate magnitude of 10% per second, which is within the range of loading rates reported in the literature, and then unloaded to their initial configuration at the same axial strain-rate magnitude. This was performed for 10 cycles.

The compressive axial nominal stress is calculated as $\sigma = -F/(\pi {r_o}^2)$, where F was the measured loading force and r_o is the radius of the undeformed cylindrical specimen. The nominal axial compressive strain (ε) under compression was calculated as $\varepsilon = (h_0 - h)/h_0$, where h is the deformed height of the cylindrical sample and h_0 is the undeformed height prior to load application. Note that, for clarity of presentation of experimental results, this convention results in positive values of σ and ε in

compression. Similar to Chapter 3, tangent stiffnesses were determined at various levels of strain, to compare the mechanical behaviour of the materials.

Statistical analysis of the experimental results was carried out using the general linear model ANOVA procedure in Minitab (ver. 18.1). A comparison of mean onset point was performed with a Bonferroni model (alpha = 0.05) to compare the initial stiffness, calculated at 10% strain, of the clot analogues when stored in serum and tested 1 day, 4 days, 7 days and 14 days after formation. Similarly the initial stiffness for the clot analogues stored at 4°C and 37°C were compared.

4.3.3 Stress-Relaxation

Unconfined compression stress-relaxation tests were also carried out on clot samples ($n \geq 15$ for each clot type). Samples were instantaneously loaded to a nominal compressive axial strain of $\varepsilon = 60\%$. The applied strain is then held constant at this value for 1000 seconds. During this period the changes in nominal axial compressive stress, σ, were recorded.

4.3.4 Scanning Electron Microscopy (SEM)

The analogue samples were fixed with 2.5% glutaraldehyde and dehydrated in a series of ethanol concentrations up to 100%. The samples were frozen in liquid nitrogen and fractured so that the interior surface of the clot analogues could be examined. The samples were then critical-point dried, mounted and sputter-coated with iridium.

4.3.5 Constitutive Model

A preliminary assessment of established hyperelastic material models reveals that the Yeoh provides a reasonably accurate fit to unconfined compression test results of clot analogue material. The Yeoh strain energy density function, W is given as

$$W = \sum_{i=1}^{3} C_{i0}(\bar{I}_1 - 3)^i + \sum_{i=1}^{3} \frac{K}{2}(J-1)^{2i} \quad (4.1)$$

The parameters C_{i0} describe the non-linear shear stiffness, while the parameter K is the bulk modulus. $\bar{I}_1$ the isochoric first strain invariant and J is the volume jacobian. In all cases near incompressible material behaviour, based on previous assumptions for material models of clot material (Wang *et al.*, 2001; Xie *et al.*, 2005; van Dam *et al.*, 2006, 2008; Hinnen *et al.*, 2007; Gasser *et al.*, 2008), was enforced by setting a value for the bulk modulus (K) that was three orders of magnitude greater than the effective shear moduli C_{i0}.

Rate dependent viscoelasticity is implemented through the specification of a non-dimensional stress-relaxation curve, parameterised through a Prony series. The effective shear-relaxation modulus is given as

$$\bar{g}(t) = 1 - \sum_{i=1}^{n} g_i\left(1 - e^{-\frac{t}{\tau_i}}\right) \quad (4.2)$$

where n is the number of the terms in the Prony series, τ_i are the relaxation time constants for each term of the series, while the parameters g_i sets the ratio of long-term to instantaneous effective shear modulus.

A series of finite element analyses were performed to identify a set of material law parameters for each clot type so that a good agreement was obtained between model predictions and experimental cyclic compression and stress-relaxation tests. The clot sample was modelled as a unit cube meshed with 400 3D bilinear rigid quadrilateral elements (R3D4). The loading platens modelled as rigid surfaces and frictionless hard contact between the platens and the clot was assumed.

4.4 Results

4.4.1 Mechanical Testing

Representative curves showing nominal stress versus time for 10 loading-unloading cycles for a 5% and 40% H clot is shown in Figure 4.2 A. Each of the clot groups were found to exhibit dynamic stress relaxation, suggesting that the clot exhibits viscoelastic behaviour. Corresponding stress-strain curves are shown in Figure 4.2 B, demonstrating non-linear hyperelastic strain stiffening, with loading-unloading hysteresis again demonstrating material viscoelasticity.

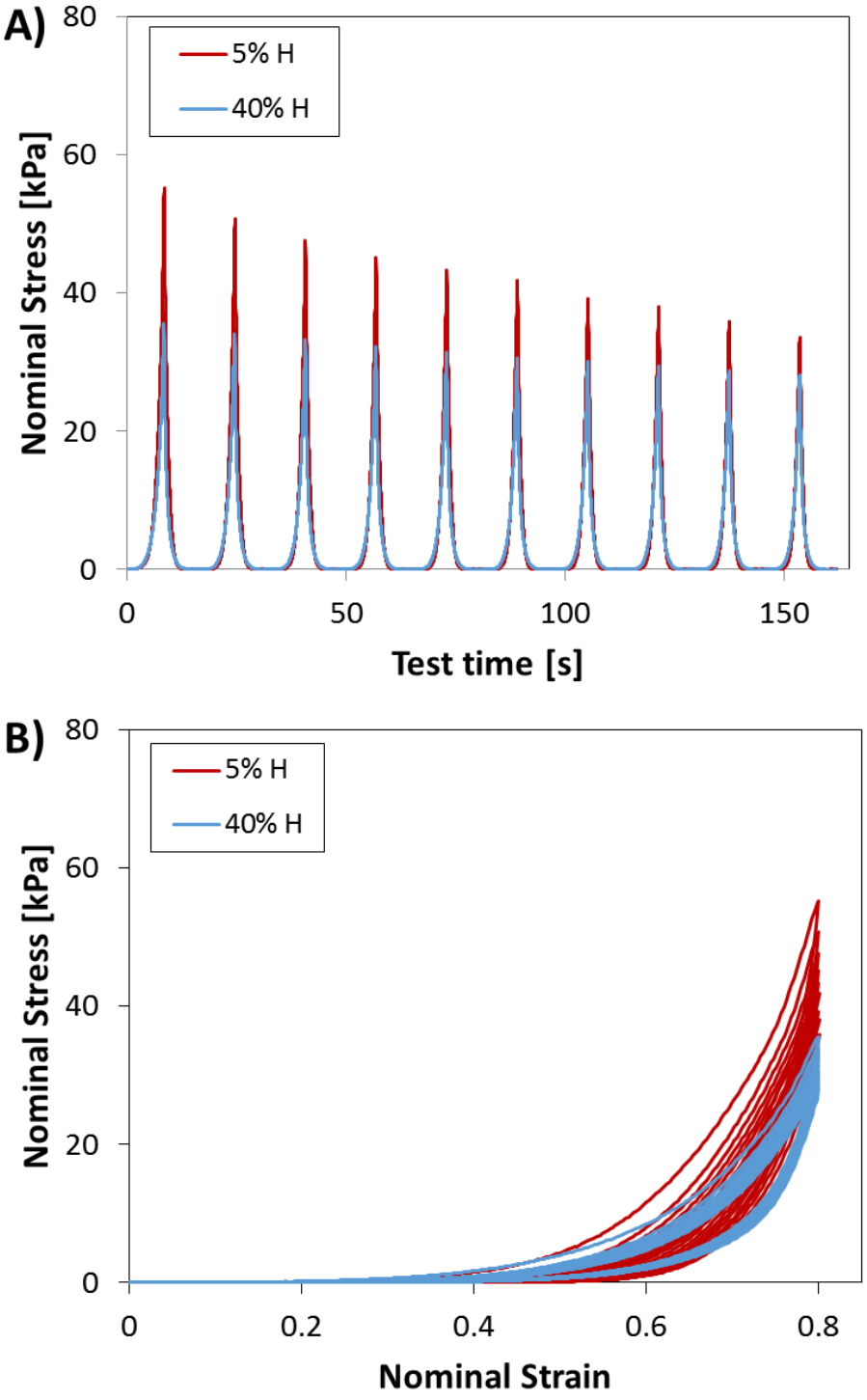

Figure 4.2 Representative curves showing the typical response of a 5% H clot and a 40% H clot analogue during cyclic compression. Plot of (A) nominal stress versus time and (B) nominal stress versus nominal strain showing the typical loading-unloading curves for 10 cycles. From both curves, the viscoelastic nature of the material is apparent through the dynamic stress-relaxation and energy-dissipation after each cycle evident in A and B respectively.

Stress-strain curves (mean ± st. dev.) are shown in Figure 4.3 A-B. All of the clot compositions exhibited loading-unloading hysteresis, suggesting that the analogue material is viscoelastic (Figure 4.3A). The stress-strain curves (mean ± st. dev.) for the first loading half-cycle to 80% compression is shown in Figure 4.3 B. The 5% H clot had the greatest peak stress at 80% strain, followed by the 0% H clot and the WB clot respectively, with the 40% H clot having the lowest peak stress at maximum strain (Figure 4.3 A-B). However from Figure 4.3 B and C, the 0% H clot appears to have the highest initial stiffness at low levels of strain, whereas the 5% H clot was found to have the greatest stiffness at strains of < 30%. The 40% H clot was found to have the lowest stiffness of the three clot types at all strains (Figure 4.3 C). It is hypothesised that the ratio of RBCs to fibrin in the 5% H clot may be optimal, and thus the stiffness is increased at large strains due to the reinforcement effect of the RBCs on the fibrin matrix. However, adding more RBCs to the matrix causes a reduction in stiffness, as demonstrated by the 40% H clot.

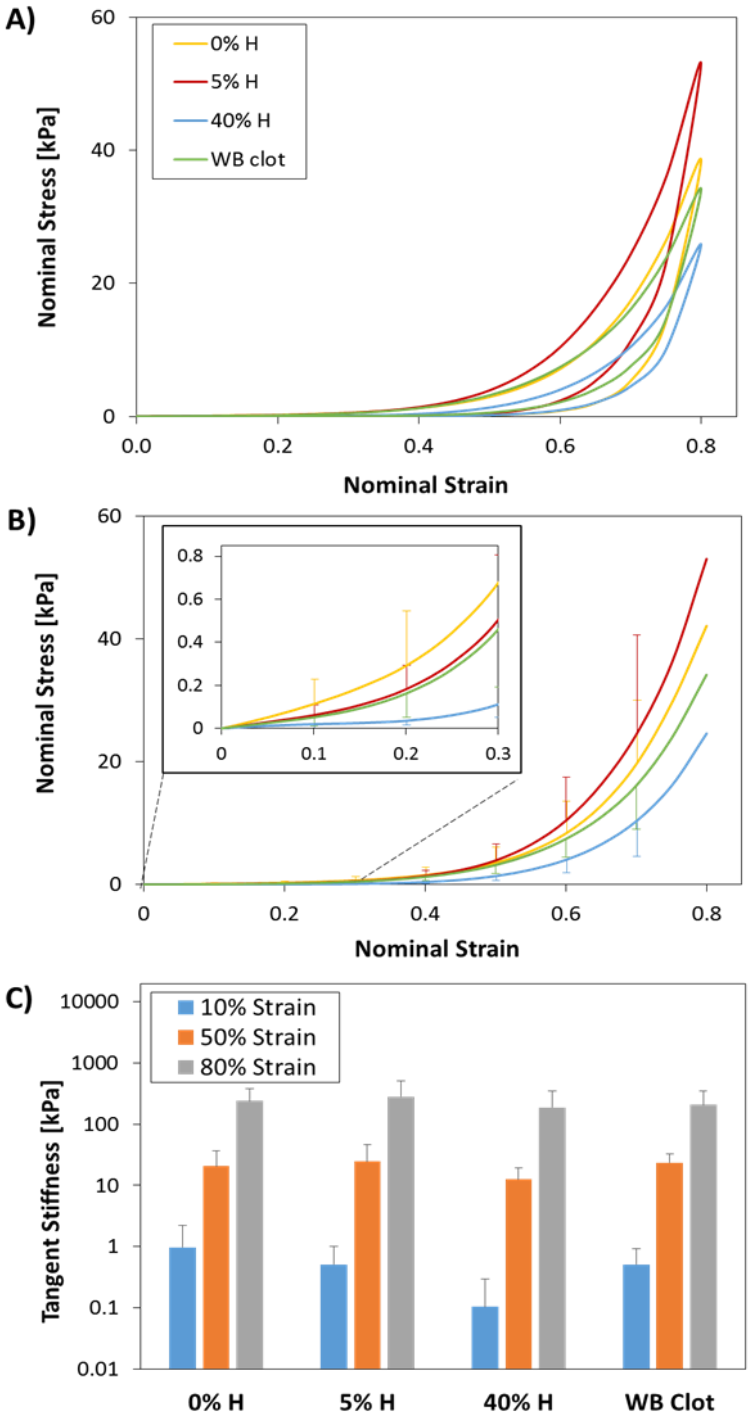

Figure 4.3 (A) Average nominal stress-strain curves (minimum of n = 15 for each clot type), shown as positive values for clarity, comparing the loading-unloading curves from the first cycle of the compression testing, for the 4 clot types with varying hematocrit. (B) Average stress-strain curves comparing the first loading half-cycle to 80% compression, including error bars representing standard deviation, for each clot group. Inset, is a zoomed-in image of the behaviour at low levels of strain. (C) Comparison of tangent stiffness values (mean ± st. dev.) at various levels of strain.

0%, 5% and 40% H clot analogues were stored in their own serum at 4°C and subjected to unconfined parallel plate compression testing at time-points of 1 day, 4 days, 7 days and 14 days after formation(Figure 4.4 A-C). No statistically significant difference in mechanical behaviour was observed when comparing the initial tangent stiffness, calculated at 10% strain, for a freshly formed clot analogue and aged analogues each time-point. This was true across all hematocrits with the exception of the 0% H clot when comparing the initial stiffness at day 1 and day 7.

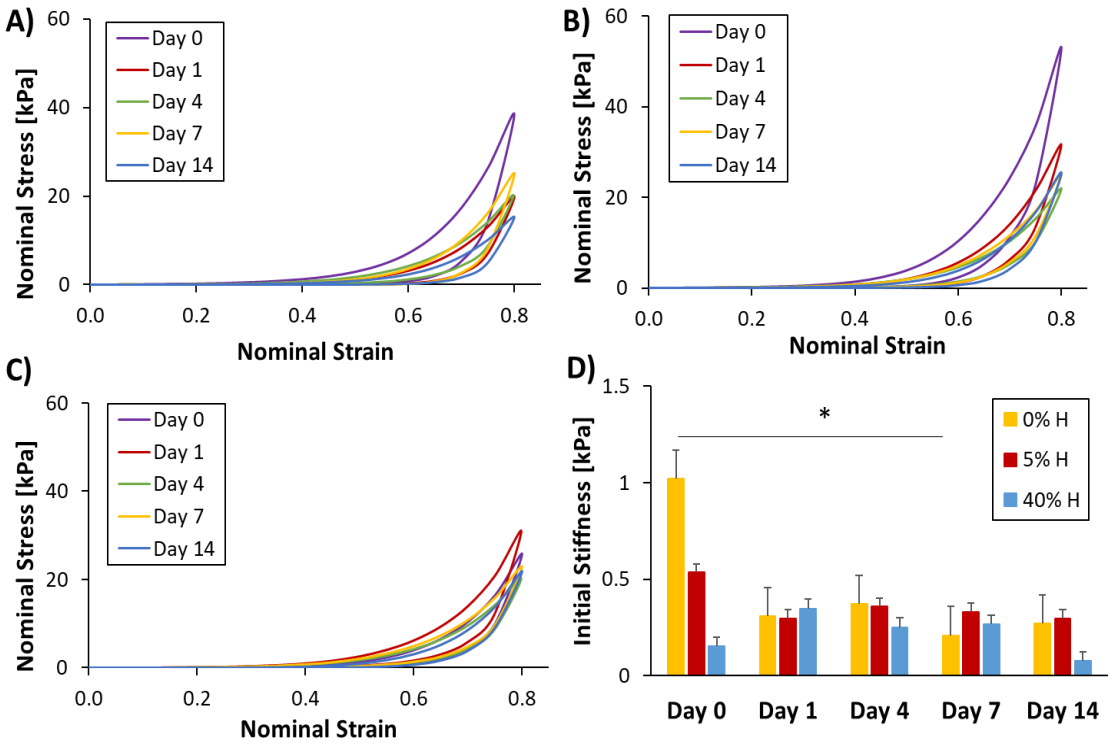

Figure 4.4 Plots of nominal stress versus nominal strain showing the average curves (n≥8 for each timepoint) for (A) the 0% H clot, (B) 5% H clots and (C) 40% H clots, comparing their mechanical behaviour after aging for 1,4, 7 and 14 days at 4°C in serum with a clot tested immediately after formation (Day 0). (D) Plot comparing the initial tangent stiffness calculated at 10% strain for the aged clots with the freshly formed clot analogue, with error bars indicating standard error. There was no statistical significance in the initial stiffness of the clots compared to the fresh clot analogue when aged over 14 days, with the exception of the 0% H clot at 7 days (statistical significance is denoted by *).

Similarly, no significant difference in the mechanical behaviour was observed between clots stored at 4°C and 37°C, when comparing their initial tangent stiffness (Figure 4.5). However, the 0% and 5% H clots were found to disintegrate if stored at 37°C for longer than 4 days and the 40% H clots stored at 37°C were found to disintegrate if stored for longer than one day.

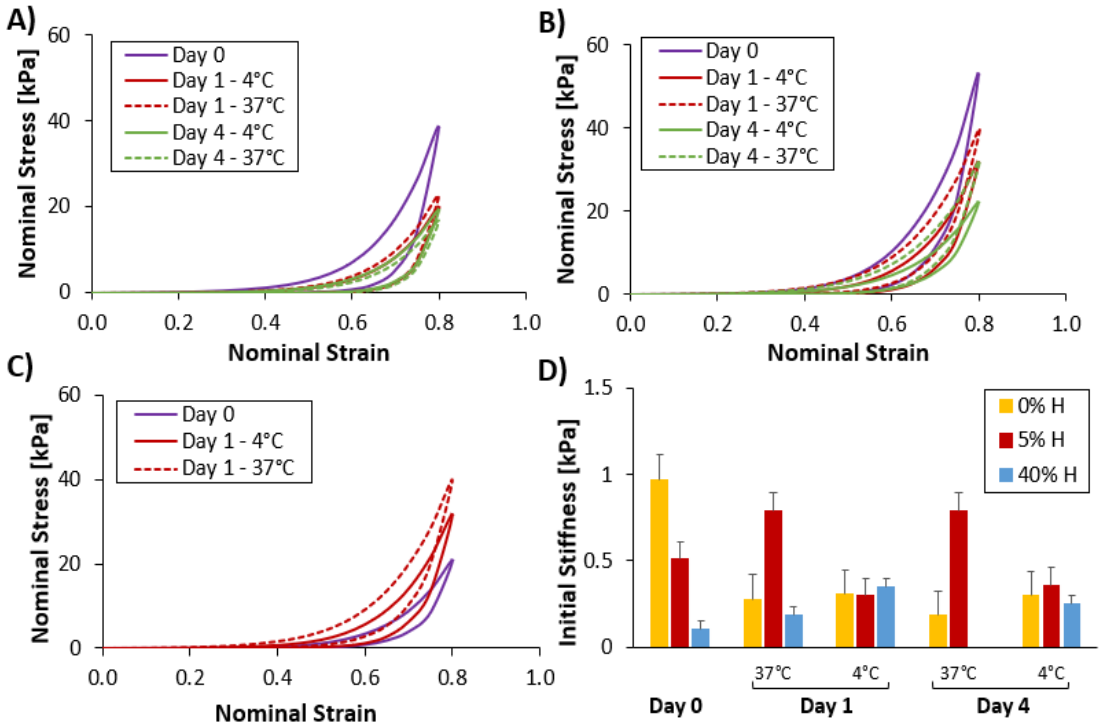

Figure 4.5 Plots of nominal stress versus nominal strain showing the average curves ($n \geq 5$ for each timepoint) for (A) the 0% H clot, (B) 5% H clots and (C) 40% H clots, comparing their mechanical behaviour after aging in serum at 4°C and 37°C at various time-points, with a clot tested immediately after formation (Day 0). (D) Plot comparing the initial tangent stiffness, calculated at 10% strain, for the clots aged at aged at 4°C and 37°C with the freshly formed clot analogue, with error bars indicating standard error. There is no data for the 40% clot at 37°C at 4 days as all clots disintegrated when stored at 37°C for more than 1 day. There was no statistical significance in the initial stiffness of the aged clots compared to the fresh clot analogue.

Measured stress-relaxation curves under an applied compressive strain of 60% are shown in Figure 4.6 A for each clot composition. The percentage relaxation following 1000 s of constant applied strain is quantified (mean ± SD) in Figure 4.6 B. While all clot compositions exhibit significant relaxation, 0% H clots exhibit the greatest stress relaxation (97.35% ± 4.76%), followed by the 5% H clot (89.08% ± 8.24%), the WB clot (61.83% ± 19.24%) and the 40% H clot (53.55% ± 19.81%) .

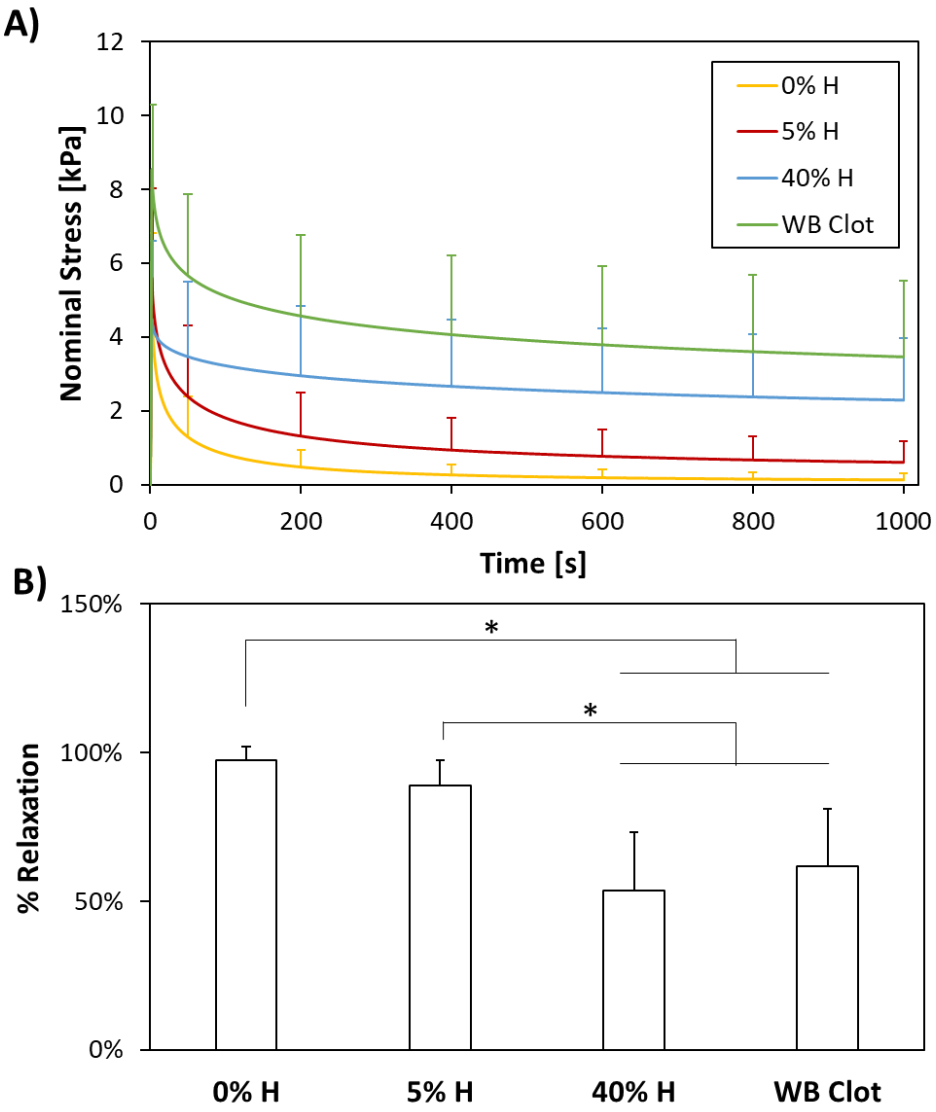

Figure 4.6 (A) Average stress-relaxation curves (n = 15 for each clot type), including error bars representing the standard deviation. (B) Plot comparing the average percentage stress-relaxation at 1000 seconds for each of the clot analogues. Error bars represent standard deviation and * denotes statistical significance where $p<0.05$.

4.4.2 SEM

Figure 4.7 shows SEM images of the interior of the clot analogues. The 0% H clot is composed of thick fibrin fibres and areas of very dense compressed fibrin (Figure 4.7 A). The 5% H clot consists of very dense fibrin compacted around compressed RBCs, indicated by the white arrows in Figure 4.7 B. The 40% H, shown in Figure 4.7 C, clot consists mainly of compacted RBCs entrapped in a network of thick fibrin fibres. There is also evidence of a thin hyper-branched fibrin network that has been significantly compressed through the action of clot contraction, appearing as a very thin layer on the faces of closely packed polyhedron-shaped RBCs (also referred to as ”polyhedrocytes” (Cines *et al*., 2014; Tutwiler *et al*., 2018)). All clots were found to have a fibrous outer layer.

Figure 4.7 C-F also compares the microstructure of the 40% H clots stored in serum and saline for various time points. At day 1 both clot groups had a relatively similar microstructure with compacted fibrin compressing around RBCs as described previously. However, at day 7, the clots stored in serum appear to have compressed further, with polyhedrocyte shapes becoming more apparent (Figure 4.7 C-D). However, this was not the case for the clots stored and aged in saline. Although the compressed fibrin network is still apparent, the RBCs appear to have returned to a spherical shape and to have become dislodged from the surrounding fibrin, leaving spherical cavities where the RBCs once were empty (Figure 4.7 E-F).

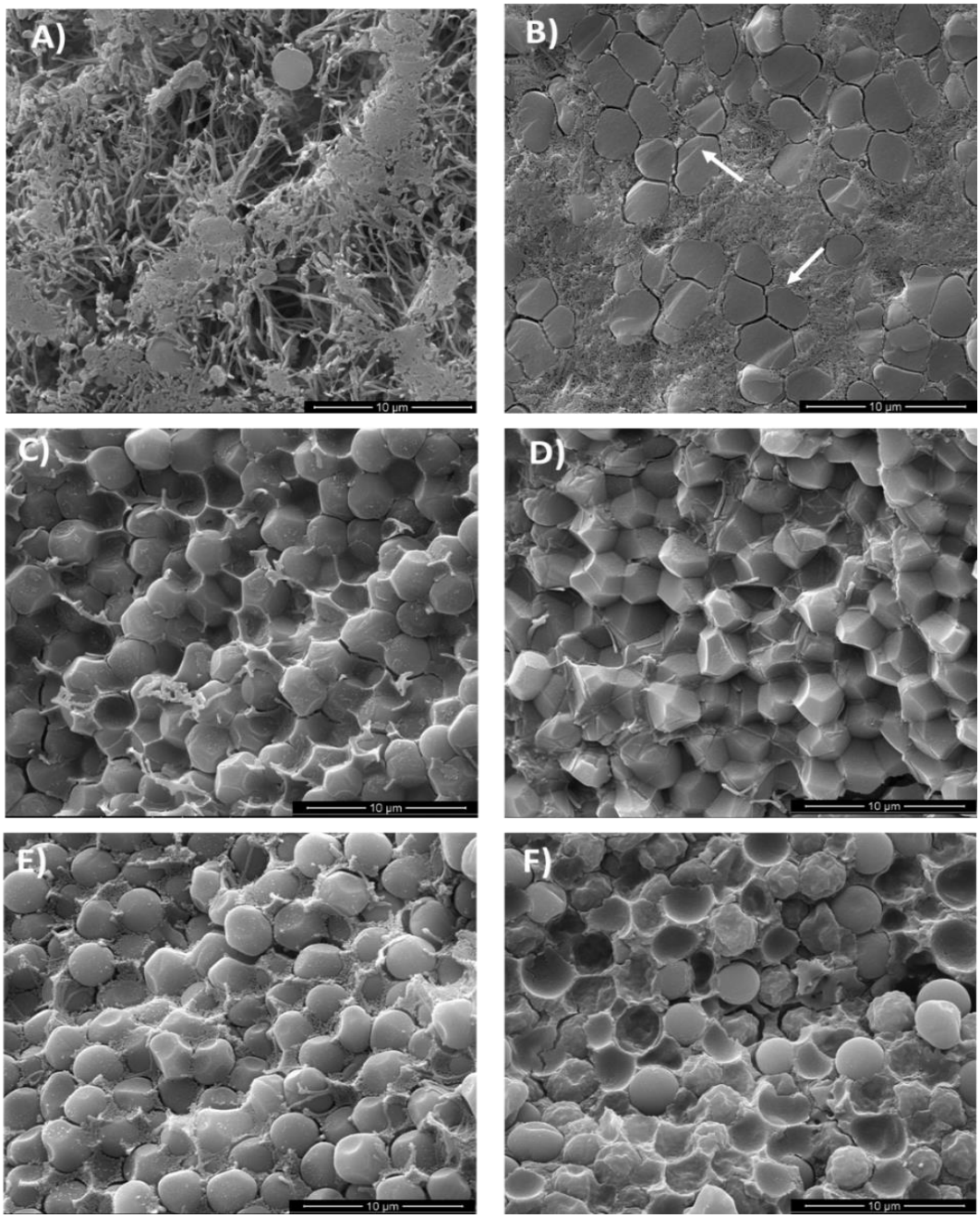

Figure 4.7 SEM images of the interior of clot analogues. (A) Interior of a 0% H clot, consisting of areas of loose thick fibrin strands and highly compacted fibrin. (B) Interior of a 5% H clot, with the white arrows indicating the red blood cells (RBCs), surrounded by a compacted fibrin network. (C) Interior of a 40% H clot stored in serum at 4°C for 1 day and (D) 7 days. The closely packed polyhedrocytes are surrounded by a network of thick fibrin fibres, with evidence of a thin hyper-branched fibrin network appearing as a very thin layer on the faces of closely packed RBCs. (E) Interior of a 40% H clot stored in saline at 4°C for 1 and (F) 7 days. The RBCs appear to have retained their natural spherical shape.

4.4.3 Material Law Calibration

As shown in Figure 4.8, the hyper-viscoelastic material law outlined in the methods section, is found to provide a reasonable fit to the experimental cyclic compression and stress-relaxation tests. The Yeoh hyperelastic formulation with three term-Prony series modulus-relaxation was found to provide reasonable agreement with experimentally measured stress-relaxation data (R^2 > 0.77 in all cases) and compression data (R^2 > 0.76 in all cases). This suggests that the material behaviour of each clot composition can be approximately captured using a hyper-viscoelastic material law. Calibrated model parameters for the clot analogue materials are shown in Table 4.1.

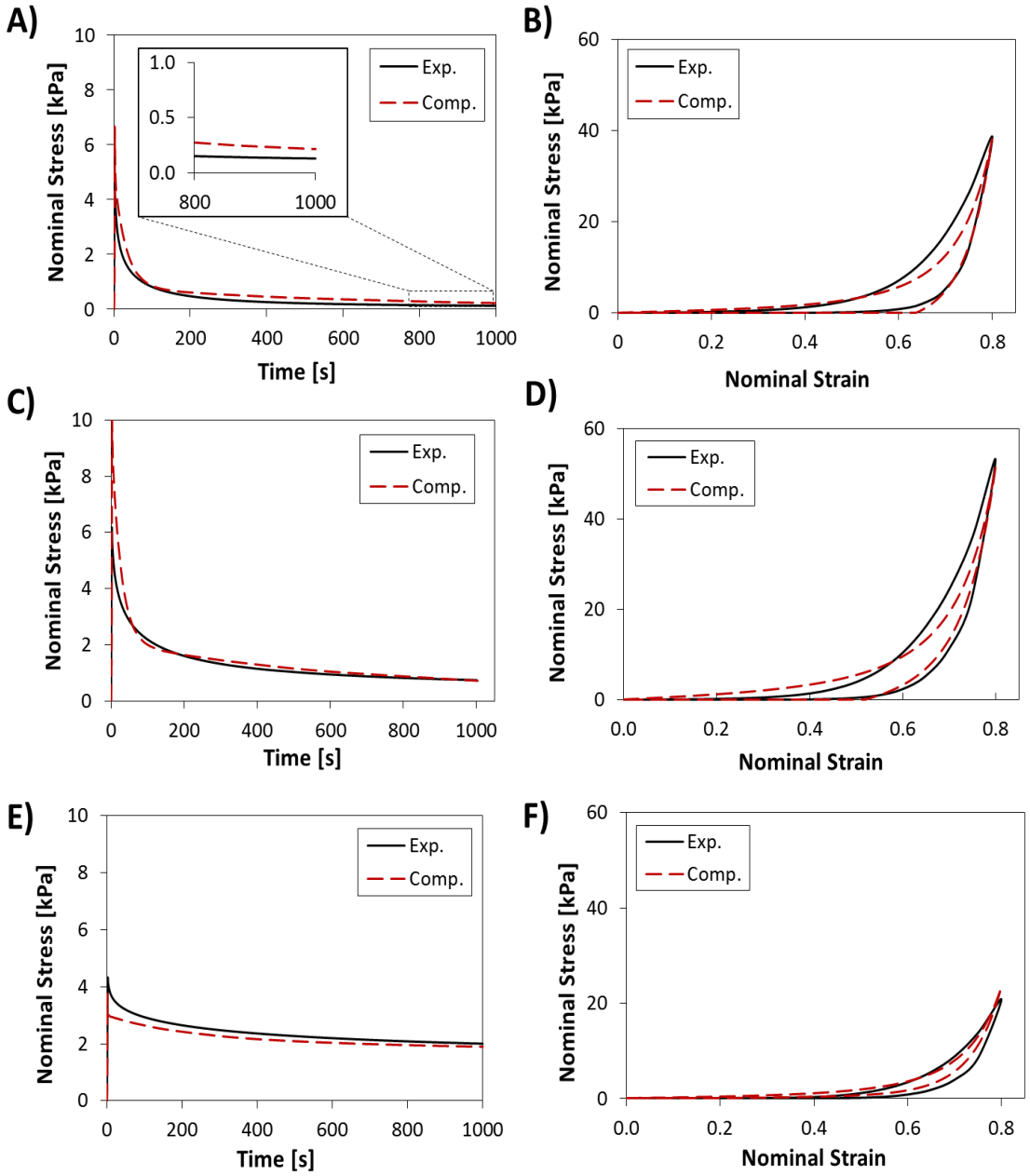

Figure 4.8 Graphs comparing the experimental results with the computational fit for the stress-relaxation experiment (left), and the first cycle of the load-unload compression experiment (right) for the 0% H clot (A-B), the 5% H clot (C-D) and the 40% H clot (E-F). Inset of (A), is a zoomed-in image of the nominal stress at a time of 1000 s.

Table 4.1 Fitted Material parameters for the material law calibration to the compression and stress-relaxation experiments.

	0% H Clot	**5% H Clot**	**40% H Clot**
C10 (Pa)	520	880	250
C20 (Pa)	40	30	28
C30 (Pa)	-0.1	-0.1	-0.4476
$\boldsymbol{K}$ **(Pa)**	100000	100000	100000
$\boldsymbol{g_1}$	0.4	0.2	0.25
$\boldsymbol{\tau_1}$	1	1	1
$\boldsymbol{g_2}$	0.5	0.62	0.2
$\boldsymbol{\tau_2}$	30	25	200
$\boldsymbol{g_3}$	0.09	0.15	0.2
$\boldsymbol{\tau_3}$	600	650	2000

4.5 Discussion

This chapter further investigated the mechanical behaviour of clot analogues with varying composition, previously described in Chapter 3, under compressive loading. The experimentally observed material behaviour was shown to be accurately predicted by a hyper-viscoelastic material law for all clot compositions.

All of the clot groups were found to exhibit the typical behaviour of a nonlinear hyperelastic material, with low stiffness behaviour occurring at low compressive strains (< 30%), and significant strain stiffening occurring at higher strains (> 30%), similar to previously published data for clot material (Johnson *et al*. 2019; Chueh *et*

al. 2011; Malone *et al*. 2018; Ashton *et al*. 2009; Krasokha *et al*. 2010). The 0% H clot was found to have the largest initial stiffness, followed by the 5% H and the WB clot, which had very a very similar stiffness as low levels of strain (< 30% strain). However, the 5% H clot appears to stiffen significantly for strains greater than 30%, and was found to have the greatest large strain stiffness, followed by the 0% H and the WB clot groups.

The behaviour observed from the results of the unconfined compression and stress-relaxation experiments suggest that the material is viscoelastic (Bird & Marsh 1968). This is supported by previous studies in the literature which have also reported on the viscoelastic behaviour of clot material (Saldívar *et al.*, 2002; van Dam *et al.*, 2006; Ashton *et al.*, 2009; Chueh *et al.*, 2011; Huang *et al.*, 2013; Malone *et al.*, 2018). However, the rate-dependent viscoelasticity has not previously been characterised for clot analogue material or for hemorrhagic stroke clots removed by mechanical thrombectomy. The characterisation of rate-dependent viscoelasticity is important for design of aspiration and MT devices.

Similarly, the effect of clot composition on the viscoelastic behaviour of clot material has not been investigated to date. The results from the mechanical testing show the behaviour of the clot analogues varied with hematocrit for both test types. Clots with a greater hematocrit were found to have a lower stiffness than clots with a lower hematocrit. This is assumed to be due to the high RBC content and low fibrin content in these analogues. In contrast the lower hematocrit clots, the 0% H and 5% H clot groups, experienced greater stress-relaxation. The larger fibrin network in these clots can allow for further fibre rearrangement and in turn, greater relaxation.

The variation in mechanical behaviour can also be explained by examining the material microstructure. The lower hematocrit clot analogues have a very dense fibrin network, due to the contracting platelets pulling on the fibrin fibres causing them to become compacted around the few RBCs present (Johnson *et al*. 2019), (Cines *et al*., 2014; Tutwiler *et al*., 2018). In contrast, the 40% H clot consists of closely packed RBCs with little fibrin present. Fibrin therefore appears to make a strong contribution to the stiffness and relaxation of the material.

Although there are few reports in the literature on the effects of storage conditions on clot material (Krasokha *et al*. 2010; Krueger *et al*. 2004), the impact on clot mechanical behaviour is not fully understood. Previous studies have reported an decrease in clot stiffness and stability due to aging (Krasokha *et al*. 2010; Krueger *et al*. 2004). However, in this chapter, aging was not found to have a significant impact on the mechanical behaviour of the clot analogues stored in serum at 4°C when tested under compression after 14 days. Although this is not consistent with the previously reported findings, it may be explained by the difference in protocols for the formation of the clot analogues, as both of the previous studies included thrombin.

Likewise, storage temperature was found to have little impact on clot mechanical behaviour of the lower haematocrit clot analogues, with no statistical difference between the initial tangent stiffness of the clots stored at 37°C versus 4°C. However the 40% H clot was found to completely disintegrate when stored at 37°C for longer than one day. Similarly, the 0% and 5% H clots were found to disintegrate when stored at 37°C for longer than four days. Although aging appeared to have little effect on the clot mechanical behaviour, it is likely that the viability of components within the clot, such as the RBCs, is affected after storing for long periods of time and therefore they

are not an accurate representation of a 'live' clot. Therefore, it is recommended that clots are tested as soon as possible after formation/collection to ensure cell viability.

Although the impact of the storage solution on the mechanical behaviour of the clot analogues was not investigated in this study, there were obvious effects on the clot microstructure. The clots stored in serum were found to have further compaction of the RBCs to a polyhedron shape between day 1 and day 7, than the clots stored in saline, where the RBCs appeared to swell and return to their native shape. This is likely due to the saline solution being hypotonic (i.e. has a lower solute concentration to the RBCs), and therefore causes water to move into the RBCS, causing them to swell and burst. The serum appears to be an isotonic solution for the RBCs (i.e. has the same solute concentration as the RBCs) and therefore the RBCs maintain their polyhedron shape.

There is little information in the literature regarding optimal storage conditions for analogue clot material. However, from the observations in this study, it is recommended that clot analogues are stored in their own serum where possible, and stored at 4°C to ensure that the mechanical properties and microstructure are preserved. It is also recommended that clots are tested as soon as possible after formation to ensure accurate results.

The calibrated hyper-viscoelastic constitutive model was found to give a good fit for the experimental data. The model adopted in this study is similar to models described previously in the literature for clot material, where similar hyperelastic models, such as the Neo-Hookean and Mooney-Rivlin Models, (Malone *et al*. 2018; van Dam *et al*. 2008) and viscoelastic models, using the generalised Maxwell model, (van Dam *et al.*, 2008; Schmitt *et al.,* 2011; van Kempen *et al,*. 2015) have been proposed. An

improved fit could have been achieved by fitting to each experimental data separately i.e. one fit for the loading-unloading and one for the stress-relaxation. However, that would not be particularly useful in relation to the aim of this study which was to determine one set of parameters for each clot type that could model the behaviour observed across both experiments. Therefore, this paper reports the first model to successfully capture the loading-unloading hysteresis and stress-relaxation of the thrombus material and provides a significant advance in the current understanding of the relationship between clot composition and rate-dependent non-linear mechanical behaviour.

4.5.1 Limitations

The author acknowledges that there are some limitations to this study. In particular, the clot analogues produced are homogeneous. This is due to the preparation of the analogue material in a controlled environment and may make the analogue material slightly less clinically relevant as clots retrieved from patients have been found to be heterogeneous (Chueh *et al*. 2011). However, for the purpose of mechanical testing, it is useful to use homogeneous samples as this allows for repeatable and comparable results. These protocols could be adapted to be formed under flow conditions to form more physiologically representative clot analogues as this has been shown to induce heterogeneity (Duffy *et al*. 2016).

4.6 Conclusion

This chapter presents an experimental characterisation of analogue clot material with varying composition under two loading procedures; cyclic compression and stress-relaxation. The experimental testing and constitutive law calibration presented in this study provides the first detailed characterisation of cyclic loading-unloading hysteresis

and stress-relaxation for a range of clot analogue compositions, which are essential for the future development and evaluation of mechanical thrombectomy devices. This chapter also provides some recommendations for the storage of clot analogues before testing.

4.7 References

Ashton, J. H. *et al.* (2009) 'Compressive mechanical properties of the intraluminal thrombus in abdominal aortic aneurysms and fibrin-based thrombus mimics', Journal of Biomechanics, 42(3), pp. 197–201. doi: 10.1016/j.jbiomech.2008.10.024.

Bird, R. B. and Marsh, B. D. (1968) 'Viscoelastic Hysteresis. Part I. Model Predictions', Transactions of the Society of Rheology. The Society of Rheology, 12(4), pp. 479–488. doi: 10.1122/1.549096.

Chueh, J. Y. *et al.* (2011) 'Mechanical characterization of thromboemboli in acute ischemic stroke and laboratory embolus analogs.', AJNR. American journal of neuroradiology, 32(7), pp. 1237–44. doi: 10.3174/ajnr.A2485.

Cines, D. B. *et al.* (2014) 'Clot contraction: compression of erythrocytes into tightly packed polyhedra and redistribution of platelets and fibrin.', Blood. American Society of Hematology, 123(10), pp. 1596–603. doi: 10.1182/blood-2013-08-523860.

van Dam, E. A. *et al.* (2006) 'Determination of linear viscoelastic behavior of abdominal aortic aneurysm thrombus.', Biorheology, 43(6), pp. 695–707.

van Dam, E. A. *et al.* (2008) 'Non-linear viscoelastic behavior of abdominal aortic aneurysm thrombus', Biomechan Model Mechanobiol, 7, pp. 127–137.

Duffy, S. *et al.* (2016) 'Novel methodology to replicate clot analogs with diverse composition in acute ischemic stroke', Journal of Neurointerventional Surgery, 0, pp. 1–7.

Ferry, J. D. and Morrison, P. R. (1944) 'Chemical, Clinical, And Immunological Studies On The Prodcuts Of Human Plasma Fractionation. XVI. Fibrin Clots, Fibrin Films, And Fibrinogen Plastics.', The Journal of clinical investigation, 23(4), pp. 566–72. doi: 10.1172/JCI101523.

Gasser, T. C. *et al.* (2008) 'Failure properties of intraluminal thrombus in abdominal aortic aneurysm under static and pulsating mechanical loads.', Journal of vascular surgery, 48(1), pp. 179–88. doi: 10.1016/j.jvs.2008.01.036.

Vande Geest, J. P. *et al.* (2006) 'A planar biaxial constitutive relation for the luminal layer of intra-luminal thrombus in abdominal aortic aneurysms.', Journal of biomechanics. Elsevier, 39(13), pp. 2347–54. doi: 10.1016/j.jbiomech.2006.05.011.

Goyal, M. *et al.* (2015) 'Randomized assessment of rapid endovascular treatment of ischemic stroke.', The New England journal of medicine. Massachusetts Medical Society, 372(11), pp. 1019–30. doi: 10.1056/NEJMoa1414905.

Gunning, G. M. *et al.* (2016) 'Clot friction variation with fibrin content; implications for resistance to thrombectomy', Journal of Neurointerventioal Surgery, 372(1), pp. 1019–1030. doi: 10.1136/.

Hinnen, J. W. *et al.* (2007) 'Development of fibrinous thrombus analogue for in-vitro abdominal aortic aneurysm studies.', Journal of biomechanics, 40(2), pp. 289–95. doi: 10.1016/j.jbiomech.2006.01.010.

Huang, C.-C., Chen, P.-Y. and Shih, C.-C. (2013) 'Estimating the viscoelastic modulus of a thrombus using an ultrasonic shear-wave approach', Medical Physics. American Association of Physicists in Medicine, 40(4), p. 042901. doi: 10.1118/1.4794493.

Johnson, S. *et al.* (2019) 'Mechanical behavior of in vitro blood clots and the implications for acute ischemic stroke treatment.', Journal of neurointerventional surgery. British Medical Journal Publishing Group. doi: 10.1136/neurintsurg-2019-015489.

van Kempen, T. H. S., Peters, G. W. M. and van de Vosse, F. N. (2015) 'A constitutive model for the time-dependent, nonlinear stress response of fibrin networks.', Biomechanics and modeling in mechanobiology, 14(5), pp. 995–1006.

Kim, J. and Srinivasan, M. A. (2005) 'Characterization of Viscoelastic Soft Tissue Properties from In Vivo Animal Experiments and Inverse FE Parameter Estimation', in. Springer, Berlin, Heidelberg, pp. 599–606. doi: 10.1007/11566489_74.

Kim, O. V. *et al.* (2017) 'Quantitative structural mechanobiology of platelet-driven blood clot contraction', Nature Communications. Nature Publishing Group, 8(1), p. 1274. doi: 10.1038/s41467-017-00885-x.

Krasokha, N. *et al.* (2010) ‘Mechanical properties of blood clots - a new test method. Mechanische Eigenschaften von Thromben - Neue Untersuchungsmethoden’, Materialwissenschaft und Werkstofftechnik, 41(12), pp. 1019–1024. doi: 10.1002/mawe.201000703.

Krueger, K. *et al.* (2004) ‘How thrombus model impacts the in vitro study of interventional thrombectomy procedures.’, Investigative radiology, 39(10), pp. 641–8. doi: 10.1097/01.RLI.0000139009.65226.17.

Liebeskind, D. S. *et al.* (2011) ‘CT and MRI Early Vessel Signs Reflect Clot Composition in Acute Stroke’, Stroke, 42(5), pp. 1237–1243. doi: 10.1161/STROKEAHA.110.605576.

Liebig, T. *et al.* (2008) ‘Comparative in vitro study of five mechanical embolectomy systems: effectiveness of clot removal and risk of distal embolisation.’, Neuroradiology, 50(1), pp. 43–52. doi: 10.1007/s00234-007-0297-y.

Malone, F. *et al.* (2018) ‘The Mechanical Characterisation of Bovine Embolus Analogues Under Various Loading Conditions’, Cardiovascular Engineering and Technology. Springer US, 9(3), pp. 489–502. doi: 10.1007/s13239-018-0352-3.

Marder, V. J. *et al.* (2012) Hemostasis and Thrombosis: Basic Principles and Clinical Practice. Lippincott Williams & Wilkins.

Di Martino, E. *et al.* (1998) ‘Biomechanics of abdominal aortic aneurysm in the presence of endoluminal thrombus: Experimental characterisation and structural static computational analysis’, European Journal of Vascular and Endovascular Surgery, 15(4), pp. 290–299. doi: 10.1016/S1078-5884(98)80031-2.

Riha, P. *et al.* (1999) ‘Elasticity and fracture strain of whole blood clots.’, Clinical Hemorheology and Microcirculation, 21, pp. 45–49.

Saldívar, E., Orje, J. N. and Ruggeri, Z. M. (2002) ‘Tensile destruction test as an estimation of partial proteolysis in fibrin clots.’, American journal of hematology, 71(2), pp. 119–27. doi: 10.1002/ajh.10199.

Schmitt, C., Hadj Henni, A. and Cloutier, G. (2011) 'Characterization of blood clot viscoelasticity by dynamic ultrasound elastography and modeling of the rheological behavior', Journal of Biomechanics, 44(4), pp. 622–629. doi: 10.1016/j.jbiomech.2010.11.015.

Siller-Matula, J. M. *et al.* (2008) 'Interspecies differences in coagulation profile.', Thrombosis and haemostasis, 100(3), pp. 397–404.

Slaboch, C. L. *et al.* (2012) 'Mechano-rheological properties of the murine thrombus determined via nanoindentation and finite element modeling.', Journal of the mechanical behavior of biomedical materials, 10, pp. 75–86. doi: 10.1016/j.jmbbm.2012.02.012.

Teng, Z. *et al.* (2015) 'Layer- and Direction-Specific Material Properties, Extreme Extensibility and Ultimate Material Strength of Human Abdominal Aorta and Aneurysm: A Uniaxial Extension Study.', Annals of biomedical engineering. Springer, 43(11), pp. 2745–59. doi: 10.1007/s10439-015-1323-6.

Tutwiler, V. *et al.* (2018) 'Shape changes of erythrocytes during blood clot contraction and the structure of polyhedrocytes', Scientific Reports. Nature Publishing Group, 8(1), p. 17907. doi: 10.1038/s41598-018-35849-8.

Wang, D. H. *et al.* (2001) 'Mechanical properties and microstructure of intraluminal thrombus from abdominal aortic aneurysm.', Journal of biomechanical engineering, 123(6), pp. 536–9.

Weafer, F. M. *et al.* (2019) 'Characterization of strut indentation during mechanical thrombectomy in acute ischemic stroke clot analogs', Journal of NeuroInterventional Surgery, 11(9), pp. 891-897 neurintsurg-2018-014601. doi: 10.1136/neurintsurg-2018-014601.

Van Der Worp, H. B. and Van Gijn, J. (2007) 'Acute Ischemic Stroke', The New England journal of medicine, 357(6), pp. 572–579.

Xie, H. *et al.* (2005) 'Correspondence of ultrasound elasticity imaging to direct mechanical measurement in aging DVT in rats.', Ultrasound in medicine & biology, 31(10), pp. 1351–9. doi: 10.1016/j.ultrasmedbio.2005.06.005.

Chapter 5

Development of an In-Vitro Model of Calcified Cerebral Emboli in Acute Ischemic Stroke for Mechanical Thrombectomy Evaluation

5.1 Chapter Overview

In this chapter we report the development of a calcified clot analogue, representative of calcified cerebral emboli (CCEs) and the development of an *in-vitro* model that is capable of evaluating different endovascular treatment approaches, using contemporary devices, for the retrieval of a CCE lodged in the M1 segment of the middle cerebral artery. The *in-vitro* model consists of a CCE analogue placed in a silicone neurovascular model. Development of an appropriate CCE analogue is based on the characterisation of human calcified tissues (from carotid endarterectomy procedures and from cardiac valves removed during open cardiac surgery) that represent likely sources of CCEs. Feasibility of the model is demonstrated in a small number of mechanical thrombectomies using four common procedural techniques. Contact aspiration with a local aspiration intermediate catheter, a stent-retriever alone and a combined approach, all with the use of flow arrest and concomitant aspiration using a balloon guide catheter (BGC), is assessed. The combined technique is also evaluated without the use of a BGC.

The content of this chapter is published in the *Journal for NeuroInterventional Surgery* (Johnson *et al*. 2020). The author wishes to clarify the histology presented in this

chapter to support the characterisation of the human calcified material was performed by Dr. Seán Fitzgerald, a co-author on the above-mentioned paper by Johnson *et al.*, (2020). Similarly, the thrombectomy simulations presented were carried out in one day by an experienced neuro-interventionalist, Prof. Frédèric Clarençon, with the author's assistance. All other work reported in this chapter were performed by the author.

5.2 Introduction

In a review of major clinical studies (Albers *et al*., 2018; Berkhemer *et al*., 2014; Bracard *et al*., 2016; Campbell *et al*., 2015; Goyal *et al*., 2016; Lapergue *et al*., 2017; Molina *et al*., 2015; Muir *et al*., 2017; Nogueira *et al*., 2012, 2018, 2018, Saver *et al*., 2015, 2012), the proportion of patients experiencing procedural revascularization success (defined as TICI scores of 2b to 3) (Table 5.1) ranged from 76% in (Saver *et al*., 2015) to 85.4% in (Lapergue *et al*. 2016) when reported after all procedures. Although some retrieval failures are associated with factors other than the nature of the clot, such as difficult anatomical access (Leischner *et al*. 2018), many investigators generally seek to improve interaction between thrombectomy devices and thrombus to improve successful revascularization rates (Lapergue *et al*., 2017; Maus *et al*., 2018; Nogueira *et al*., 2018; Wiesmann *et al*., 2017).

Table 5.1 Table describing TICI scoring system (Tung *et al*. 2017).

TICI Grade	Original TICI	Modified TICI	Modified TICI With 2c
0/1	No/minimal reperfusion	No/minimal reperfusion	No/minimal reperfusion
2a	Partial filling <2/3 territory	Partial filling <50% territory	Partial filling <50% territory
2b	Partial filling ≥2/3 territory	Partial filling ≥50% territory	Partial filling ≥50% territory
2c	…	…	Near complete perfusion except slow flow or few distal cortical emboli
3	Complete perfusion	Complete perfusion	Complete perfusion

TICI indicates thrombolysis in cerebral infarction.

Calcified Cerebral Emboli (CCE) represent an uncommon cause of acute ischemic stroke (AIS), present in approximately 1-3% of all cases (Walker *et al.*, 2014; Koh *et al.*, 2017; Dobrocky *et al.*, 2018). The material properties of CCEs differ significantly from those of thrombus emboli (Chueh *et al*. 2011), and are responsible for lower recanalisation rates with standard endovascular techniques (Walker *et al.*, 2014; O'Cearbhaill *et al.*, 2016). Working under the assumption that the nature of the clot accounts for a large part of all MT failures, and owing to the difficulty to retrieve CCEs, it may be reasoned that the occurrence of AIS with CCEs is proportionally larger in the failed thrombectomy cases than in the overall AIS population undergoing MT.

CCEs consist of one (or several) build up(s) of calcium that embolise to the cerebral vasculature, leading to large vessel occlusion (LVO). In the experience from Pitié-Salpêtrière Hospital, CCEs usually occur after cardiovascular interventions, such as cardiac valve surgery/percutaneous procedures or carotid endarterectomy, however some studies have reported higher levels of spontaneous CCEs (Walker *et al.*, 2014). The presence of dense calcified material enables reliable identification of CCEs using non-contrast CT (Figure 5.1) (Christian *et al.*, 2009; Walker *et al.*, 2014), however CCEs remain among the most difficult clots to recanalise (Walker *et al.*, 2014; O'Cearbhaill *et al.*, 2016).

Contemporary treatment of AIS relies on targeting the occlusive clot using medical and endovascular therapy, which exploit the properties of thrombus to lyse or capture the occlusive material. Resistant CCEs represent a different paradigm, they are neither amenable to fibrinolysis (Kavanagh *et al.*, 2014) or mechanical engagement in the same way as thrombi (Koh *et al.*, 2017; Dobrocky *et al.*, 2018). While composite emboli occur, consisting of a mixture of thrombus and small calcified inclusions, CCEs that consist of a large solitary calcified fragment cannot be dissolved by fibrinolysis or engaged and broken apart by contemporary MT devices.

This chapter reports the development of an *in-vitro* model to evaluate different procedural approaches using contemporary endovascular treatment devices in the M1 segment of the middle cerebral artery and outlines the development of a calcified clot analogue for the first time. The objective of this chapter is to recreate a LVO involving a CCE using an *in-vitro* silicone model of the intracranial vessels. This was achieved by developing a CCE analogue that shares the biomechanical properties of calcified tissues that pose a high potential source of CCEs. The feasibility of this *in-vitro* AIS CCE model, to test different endovascular strategies to recanalise an occlusion of the M1 segment of the MCA, was demonstrated.

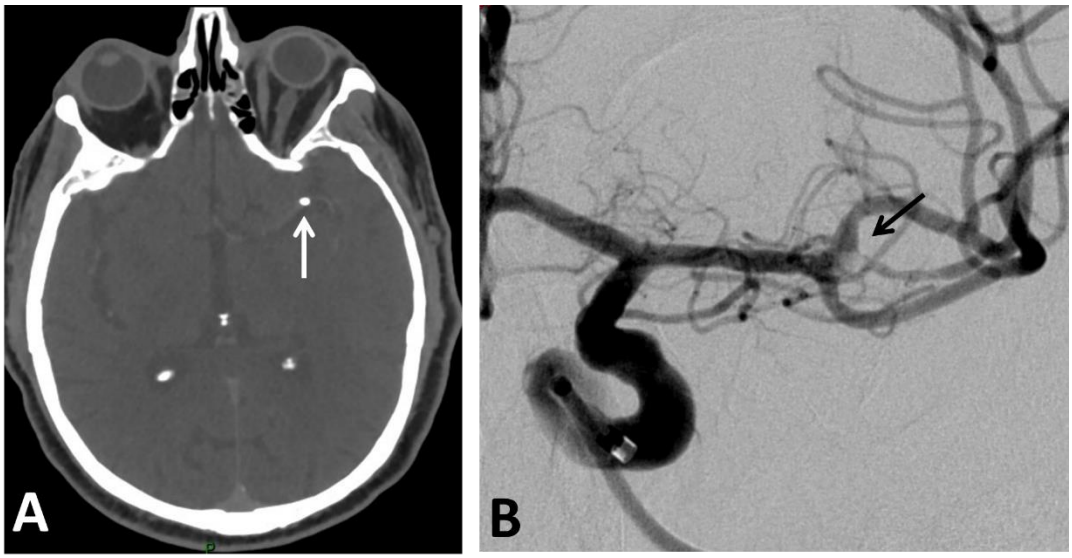

Figure 5.1 71 year old male presenting an acute onset of right hemiplegia after a transaortic valve implantation (TAVI) procedure. (A) Unenhanced CT-scan, axial slice, showing a calcified embolus (CCE) located on the course of the left M1 segment of the middle cerebral artery (MCA) (white arrow). (B) Digital subtraction angiography performed at the beginning of the mechanical thrombectomy procedure (anteroposterior projection), showing the calcified embolus located in the left MCA trifurcation (black arrow). Despite five passes using different techniques (aspiration, stent retriever), the calcified embolus could not be removed.

5.3 Materials and Methods

5.3.1 Ethical Statement

The Institutional Review board (IRB) and Research Ethics Committee (National University of Ireland Galway REC 16-SEPT-08) gave approval for this study. No informed consent was requested by the IRB since tissues harvested are considered as human waste.

5.3.2 Sample Collection

Calcified aortic valve leaflets were collected from Amiens University Hospital during open cardiac surgery procedures for cardiac valve replacement, and calcified carotid plaques were collected from endarterectomy cases at the Pitié-Salpêtrière Hospital. The calcified tissue samples were sent to NUI Galway for mechanical, histological and micro-CT analysis. The samples used for histology were preserved in formaldehyde and the samples for mechanical testing and micro-CT were preserved in an EDTA/PBS solution and were tested within 5 days of collection.

5.3.3 Clot Analogues

Calcified clot analogues were fabricated using ovine trabecular (spongy) bone from juvenile sheep (*Ovis aries*). Preliminary testing was performed on cortical and trabecular bone from different animal species under compression to determine a suitable analogue material. The trabecular ovine bone was found to provide a good match for the calcified tissue and therefore was selected to produce the CCE analogues. Bones were collected from a local butcher (Galway, Ireland) the day after slaughter. The outer, cortical bone was removed to allow isolation of the inner, trabecular bone. The bone was cut to the target size of 3.5 mm in length and 3 mm

width, according to CCE dimensions observed clinically, using a blade and smoothed with sandpaper.

Two types of CCE analogues were formed – with and without the surrounding thrombus matrix. The first consisted of the above-described bone fragments only, and the latter were prepared by forming a thrombus around a bone fragment. Venous ovine blood was collected using methods similar to those reported previously in Chapters 3 and 4 (Duffy *et al*. 2016; Johnson *et al*. 2019). Platelet rich plasma (PRP) was isolated from the citrated blood by spinning at 180g for 10 minutes. The remaining fraction of blood was spun again at 2200g to isolate the red blood cells (RBCs) (Johnson *et al*. 2019). A blood mixture of 1% hematocrit was created with the PRP and RBCs. The anticoagulant was reversed with a 2.06% calcium chloride solution in a 1:9 ratio with the plasma. After immediate mixing, the blood mixture was placed in a close-ended glass tube along with a single bone fragment to allow formation of blood clot around the bone and kept at 37°C overnight to allow the clot to mature and attach to the bone. The clot was brought to its final size by trimming away excess thrombus surrounding the bone fragment.

5.3.4 Micro-Computed Tomography

Samples were scanned using micro-computed tomography (μCT) (Scanco Medical μCT100), in the axial direction, at intensity settings of 45 kV, 200 μA and 9 W. An air filter was used with an integration time of 55 ms. A voxel size of 20 μm was achieved allowing for sufficient resolution of the sample constituents. Samples were submerged in mineral oil during scanning to create a sufficiently large density differential between the medium and the fibrous material, allowing for identification of the outer boundary of the tissue samples. A selection of full, intact samples of both

cardiac valve leaflets and endarterectomy plaques (n = 3 in each group) were scanned to quantify the extent of calcified material present in the tissue samples and to determine the size of the isolated calcified deposits.

The scans were processed, and the constituents of the samples were discretised using a greyscale value range of 50-600 for fibrous tissue with grayscale values of 600-1000 used for calcifications (Figure 5.2 A-B). 3D models of composite tissue samples, consisting of fibrous tissue and embedded calcifications were then generated.

Image J software was used to quantify the size of the calcifications within the material. As the cross-section of the isolated calcified inclusions in the tissue were not perfectly circular, the Feret's diameter (mm), which is defined as the longest distance between any two points along the boundary of the region of interest, was used to compare the size of the particles (Figure 5.2 C).

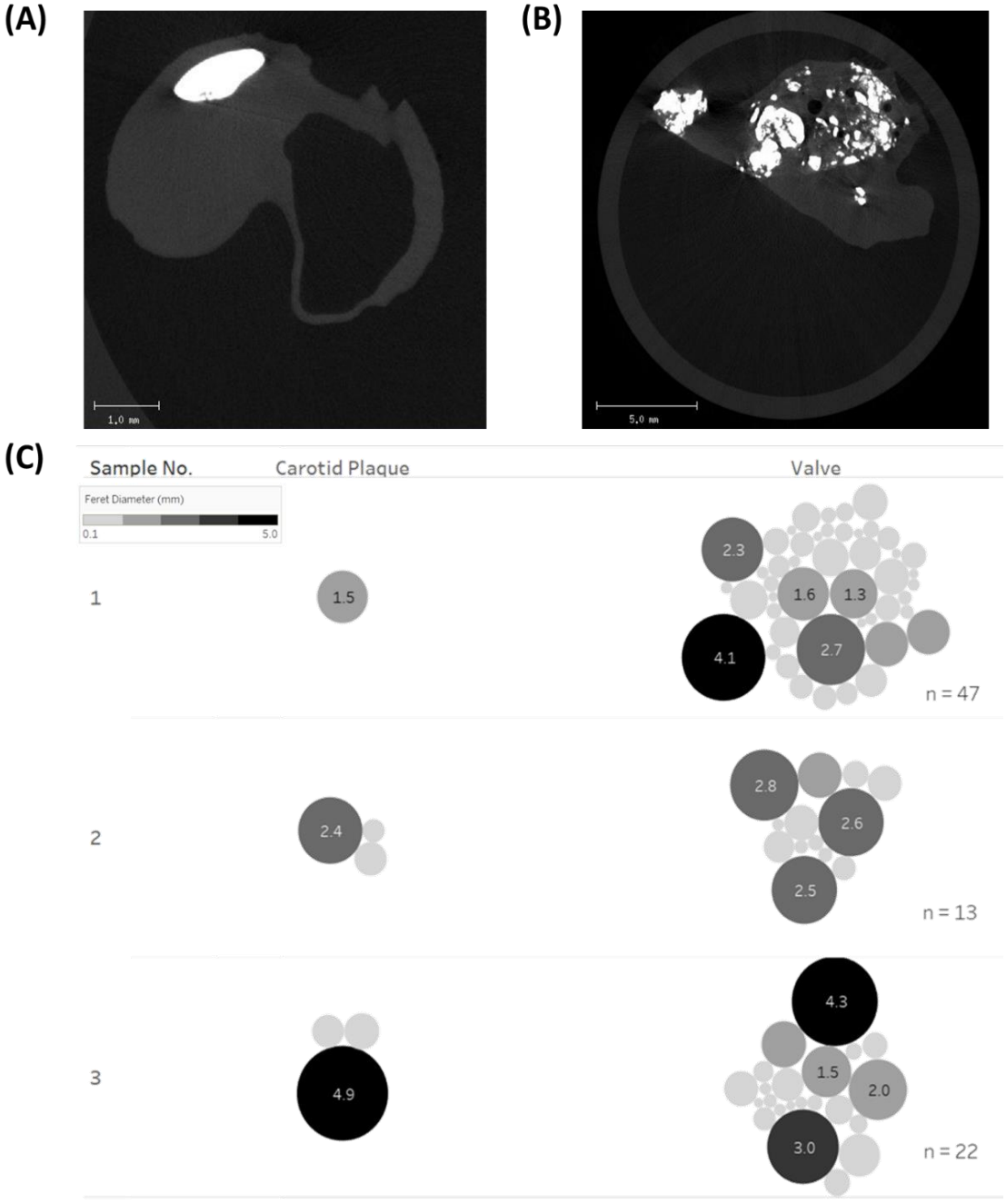

Figure 5.2 Representative transverse cross-sectional slices obtained from µCT of (A) a carotid plaque and (B) a calcified valve leaflet. (C) Bubble charts showing the relative size and quantity (dictated by the number of bubbles and the n-number) of isolated calcified inclusions in 3 separate samples of carotid plaques and valve leaflets. The Feret's diameter (mm) of each isolated calcified inclusion is used to determine the bubble size, with values for some of the largest inclusions provided within the bubble.

5.3.5 Histological Analysis

Following μCT analysis, the samples were fixed in 10% Neutral Buffered Formalin for 24 hours. Gross photographs were taken of each sample (Figure 5.3 A-B). The samples were then decalcified in Leica Surgipath Decalcifier II solution for three days, and the decalcification solution was changed daily. Following decalcification, the samples were processed using a standard tissue processing protocol, embedded in paraffin and cut into 3 μm sections and one section was mounted on each slide. Representative slides from each sample were stained with Alizarin Red stains and Martius Scarlett Blue (MSB) (Figure 5.3 C-D). Following staining, the slides were scanned at 20x magnification on an Olympus VS120 slide scanner and digital whole-slide scan images were generated. Percentage area of tissue components and mineralisation within the sample was calculated for the MSB and Alizarin Red stained images using Orbit Image Analysis Software.

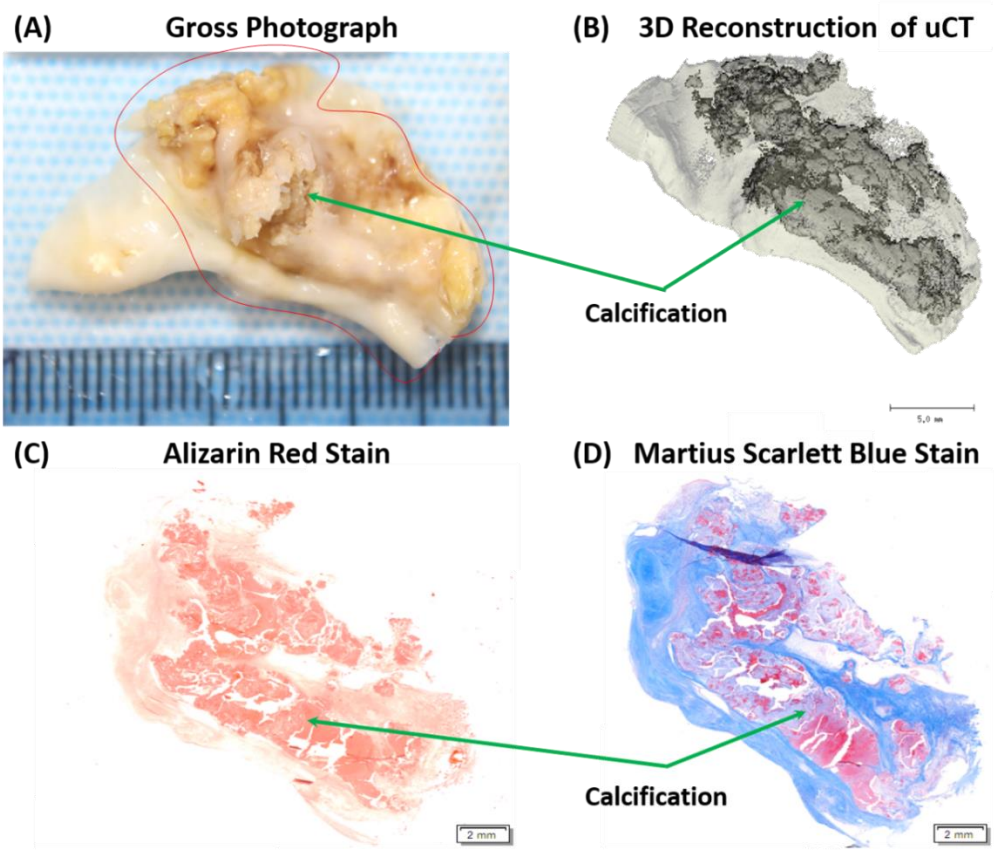

Figure 5.3 (A) Gross photograph of calcified cardiac valve leaflet. (B) 3D reconstruction of the same calcified cardiac valve leaflet from the µCT imaging. (C) Alizarin red stained section of the leaflet with the darker red/brown colour indicating areas of mineralisation. (D) Martius scarlet blue stained section highlighting areas of mineralisation in red and regions of connective tissue in blue.

5.3.6 Mechanical Analysis

Unconfined compression testing was used to determine the material behaviour. Testing was carried out at ambient temperature, on a Zwick uniaxial tensile machine (Zwick Z2.5, Ulm, Germany), using customised aluminium platens. Test samples were isolated from calcified human cardiac valves and carotid plaques (minimum of n = 10 for each group) and were pre-shaped to have a cubic shape with flat upper and lower surfaces for parallel plate compression. With the sample positioned in the centre of the bottom platen, the crosshead position of the machine was adjusted so that the

top platen was almost touching the top of the sample at the beginning of the test. The specimens were loaded to a compressive nominal strain of 30% at a strain rate of 10% per second. The same procedure was followed when testing the CCE analogues (n = 8). To compare the mechanical behaviour of the materials, the initial stiffnesses were determined from the slopes of straight lines fitted to the initial linear portions of the nominal stress-strain curves.

5.3.7 Device Selection

For this study, three stent-retriever device designs were selected; Solitaire2 4x40 mm (Medtronic, CA, USA), Trevo XP ProVue 4x20 mm (Stryker, MI, USA) and EmboTrapII 5x33 mm (Cerenovus, Galway, Ireland). The Solitaire and Trevo devices employ a 'typical' cylindrical closed-cell design, meanwhile the EmboTrap has a segmented design. An ACE 68 intermediate catheter (Penumbra, Alameda, CA, USA) was used for local aspiration and for the combined technique with stent-retriever. A Rebar 18 microcatheter (Medtronic, Irvine, CA, USA) was used to deliver the stentriever, a Merci 9F BGC (Stryker) was used to achieve flow arrest and a 6F NeuronMax long sheath (Penumbra) when flow was not arrested.

5.3.8 Silicone Vascular *In-Vitro* Model

Simulated *in-vitro* MT procedures were performed using a 3D silicone model of the human cerebral vasculature (Figure 5.4 A-B). This patient vascular replica model (Elastrat Sàrl, Geneva, Switzerland) is comprised of the complete intracranial circulation with both internal carotid and vertebral arteries, complete circle of Willis, and functional anterior and posterior communicating arteries with distal circulation up to M2 and A2 segments of the MCA and ACA, respectively. An isotonic saline solution, heated to 37°C to simulate human body temperature, was circulated through

the model using a continuous flow pump. The flow rate of the circulating fluid was maintained at 680 ± 50 ml/min for the full model, and 287 ± 35 ml/min in ICA.

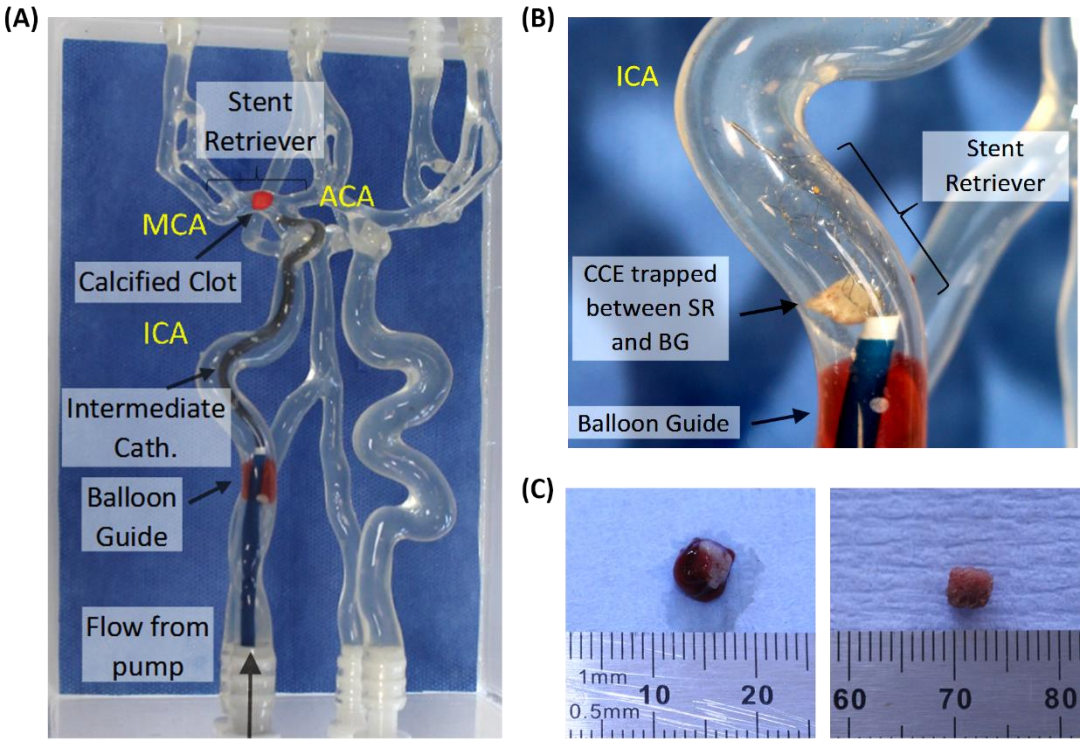

Figure 5.4 (A) Silicone vascular model showing the balloon guide catheter inflated, intermediate catheter (for local aspiration) and location of the stent retriever. The calcified clot position in the mid M1 segment of the MCA. (B) Image of the CCE analogue trapped between the stent retriever and balloon guide catheter tip. (C) CCE analogue with (left) and without thrombus attached (right).

5.3.9 *In-Vitro* Procedural Technique

Thrombectomy simulations were carried out in one day by an experienced neuro-interventionalist (FC). Revascularization of an M1 segment occlusion of the MCA was attempted with four different procedural approaches to assess the ability of the *in-vitro* model to differentiate recanalisation success between approaches; (1) Contact aspiration with an intermediate catheter, (2) stent-retriever alone, (3) a combined approach, all with the use of flow arrest and manual aspiration using a balloon guide catheter (BGC), and (4) a combined technique without the use of a BGC but with a

long guide sheath instead. For each MT procedure, one CCE analogue sample was introduced into the internal carotid artery (ICA) through a side port of the silicone model off the external carotid artery (ECA) branch, and allowed to migrate to the M1 segment of the MCA, causing an occlusion. To consistently target the same region of the anatomy, all clot samples were cut to the same approximate size of 3.5 mm (Figure 5.4 C). The flow in the MCA in the region distal to the clot was measured using a flow meter (T110 Flow meter, Transonic Systems Inc., Ithaca, NY, USA) clamped to the outside of the vessel.

For each procedure an access catheter (I.D. 0.088") was positioned at the cervical ICA. The 0.014" micro guidewire and microcatheter (I.D. 0.021") were used to position the stent-retriever at the site of the occluding clot. All devices were used according to their instructions for use. A maximum of three attempts was tried to retrieve the CCE. A video recording of each procedure was collected. When local aspiration was used, a mechanical pump (Hersill V7 Plus AC), which can be set to 'High' or 'Low', was set to 'High', and was used prior to initiating retrieval. Manual aspiration with a syringe, through the guide catheter was carried out during retrievals. Success was defined as complete capture of the CCE, with no clot remaining in the model after three passes. If the clot was lost upon retrieval, the location at which engagement was lost was noted.

5.3.10 Statistical Analysis

Statistical analysis for the mechanical test data was carried out using the general linear model ANOVA (analysis of variance) procedure in Minitab (version 18.1). A comparison of the initial moduli was performed with a Bonferroni model ($\alpha = 0.05$) to

compare the initial moduli of the calcified tissue and the CCE analogue material with the thrombus analogue.

Descriptive statistics for the μCT analysis are included in the results section. To compare the success/failure rates of each procedural approach for each retrieval attempt, statistical analysis was carried out using the Chi-square test for association procedure.

5.4 Results

5.4.1 μCT and histological characterisation of *ex-vivo* calcified tissue

The calcified tissue samples were divided into two groups; calcified cardiac valve leaflets and calcified carotid plaques. The μCT analysis found that the carotid plaques contained fewer isolated calcified deposits than the cardiac valve samples (Figure 5.2 A-B). The carotid plaques were determined to be in majority composed of fibrous tissue (98.45% ± 1.67%) with isolated calcified deposits present in low abundance (1.55% ± 1.67%). The calcified material consisted of one or two large calcifications surrounded by the fibrous tissue. In contrast, the valve leaflet material was found to contain both small and large isolated calcified deposits (22.85% ± 4.31%) scattered throughout the fibrous tissue (75.84% ± 2.10%) and along the surface of the material. This result was supported by the histological analysis.

The dimensions of the calcifications present in the *ex-vivo* tissue were measured from the μCT images, and the Feret's diameter was used to quantify the size of the calcified particles (image provided in supplementary material). The mean Feret's diameter for calcifications within the carotid plaque tissue was found to be 1.112 mm ± 1.103, with a minimum diameter of 0.056 mm and maximum of 4.901 mm. The cardiac valve tissue was found to have a mean Feret's diameter of 0.6162 mm ± 0.9533, with a

minimum of 0.006 mm and a maximum of 7.196 mm. Therefore, many of the individual calcifications were found to be within the same size range as CCEs seen clinically (Walker *et al.*, 2014; Dobrocky *et al.*, 2018).

The histological quantification of the Alizarin Red stained slide identified that there was 30.4% mineralisation and 69.6% of tissue components in the sample (Figure 5.3 C). The MSB staining identified that there was 29.3% mineralisation, 57.7% collagen and 13.0% of other tissue components in the sample. Collagen, shown in blue in Figure **5.** 5.3 D, is seen to encapsulate the regions of mineralisation, with just minimal collagen infiltration through these regions.

5.4.2 Mechanical characterisation of *ex-vivo* and CCE analogue samples

The initial stiffness values for the carotid plaque and cardiac valve samples were similar, 13.71 kPa ± 12.52 and 19.74 kPa ± 28.78 (mean ± st. dev.), respectively (Figure 5.5 A). A marginally higher stiffness and larger variation seen in the valve leaflets is likely due to heavier calcification than the carotid plaques.

The mechanical testing of the ex-vivo calcified tissue was used as a reference to develop an analogue material with similar mechanical properties that could be used to replicate the material behaviour *in-vitro*. Cortical and trabecular bone from different animal species were tested to determine a suitable material to produce the CCE analogues (results not provided here). Mechanical testing showed the CCEs, constructed from ovine trabecular bone, mimicked the behaviour of the *ex-vivo* material well (Figure 5.5 B) and had similar stiffness values of 16.26 kPa ± 17.29. Both the *ex-vivo* calcified tissue and the CCE analogues were found to be approximately four to five times stiffer than *in-vitro* blood clots (Figure 5.5 C), which were found to have an initial stiffness of 4.21 kPa ± 1.73.

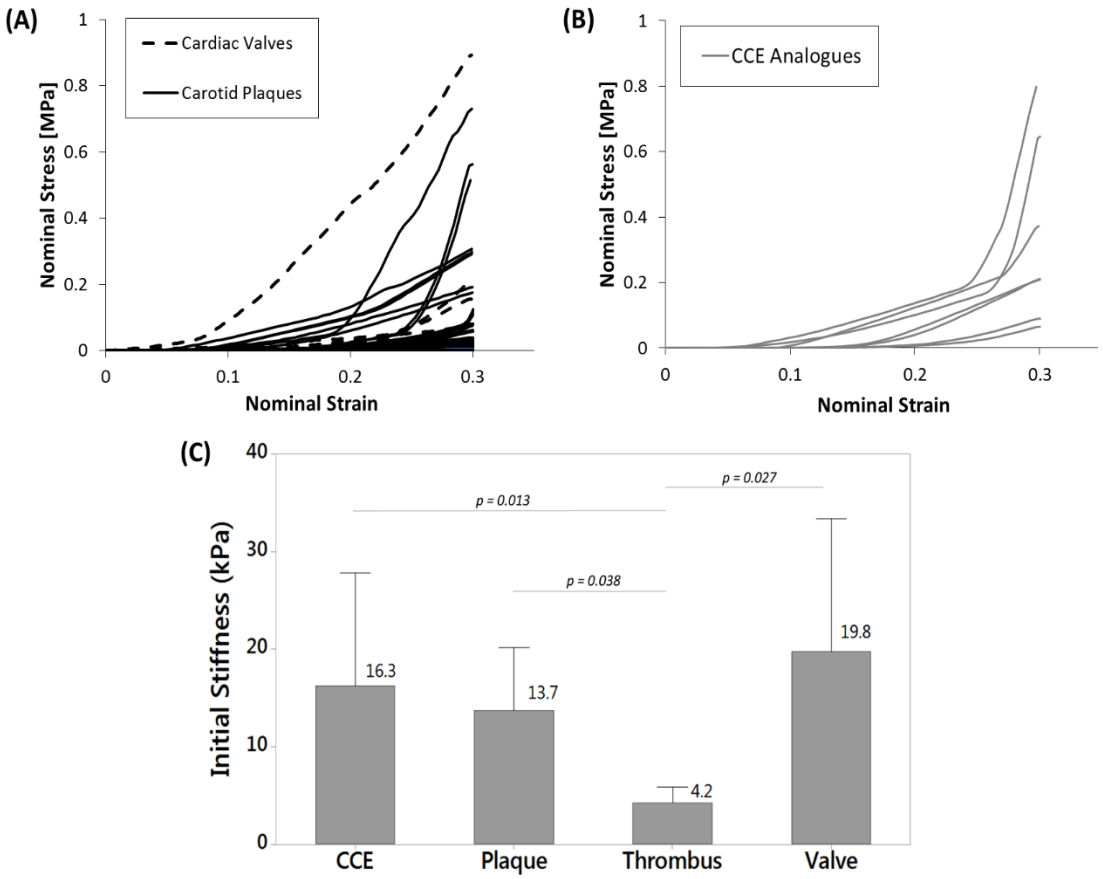

Figure 5.5 Plot of nominal stress vs strain in compression for (A) the ex-vivo calcified material obtained from cardiac valves and carotid plaques and (B) the CCE analogues. (C) Plot comparing the mean initial stiffness values for the CCE analogues (n = 8) with the ex-vivo carotid plaques (n = 12) and cardiac valves (n = 14) with the thrombus analogue material (n = 5) with error bars showing standard deviation.

5.4.3 Thrombectomy Simulations

Thrombectomy procedures were attempted using CCEs with and without adherent thrombus. The presence of thrombus did not affect the success of the procedures however it did impact crossing using the guidewire. It was more difficult to cross CCEs with adhered thrombus, sometimes taking several attempts with a guidewire. However, in all procedures that required the guidewire to cross the CCE, placement of the guidewire was eventually successful. In addition, the presence of attached thrombus led to a complete loss of flow in the MCA in the region distal to the clot, whereas CCE analogues of bone alone reduced flow to approximately 20% of the flow in the unobstructed vessel. This indicates the porous nature of the CCE analogue, which may not be physiologically relevant, Adherent thrombus was stripped from the bone fragment following one or two passes with a stent-retriever, which also resulted in partial restoration of flow to the MCA region distal to the CCE. In two out of nineteen attempts to position the microcatheter in a suitable location distal to the CCE, a sub-optimal position was achieved because of failure to fully cross the CCE, thereby resulting in non-ideal stent-retriever placement in a more proximal location than desired.

During clot retrieval with up to three passes, contact aspiration alone with flow-arrest was the least effective, with the force of aspiration alone unable to dislodge the CCE in any of the attempts (Figure 5.6). The most effective approach was the combined technique and BGC, where the CCE was retrieved to the tip of the BGC and subsequently removed in all attempts. Recovery of the CCE was achieved by removing the entire device system and CCE en-bloc, with the CCE secured between the tip of the BGC and SR. The combination of SR and local aspiration without flow arrest enabled CCE dislodgement from the mid M1 segment but the CCE was lost at the

proximal MCA/ICA terminus in each attempt. One of three attempts with a SR alone and BGC was successful at recovering the CCE fully, with the CCE being brought back to the distal cavernous segment in the other two attempts.

For an average of eleven procedures and a total of twenty-nine passes, 84% of passes failed and only 16% of passes were successful. In the *in-vitro* experiments, where four procedure approaches were used, there was a statistical difference among the outcomes when comparing techniques using the Chi-Square test for association ($p = 0.029$). Therefore, there is an association between the outcome and the procedural approach used, and hence, the CCE AIS model is capable of differentiating between techniques.

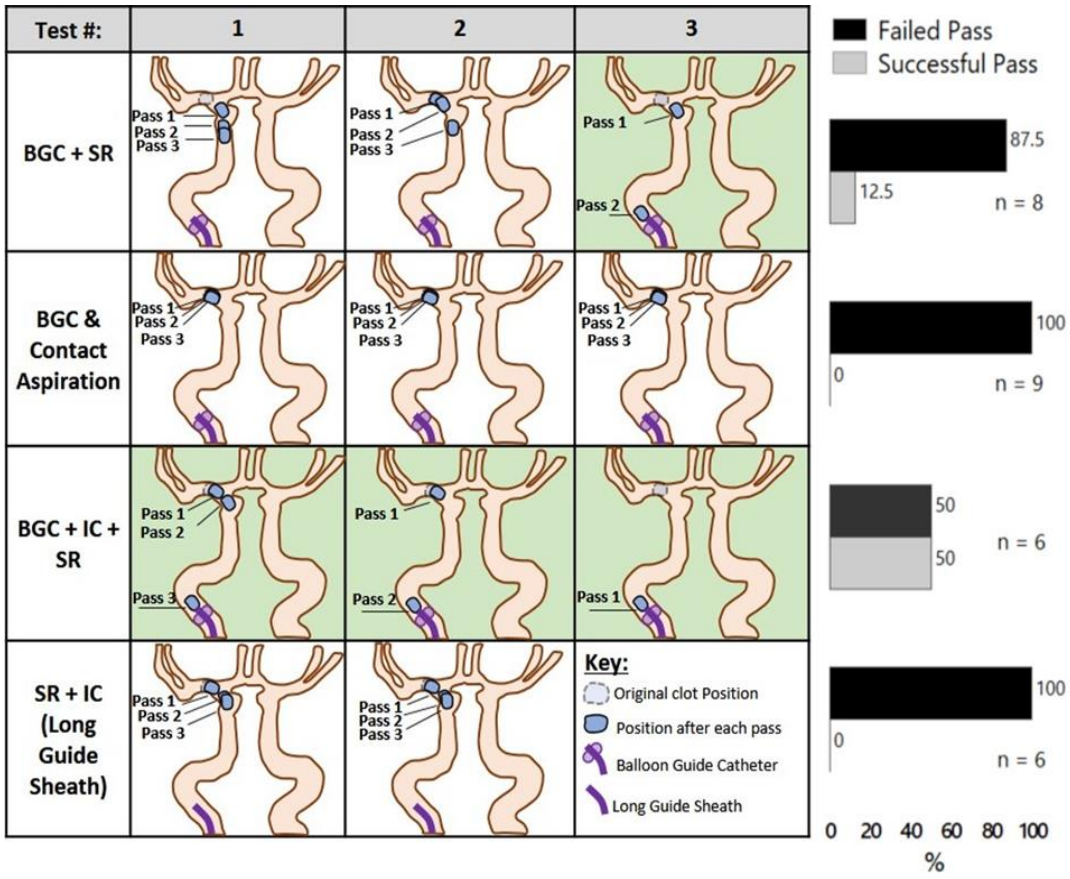

Figure 5.6 Schematic diagram showing the position in the anatomical model at which engagement with the CCE was lost after each pass (left), and plot outlining the breakdown of the percentage of successful and failed passes per procedural technique (right). The original clot position for all tests is located in the mid M1 segment of the MCA. The successful cases are indicated by the green coloured background. The CCE was successfully removed in every case in which the CCE was retrieved to the balloon guide catheter (BGC). IC: Intermediate Catheter. SR: Stentretriever

5.5 Discussion

This chapter reports the development of an *in-vitro* AIS model of a CCE occlusion, that can be used to evaluate different mechanical thrombectomy procedural approaches and devices in the M1 segment of the middle cerebral artery *in-vitro*. Silicone anatomical models of the neurovasculature have been widely used for AIS simulation, and their accuracy has been improved through the use of actual blood clot analogues, rather than analogues consisting of synthetic alternatives made of different

materials. In the same way we hypothesised, for an AIS model of a CCE occlusion, that a CCE analogue consisting of similar material to an actual CCE would provide the most accurate *in-vitro* model.

Since CCEs in clinical cases prove difficult to retrieve by endovascular means (Walker *et al.*, 2014; O'Cearbhaill *et al.*, 2016; Koh *et al.*, 2017), analysis of their composition is usually not possible. Therefore, in order to make a representative CCE analogue, we chose to study the isolated biological tissues from where they originate: calcified cardiac valves and calcified carotid artery stenosis. Micro-CT and histological analysis clearly show the calcifications organised in distinctive ways in both tissue types, which is unsurprising considering differences in the underlying pathophysiology, however some common features exist.

µCT examination shows the presence of isolated calcified inclusions surrounded by connective tissue. It is possible to envisage calcified deposits being liberated from the surrounding soft tissue during invasive procedures such as transcatheter valve placement and carotid endarterectomy (Ramírez-Moreno *et al*. 2017). A larger quantity of isolated calcified deposits, of various sizes, were observed in the cardiac valve samples than in the carotid plaques. However, many of the individual deposits within both tissue sample groups were of sufficient size to obstruct a large vessel in the intracranial vasculature (Walker *et al.*, 2014; Dobrocky *et al.*, 2018). Apart from LVOs caused by one or two large CCEs, another common observation is the so-called 'salted pretzel' sign, where several small calcified emboli are found scattered throughout a large vascular territory in the brain (Christian *et al*. 2009; Raghib *et al*. 2018; Gschwind *et al*. 2013). The observation of a large quantity of small isolated calcified deposits of less than 1 mm in diameter, particularly in the cardiac valve

samples, indicate that these calcified tissues are also a potential source for these clinical observations.

Histological examination of the calcified tissues did not identify thrombus. The arrangement of collagen and other soft tissue around isolated calcified deposits suggest that particles consisting mostly of calcified material could occur if the surrounding collagen is disrupted during vascular interventions resulting in calcified emboli predominantly made up of a hard, mineralized deposit without softer tissue attached. Whether or not CCEs already have attached thrombus before they cause an occlusion, it is highly probable that thrombus will form at the site of the intracranial occlusion. High shear blood flow around a CCE wedged in the vessel lumen will lead to platelet activation and thereby thrombus formation (Hathcock 2006). The presence of a platelet-rich thrombus attached to a CCE was evaluated in the *in-vitro* model and was shown to increase the difficulty of crossing the occlusion with a guidewire. A partial restoration of blood flow following passes with a stent-retriever was also observed as the softer thrombus was stripped from the calcified material. However, the likelihood of the vessel fully re-occluding is high unless the CCE is removed.

The CCE analogues were found to successfully replicate the mechanical behaviour of *ex-vivo* calcified tissue when tested under compression, with similar initial stiffness values. When the compressive stiffness of the calcified material and CCE analogues are compared to those of blood thrombus, they were found to be approximately 4-5 times greater. Similar results were reported by Chueh *et al.* where calcified human thromboemboli were found to be significantly stiffer than regular thrombi, when tested in compression (Chueh *et al*. 2011). This is to be expected as the calcifications greatly increases the overall stiffness of the material matrix.

Due to the stiffness of the CCE analogues in the *in-vitro* model, they could not be deformed by the thrombectomy devices during the retrieval attempts. Therefore, it was impossible to pull a 3.5 mm CCEs, even in part, into a 9F guide catheter, or the smaller distal access catheter. This is a limitation of the current treatment strategies as the clot must be removes en-bloc by dragging the CCE along the vessel wall in-vivo which could cause further vessel damage, thus inducing thrombosis.

The most successful strategy in removing the CCEs from the *in-vitro* model was a combined technique, using a stent-retriever with local aspiration under flow arrest conditions. This reflects previous studies which report the success of a combined technique with a BGC in thrombus retrievals (Chueh *et al*. 2013; Maegerlein *et al*. 2018; Nikoubashman *et al*. 2018). The combination of each of the three devices had a critical and different part to play in this success, with each on their own or in dual combination proving to be mostly ineffective. Firstly, the stent-retrievers enabled enough mechanical engagement with CCEs to allow them to be dragged from the mid M1 segment of the MCA to more proximal vessel segments with larger diameter. Without this mechanical engagement it would not be possible to dislodge the CCE as seen when aspiration on its own was used. The ineffectiveness of contact aspiration alone has been previously reported (Koh *et al.*, 2017). Larger bore aspiration catheters have been showing promise in recent clinical studies, however they were not investigated in this study (Nikoubashman *et al*. 2017).

The stent-retriever allowed control of the CCEs by pinning it against the vessel wall. Once in the proximal ICA, the CCEs became ensnared in the stent-retrievers which allowed them to be securely trapped at the tip of the BGC during subsequent withdrawal. Secondly, co-aspiration using a distal access catheter acted to enhance the engagement of the CCE between the stent-retriever and the vessel wall, particularly at

the ICA terminus and the cavernous ICA, where the CCE otherwise tended to roll off the stent-retriever. Aspiration in the stagnant column of fluid in the proximal ICA encouraged the CCEs into the inner lumen of the fully opened stent-retrievers. Finally, flow arrest with the BGC reduced the flow in the MCA and the distal ICA sufficiently to maintain CCE engagement with the stent-retriever. Once the stent-retriever dislodged the CCEs from the MCA and began to move into a larger proximal vessel, the CCEs became very mobile under full flow conditions and it was difficult to retain engagement, even with local aspiration. The establishment of flow arrest in the proximal ICA also enabled flow reversal using aspiration, which in each successful case resulted in pulling the CCE into the fully expanded stent-retriever.

This chapter has included preliminary experiments to highlight the capability of the *in-vitro* model. A more comprehensive analysis is required to draw definitive conclusions when comparing techniques. However, this result supports the benefit of a combined approach (stent retriever + aspiration) with a BGC. Interestingly, in the previous studies focused on MT in CCEs, which showed recanalisation failure in most cases, BGC was not used in the majority of the cases previously reported clinical observations in thrombectomy procedures, which have demonstrated high success rates when removing thrombi, but are often unsuccessful when attempting to remove CCEs (Koh *et al.*, 2017; Dobrocky *et al.*, 2018). Thrombectomy devices, as the name implies, have been developed to capture thrombi that are much softer and more deformable than the stiffer and more rigid CCEs. The contemporary thrombectomy devices are thus probably less effective in removing hard embolic material such as CCEs, thus explaining the poorer clinical outcomes observed in patients treated by MT.

5.5.1 Limitations

Although silicone models are widely utilised for *in-vitro* simulation of AIS and treatment procedures, they can behave quite differently to native vessels, in terms of vessel compliance and friction. This study presents one model of patient-specific anatomy, though many varying patient anatomies exist. Similarly, vessel dissections, which are commonly observed clinically when removing CCEs, are not represented in the model, as well as other limiting factors such as the ICA/MCA angle, the presence of vessel disease and patient comorbidities.

Additionally, the interventionalist preforming the retrievals could see the CCEs and the retrieval devices within the model. This was not realistic as the interventionalist can only see device markers when preforming these procedures *in-vivo* and can only barely see the hyperdense clot.

Another limitation of this study is that we examined the removal of CCEs from one vessel only – the M1 segment of the MCA. Different behaviours may be observed in other vessels or in the distal MCA.

5.6 Conclusion

In the absence of specific devices for CCEs, this chapter reports an *in-vitro* model of a LVO in the anterior circulation with a CCE that may be used to evaluate different endovascular MT approaches. This *in-vitro* model suggests that the most successful procedure involved a stent-retriever combined with local aspiration through an intermediate catheter and importantly, with flow arrest and dual aspiration using a BGC. However, a more comprehensive analysis is required to draw definitive conclusions when comparing techniques. The *in-vitro* model provides a test platform

for the evaluation of future purpose-designed devices for this unresolved clinical scenario.

5.7 References

Albers, G. W. *et al.* (2018) 'Thrombectomy for Stroke at 6 to 16 Hours with Selection by Perfusion Imaging', New England Journal of Medicine. Massachusetts Medical Society, 378(8), pp. 708–718. doi: 10.1056/NEJMoa1713973.

Berkhemer, O. A. *et al.* (2014) 'A Randomized Trial of Intraarterial Treatment for Acute Ischemic Stroke', New England Journal of Medicine. Massachusetts Medical Society, (372), pp. 11–20.

Bracard, S. *et al.* (2016) 'Mechanical thrombectomy after intravenous alteplase versus alteplase alone after stroke (THRACE): a randomised controlled trial', The Lancet Neurology. Elsevier, 15(11), pp. 1138–1147. doi: 10.1016/S1474-4422(16)30177-6.

Campbell, B. C. V. *et al.* (2015) 'Endovascular Therapy for Ischemic Stroke with Perfusion-Imaging Selection', New England Journal of Medicine. Massachusetts Medical Society, 372(11), pp. 1009–1018. doi: 10.1056/NEJMoa1414792.

Christian, B. A. *et al.* (2009) 'Showered calcific emboli to the brain, the "salted pretzel" sign, originating from the ipsilateral internal carotid artery causing acute cerebral infarction.', Stroke, 40(5), pp. e319-21. doi: 10.1161/STROKEAHA.108.538009.

Chueh, J. Y. *et al.* (2013) 'Reduction in Distal Emboli With Proximal Flow Control During Mechanical Thrombectomy', Stroke, 44(5), pp. 1396–1401. doi: 10.1161/STROKEAHA.111.670463.

Chueh, J. Y. *et al.* (2011) 'Mechanical characterization of thromboemboli in acute ischemic stroke and laboratory embolus analogs.', AJNR. American journal of neuroradiology, 32(7), pp. 1237–44. doi: 10.3174/ajnr.A2485.

Dobrocky, T. *et al.* (2018) 'Thrombectomy of calcified emboli in stroke. Does histology of thrombi influence the effectiveness of thrombectomy?', Journal of neurointerventional surgery. British Medical Journal Publishing Group, 10(4), pp. 345–350. doi: 10.1136/neurintsurg-2017-013226.

Duffy, S. *et al.* (2016) 'Novel methodology to replicate clot analogs with diverse composition in acute ischemic stroke', Journal of Neurointerventional Surgery, 0, pp. 1–7.

Goyal, M. *et al.* (2016) 'Endovascular thrombectomy after large-vessel ischaemic stroke: a meta-analysis of individual patient data from five randomised trials', The Lancet. Elsevier, 387(10029), pp. 1723–1731. doi: 10.1016/S0140-6736(16)00163-X.

Gschwind, M. *et al.* (2013) 'Neurological picture. Dispersion and "salted pretzel sign" from thrombolysis of a spontaneous calcified embolus in an acute stroke.', Journal of neurology, neurosurgery, and psychiatry. BMJ Publishing Group Ltd, 84(1), pp. 111–2. doi: 10.1136/jnnp-2012-303298.

Hathcock, J. J. (2006) 'Flow effects on coagulation and thrombosis.', Arteriosclerosis, thrombosis, and vascular biology, 26(8), pp. 1729–37. doi: 10.1161/01.ATV.0000229658.76797.30.

Johnson, S. *et al.* (2019) 'Mechanical behavior of in vitro blood clots and the implications for acute ischemic stroke treatment.', Journal of neurointerventional surgery. British Medical Journal Publishing Group. doi: 10.1136/neurintsurg-2019-015489.

Johnson, S. *et al.* (2020) 'Development of an in vitro model of calcified cerebral emboli in acute ischemic stroke for mechanical thrombectomy evaluation.', Journal of neurointerventional surgery. British Medical Journal Publishing Group. doi: 10.1136/neurintsurg-2019-015595.

Kavanagh, E., Fenton, D. and Heran, M. (2014) 'Calcified cerebral emboli.', American Journal of Neuroradiology. American Journal of Neuroradiology, 27(9), pp. 1996–1999. doi: 10.3174/ajnr.a3892.

Koh, E. *et al.* (2017) 'Manual Aspiration Thrombectomy in Patients with Acute Stroke-Related Calcified Cerebral Emboli.', Journal of stroke and cerebrovascular diseases : the official journal of National Stroke Association. Elsevier, 26(10), pp. 2050–2054.

Lapergue, B. *et al.* (2016) 'A Direct Aspiration, First Pass Technique (ADAPT) versus Stent Retrievers for Acute Stroke Therapy: An Observational Comparative

Study', American Journal of Neuroradiology, 37(10), pp. 1860–1865. doi: 10.3174/ajnr.A4840.

Lapergue, B. *et al.* (2017) 'Effect of Endovascular Contact Aspiration vs Stent Retriever on Revascularization in Patients With Acute Ischemic Stroke and Large Vessel Occlusion', JAMA. American Medical Association, 318(5), p. 443. doi: 10.1001/jama.2017.9644.

Leischner, H. *et al.* (2018) 'Reasons for failed endovascular recanalisation attempts in stroke patients', Journal of NeuroInterventional Surgery , 0, pp. 1–5.

Maegerlein, C. *et al.* (2018) 'Further Development of Combined Techniques Using Stent Retrievers, Aspiration Catheters and BGC', Clinical Neuroradiology. Springer Berlin Heidelberg, pp. 1–7. doi: 10.1007/s00062-018-0742-9.

Maus, V. *et al.* (2018) 'Maximizing First-Pass Complete Reperfusion with SAVE', Clinical Neuroradiology. Springer Berlin Heidelberg, 28(3), pp. 327–338. doi: 10.1007/s00062-017-0566-z.

Molina, C. A. *et al.* (2015) 'REVASCAT: A Randomized Trial of Revascularization with Solitaire FR® Device vs. Best Medical Therapy in the Treatment of Acute Stroke Due to Anterior Circulation Large Vessel Occlusion Presenting within Eight-Hours of Symptom Onset', International Journal of Stroke. John Wiley & Sons, Ltd (10.1111), 10(4), pp. 619–626. doi: 10.1111/ijs.12157.

Muir, K. W. *et al.* (2017) 'Endovascular therapy for acute ischaemic stroke: the Pragmatic Ischaemic Stroke Thrombectomy Evaluation (PISTE) randomised, controlled trial.', Journal of neurology, neurosurgery, and psychiatry. BMJ Publishing Group, 88(1), pp. 38–44. doi: 10.1136/jnnp-2016-314117.

Nikoubashman, O. *et al.* (2017) 'Necessary Catheter Diameters for Mechanical Thrombectomy with ADAPT', American Journal of Neuroradiology. American Journal of Neuroradiology, 38(12), pp. 2277–2281. doi: 10.3174/AJNR.A5401.

Nikoubashman, O. *et al.* (2018) 'Balloon-Guide Catheters Are Needed for Effective Flow Reversal during Mechanical Thrombectomy.', AJNR. American journal of neuroradiology. American Journal of Neuroradiology, 39(11), pp. 2077–2081. doi: 10.3174/ajnr.A5829.

Nogueira, R. G. *et al.* (2012) ‘Trevo versus Merci retrievers for thrombectomy revascularisation of large vessel occlusions in acute ischaemic stroke (TREVO 2): a randomised trial.’, Lancet (London, England). NIH Public Access, 380(9849), pp. 1231–40. doi: 10.1016/S0140-6736(12)61299-9.

Nogueira, R. G., Frei, D., *et al.* (2018) ‘Safety and Efficacy of a 3-Dimensional Stent Retriever With Aspiration-Based Thrombectomy vs Aspiration-Based Thrombectomy Alone in Acute Ischemic Stroke Intervention: A Randomized Clinical Trial.’, JAMA neurology. American Medical Association, 75(3), pp. 304–311. doi: 10.1001/jamaneurol.2017.3967.

Nogueira, R. G., Jadhav, A. P., *et al.* (2018) ‘Thrombectomy 6 to 24 Hours after Stroke with a Mismatch between Deficit and Infarct’, New England Journal of Medicine. Massachusetts Medical Society, 378(1), pp. 11–21. doi: 10.1056/NEJMoa1706442.

O’Cearbhaill, R. M. *et al.* (2016) ‘Calcified cerebral emboli: A case series and review of literature’, Journal of Systems and Integrative Neuroscience, 2(3), pp. 180–13. Available at: https://www.oatext.com/pdf/JSIN-2-133.pdf (Accessed: 13 September 2019).

Raghib, M. F. *et al.* (2018) ‘Acute treatment of stroke due to spontaneous calcified cerebral emboli causing large vessel occlusion’, Journal of Clinical Neuroscience, 47, pp. 56–61. doi: 10.1016/j.jocn.2017.10.042.

Ramírez-Moreno, J. M. *et al.* (2017) ‘Mechanical thrombectomy during ischaemic stroke due to a calcified cerebral embolism’, Neurología (English Edition). Elsevier, 32(4), pp. 270–273. doi: 10.1016/j.nrleng.2015.06.008.

Saver, J. L. *et al.* (2012) ‘Solitaire flow restoration device versus the Merci Retriever in patients with acute ischaemic stroke (SWIFT): a randomised, parallel-group, non-inferiority trial.’, Lancet (London, England). Elsevier, 380(9849), pp. 1241–9. doi: 10.1016/S0140-6736(12)61384-1.

Saver, J. L. *et al.* (2015) ‘Stent-Retriever Thrombectomy after Intravenous t-PA vs. t-PA Alone in Stroke’, New England Journal of Medicine. Massachusetts Medical Society, 372(24), pp. 2285–2295. doi: 10.1056/NEJMoa1415061.

Tung, E.L. *et al.* (2017). Rethinking Thrombolysis in Cerebral Infarction 2b: Which Thrombolysis in Cerebral Infarction Scales Best Define Near Complete Recanalisation in the Modern Thrombectomy Era? Stroke, 48(9), pp.2488–2493.

Walker, B. S. *et al.* (2014) 'Calcified cerebral emboli, a "do not miss" imaging diagnosis: 22 new cases and review of the literature', American Journal of Neuroradiology, 35(8), pp. 1515–1519. doi: 10.3174/ajnr.A3892.

Wiesmann, M. *et al.* (2017) 'Active push deployment technique improves stent/vessel-wall interaction in endovascular treatment of acute stroke with stent retrievers.', Journal of neurointerventional surgery. British Medical Journal Publishing Group, 9(3), pp. 253–256. doi: 10.1136/neurintsurg-2016-012322.

Chapter 6

Investigating the Effect of Mechanical Properties and Composition on Clot Behaviour during Vessel Occlusion

6.1 Chapter Overview

The aim of this chapter is to investigate the occlusion dynamics of clots with various mechanical properties over the relevant timeline for stroke. The previously characterised clot analogues, described in Chapters 3 and 4, were used to investigate the effect of clot mechanical properties and composition on the deformation and angiographic appearance of clot when lodged in an *in-vitro* model under physiological conditions of pressure and flow. A finite element model of the experiment is also presented to allow a comparison with the experimental results.

A journal paper based on the content of this chapter is currently in preparation.

6.2 Introduction

There is strong evidence for mechanical thrombectomy (MT) in the treatment of acute ischemic stroke (AIS). The evolution of endovascular devices and strategies, such as stent-retrievers (SR), balloon-guiding catheters and the contact aspiration technique (CA), has led to a dramatic increase in recanalisation rates of between 70-88%, as reported in the most recent randomised trials (Goyal *et al*. 2016; Lapergue *et al*. 2016; Turk *et al*. 2014; Kim *et al*. 2016). However, in some cases, adequate recanalisation is obtained only after multiple manoeuvres, which involve longer procedural times

and a potentially higher risk of intraprocedural complications, such as new territory embolisation secondary to clot fragmentation.

Prior studies have suggested that the thrombus composition can be predictive of successful recanalisation following both intravenous (IV) thrombolysis and mechanical thrombectomy (Mehta & Nogueira 2012; Froehler *et al*. 2013; Shin *et al*. 2018b; Goyal *et al*. 2016; Brinjikji *et al*. 2017). In fact, recent *in-vitro* studies have suggested that clot composition can affect the ideal choice of techniques used during clot retrieval and does, in fact, play a role in device-clot interaction (Weafer *et al*. 2019; Gunning *et al*. 2016; Yoo & Andersson 2017; van der Marel *et al*. 2016). Therefore determining the clot composition and clot age has potential to be useful in evaluating what treatment method to pursue (Fang *et al*. 2015b).

Some authors have proposed different predictors of recanalisation according to the clot imaging characteristics, such as the susceptibility vessel sign on MRI (Fujimoto *et al*. 2013; Bourcier *et al*. 2019; Liebeskind *et al*. 2011) and attenuation on CT scan (Fitzgerald *et al*. 2019; Kirchhof *et al*. 2003; Riedel *et al*. 2010), as well as the thrombus length (Ganeshan *et al*. 2018), clot perviousness (Benson *et al*. 2019; Santos *et al*. 2016) and the clot burden score (Mokin *et al*. 2017; Cenic *et al*. 1999).

The determination of clot characteristics that are associated with successful recanalisation could help to inform treatment decisions and identify patients at risk (Minnerup & Kleinschnitz 2011). From a clinical aspect, imaging of a clot *in-situ* before treatment could assist in establishing the clot type, and thus its expected behaviour during treatment. Prior knowledge of the expected behaviour of the clot could assist the physician in selecting the most appropriate treatment methods to increase the rate of successful clinical outcomes.

Recent studies have examined the angiographic appearance of an occlusion in AIS patients on digital subtraction angiography (DSA) as a method to determine the occlusion etiology and to predict likelihood of successful recanalisation (Yamamoto *et al*. 2019; Garcia-Bermejo *et al*. 2019; Pillai *et al*. 2001; Mönch *et al*. 2019; Consoli *et al*. 2019; Consoli *et al*. 2018). Four to five clot morphology classifications were identified on DSA and their relationship with successful recanalisation rates and clinical outcomes were investigated (Pillai *et al*. 2001; Mönch *et al*. 2019; Garcia-Bermejo *et al*. 2019). Similarly, Yamamoto *et al.* (2019) proposed what they refer to as the "claw signal" to predict successful recanalisation in AIS patients. The "claw sign" is defined as the contrast morphology of the occlusion site in which a convexity protruded to the proximal side with a protrusion length that was more than half the arterial vessel diameter (Yamamoto *et al*. 2019).

However, these methods can be quite complex and time-consuming for a neurointerventionalist to measure and distinguish in the limited time available to them to decide on the best treatment strategy for the patient. Therefore, Consoli *et al.* (2018, 2019) suggested a more simplified approach by proposing only 2 appearances: "regular" when the profile of the occlusion was smooth and straight, with a linear interruption of the flow in the artery that appeared to be abruptly cut off, and "irregular" where there was any evident modification of the linearity of the occlusion, such as concave or convex shapes or the presence of multiple contrast filling defects on the profile of the occlusion (Figure 6.1) (Consoli *et al*. 2018). The relationship of the clot phenotype classification and the recanalisation rates achieved with the two most frequently used endovascular techniques, SR and CA, were investigated. The results of the study show both techniques have similar outcomes for regular phenotype occlusions, however irregular occlusions treated with SR as the front-line strategy

were associated with better procedural and clinical outcomes (Consoli *et al*. 2019). The different morphological aspects of the occlusion site, regular, or irregular were found to be associated with the efficacy of the endovascular technique, SR or CA, and may strongly impact the choice of the first-line endovascular procedure device in the future.

Little is still known about the underlying factors that determine the clot phenotype. It has been proposed that the mechanical properties and composition of the thrombus may have an influence (Consoli *et al*. 2018), and thus underlines the importance of future investigations about the mechanical nature of the occluding thrombus. The study by Mönch *et al.* (2019) found that there was no association of the proximal thrombus appearance on digital subtraction angiography (DSA) with stroke etiology, clinical outcome and thrombus-specific parameters, such as perviousness and histological features and therefore suggested that further investigations with higher numbers of patients would be desirable.

This chapter investigates the relationship between clot mechanical properties, which are composition dependent and which were previously characterised in Chapters 3 and 4, and clot deformation and angiographic appearance, when lodged in an *in-vitro* model under physiological conditions. The deformation of the clot during lodgement is observed and the shape of the proximal face is monitored over a period of 5 hours. The results from the *in-vitro* model are then analysed to examine the effect of clot composition and mechanical properties on clot behaviour during lodgement.

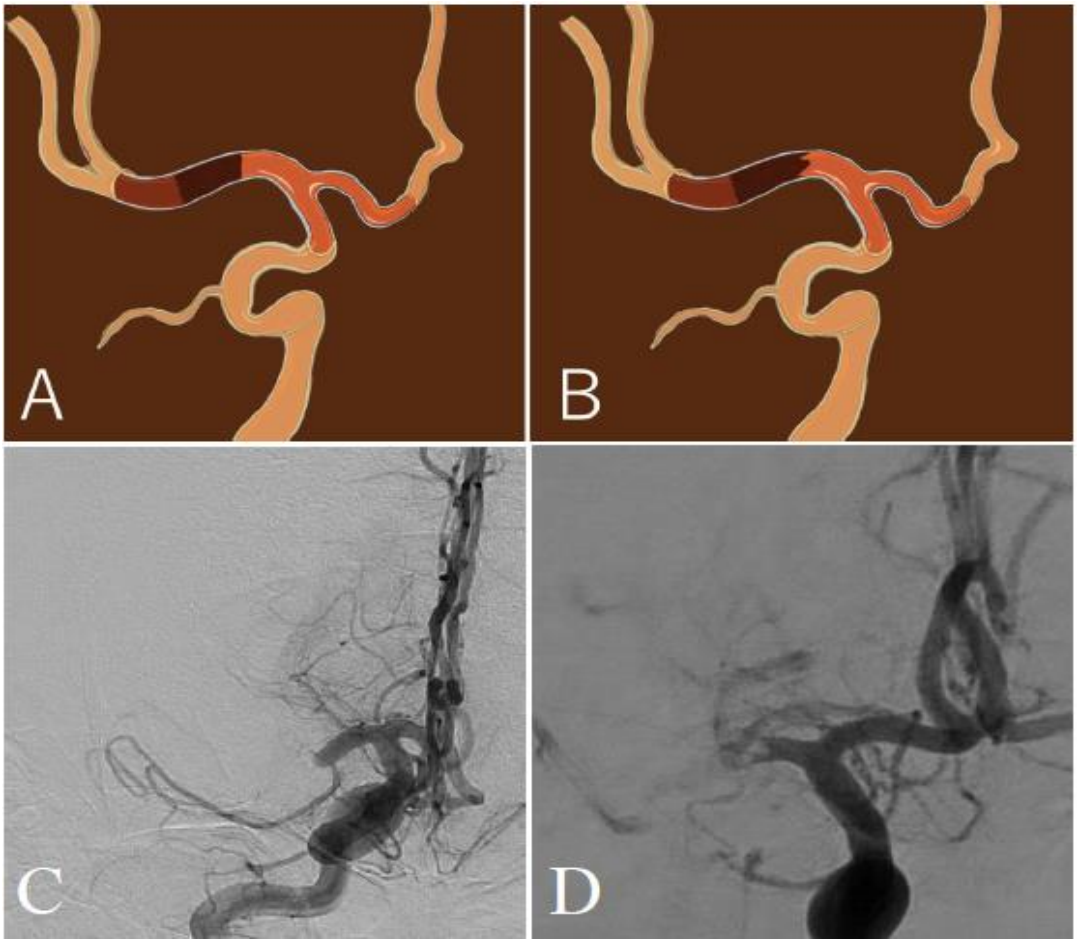

Figure 6.1 Regular (A,C) and irregular (B,D) phenotype of the M1-Middle cerebral artery occlusion shown in the artwork (A, B) and at DSA (C, D) according to Consoli *et al*. definition (2018, 2019).

6.3 Materials and Methods

6.3.1 Sample Preparation

Fresh venous ovine blood was collected using methods similar to those reported previously (Duffy *et al*. 2016; Johnson *et al*. 2019). The blood was then transported to the lab and stored at room temperature until used. All clots were prepared within 5 hours of blood collection. Platelet rich plasma (PRP) was isolated from the citrated blood by spinning at 180 g for 10 minutes. The remaining fraction of blood was spun again at 2200 g for 10 minutes to isolate the red blood cells.

The clots were prepared according to the procedure for the previously characterised clot analogues (Chapters 3 (Johnson *et al*. 2019) and 4). Two groups of clot analogues were produced – platelet-contracted clots (PCC) and non-contracted clots (NCC). PCCs were formed from blood mixtures with different hematocrit (%H), i.e. the volume percentage of RBCs in the mixture, by mixing RBCs with PRP in controlled ratios to prepare clots with a 5%, 40%. Similarly, the NCCs were produced by mixing PPP with RBCs to prepare clots with a 5% and 40% H. Coagulation of the blood mixtures was initiated by adding a 2.06% calcium chloride solution in a 1:9 ratio and were matured overnight at 37°C. Confirmation of contraction was assessed gravimetrically by weighing the solid and liquid phases in the clot moulds, and monitoring the colour of the serum to ensure the RBCs had been incorporated.

A third clot group – mechanically contracted clots (MCC) – were formed by mechanically compressing non-contracted clot analogues with a 5% and 40% hematocrit, by spinning in the centrifuge for 10 minutes at 2200 g, to remove entrapped serum, until the final clot weight was similar those of the platelet-contracted clots for the specific hematocrit levels. This method is also described in Chapter 3 and was found to be an effective method to remove excess serum from the clot and to reduce the weight of the clot to a similar weight to that of the PCCs (Johnson *et al*. 2019).

The cylindrical clot samples were cut to have a length of approximately 15 mm with a flat distal end and a pointed tail at the proximal end, similar to a pencil shape (Figure 6.2 A). The weight and diameter of the clot samples were recorded before introducing them into the flow model.

6.3.2 Experimental Set-up

The experimental set-up consisted of a tapered silicone tube (BioMET, GMIT, Galway, Ireland), with a maximum diameter of 10 mm and a minimum diameter of 1.4 mm, connected to a pulsatile pump (PD-1100 pulsatile pump, BDC Laboratories), which precisely controlled the pulse rate, pressure and temperature of the system. Saline solution, which was heated to 37°C was pumped through the model with a pulse rate of 75 BPM. The tapered tube was mounted at an angle using a retort stand to allow any RBCs that had been liberated from the clot to flow away from the proximal face of the clot to ensure a clear view of the proximal clot face was maintained.

The clot samples were introduced to the tapered vessel through a side port and allowed to flow to the lodgement site, ensuring that the "irregular" face was in the proximal position. Two pressure sensors were attached to the model, before and after the tapered vessel (Figure 6.2 B-D) to monitor the pressure and to ensure that there was a mean pressure of approximately 90 mmHg at the proximal face of the clot and a pressure of approximately 30 mmHg at the distal face of the clot, thereby maintaining a pressure drop of 60 mmHg across the clot, based on *in-vivo* measurements that had previously been reported in the literature (Sorimachi *et al*. 2011). The clot remained in the model for a period of 5 hours. This time period was selected as it was determined to span the period of time of stroke onset to treatment time for the majority of cases (Tong *et al*. 2012; Strbian *et al*. 2013). The lodgement time was recorded and the clot was then monitored by taking images every 2 minutes. Images were taken from two angles; v_1 and v_2, at 90° to one another, so that deformation in two orthogonal planes was monitored during the experiment (see Figure 6.2 C). The v_2 direction is essentially horizontal, in the "plane" of the flow model, as shown in 6.2 C, and this view corresponds to the mediolateral image perspective of the brain using digital

subtraction angiography (DSA). The v_1 direction is perpendicular to this, looking down on the flow model and corresponds to the anteroposterior image perspective of the brain on DSA. Once the clot was removed from the model, the length and weight of the sample were recorded, and the mass loss and elongation of the sample were calculated. A minimum of n = 5 samples were tested for each clot type.

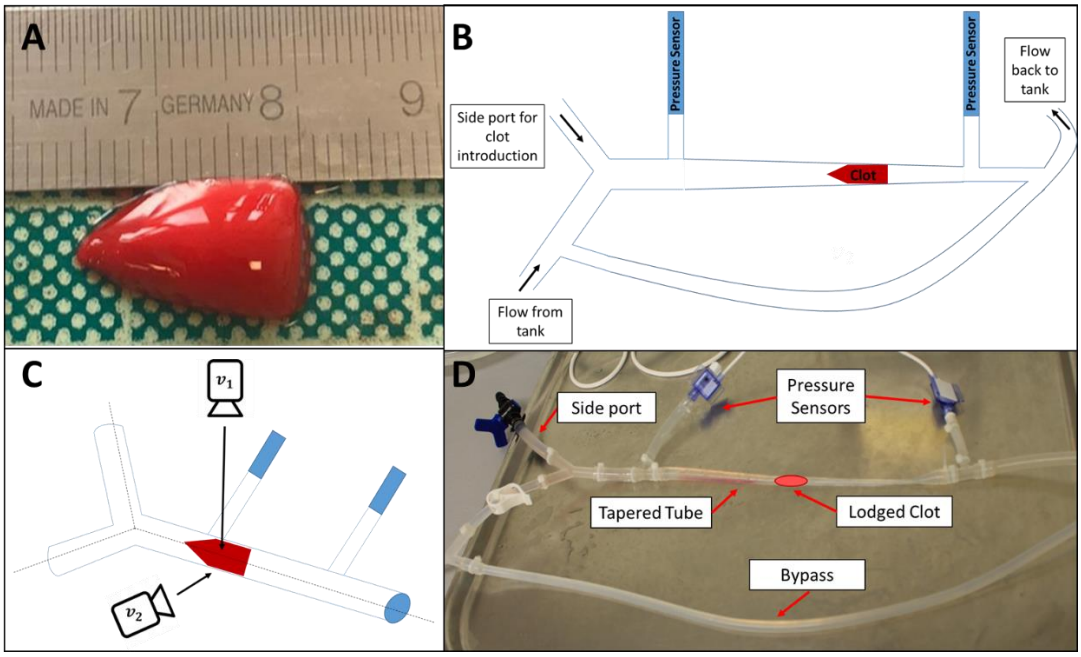

Figure 6.2 Image of (A) 5% H clot sample. (B) Schematic diagram showing the experimental set-up, with (C) showing the camera set-up for views v_1 *and* v_2 at 90° to one another. (D) Image of the *in-vitro* flow model.

A subset of clots were imaged using fluoroscopy to compare with the images taken with the camera. Fluoroscopy imaging was carried out at BioMET, GMIT, Galway, Ireland, using a Ziehm Vision R Smart Vascular fluoroscope. The clots were initially introduced into the side port of the *in-vitro* model using saline. Contrast medium (Optiray 350, Liebel-Flarsheim Company LLC, Raleigh, NC, USA) was then used to lodge the clot in the model, so that the proximal face of the clot would be visible under the fluoroscope.

6.3.3 Analysis of Proximal Clot Face

The deformation of the proximal face of the clot samples were analysed using two different methods.

Firstly, the Consoli approach was adopted by analysing v_1 of the occlusion only, which correspond to the anteroposterior image perspective of the brain using DSA. The clots were classified as "regular" when the profile of the occlusion was smooth and straight, or "irregular" where there was any evident modification of the linearity of the occlusion, such as concave or convex shapes or the presence of multiple contrast filling defects on the profile of the occlusion (Consoli *et al*. 2019; Consoli *et al*. 2018).

For the second approach, the two classifications used by Consoli *et al.* were expanded further and four common appearances were identified from the experiment (Figure 6.3 A). For this method, both views of the clot were analysed, v_1 and v_2, which correspond to the anteroposterior or mediolateral image perspectives on DSA respectively. For the purpose of the statistical analysis, if the clot appearance from both views, v_1 and v_2 were scored as combinations of 1 and 1, 1 and 2 or 2 and 2, the clot was classified as "regular". Similarly, if the clot appearance from both views were scored as a combination of 3 and 3, 3 and 4 or 4 and 4, the clot was classified as "irregular". All other combinations, such as 1 and 3, 1 and 4, 2 and 3 or 2 and 4, were classified as "mixed".

Measurements were also taken from the proximal face of the clot, as shown in Figure 6.3 B and C, to determine the shape change of the proximal face of the clot as it lodged in the tapered vessel. These measurements include the diameter of the vessel at the point of clot lodgement, *z*, the distance from the top of the apex of the clot from the point of contact on both sides of the vessel, *x* and *y*, and the distance of the apex from

both sides of the vessel, *i* and *j*. The apex height, *h*, and the distance between the two contact points, *d*, were then calculated from these measurements (See Figure 6.3 B and C).

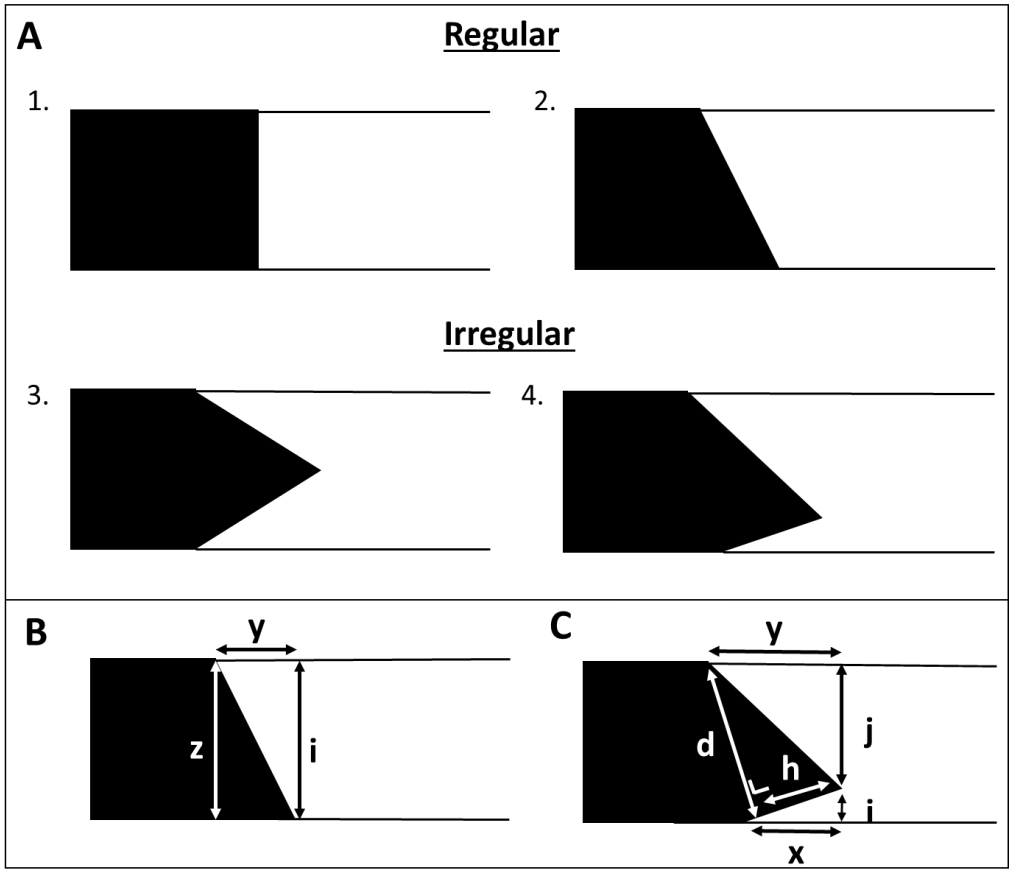

Figure 6.3 (A) Expanded classification of the appearance of the proximal clot face, to include the four commonly observed shapes of the occlusion during the experiment. The clot is shown in black. (B) and (C) show the various measurements that were taken from the images obtained during the experiment, as discussed in the text.

6.3.4 Statistical Analysis

Statistical analysis of the experimental results was carried out using the general linear model ANOVA procedure in Minitab (ver. 18.1). A comparison of mean onset point was performed with a Bonferroni model (alpha = 0.05) to compare the mass loss and change in diameter for each clot group.

6.3.5 Computational Methods

The deformation of the proximal face of the clot was then simulated using finite element (FE) analysis in Abaqus/Standard (DS SIMULIA, USA). The clot geometry was representative of the clot samples before they were placed in the flow model. To simplify the model, the clot was modelled as 2D axisymmetric. Boundary conditions were applied to simulate its lodgement within the vessel. The lodged clot was simulated by applying displacement boundary conditions to the distal face of the clot to constrain the clot in the x-direction (axial direction) and also to the side of the clot to constrain the clot in the y-direction (radial direction) so simulate the constraint of the vessel wall. A pressure of 0.012 MPa was applied to clot tip to simulate experimental pressure conditions. The clot material was meshed with 4962 hexahedral elements of type CAX4RH, with reduced integration and hybrid formulation The Yeoh hyperelastic material model was used to describe the behaviour of the clot material, under the assumption of large deformation kinematics within Abaqus (NLGEOM activated within Abaqus). The fitted hyperelastic material parameters obtained in Chapter 4 were used to simulate the deformation of a contracted clot analogue, with a large bulk modulus (K). The FE model was then used to examine the effect of altering the effective shear modulus (G), by changing the C_{10} parameter, and the bulk modulus (K), on the deformation of the clot tip.

6.4 Results

6.4.1 Experimental Results

From the images taken during the experiment, the proximal face of the clot was classified as either “regular” or “irregular” (Figure 6.4 A and C). Images were also taken under fluoroscopy to validate the results (Figure 6.4 B and D).

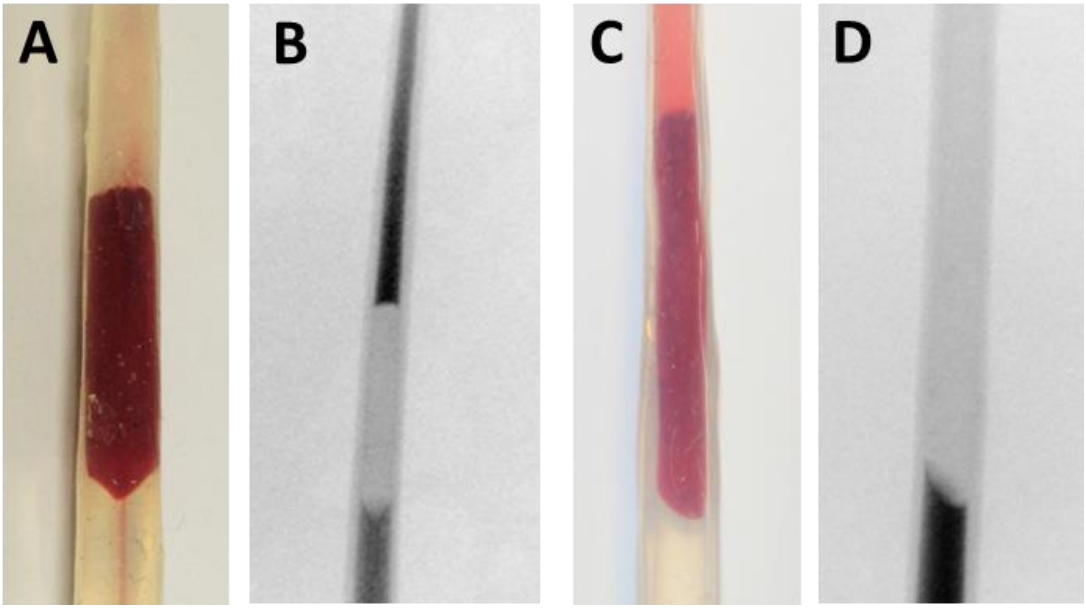

Figure 6.4 Image of a clot with an “irregular” proximal face (A) after lodgement in the silicone vessel and (B) under fluoroscopy, with the clot shown in light grey and the contrast media shown in black. (C) Photograph of a “regular” clot lodged in the experimental model. (D) Image of the clot under fluoroscopy.

The clots were classified using images from 2 views of the clot, as described in the methods section (Figure 6.5), and the combinations were described as “regular”, “irregular” or “mixed”. The breakdown of the classifications for each clot group are shown in Figure 6.5. For the PCCs and MCCs, across both hematocrits, the majority of the clots were classified as “irregular”. In contrast, the majority of the clots in the NCC group were classified as “mixed”.

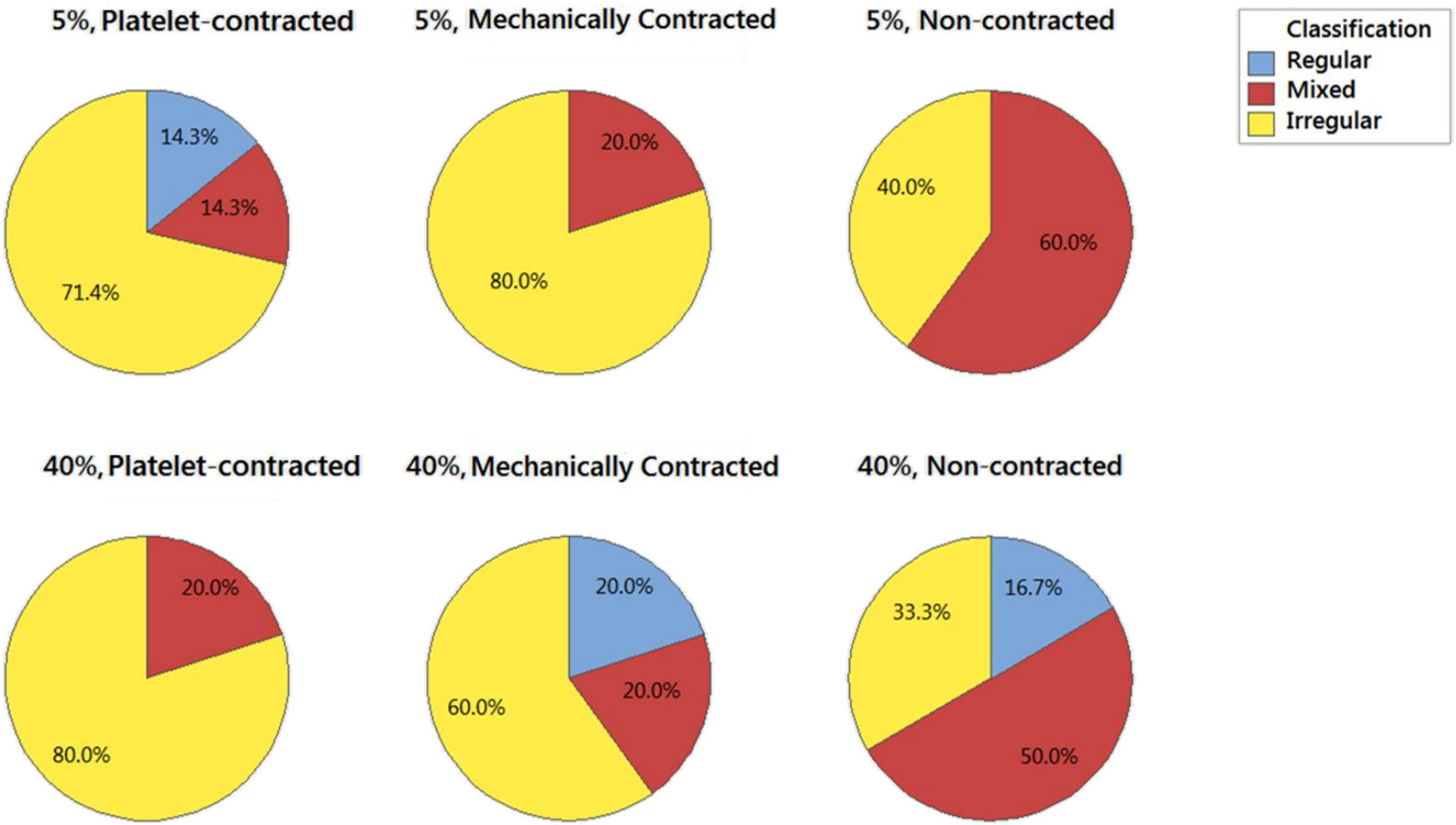

Figure 6.5 Pie chart showing the breakdown of the classification of the clot shape per clot group (minimum of n = 5 per group).

Figure 6.6 compares the clot diameter outside of the model before lodgement to the vessel diameter at the point of lodgement, captured by the '*z*' measurement from the experimental images, and after 30 seconds, 5 minutes and 5 hours respectively. As the silicone vessel used for the experiment was tapered, a lower clot diameter indicates that the clot travelled further into the vessel before lodgement. Overall the 5% H clot groups were found to have a lower diameter and therefore travelled further into the silicone vessel before lodgement. The PCCs were found to have the greatest diameter, followed by the MCCs, with the NCCs having the lowest. For the 40% H group, there was little difference in the lodgement diameter across all contraction groups. Overall the diameter measurement for the 40% H clots were larger than for the 5% H clots, indicating that they did not travel as far into the silicone vessel as the 5% H clots, with the exception of the PCC group, which was found to have a similar diameter measurement across both hematocrits.

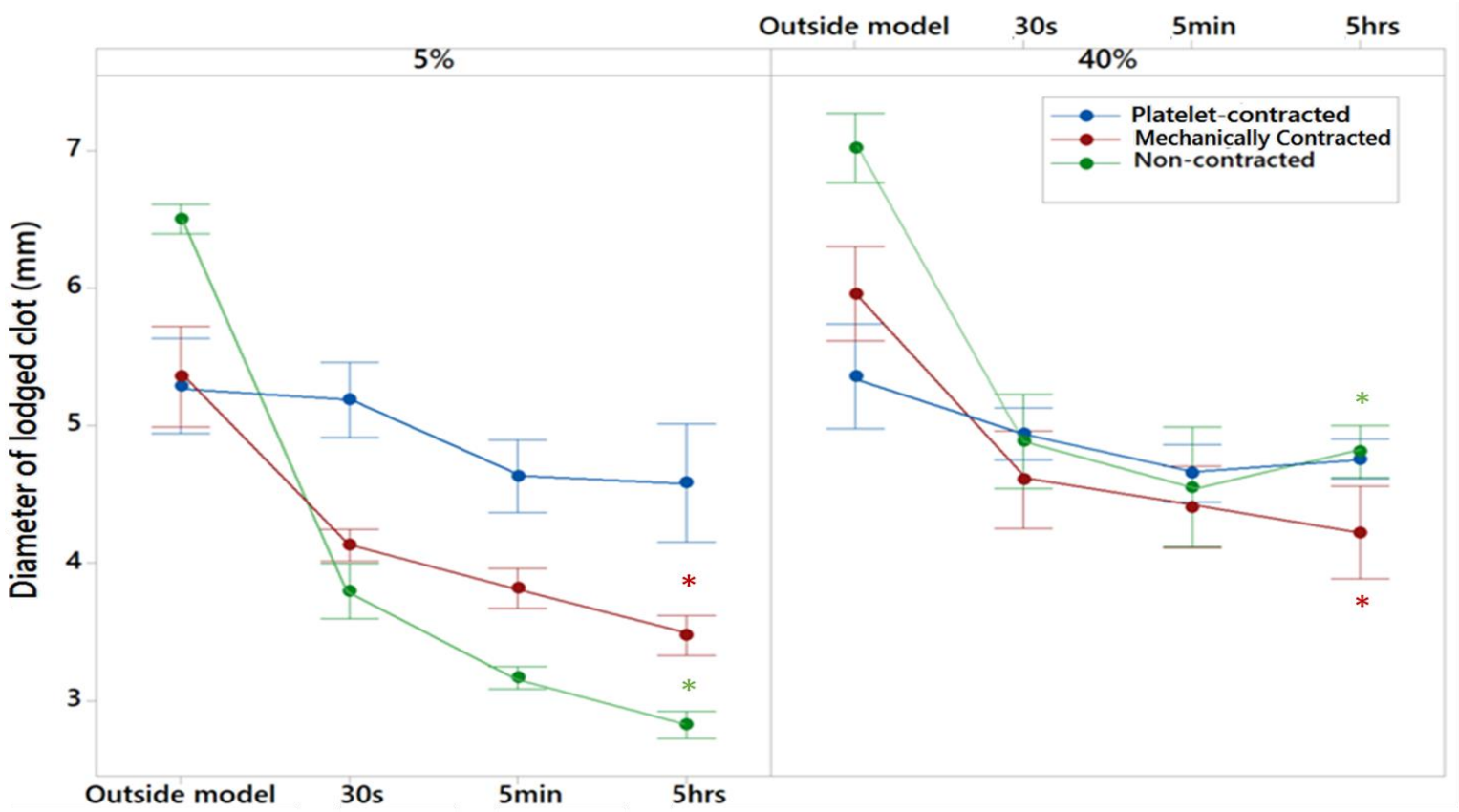

Figure 6.6 Plot of vessel diameter at point of vessel occlusion, *z*, after 30 seconds, 5 minutes and 5 hours, for the 5% H clots (left) and the 40% H clots (right), compared with the clot diameter outside of the model before lodgement. The error bars represent standard error and * denotes statistical significance ($p<0.05$) when compared to the initial diameter of the clot outside of the model.

The weight of the clots were measured before and after the experiment and the mass loss of the samples was calculated and is shown in Figure 6.7. For both hematocrits, the PCCs and the MCCs were found to experience a similar % mass loss, with the 5% H clots experiencing more mass loss than the 40% H clots. The NCC group had significantly greater mass loss than the MCCs and PCCs across both hematocrits.

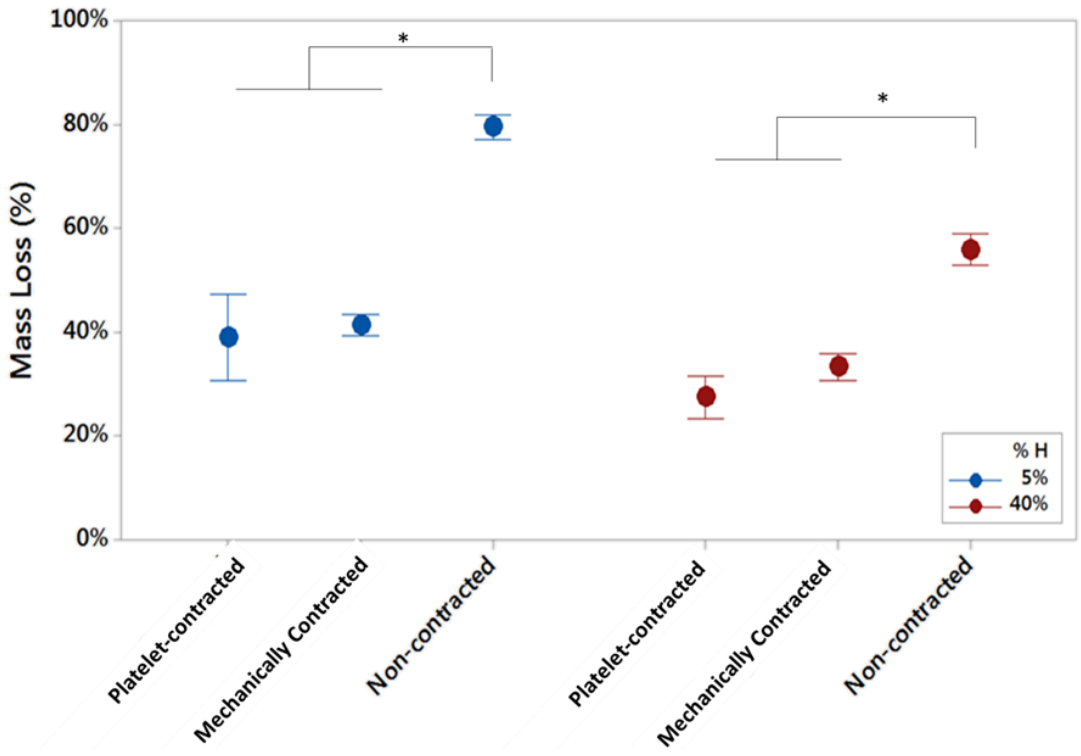

Figure 6.7 Graph illustrating the average percentage mass loss for each clot type (n=5 per group), with the 5% hematocrit clots shown in blue and the 40% hematocrit clots shown in red. The error bars show standard error and * denotes statistical significance ($p<0.05$).

Figure 6.8 A-B presents the results for the apex height, '*h*', normalised by the vessel diameter at the point of clot lodgement, '*z*', for both views v_1 and v_2 respectively. The greater the ratio of *h/z*, the greater the irregularity of the proximal face of the clot. The results in Figure 6.8 show that a similar trend was evident from both camera views.

For the 5% H group, the PCCs had the lowest *h/z* ratio. The MCCs and NCCs were found to have a greater *h/z* ratio, however there was little difference between the two groups. This indicates that the MCCs and NCCs had a more "irregular" shape. This is due to the proximal face of the clot maintaining its "irregular" shape, while moving further into the vessel. For the 40% H group, the opposite trend was observed, where the MCCs and NCCs had a lower *h/z* ratio. As all of the clot samples begin with an "irregular" shape, this measurement indicates the tendency of the clots to become "regular" as a function of composition.

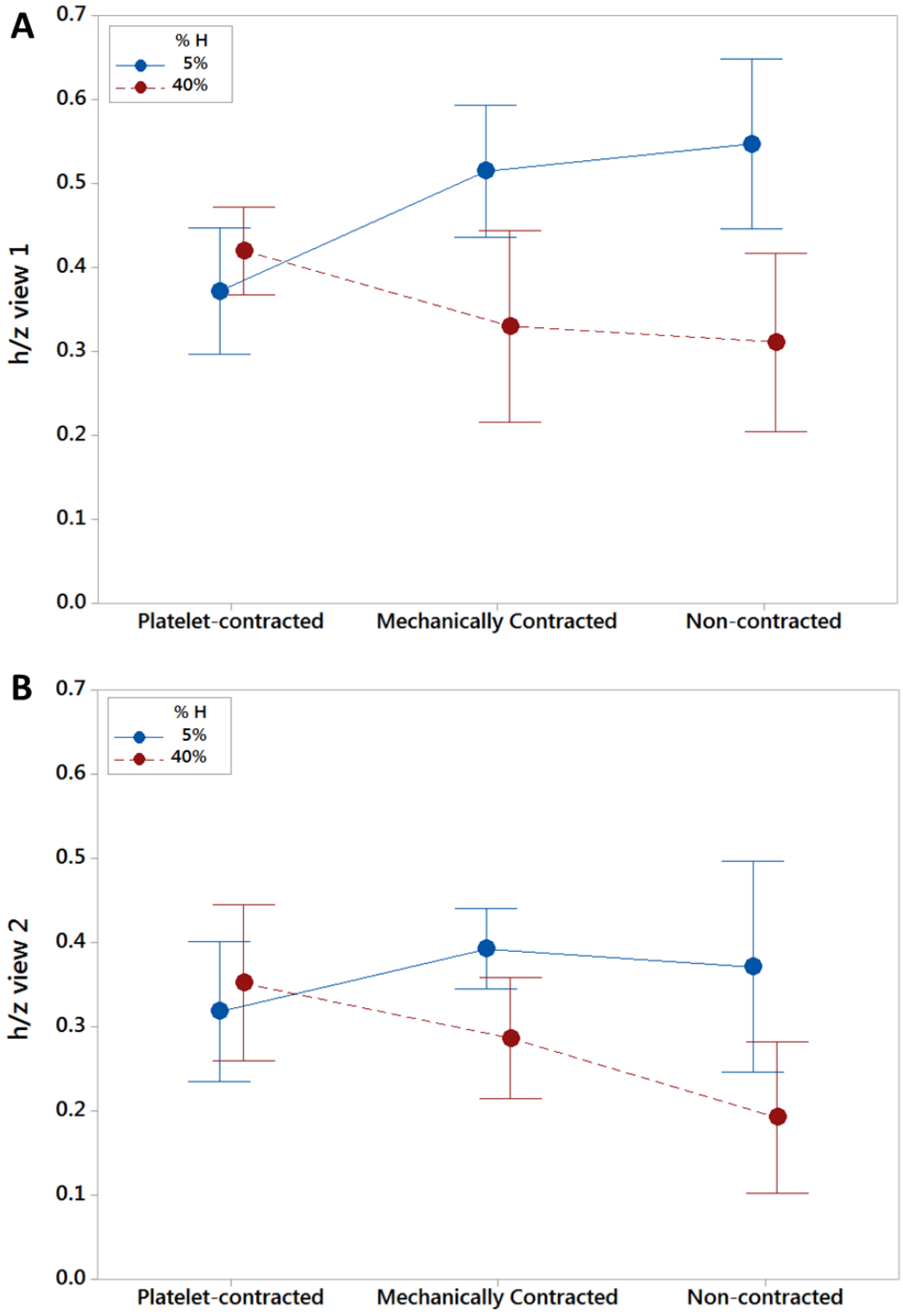

Figure 6.8 Plot of the ratio of *h/z* for (A) view v_1 and (B) view v_2, for each of the clot groups, with error bars denoting standard error.

6.4.2 Computational Results

The results from the FE analysis are shown in Figures 6.9 and 6.10.

Figure 6.9 A-D shows the effect of varying the effective shear modulus (*G*) on the deformation of the clot tip, for a material with a large bulk modulus (*K*). The results show that the change in the effective shear modulus had little effect on the deformation of the clot tip for a nearly incompressible material.

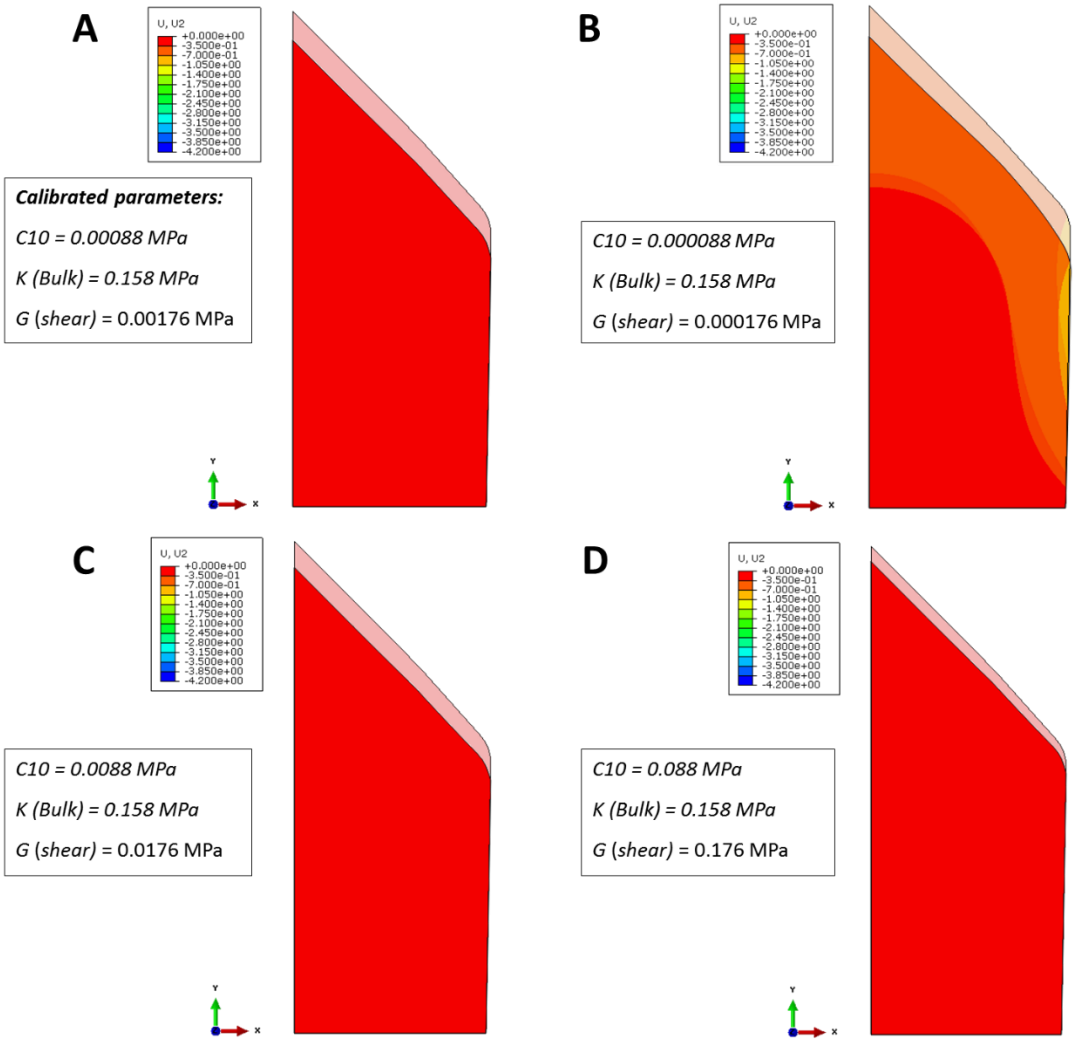

Figure 6.9 (A) Finite element simulations using the calibrated material parameters for a contracted clot from Chapter 4. (B-D) Finite element simulations showing the effect of altering the effective shear modulus (*G*) on the deformation of the clot tip, for a constant large bulk modulus (*K*).

Figure 6.10 A-D demonstrates the effect of varying the bulk modulus (*K*) on the deformation of the clot tip, while maintaining a constant shear modulus (*G*). The reduction of the bulk modulus, and thus an increase in the compressibility of the clot material, allowed for significant deformation of the clot tip to occur.

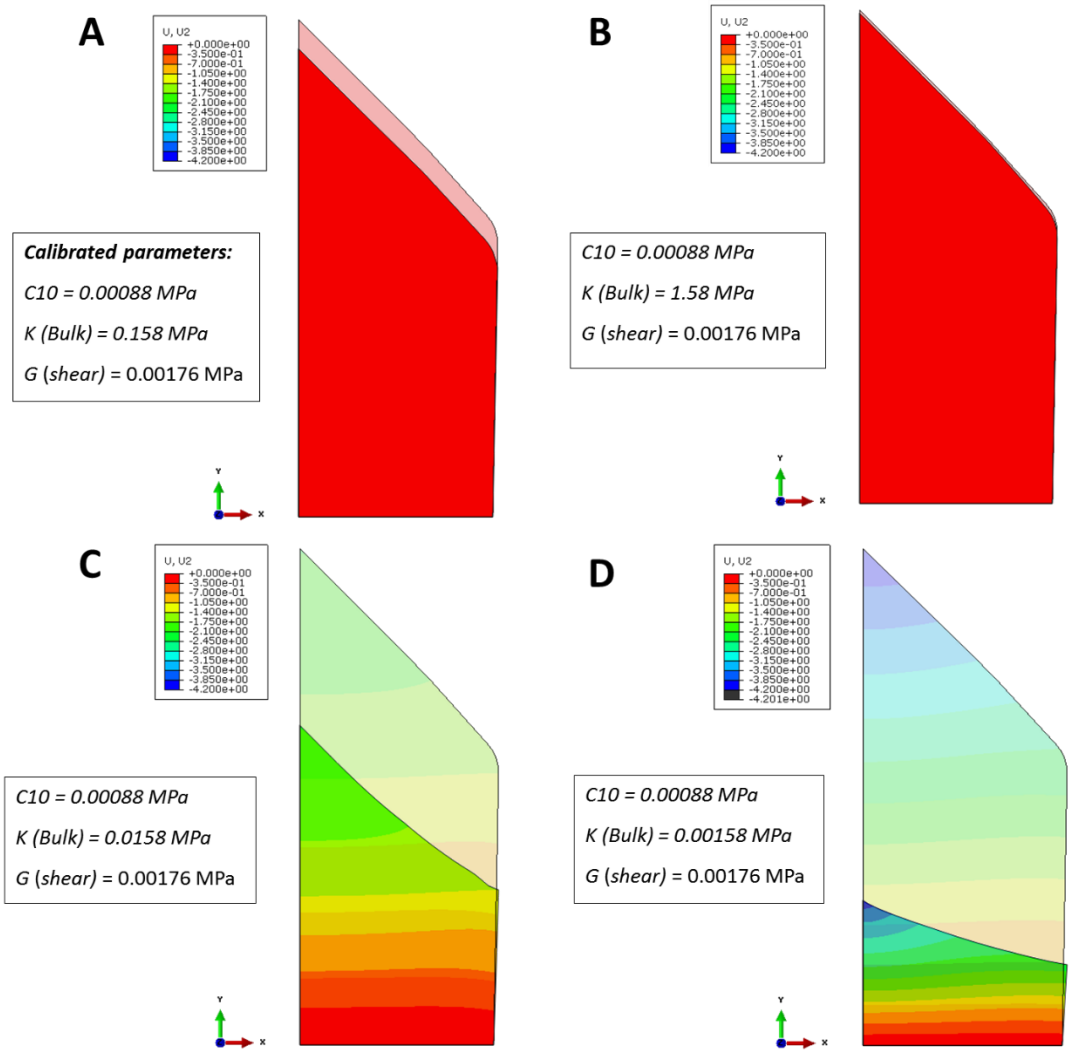

Figure 6.10 (A) Finite element simulations using the calibrated material parameters for a contracted clot from Chapter 4. (B-D) Finite element simulations showing the effect of altering the bulk modulus (*K*) on the deformation of the clot tip, for a constant effective shear modulus.

6.5 Discussion

This chapter investigates the effect of clot mechanical properties and composition on the appearance of the proximal face of an occluding clot and the clot deformation during lodgement in an *in-vitro* model under physiological conditions of pressure and flow. The clot analogues used in this experiment were previously described and characterised in Chapters 3 (Johnson *et al*. 2019) and 4. All samples lodged in the *in-vitro* model were cut to have an "irregular" proximal face before lodgement and the shape of the proximal face of the clot was monitored.

Many recent studies have investigated the relationship between angiographic appearance of an occlusion in AIS patients on DSA to the occlusion etiology and to clinical outcomes (Yamamoto *et al*. 2019; Garcia-Bermejo *et al*. 2019; Pillai *et al*. 2001; Mönch *et al*. 2019; Consoli *et al*. 2019; Consoli *et al*. 2018). However, some of the reported methods are quite complex and may be time-consuming for a neurointerventionalist to measure in the limited time available before treatment. This study explores the underlying factors that may affect the clot classifications previously described by Consoli *et al.* (2018, 2019), which classified the angiographic appearance of occluding thrombi as "regular" or "irregular".

A limitation of the aforementioned studies was that the angiographic images were only analysed from one perspective: an anteroposterior image view. Due to the nature of the *in-vitro* experiment presented here, it was possible to observe the proximal clot face from two orthogonal views. This was supported by the fluoroscopy images. However, the results demonstrated that although the proximal clot face may appear "irregular" in one view, it could appear "regular" in the other orthogonal view in some cases. Therefore, for the purpose of this study these clots were classified as "mixed".

The experimental results found that both the PCC and MCC groups were mostly classified as “irregular”, for both hematocrits. This is as expected as it is hypothesised that the shape-change of the proximal face of the occlusion is related to the clot mechanical properties (Consoli *et al*. 2018). As discussed in Chapter 3, PCCs were found to have an increased stiffness due to the rearrangement of the components within the clot network during platelet-contraction. Therefore the greater mechanical stiffness of this clot group is likely to have prevented the deformation or flattening of the clot face due to the applied pressure and flow. Although the MCCs did not undergo active platelet-contraction, they were mechanically compressed by centrifugation to reduce the weight of the clots to that of the PCCs, as previously demonstrated in Chapter 3. Therefore it is assumed that the compaction and rearrangement of the clot microstructure, and the removal of the excess serum via mechanical contraction also caused an increased stiffness in the clot material, and thus allowed the clot to maintain its “irregular” shape under the applied conditions of pressure and flow.

For the NCC group, the majority of the clots were classified as “mixed”, as there was no clear classification as “regular” or “irregular” due to variation in the classifications for both image views. However, it was found that many of these clots had an “irregular” classification in one of the two views. Although this is not evident from the proximal face analysis, this hypothesis is supported by other factors measured in this experiment.

The diameter of the silicone vessel at the point of clot lodgement was quantified by the ‘*z*’ measurement. As the silicone vessel was tapered, a lower ‘*z’* measurement indicates that the clot had travelled further into the vessel before lodgement. This measurement was also reported for time points of 30 seconds, 5 minutes and 5 hours after clot lodgement in the vessel. The 5% H MCCs and NCCs were found to

progressively move through the vessel over the 5-hour period. The 40% H MCCs and NCCs and the PCCs for both hematocrits were found to move slightly over the 5 minutes, however they remained generally in the same position after this time. Although there was slight movement of the various clot positions in the vessel over time, the behavioural trend remained the same.

For the 40% H group, there was little difference in the lodgement diameter across all contraction groups. Overall, the diameter measurements for the 40% H clots were larger than for the 5% H clots with the exception of the PCC group, where a similar change was recorded for both hematocrits. This result is as expected as the PCC group is most likely to resist compression and deformation due to its stiffness and highly compressed microstructure.

For the 5% H group, the PCCs were found to have greatest lodgement diameter, followed by the MCCs, with the NCCs respectively. Due to the porous nature of the microstructure of the NCCs, as described in Chapters 3, it is likely that the material could compress further and become more compacted when lodged in the vessel over time due to the physiological pressure. This causes the clots to lose more serum and progress further into the vessel. However, it is possible that this also causes these clots to have an increased stiffness when lodged in the vessel over a period of 5 hours.

This result is also supported by the mass loss results. The NCC group was found to have the greatest mass loss of all three groups, followed by the MCCs and the PCCS respectively, across both hematocrits. This is not surprising as the NCC group had undergone the least amount of dehydration compared to the PCC and MCC groups and therefore contained more serum. The mass loss of the NCC group, as a result of

serum being expelled from the clot due to the applied pressure and flow-rates, enabled the NCCs to shrink in size and therefore be pushed further into the tapered vessel.

In contrast, the PCCs had the lowest mass loss. This is due to the activated platelets within the clot mixture causing the network to contract and to expel any excess serum during the clotting process, and therefore the mass loss of the PCC groups was significantly less than the NCC group. The MCCs had a similar result to the PCCs as the MCCs underwent centrifugation to remove excess serum prior to the experiment. Overall, the 5% H clots were found to have greater mass loss than the 40% H clots. This result shows that the hematocrit effected the mass loss, simply due to the greater ratio of plasma to RBCs in the 5% H clots than in the 40% H clots, thus indicating that the mass loss experienced by the clots was mainly due to the loss of serum.

From the measurements taken from the experimental images, the height of the apex of the proximal clot face, *h*, was calculated. This measurement was then normalised by the diameter of the vessel at which the clot lodged, *z*, to compare clots that had lodged at different points in the tapered vessel. A lower *h/z* value indicates a greater tendency for the clot to flatten or have a "regular" shape, whereas a larger *h/z* value would indicate that the clot had maintained its initial pointed or "irregular" shape. The NCCs and MCCs for the 5% H clot group were found to have the greatest *h/z* value, however there was little difference between the two groups. Although these clot groups experienced the greatest mass loss and reduction in clot diameter, the pointed proximal shape of the clot was maintained once lodged in the vessel. This may be due to these clots experiencing an increase in stiffness as they become further compacted by the physiological pressure acting on them over the period of 5 hours, as described earlier. This is also supported the clot classification results, where the clot face had a mostly "irregular" appearance for both of these groups.

For the 40% H group, the opposite trend was observed, where the MCCs and NCCs had a lower *h/z* measurement. As all of the clot samples begin with an "irregular" shape, this measurement indicates the tendency of the clots to flatten. It is hypothesised in the 40% H group, in particular NCCs, would be most likely to flatten to a more "regular" shape due to the low stiffness of the material, previously reported in Chapter 3. The reduced stiffness is likely due to the lower levels of fibrin present, combined with the increased number of RBCs present (Johnson *et al*. 2019). This suggests that although the proximal face of these clots did not flatten completely, they did tend to flatten substantially more than the PCCs or the 5% H group.

The FE modelling presented in this chapter investigates the effect of bulk and shear modulus on the deformation of the proximal face of the clot. The fitted hyperelastic material parameters, obtained in Chapter 4, were used to simulate the deformation of a contracted clot analogue, with a large bulk modulus (*K*). A parameter study was then carried out to examine the effect of changing the effective shear modulus (*G*) and the bulk modulus values on the deformation of the proximal clot face. The results demonstrate that when the clot material is modelled as nearly incompressible, with a large *K*, the applied loading does not have a significant effect on the shape of proximal face of the clot, regardless of the effective shear modulus. Even for a very low effective shear modulus, the clot tip did not significantly change its shape under the applied pressure loading. Essentially the applied boundary conditions significantly constrain the possible deformation of the clot. Material incompressibility therefore causes the clot shape to "lock up", and thus prevents the clot from deforming, even if the material has a low shear stiffness. Additionally, the symmetry boundary conditions used in the idealised model are further constraining the geometry. If the tip was slightly mis-

aligned with the centre of the vessel then this would allow some shear (shape change) to occur, provided the applied effective shear modulus was sufficiently low.

Similarly, when the clot material is modelled as compressible, with a lower bulk modulus, then significant deformation of the tip, and indeed the entire clot, can occur. Greater compressibility may be reflective of a more non-contracted clot, or a clot with a greater haematocrit and therefore could explain why the proximal face of the clot is more likely to flatten in these clots, while it is not likely to deform very much in the case of the more incompressible contracted clots. However, the purpose of this parameter study was simply to examine the effect of varying the shear and bulk moduli on the deformation of the clot tip, and these values for the bulk modulus have not been calibrated for the all of clot analogue material in this study. Therefore, to model a broad range of clots with varying levels of contraction, compressibility of PCCs and MCCs may need to be examined further in future work to update the constitutive model accordingly, so that the material behaviour of these clots is accurately captured.

6.5.1 Limitations

One limitation of this investigation, as described previously in this thesis (Chapters 3 and 4), is the homogeneous nature of the clots, as they are prepared under static conditions in a controlled laboratory environment, whereas clots retrieved from patients tend to have irregular distribution of components. However, analogue clot material is widely accepted for use in the *in-vitro* testing of clot behaviour, as an alternative to human tissue.

Another limitation of this study is the use of a simplified silicone *in-vitro* model to replicate an *in-vivo* scenario. Silicone models are widely utilised for *in-vitro* simulation of AIS and treatment procedures, however they can behave quite

differently to native vessels, in terms of vessel compliance and friction. Similarly the simplified nature of the tapered vessel was another limitation. However the aim of this study was to observe the clot behaviour and shape change when lodged in a vessel under physiological conditions. Although the tapered vessel is a simplified representation of the neurovasculature, it allowed for consistent lodgement of the clots, which was difficult to achieve in a full intracranial model. Future work will investigate the lodgement in more a realistic model of the neurovasculature.

Similarly, a limitation of the FE modelling is the idealised 2D axisymmetric geometry. Future work could focus on a more realistic 3D geometry, to allow for more accurate analysis of the clot tip deformation.

6.6 Conclusion

This chapter investigates the effect of clot mechanical properties and composition, using the previously characterised clot analogues, described in Chapters 3 and 4, on the deformation and angiographic appearance of an occluding clot lodged in an *in-vitro* model under physiological conditions of pressure and flow.

NCCs, particularly with a lower hematocrit, were found to experience greater mass loss which in turn allowed these clots to travel further into the tapered tube before lodgement. Additionally, clots with a greater hematocrit were found to have increased flattening of the original pointed proximal face, particularly in the case of the NCC group, which is likely due to the soft nature of the clot. The FE model supports these results and highlights the possible effect of the bulk and shear moduli on the deformation of the proximal face of the clot.

Overall, this chapter gives an insight into the occlusion dynamics of clots with various mechanical properties over the relevant timeline for stroke. This result could

potentially aid the identification of particular clot types prior to treatment and could assist physicians in selecting the most appropriate treatment method to administer or on what MT technique to use, that would ensure a greater success rate in each case. Although the clot mechanical properties have previously been found to affect the thrombectomy procedures, a more comprehensive analysis, with larger sample numbers, is required to draw definitive conclusions.

6.7 References

Benson, J. C. *et al.* (2019) 'Clot permeability and histopathology: is a clot's perviousness on CT imaging correlated with its histologic composition?', Journal of NeuroInterventional Surgery. British Medical Journal Publishing Group. doi: 10.1136/NEURINTSURG-2019-014979.

Bourcier, R. *et al.* (2019) 'Susceptibility vessel sign on MRI predicts better clinical outcome in patients with anterior circulation acute stroke treated with stent retriever as first-line strategy.', Journal of neurointerventional surgery. British Medical Journal Publishing Group, 11(4), pp. 328–333. doi: 10.1136/neurintsurg-2018-014217.

Brinjikji, W. *et al.* (2017) 'Correlation of imaging and histopathology of thrombi in acute ischemic stroke with etiology and outcome: a systematic review', Journal of NeuroInterventional Surgery, 9(6), pp. 529–534. doi: 10.1136/neurintsurg-2016-012391.

Cenic, A. *et al.* (1999) 'Dynamic CT measurement of cerebral blood flow: a validation study.', AJNR. American journal of neuroradiology. American Journal of Neuroradiology, 20(1), pp. 63–73. doi: 10.3174/ajnr.a1408.

Consoli, A. *et al.* (2018) 'Thrombectomy for M1-Middle Cerebral Artery Occlusion: Angiographic Aspect of the Arterial Occlusion and Recanalisation: A Preliminary Observation.', Stroke, 49(5), pp. 1286–1289. doi: 10.1161/STROKEAHA.117.018987.

Consoli, A. *et al.* (2019) 'Effect of the phenotype of the M1-middle cerebral artery occlusion on the recanalisation rates in the ASTER trial', Journal of NeuroInterventional Surgery. British Medical Journal Publishing Group. doi: 10.1136/neurintsurg-2019-015002.

Duffy, S. *et al.* (2016) 'Novel methodology to replicate clot analogs with diverse composition in acute ischemic stroke', Journal of Neurointerventional Surgery, 0, pp. 1–7.

Fang, J. *et al.* (2015) 'Discrimination between Newly Formed and Aged Thrombi Using Empirical Mode Decomposition of Ultrasound B-Scan Image', BioMed Research International. Hindawi, 2015, pp. 1–9. doi: 10.1155/2015/403293.

Fitzgerald, S. T. *et al.* (2019) 'Platelet-rich clots as identified by Martius Scarlet Blue staining are isodense on NCCT.', Journal of neurointerventional surgery. British Medical Journal Publishing Group, 11(11), pp. 1145–1149. doi: 10.1136/neurintsurg-2018-014637.

Froehler, M. T. *et al.* (2013) 'The hyperdense vessel sign on CT predicts successful recanalisation with the Merci device in acute ischemic stroke.', Journal of neurointerventional surgery. British Medical Journal Publishing Group, 5(4), pp. 289–93. doi: 10.1136/neurintsurg-2012-010313.

Fujimoto, M. *et al.* (2013) 'Characterization of Arterial Thrombus Composition by Magnetic Resonance Imaging in a Swine Stroke Model', Stroke, 44(5), pp. 1463–1465. doi: 10.1161/STROKEAHA.111.000457.

Ganeshan, R. *et al.* (2018) 'Assessment of thrombus length in acute ischemic stroke by post-contrast magnetic resonance angiography.', Journal of neurointerventional surgery. British Medical Journal Publishing Group, 10(8), pp. 756–760. doi: 10.1136/neurintsurg-2017-013454.

Garcia-Bermejo, P. *et al.* (2019) 'Baseline Occlusion Angiographic Appearance on Mechanical Thrombectomy Suggests Underlying Etiology and Outcome.', Frontiers in neurology. Frontiers Media SA, 10, p. 499. doi: 10.3389/fneur.2019.00499.

Goyal, M. *et al.* (2016) 'Endovascular thrombectomy after large-vessel ischaemic stroke: a meta-analysis of individual patient data from five randomised trials', The Lancet. Elsevier, 387(10029), pp. 1723–1731. doi: 10.1016/S0140-6736(16)00163-X.

Gunning, G. M. *et al.* (2016) 'Clot friction variation with fibrin content; implications for resistance to thrombectomy', Journal of Neurointerventioal Surgery, 372(1), pp. 1019–1030. doi: 10.1136/.

Johnson, S. *et al.* (2019) 'Mechanical behavior of in vitro blood clots and the implications for acute ischemic stroke treatment.', Journal of neurointerventional surgery. British Medical Journal Publishing Group. doi: 10.1136/neurintsurg-2019-015489.

Kim, Y.-W. *et al.* (2016) 'Efficacy of Proximal Aspiration Thrombectomy for Using Balloon-Tipped Guide Catheter in Acute Intracranial Internal Carotid Artery Occlusion.', Journal of Korean Neurosurgical Society. The Korean Neurosurgical Society, 59(4), pp. 379–84. doi: 10.3340/jkns.2016.59.4.379.

Kirchhof, K. *et al.* (2003) 'Differentiation of White, Mixed, and Red Thrombi: Value of CT in Estimation of the Prognosis of Thrombolysis—Phantom Study', Radiology, 228(1), pp. 126–130. doi: 10.1148/radiol.2273020530.

Lapergue, B. *et al.* (2016) 'A Direct Aspiration, First Pass Technique (ADAPT) versus Stent Retrievers for Acute Stroke Therapy: An Observational Comparative Study', American Journal of Neuroradiology, 37(10), pp. 1860–1865. doi: 10.3174/ajnr.A4840.

Liebeskind, D. S. *et al.* (2011) 'CT and MRI Early Vessel Signs Reflect Clot Composition in Acute Stroke', Stroke, 42(5), pp. 1237–1243. doi: 10.1161/STROKEAHA.110.605576.

van der Marel, K. *et al.* (2016) 'Quantitative assessment of device–clot interaction for stent retriever thrombectomy', Journal of NeuroInterventional Surgery, 8(12), pp. 1278–1282. doi: 10.1136/neurintsurg-2015-012209.

Mehta, B. P. and Nogueira, R. G. (2012) 'Should clot composition affect choice of endovascular therapy?', Neurology. Wolters Kluwer Health, Inc. on behalf of the American Academy of Neurology, 79(13 Suppl 1), pp. S63-7. doi: 10.1212/WNL.0b013e3182695859.

Minnerup, J. and Kleinschnitz, C. (2011) 'Visualization of Clot Composition in Ischemic Stroke', Stroke, 42(5), pp. 1193–1194. doi: 10.1161/STROKEAHA.110.612150.

Mokin, M. *et al.* (2017) 'Association of clot burden score with radiographic and clinical outcomes following Solitaire stent retriever thrombectomy: analysis of the SWIFT PRIME trial', Journal of NeuroInterventional Surgery. British Medical Journal Publishing Group, 9(10), pp. 929–932. doi: 10.1136/NEURINTSURG-2016-012631.

Mönch, S. *et al.* (2019) 'Angiographic Baseline Proximal Thrombus Appearance of M1/M2 Occlusions in Mechanical Thrombectomy', Clinical Neuroradiology. Springer, pp. 1–8. doi: 10.1007/s00062-019-00863-4.

Pillai, J. J. *et al.* (2001) 'Initial Angiographic Appearance of Intracranial Vascular Occlusions in Acute Stroke as a Predictor of Outcome of Thrombolysis: Initial Experience', Radiology. Radiological Society of North America , 218(3), pp. 733–738. doi: 10.1148/radiology.218.3.r01mr40733.

Riedel, C. H. *et al.* (2010) 'Assessment of Thrombus in Acute Middle Cerebral Artery Occlusion Using Thin-Slice Nonenhanced Computed Tomography Reconstructions', Stroke, 41(8), pp. 1659–1664. doi: 10.1161/STROKEAHA.110.580662.

Santos, E. M. M. *et al.* (2016) 'Thrombus Permeability Is Associated With Improved Functional Outcome and Recanalisation in Patients With Ischemic Stroke', Stroke, 47(3), pp. 732–741. doi: 10.1161/STROKEAHA.115.011187.

Shin, J. W. *et al.* (2018) 'High red blood cell composition in clots is associated with successful recanalisation during intra-arterial thrombectomy', PLOS ONE. Edited by H. ten Cate. Public Library of Science, 13(5), p. e0197492. doi: 10.1371/journal.pone.0197492.

Sorimachi, T. *et al.* (2011) 'Blood pressure measurement in the artery proximal and distal to an intra-arterial embolus during thrombolytic therapy.', Journal of neurointerventional surgery. British Medical Journal Publishing Group, 3(1), pp. 43–6. doi: 10.1136/jnis.2010.003061.

Strbian, D. *et al.* (2013) 'Relationship between onset-to-door time and door-to-thrombolysis time: a pooled analysis of 10 dedicated stroke centers.', Stroke, 44(10), pp. 2808–13. doi: 10.1161/STROKEAHA.113.000995.

Tong, D. *et al.* (2012) ‘Times from symptom onset to hospital arrival in the Get with the Guidelines--Stroke Program 2002 to 2009: temporal trends and implications.’, Stroke, 43(7), pp. 1912–7. doi: 10.1161/STROKEAHA.111.644963.

Turk, A. S. *et al.* (2014) ‘Initial clinical experience with the ADAPT technique: A direct aspiration first pass technique for stroke thrombectomy’, Journal of NeuroInterventional Surgery, 6(3), pp. 231–237. doi: 10.1136/neurintsurg-2013-010713.

Weafer, F. M. *et al.* (2019) ‘Characterization of strut indentation during mechanical thrombectomy in acute ischemic stroke clot analogs’, Journal of NeuroInterventional Surgery, 11(9), pp. 891-897 neurintsurg-2018-014601. doi: 10.1136/neurintsurg-2018-014601.

Yamamoto, Y. *et al.* (2019) ‘The Claw Sign: An angiographic Predictor of Recanalisation After Mechanical Thrombectomy for Cerebral Large Vessel Occlusion’, Journal of Stroke and Cerebrovascular Diseases. W.B. Saunders, 28(6), pp. 1555–1560.

Yoo, A. J. and Andersson, T. (2017) ‘Thrombectomy in Acute Ischemic Stroke: Challenges to Procedural Success.’, Journal of stroke. Korean Stroke Society, 19(2), pp. 121–130. doi: 10.5853/jos.2017.00752.

Chapter 7

Discussion & Conclusion

7.1 Chapter Overview

This chapter summarises and discusses the outcomes of the work in this thesis. A brief overview of the novelty of the work performed is given in section 7.2. A summary of the work presented and a discussion of the main findings of the technical chapters (**Chapters 3-6**) is given in section 7.3. This is followed by recommendations for future work and final concluding remarks.

7.2 Overview and Novelty

The main novelties of the work presented in this thesis are summarised as follows:

- The preparation and production of a range of repeatable clot analogues, with varying compositions and mechanical behaviour that span the range of human thromboemboli.
- The investigation of the mechanical behaviour of clot analogues as a function of clot composition and the development of a reliable test method that can be used to test the broad range of clot types.
- The evaluation of the effect of platelet-driven contraction on clot mechanical properties and microstructure, and in turn how this can have implications for the treatment of AIS.

- The characterisation of cyclic loading-unloading hysteresis and stress-relaxation for a range of clot analogues, as a function of composition and the fitting of a hyper-viscoelastic constitutive law to capture the observed mechanical behaviour.
- The development of the first reported calcified clot analogue material, with similar mechanical properties to human calcified tissues that represent likely sources of calcified clots.
- The development of an *in-vitro* model of AIS using the clot analogues that can be used to compare the effectiveness of various mechanical thrombectomy techniques on clots with varying mechanical properties.
- The investigation of the effect of clot mechanical properties and composition on the occlusion dynamics and deformation of an occluding clot under physiological conditions *in-vitro*.

7.3 Summary and Discussion

Mechanical thrombectomy is the new gold standard for the treatment of AIS. The focus of this thesis is to further the understanding of the mechanical behaviour of thrombus material and to develop realistic thrombus analogues that can be used in the *in-vitro* testing of mechanical thrombectomy devices, with the aim of being able to facilitate the improvement of future generation of devices. This is accomplished in this work by developing a variety of clot analogues, with a range of mechanical properties, and through the development of an *in-vitro* AIS model for the evaluation of mechanical thrombectomy. A summary of the key findings of each of the results chapters presented in this thesis is provided and discussed below.

The preparation of a selection of repeatable clot analogues, with a range of mechanical properties that have been developed for the *in-vitro* modelling of AIS is presented in **Chapter 3**. Both platelet-contracted (PCCs) and non-contracted clots (NCCs) were formed, with varying hematocrit. For the first time, the effect of platelet contraction on clot microstructure and mechanical properties was examined. The large strain stiffnesses of the analogues were found to span the range measured for the human thromboemboli at large strains. Platelet contraction had the effect of increasing stiffness and together with adjustment of the haematocrit, enabled close matching of stiffness to representative thromboemboli of AIS origin. Although significant differences in mechanical properties and microstructure were observed between PCCs and NCCs, histological quantification of fibrin and RBCs in these clots did not show an appreciable difference. The implication is that RBC content alone, measured by histology, of explanted human clots may not be predictive of their mechanical behaviour during thrombectomy.

PCCs with a low %H resisted complete ingestion via contact aspiration alone or complete retrieval with stent-retrievers. PCCs with a higher %H and all NCCs were fully retrievable, although the likelihood of fragmentation is increased in clots with a greater %H. The clot analogues presented in this chapter have been shown to be useful for the evaluation of different clot behaviour during mechanical thrombectomy.

Chapter 4 presents a further investigation of the mechanical behaviour of the contracted clot analogues described in **Chapter 3**, through experimental testing and computational analysis. The experimental testing and constitutive law calibration reported in **Chapter 4** provides the first detailed characterisation of cyclic loading-unloading hysteresis and stress-relaxation for a range of clot analogue compositions.

All of the samples exhibit hysteresis between the loading and unloading curves, suggesting that the material is viscoelastic. The 0% H clot was found to have the largest initial stiffness, followed by the 5% H and the WB clot, which had a similar stiffness as low levels of strain (< 30% strain). However, the 5% H clot was found to stiffen significantly for strains greater than 30% and was found to have the greatest large strain stiffness.

The viscoelasticity of the material was investigated further by the stress-relaxation experiments. The 0% H and the 5% H clots experienced similar levels of relaxation, with the 0% H clot experiencing the greatest relaxation of all of the clots tested. The percentage relaxation for both the WB clot and the 40% H clot were significantly lower than the other two groups. Material modelling of the experiments were also presented, and an appropriate hyper-viscoelastic constitutive model was identified and calibrated based on the experimental mechanical test data. This chapter reports the first model to successfully capture the loading-unloading hysteresis and stress-relaxation of the thrombus material and provides a significant advance in the current understanding of the relationship between clot composition and rate-dependent non-linear mechanical behaviour.

Aging was not found to affect the mechanical behaviour of the clot analogues tested in compression, as clots tested after aging for 1, 4, 7 and 14 days exhibited little difference in mechanical behaviour. Likewise, there was no significant difference in the mechanical behaviour of the clot analogues stored at 4°C versus 37°C, with the exception of the 40% H clot, which was found to disintegrate when stored at 37°C for more than one day. The literature provides little information on the optimal storage conditions for analogue clot material, however from the observations in **Chapter 4**, it

is recommended that clot analogues are stored in their own serum, where possible, at 4°C to ensure that the mechanical properties and microstructure are maintained.

Scanning electron microscopy (SEM) was also used in **Chapter 4** to observe the clot microstructure at various time-points and to investigate the effect of aging and storage solution on the clot microstructure for the first time. The clots stored in serum were found to have further compaction of the RBCs to a polyhedron shape between day 1 and day 7. This was in contrast to the clots stored in saline, as the RBCs in those clot samples appeared to swell and have their native shape restored.

The development of a calcified clot analogue, representative of calcified cerebral emboli (CCEs) and the development of an *in-vitro* model that is capable of evaluating different endovascular treatment approaches, using contemporary devices, for the retrieval of a CCE lodged in the M1 segment of the middle cerebral artery is described in **Chapter 5**. Silicone anatomical models of the neurovasculature have been widely used for AIS simulation, and their accuracy has been improved through the use of actual blood clot analogues, rather than analogues consisting of synthetic alternatives made of different materials. In the same way we hypothesised, for an AIS model of a CCE occlusion, that a CCE analogue consisting of similar material to an actual CCE would provide the most accurate *in-vitro* model. Therefore, the development of a calcified clot analogue, that shares the biomechanical properties of calcified tissues that pose a high potential source of CCEs, is outlined for the first time in **Chapter 5.**

The CCE analogues were found to successfully replicate the mechanical behaviour of *ex-vivo* calcified tissue when tested under compression, with similar initial stiffness values. When the compressive stiffness of the calcified material and CCE analogues were compared to those of blood thrombus, they were found to be approximately four

to five times greater. Due to the stiffness of the CCE analogues in the *in-vitro* model, they could not be deformed by the thrombectomy devices during the retrieval attempts. Therefore, it was impossible to pull the CCEs, even in part, into the guide catheter, or the distal access catheter. The most successful strategy in removing the CCEs from the *in-vitro* model was a combined technique, using a stent-retriever with local aspiration under flow arrest conditions. The combination of each of the three devices had a critical and different part to play in this success, with each on their own or in dual combination proving to be mostly ineffective. Although a more comprehensive analysis is required to draw definitive conclusions when comparing mechanical thrombectomy techniques, the preliminary experiments do highlight the capability of this *in-vitro* model.

Chapter 6 provides an insight into the occlusion dynamics of clots with various mechanical properties and compositions over the relevant timeline for stroke. The effect of clot mechanical properties and hematocrit, using the previously characterised clot analogues described in **Chapters 3 and 4**, on the deformation and angiographic appearance of clot, when lodged in an *in-vitro* model under physiological conditions of pressure and flow, was examined. The clot behaviour during lodgement was analysed and the shape change of the proximal face of the clot was monitored for a period of 5 hours. All of the clot samples were cut to have an ‘irregular’ shape before lodgment, and the tendency of the clots to flatten, as a function of composition and contraction, was monitored.

NCCs, particularly with a lower hematocrit, were found to experience greater mass loss which in turn allowed these clots to travel further into the tapered tube before lodgement. Additionally, clots with a greater hematocrit were found to have increased flattening of the original pointed proximal face, particularly in the case of the NCC

group, which is likely due to the soft nature of the clot. The finite element modelling performed supports these results and highlights the effect of the bulk and shear moduli on the deformation of the proximal face of the clot. From the experimental and computational results in this chapter, it appears that the compressibility of the clots affects the extent of deformation of the proximal face of the clot in some cases.

The angiographic appearance of an occlusion in AIS patients on digital subtraction angiography (DSA) is emerging as a method to determine the occlusion etiology and to predict likelihood of successful recanalisation. Therefore, this result could potentially aid the identification of particular clot types prior to treatment, and could assist physicians in selecting the most appropriate treatment method to administer or on what MT technique to use, that would ensure a greater success rate in each case.

7.4 Recommendations for Future Work

The emergence of mechanical thrombectomy as the new standard of care in the treatment of AIS is a relatively recent development. Despite a considerable number of valuable studies in recent years, there is still a lot that is not fully understood about thrombus material and its interaction with the thrombectomy device during a procedure. However, the clot analogues discussed in this thesis provide a valuable tool that can be utilized in many ways to further our understanding of clot mechanics.

Chapters 3 and **4** investigate the mechanical behaviour of the thrombus analogues under compressive loading. Tensile testing of the samples was initially attempted, however reliable tensile testing did not prove possible and often resulted in tearing/rupturing at the grips due to the fragile nature of the clots. Therefore, the compression test developed in this thesis has been proven as a reliable test method that is capable of testing the broad spectrum of clot types found *in-vivo*. Few studies in the

literature have investigated the mechanical properties of thrombi retrieved from patients with AIS (Chueh *et al*. 2011). This robust and repeatable test method could be utilised in the future for the testing of retrieved human thromboemboli.

However, it is also important that behaviour of the clot material is examined under a variety of loading conditions, such as tensile or shear loading, in order to fully characterise the material. Similarly, the fracture properties of clot material are essential for understanding the embolisation of this material during thrombectomy. These properties would also be crucial for the development of accurate computational modelling of the mechanical thrombectomy procedure and therefore should be examined further.

The research presented in this thesis investigated the effect of activated platelets and hematocrit on the mechanical behaviour and microstructure of the clot analogues. However, the range of clot compositions examined could be expanded greatly by examining additional hematocrit ratios, by investigating the effect of platelet concentration and by examining the effect of thrombin to name a few. By investigating and varying these components, clot analogues with a greater stiffness, that more closely match those of human thromboemboli may be developed.

Similarly, a limitation of the clot analogues presented in this thesis is the homogeneous nature of the clots as they are prepared under static conditions in a controlled laboratory environment. In reality, clots retrieved from patients tend to have irregular distribution of components. Heterogeneous clot analogues could be produced following a similar protocol to those described in this thesis, and by forming them under dynamic conditions (Krueger *et al*. 2004; Campbell *et al*. 2015; Duffy *et al*. 2016) to more accurately capture the nature of human thrombi.

The changes in clot microstructure due to platelet contraction of the clot analogues, and the impact on the clot mechanical properties were investigated in **Chapter 3**. The association between these clot properties and their behaviour during mechanical thrombectomy was also investigated. As platelet contraction can also affect the clot permeability, it is hypothesised that this may also impact the effectiveness of other stroke treatments such as thrombolysis. Therefore, it is proposed that the effect of tPA on both platelet contracted and non-contracted clots is investigated in future work.

Analysis of retrieved thrombi can provide information to enhance our understanding of AIS pathophysiology. The efficacy of removing an occluding clot during mechanical thrombectomy has been shown to be influenced by histologic characteristics. Therefore clot composition has been assessed using various histological methods (Yuki *et al*. 2012; Chueh *et al*. 2011; Duffy *et al*. 2016; Fitzgerald *et al*. 2019; De Meyer *et al*. 2017) to determine a potential relationship between thrombus histology and clot stability. However, the results from **Chapter 3**, highlight that although significant differences in mechanical properties and microstructure was observed between PCCs and NCCs, histological quantification of fibrin and RBCs in these clots did not show an appreciable difference. The implication is that RBC content alone, measured by histology, of explanted human clots may not be predictive of their mechanical behaviour during thrombectomy. More recent studies of clot histology have begun to quantify the platelet concentration to investigate the relationship between the platelet-rich clots and successful recanalisation (De Meyer *et al*. 2017; Fitzgerald *et al*. 2019). Similarly, platelet-concentration has been shown to significantly affect clot microstructure (Cines *et al*., 2014; Johnson *et al*., 2019; Tutwiler *et al*., 2017). Therefore, it may be useful to also examine the microstructure

of retrieved thrombi to further understand the impact of the clot microstructure on recanalisation rates and successful procedures.

In recent years, significant developments have been made in the field of AIS treatment. Contemporary treatment of AIS relies on targeting the occlusive clot using medical and endovascular therapy, which exploit the properties of thrombus to lyse or capture the occlusive material. There has been rapid evolution in thrombectomy devices and approaches over the past decade; however, to date, there are no universally accepted standards for device or treatment selection due to little-known scientific information about what combinations of techniques or devices will yield the best outcome (Spiotta *et al*. 2015). Prior studies have suggested that the thrombus composition can be predictive of successful recanalisation following both intravenous (IV) thrombolysis and mechanical thrombectomy (Mehta & Nogueira 2012; Froehler *et al*. 2013; Shin *et al*. 2018b; Goyal *et al*. 2016; Brinjikji *et al*. 2017) and these studies have suggested that clot composition can affect the ideal choice of techniques used during clot retrieval and does, in fact, play a role in device/clot interaction (Weafer *et al*. 2019; Gunning *et al*. 2016; Yoo & Andersson 2017; van der Marel *et al*. 2016). The clot analogues described in this thesis have a range of mechanical properties and therefore may be used to perform a comprehensive analysis to compare the success of each techniques with clot analogues with varying compositions and mechanical properties.

From a clinical perspective, imaging of a clot *in-situ* before treatment could assist in establishing the clot type, and in turn, could assist the physician in selecting the most appropriate treatment method to administer or what device to use, that would ensure a greater success rate in each case. Many studies have proposed different predictors of recanalisation according to the clot imaging characteristics, (Fujimoto *et al*. 2013; Bourcier *et al*. 2019; Liebeskind *et al*. 2011; Kirchhof *et al*. 2003; Riedel *et al*. 2010;

Fitzgerald *et al*. 2019; Ganeshan *et al*. 2018; Santos *et al*. 2016; Benson *et al*. 2019; Cenic *et al*. 1999; Mokin *et al*. 2017). The definition of clot characteristics that are associated with successful recanalisation could help to inform treatment decisions and identify patients at risk (Minnerup & Kleinschnitz 2011). In **Chapter 6**, the clot analogues were utilised to investigate the relationship between the angiographic appearance of an occlusion in AIS patients on digital subtraction angiography (DSA) and the clot mechanical properties and composition, to validate this emerging method as a way to determine the occlusion etiology and to predict likelihood of successful recanalisation. Similarly, these characterized clot analogues can be utilised in the validation of other imaging techniques *in-vitro*. In the near future, these imaging strategies may enable identification of AIS patients who may or may not benefit from a particular treatment and may also offer the physician with an insight into what to expect during the procedure.

A hyper-viscoelastic constitutive model is fitted to the experimental test data for thrombus analogue material in **Chapter 4**. Although this model is relatively simple, is still manages to achieve a reasonably good fit for the loading-unloading hysteresis and stress-relaxation behaviour of the material. The results from **Chapter 6** suggest that future experiments should provide a detailed characterisation of the compressibility and plasticity of the thrombus analogue material as a function of contraction and composition.

Similar material models to the constitutive law proposed in **Chapter 4** have previously been proposed in the literature for clot material, however the constitutive modelling of calcified clots have not been reported. Although this material has been shown to be quite different to regular thrombus material, there are many studies on the characterisation and constitutive modelling of calcified tissue in the literature (Pham

& Sun 2014; Li *et al*. 2008; Hoshino *et al*. 2009). Future constitutive model development for calcified clot material could combine the current models proposed for both thrombus and calcified material to capture the behaviour of this heterogeneous composite material.

7.5 Concluding Remarks

In conclusion, the focus of this thesis was on the development of a range of repeatable clot analogues with varying compositions and to use these to gain a better understanding of the mechanical behaviour of clot material, than has been possible to date. These clot analogues were then used in *in-vitro* AIS models to allow for the analysis of the mechanics of an occluding clot and for the performance assessment of various AIS treatment techniques.

The analysis of the clot analogues presented in this thesis have led to an improved understanding of clot mechanics and the implications for stroke treatment, in particular mechanical thrombectomy. The work presented here has also provided practical recommendations on how these analogues can be utilised in the future to further understand the clot material behaviour and for the development of future treatment devices and strategies.

7.6 References

Benson, J. C. *et al.* (2019) 'Clot permeability and histopathology: is a clot's perviousness on CT imaging correlated with its histologic composition?', Journal of NeuroInterventional Surgery. British Medical Journal Publishing Group. doi: 10.1136/NEURINTSURG-2019-014979.

Bourcier, R. *et al.* (2019) 'Susceptibility vessel sign on MRI predicts better clinical outcome in patients with anterior circulation acute stroke treated with stent retriever as first-line strategy.', Journal of neurointerventional surgery. British Medical Journal Publishing Group, 11(4), pp. 328–333. doi: 10.1136/neurintsurg-2018-014217.

Brinjikji, W. *et al.* (2017) 'Correlation of imaging and histopathology of thrombi in acute ischemic stroke with etiology and outcome: a systematic review', Journal of NeuroInterventional Surgery, 9(6), pp. 529–534. doi: 10.1136/neurintsurg-2016-012391.

Campbell, B. C. V. *et al.* (2015) 'Endovascular Therapy for Ischemic Stroke with Perfusion-Imaging Selection', New England Journal of Medicine. Massachusetts Medical Society, 372(11), pp. 1009–1018. doi: 10.1056/NEJMoa1414792.

Cenic, A. *et al.* (1999) 'Dynamic CT measurement of cerebral blood flow: a validation study.', AJNR. American journal of neuroradiology. American Journal of Neuroradiology, 20(1), pp. 63–73. doi: 10.3174/ajnr.a1408.

Chueh, J. Y. *et al.* (2011) 'Mechanical characterization of thromboemboli in acute ischemic stroke and laboratory embolus analogs.', AJNR. American journal of neuroradiology, 32(7), pp. 1237–44. doi: 10.3174/ajnr.A2485.

Cines, D. B. *et al.* (2014) ‘Clot contraction: compression of erythrocytes into tightly packed polyhedra and redistribution of platelets and fibrin.’, Blood. American Society of Hematology, 123(10), pp. 1596–603. doi: 10.1182/blood-2013-08-523860.

Duffy, S. *et al.* (2016) ‘Novel methodology to replicate clot analogs with diverse composition in acute ischemic stroke’, Journal of Neurointerventional Surgery, 0, pp. 1–7.

Fitzgerald, S. T. *et al.* (2019) ‘Platelet-rich clots as identified by Martius Scarlet Blue staining are isodense on NCCT.’, Journal of neurointerventional surgery. British Medical Journal Publishing Group, 11(11), pp. 1145–1149. doi: 10.1136/neurintsurg-2018-014637.

Froehler, M. T. *et al.* (2013) ‘The hyperdense vessel sign on CT predicts successful recanalisation with the Merci device in acute ischemic stroke.’, Journal of neurointerventional surgery. British Medical Journal Publishing Group, 5(4), pp. 289–93. doi: 10.1136/neurintsurg-2012-010313.

Fujimoto, M. *et al.* (2013) ‘Characterization of Arterial Thrombus Composition by Magnetic Resonance Imaging in a Swine Stroke Model’, Stroke, 44(5), pp. 1463–1465. doi: 10.1161/STROKEAHA.111.000457.

Ganeshan, R. *et al.* (2018) ‘Assessment of thrombus length in acute ischemic stroke by post-contrast magnetic resonance angiography.’, Journal of neurointerventional surgery. British Medical Journal Publishing Group, 10(8), pp. 756–760. doi: 10.1136/neurintsurg-2017-013454.

Goyal, M. *et al.* (2016) ‘Endovascular thrombectomy after large-vessel ischaemic stroke: a meta-analysis of individual patient data from five randomised trials’,

The Lancet. Elsevier, 387(10029), pp. 1723–1731. doi: 10.1016/S0140-6736(16)00163-X.

Gunning, G. M. *et al.* (2016) 'Clot friction variation with fibrin content; implications for resistance to thrombectomy', Journal of Neurointerventioal Surgery, 372(1), pp. 1019–1030. doi: 10.1136/.

Hoshino, T. *et al.* (2009) 'Mechanical stress analysis of a rigid inclusion in distensible material: a model of atherosclerotic calcification and plaque vulnerability', American Journal of Physiology-Heart and Circulatory Physiology. American Physiological Society, 297(2), pp. H802–H810. doi: 10.1152/ajpheart.00318.2009.

Johnson, S. *et al.* (2019) 'Mechanical behavior of in vitro blood clots and the implications for acute ischemic stroke treatment.', Journal of neurointerventional surgery. British Medical Journal Publishing Group. doi: 10.1136/neurintsurg-2019-015489.

Kirchhof, K. *et al.* (2003) 'Differentiation of White, Mixed, and Red Thrombi: Value of CT in Estimation of the Prognosis of Thrombolysis—Phantom Study', Radiology, 228(1), pp. 126–130. doi: 10.1148/radiol.2273020530.

Krueger, K. *et al.* (2004) 'How thrombus model impacts the in vitro study of interventional thrombectomy procedures.', Investigative radiology, 39(10), pp. 641–8. doi: 10.1097/01.RLI.0000139009.65226.17.

Li, Z.-Y. *et al.* (2008) 'Impact of calcification and intraluminal thrombus on the computed wall stresses of abdominal aortic aneurysm', Journal of Vascular Surgery. Mosby, 47(5), pp. 928–935. doi: 10.1016/J.JVS.2008.01.006.

Liebeskind, D. S. *et al.* (2011) 'CT and MRI Early Vessel Signs Reflect Clot Composition in Acute Stroke', Stroke, 42(5), pp. 1237–1243. doi: 10.1161/STROKEAHA.110.605576.

van der Marel, K. *et al.* (2016) 'Quantitative assessment of device–clot interaction for stent retriever thrombectomy', Journal of NeuroInterventional Surgery, 8(12), pp. 1278–1282. doi: 10.1136/neurintsurg-2015-012209.

Mehta, B. P. and Nogueira, R. G. (2012) 'Should clot composition affect choice of endovascular therapy?', Neurology. Wolters Kluwer Health, Inc. on behalf of the American Academy of Neurology, 79(13 Suppl 1), pp. S63-7. doi: 10.1212/WNL.0b013e3182695859.

De Meyer, S. F. *et al.* (2017) 'Analyses of thrombi in acute ischemic stroke: A consensus statement on current knowledge and future directions', International Journal of Stroke, 12(6), pp. 606–614. doi: 10.1177/1747493017709671.

Minnerup, J. and Kleinschnitz, C. (2011) 'Visualization of Clot Composition in Ischemic Stroke', Stroke, 42(5), pp. 1193–1194. doi: 10.1161/STROKEAHA.110.612150.

Mokin, M. *et al.* (2017) 'Association of clot burden score with radiographic and clinical outcomes following Solitaire stent retriever thrombectomy: analysis of the SWIFT PRIME trial', Journal of NeuroInterventional Surgery. British Medical Journal Publishing Group, 9(10), pp. 929–932. doi: 10.1136/NEURINTSURG-2016-012631.

Pham, T. and Sun, W. (2014) 'Material properties of aged human mitral valve leaflets', Journal of Biomedical Materials Research Part A. John Wiley & Sons, Ltd, 102(8), pp. 2692–2703. doi: 10.1002/jbm.a.34939.

Riedel, C. H. *et al.* (2010) 'Assessment of Thrombus in Acute Middle Cerebral Artery Occlusion Using Thin-Slice Nonenhanced Computed Tomography Reconstructions', Stroke, 41(8), pp. 1659–1664. doi: 10.1161/STROKEAHA.110.580662.

Santos, E. M. M. *et al.* (2016) 'Thrombus Permeability Is Associated With Improved Functional Outcome and Recanalisation in Patients With Ischemic Stroke', Stroke, 47(3), pp. 732–741. doi: 10.1161/STROKEAHA.115.011187.

Shin, J. W. *et al.* (2018) 'High red blood cell composition in clots is associated with successful recanalisation during intra-arterial thrombectomy', PLOS ONE. Edited by H. ten Cate. Public Library of Science, 13(5), p. e0197492. doi: 10.1371/journal.pone.0197492.

Spiotta, A. M. *et al.* (2015) 'Evolution of thrombectomy approaches and devices for acute stroke: a technical review.', Journal of neurointerventional surgery, 7(1), pp. 2–7. doi: 10.1136/neurintsurg-2013-011022.

Tutwiler, V. *et al.* (2017) 'Contraction of Blood Clots Is Impaired in Acute Ischemic Stroke.', Arteriosclerosis, thrombosis, and vascular biology, 37(2), pp. 271–279. doi: 10.1161/ATVBAHA.116.308622.

Weafer, F. M. *et al.* (2019) 'Characterization of strut indentation during mechanical thrombectomy in acute ischemic stroke clot analogs', Journal of NeuroInterventional Surgery, 11(9), pp. 891-897 neurintsurg-2018-014601. doi: 10.1136/neurintsurg-2018-014601.

Yoo, A. J. and Andersson, T. (2017) ‘Thrombectomy in Acute Ischemic Stroke: Challenges to Procedural Success.’, Journal of stroke. Korean Stroke Society, 19(2), pp. 121–130. doi: 10.5853/jos.2017.00752.

Yuki, I. *et al.* (2012) ‘The Impact of Thromboemboli Histology on the Performance of a Mechanical Thrombectomy Device’, American Journal of Neuroradiology, 33(4), pp. 643–648. doi: 10.3174/ajnr.A2842.